NON-CODING RNAs IN REPRODUCTIVE BIOLOGY

EDITED BY: Linjun Hong, Katja Teerds, Tang Zhonglin, Zuo Bo and Li Meng
PUBLISHED IN: Frontiers in Cell and Developmental Biology

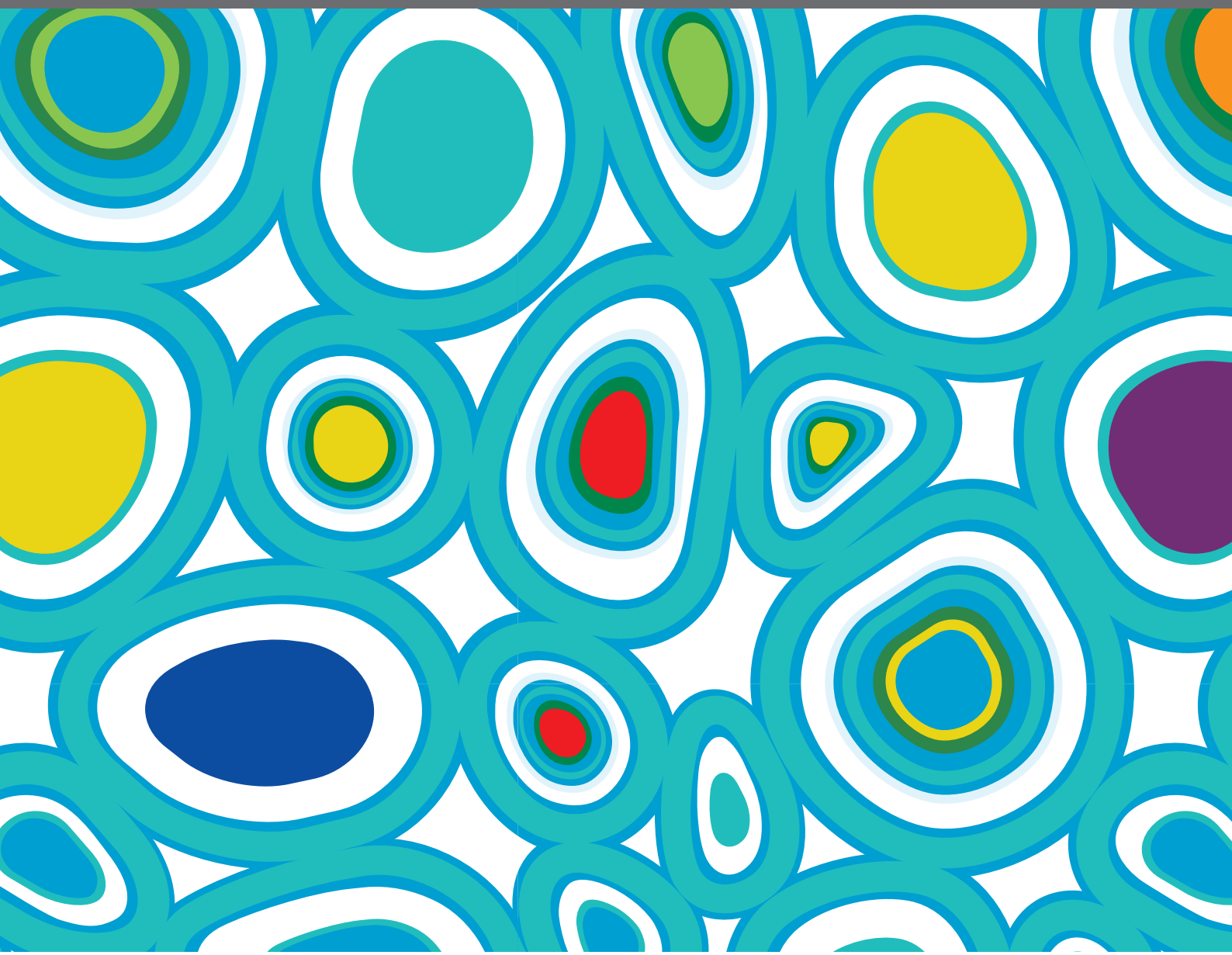

frontiers Research Topics

frontiers

ISSN 1664-8714
ISBN 978-2-88971-227-4
DOI 10.3389/978-2-88971-227-4

About Frontiers

Frontiers is more than just an open-access publisher of scholarly articles: it is a pioneering approach to the world of academia, radically improving the way scholarly research is managed. The grand vision of Frontiers is a world where all people have an equal opportunity to seek, share and generate knowledge. Frontiers provides immediate and permanent online open access to all its publications, but this alone is not enough to realize our grand goals.

Frontiers Journal Series

The Frontiers Journal Series is a multi-tier and interdisciplinary set of open-access, online journals, promising a paradigm shift from the current review, selection and dissemination processes in academic publishing. All Frontiers journals are driven by researchers for researchers; therefore, they constitute a service to the scholarly community. At the same time, the Frontiers Journal Series operates on a revolutionary invention, the tiered publishing system, initially addressing specific communities of scholars, and gradually climbing up to broader public understanding, thus serving the interests of the lay society, too.

Dedication to Quality

Each Frontiers article is a landmark of the highest quality, thanks to genuinely collaborative interactions between authors and review editors, who include some of the world's best academicians. Research must be certified by peers before entering a stream of knowledge that may eventually reach the public - and shape society; therefore, Frontiers only applies the most rigorous and unbiased reviews.
Frontiers revolutionizes research publishing by freely delivering the most outstanding research, evaluated with no bias from both the academic and social point of view. By applying the most advanced information technologies, Frontiers is catapulting scholarly publishing into a new generation.

What are Frontiers Research Topics?

Frontiers Research Topics are very popular trademarks of the Frontiers Journals Series: they are collections of at least ten articles, all centered on a particular subject. With their unique mix of varied contributions from Original Research to Review Articles, Frontiers Research Topics unify the most influential researchers, the latest key findings and historical advances in a hot research area! Find out more on how to host your own Frontiers Research Topic or contribute to one as an author by contacting the Frontiers Editorial Office: frontiersin.org/about/contact

NON-CODING RNAs IN REPRODUCTIVE BIOLOGY

Topic Editors:
Linjun Hong, South China Agricultural University, China
Katja Teerds, Wageningen University, Netherlands
Tang Zhonglin, Agricultural Genomics Institute at Shenzhen, Chinese Academy of Agricultural Sciences, China
Zuo Bo, Huazhong Agricultural University, China
Li Meng, The Chinese University of Hong Kong, China

Citation: Hong, L., Teerds, K., Zhonglin, T., Bo, Z., Meng, L., eds. (2021). Non-Coding RNAs in Reproductive Biology. Lausanne: Frontiers Media SA.
doi: 10.3389/978-2-88971-227-4

Table of Contents

frontiers in Cell and Developmental Biology

EDITORIAL
published: 24 June 2021
doi: 10.3389/fcell.2021.712467

Editorial: Non-coding RNAs in Reproductive Biology

Li Meng[1,2]*, *Katja Teerds*[3], *Zhonglin Tang*[4,5], *Bo Zuo*[6] and *Linjun Hong*[1,7]*

[1] National Engineering Research Center for Breeding Swine Industry, College of Animal Science, South China Agricultural University, Guangzhou, China, [2] Department of Obstertrics and Gynecology, Faculty of Medicine, The Chinese University of Hong Kong, Shatin, China, [3] Human and Animal Physiology, Wageningen University, Wageningen, Netherlands, [4] Shenzhen Branch, Guangdong Laboratory for Lingnan Modern Agriculture, Agricultural Genomics Institute at Shenzhen, Chinese Academy of Agricultural Sciences, Shenzhen, China, [5] Kunpeng Institute of Modern Agriculture at Foshan, Foshan, China, [6] Key Laboratory of Agriculture Animal Genetics, Breeding and Reproduction of the Ministry of Education, Huazhong Agricultural University, Wuhan, China, [7] Guangdong Provincial Key Laboratory of Agro-Animal Genomics and Molecular Breeding, College of Animal Science, South China Agricultural University, Guangzhou, China

Keywords: ncRNAs, reproduction, embryo, development, epigenetic regulation

Editorial on the Research Topic

Non-coding RNAs in Reproductive Biology

Non-coding RNAs (ncRNAs) consist of several classes of transcripts that can be classified according to their function into housekeeping (e.g., ribosomal RNA and transfer RNA) and regulatory RNAs. The main categories of regulatory RNAs include microRNAs (miRNAs), small interfering RNAs (siRNAs), PIWI-interacting RNAs (piRNAs), long non-coding RNAs (lncRNAs) and circular RNAs (circRNAs). ncRNAs are considered as master regulators of transcription, transcript stability, and post-transcriptional and epigenetic regulators of protein-coding transcripts, with functions in both physiological processes and human diseases. To date, much emphasis in research on reproductive biology is put on the identification of protein-coding genes that play important roles in the development of organs and tissues involved in reproduction. Mutations in these genes can have devastating effects on the reproductive system. Surprisingly, much less attention is paid to the possible importance of ncRNAs in reproduction. Several examples in reproductive physiology and disease clearly demonstrate that ncRNAs are essential for proper cellular interactions such as ovarian follicle and embryo development, and that alterations in ncRNAs may play a role in various diseases such as ovarian and prostate cancer.

The Research Topic on "Non-Coding RNAs in Reproductive Biology" in *Frontiers in Cell and Developmental Biology* includes a series of 9 articles that discuss recent advances regarding the biological and molecular roles of ncRNAs in reproductive processes and highlight challenges and outstanding questions, that need to be addressed in future researches.

The gonadal organs testis and ovary function not only as gamete producers but also as endocrine organs involved in the synthesis of sex steroid hormones which are crucial for successful reproduction. In the testis, somatic Sertoli cells directly support and nurse male germ cells in different stages of development, thus playing an essential role in spermatogenesis. Liu et al. explored the expression, function, and mechanism of action of human miR-100-3p in Sertoli cell development, using molecular and physiological methods. The authors demonstrate that miR-100-3p is more highly expressed in the Sertoli cells cultured in the presence of 10% fetal bovine serum (FBS) than 0.5% FBS,

OPEN ACCESS

Edited and reviewed by:
Philipp Kaldis,
Lund University, Sweden

***Correspondence:**
Li Meng
limeng@cuhk.edu.hk
Linjun Hong
linjun.hong@scau.edu.cn

Specialty section:
This article was submitted to Cell Growth and Division, a section of the journal Frontiers in Cell and Developmental Biology

Received: *20 May 2021*
Accepted: *28 May 2021*
Published: *24 June 2021*

Citation:
Meng L, Teerds K, Tang Z, Zuo B and Hong L (2021) Editorial: Non-coding RNAs in Reproductive Biology. Front. Cell Dev. Biol. 9:712467. doi: 10.3389/fcell.2021.712467

promoting DNA synthesis and cell proliferation, while reducing apoptosis simultaneously. Through a loss of function study, authors prove that miR-100-3p directly binds the downstream target gene, serum/glucocorticoid regulated kinase family member 3 (*SGK3*), which main function is related to stimulation of Sertoli cell development. Next to miRNAs, another new type of ncRNAs, circRNAs with closed loop structure, have been reported to play an important role in ovarian follicular development. Li et al. recently identified an N6-methyladenosine (m6A)-modified circRNA, circGFRa1, which is abundantly expressed in the mouse ovary and stage-specifically expressed in cells that are by the authors considered to be mouse female germline stem cells (FGSCs). The authors demonstrate that silencing circGFRa1 in FGSCs significantly reduces their self-renewal capabilities, while overexpression of circGFRa1 significantly enhances FGSC self-renewal. Furthermore, authors show that circGFRa1 can enhance the expression of the downstream target GFRa1, leading to activation of the glial cell derived neurotrophic factor (GDNF) signaling pathway by sponging miR-449 in FGSC. Although these data are very exciting, some caution is necessary, as the presence of FGSC in the postnatal (adult) mammal ovary continues to be under debate.

Embryo implantation failure is recognized as a leading cause of infertility. The review by Zhou and Dimitriadis surveys a group of secreted miRNAs, that are potentially useful in predicting implantation outcome using materials that can be collected in a relatively non-invasive way, such as follicular fluid, blood and uterine fluid. Secreted or extracellular miRNAs are highly stable in body fluids and can be used as a reflection of disease state. A further advantage of these miRNAs is that they are easily detectable in a short time frame. These advantages make them promising biomarkers for the detection of (successful) embryo implantation.

The placenta is the structure where exchange of blood borne factors between mother and fetus occur and as such plays a central role in maternal and fetal health during pregnancy. Xu et al. in their mini-review address the role of placenta-derived miRNAs in the pathophysiology of human pregnancy. miRNAs produced by the maternal site of the placenta can be selectively incorporated into exosomes and potentially transferred into fetal cells to provide intercellular communication between mother and fetus. In this review, the authors especially focus on the role of exosome miRNAs as possible biomarkers for the prediction of pregnancy related diseases, such as preeclampsia.

Next to embryo implantation, proper trophoblast invasion and fusion are also pivotal processes for the establishment of a successful pregnancy. Two original research papers discuss the emerging findings that non-coding RNAs are involved in regulating trophoblast differentiation, invasion, and fusion. You et al. delineated the precise molecular physiological processes by which BMP2 regulates trophoblast invasion. The authors show that serum BMP2 concentrations are significantly lower in women with early pregnancy loss than in women with an ongoing early pregnancy. In mice, exogenous BMP2 promotes embryonic development by stimulating blastocyst formation and hatching. Using primary extravillous trophoblast cells, the authors observed that BMP2 upregulates the downstream LncRNA NR026833.1, promoting SNAIL expression via sponging miR-502-5p. SNAIL then enhances MMP2 expression and promotes cell invasion. Apicella et al. identified two non-coding transcripts, miR-193b and lncRNA UCA1, in the BeWo trophoblast cell model and in placental diseases. The authors show that miR-193b is a hub for the downregulation of 135 targets genes mainly involved in cell cycle progression and energy usage/nutrient transport. Furthermore, it is reported that UCA1 knockdown leads to an altered gene expression profile which may affect trophoblast cell fusion.

Successful reproduction is highly dependent on the health status of the reproductive organs. Finding cures for diseases such as ovarian and prostate cancer is of the utmost importance not only from a reproductive perspective but also from the point of human well-being. Takeiwa et al. provide an outstanding review of the regulatory effects of some lncRNAs in apoptosis of ovarian cancer cells. In particular the authors focus on the molecular characteristics of apoptosis-related lncRNAs, involved in the regulation of transcription factors, histone modification complexes, miRNAs, and protein stability. The authors provide insight in the possible role of apoptosis-related lncRNAs as biomarkers for ovarian cancer diagnosis, prognosis, and therapy. In line with the review by Takeiwa et al.; Hu et al. execute an extensive integrated bioinformatic analysis to characterize lncRNA-immune interactions in prostate cancer. Prostate cancer-specific dysregulated lncRNAs such as RP11-627G23.1 and RP11-465N4.5 are identified and seem to be closely associated with immune-related hallmarks of prostate cancer.

At last, we are pleased with the article by Luo et al. investigating the regulatory roles of non-coding RNAs in fetal and postnatal muscle development. The focus of this study is on fetal development with the emphasis on muscle development as part of fetal well-being. In this review, the authors provide an up-to-date research overview of miRNAs, circRNAs, and lncRNAs involved in regulating myoblast proliferation, differentiation, and postnatal muscle development through multiple molecular mechanisms.

In conclusion, with this Research Topic we have collected a series of reviews and original research papers describing the role of non-coding RNAs in both physiological and pathological processes related to male and female reproduction. The papers comprising this Research Topic greatly contributed to our further understanding of the regulatory mechanisms and potential applications of ncRNAs, although we also learnt that many questions remain still unanswered.

AUTHOR CONTRIBUTIONS

LM and LH drafted and further revised the manuscript. KT critically reviewed the manuscript and significantly improved it.

ZT and BZ have critically reviewed it. All authors listed have read this editorial and approved it for publication.

FUNDING

This work was supported by the National Natural Science Foundation of China (31802033) and the Science & Technology Planning Project of Guangzhou (201904010434).

ACKNOWLEDGMENTS

As Research Topic editors we would like to express our sincerely thank to all authors and referees for their valuable contributions, which made it possible for us to compile this interesting Research Topic on Non-Coding RNAs in Reproductive Biology.

Conflict of Interest: The authors declare that the research was conducted in the absence of any commercial or financial relationships that could be construed as a potential conflict of interest.

frontiers in Cell and Developmental Biology

REVIEW
published: 22 September 2020
doi: 10.3389/fcell.2020.586510

Secreted MicroRNA to Predict Embryo Implantation Outcome: From Research to Clinical Diagnostic Application

Wei Zhou[1,2] *and Evdokia Dimitriadis*[1,2]*

[1] Department of Obstetrics and Gynaecology, The University of Melbourne, Parkville, VIC, Australia, [2] Gynaecology Research Centre, The Royal Women's Hospital, Parkville, VIC, Australia

Embryo implantation failure is considered a leading cause of infertility and a significant bottleneck for *in vitro* fertilization (IVF) treatment. Confirmed factors that lead to implantation failure involve unhealthy embryos, unreceptive endometrium, and asynchronous development and communication between the two. The quality of embryos is further dependent on sperm parameters, oocyte quality, and early embryo development after fertilization. The extensive involvement of such different factors contributes to the variability of implantation potential across different menstrual cycles. An ideal approach to predict the implantation outcome should not compromise embryo implantation. The use of clinical material, including follicular fluid, cumulus cells, sperm, seminal exosomes, spent blastocyst culture medium, blood, and uterine fluid, that can be collected relatively non-invasively without compromising embryo implantation in a transfer cycle opens new perspectives for the diagnosis of embryo implantation potential. Compositional comparison of these samples between fertile women and women or couples with implantation failure has identified both quantitative and qualitative differences in the expression of microRNAs (miRs) that hold diagnostic potential for implantation failure. Here, we review current findings of secreted miRs that have been identified to potentially be useful in predicting implantation outcome using material that can be collected relatively non-invasively. Developing non-invasive biomarkers of implantation potential would have a major impact on implantation failure and infertility.

Keywords: embryo implantation, non-invasive prediction, microRNAs, male factor, spent blastocyst culture medium, blood, uterine fluid, oocyte quality

OPEN ACCESS

Edited by:
Katja Teerds, Wageningen University & Research, Netherlands

Reviewed by:
Rajprasad Loganathan, Johns Hopkins University School of Medicine, United States
Andrew Swan, University of Windsor, Canada

***Correspondence:**
Evdokia Dimitriadis
eva.dimitriadis@unimelb.edu.au

Specialty section:
This article was submitted to Cell Growth and Division, a section of the journal Frontiers in Cell and Developmental Biology

Received: *23 July 2020*
Accepted: *24 August 2020*
Published: *22 September 2020*

Citation:
Zhou W and Dimitriadis E (2020) Secreted MicroRNA to Predict Embryo Implantation Outcome: From Research to Clinical Diagnostic Application. Front. Cell Dev. Biol. 8:586510. doi: 10.3389/fcell.2020.586510

INTRODUCTION

Infertility affects a staggering one in six couples worldwide (Wilcox et al., 1988) and can be a devastating condition for couples, with the failure to conceive recognized as a leading cause of psychological distress, depression, low self-esteem, and domestic violence (Chachamovich et al., 2010; Cui, 2010). A major contributor to infertility is the failure of blastocysts to implant, accounting for >50% of all failed pregnancies (Craciunas et al., 2019). While *in vitro* fertilization (IVF) has increasingly assisted couples to conceive, success rates have stagnated as still, ∼50%

of good quality blastocysts fail to implant (Gardner and Balaban, 2016). Implantation is a highly complex biological process that requires the coordination between a healthy embryo and a receptive endometrium. The process is initiated via fertilization of a healthy oocyte, which occurs in the Fallopian tube. During fertilization, the female reproductive tract serves as a natural selection system to guarantee that the best quality sperm reaches and fertilizes the oocyte (Ralt et al., 1991). Once fertilized, the zygote travels through the Fallopian tube and develops to the morula stage when it reaches the uterine cavity. The morula stage embryo continues to develop to the blastocyst stage in the uterine cavity before implantation (Norwitz et al., 2001). This can take up to 72 h within which time the embryo and the endometrium communicate via secreted and cell surface factors to prepare for the initial adhesion and attachment (Ashary et al., 2018). Once the outer layer of the embryo, namely, the trophectoderm firmly attaches to the endometrial luminal epithelium, it initiates implantation. Failure of firm adhesion leads to implantation failure.

Successful implantation is based on the cumulative success of the above events. Implantation can be affected by many factors including sperm and oocyte quality, early development of the embryo, the endometrium, and the reciprocal communication between blastocysts and endometrium. During an IVF clinical setting, embryo quality is generally scored via assessment of morphology, expansion and hatching, development of inner cell mass, and the formation of the trophectoderm layer (Giorgetti et al., 1995; Gardner et al., 2000). The transfer of embryos graded as good or "transferable" can improve implantation and pregnancy outcome (Giorgetti et al., 1995; Gardner et al., 2000). However, these morphological criteria do not necessarily correlate with implantation potential. Embryos with similar morphologically good scores assessed to be of transferable quality from aged women (>38 years) have a significantly lower pregnancy rate compared to those of younger women (<38 years) (Giorgetti et al., 1995). It is estimated that overall, 50% of good quality embryos fail to implant (Gardner and Balaban, 2016). In addition to scores based on morphology, pre-implantation genetic testing is also used in some IVF clinics. This testing requires the collection of trophectoderm cells to assess the ploidy of blastocysts and can reveal one of the many characters that may affect implantation. Another clinical approach to improve implantation success is via the assessment of endometrial receptivity. A current clinical test, called endometrial receptivity array, is used to evaluate whether the endometrium is in phase or receptive (Díaz-Gimeno et al., 2011). However, this method is invasive as it requires an endometrial biopsy and does not diagnose a disrupted or dysregulated endometrium, and while promising, there is still a need to develop non-invasive methods to recognize a disrupted endometrium (Díaz-Gimeno et al., 2011). In addition to the endometrium, sperm quality also can affect implantation. Current clinical analysis of sperm quality relies on the basic assessments of sperm morphology and motility, which do not necessarily reflect their capability in facilitating embryo development and implantation.

Despite the available tests, abnormalities in sperm, oocytes, disrupted endometrium, and embryo–endometrial interactions that contribute to implantation failure are not able to be effectively determined, and implantation failure remains a significant bottleneck for IVF treatment. To improve this, emerging work focuses on assessing biomarkers in samples that can be collected relatively non-invasively and examining whether they reflect the implantation potential. While many different classes of potential biomarkers have been proposed, microRNAs (miRs) stand out as promising biomarkers to determine the quality of sperm, oocytes, embryos, and endometrium that could be used to predict implantation outcome. miRs are small non-coding RNAs that regulate gene expression and protein production (Bushati and Cohen, 2007). Secreted or extracellular miRs are highly stable in body fluids, reflect disease states, and are easily detectable in a short time frame making them highly suitable for biomarker detection (Cuman et al., 2015). Emerging evidence strongly suggests that miRs regulate human embryo implantation (Paul et al., 2019). Recent studies support their use as non-invasive biomarkers for sperm, oocyte, and blastocyst quality, endometrial receptivity, and blastocyst–endometrial interactions (Cuman et al., 2015; Machtinger et al., 2017; Li et al., 2019; Abu-Halima et al., 2020). This review aims to discuss the use of miRs for screening blastocyst quality and implantation potential, focusing on using human samples that can be collected relatively non-invasively.

LABORATORY IDENTIFICATION OF MIRS WITH TRANSLATIONAL POTENTIAL FOR IMPLANTATION PREDICTION

A standard IVF treatment broadly requires egg retrieval, sperm collection, IVF, and embryo culture before transfer. The collection of cumulus cells and follicular fluid is possible during egg retrieval without affecting IVF (**Figure 1**). Analysis of gene and miR expression in follicular fluid and cumulus cells indicates oocyte and embryo quality, thus the implantation potential from an embryo's perspective (Hamel et al., 2008; Fu et al., 2018). Embryos are generally cultured up to 5–6 days to reach the blastocyst stage before transfer (**Figure 1**). Embryos secrete specific profiles of miRs that may reflect their quality and implantation potential (Kropp et al., 2014; Capalbo et al., 2016). The endometrial epithelium secretes factors into the uterine cavity to regulate implantation and uterine fluid, or uterine lavage washings can potentially be used to detect miRs as biomarkers for the prediction of receptivity and implantation (Boomsma et al., 2009). Blood contains extracellular miRs with expression levels of some miRs positively correlating with endometrial levels and can potentially indicate whether the endometrium is dysregulated or receptive (Kresowik et al., 2014). Abnormalities in sperm contribute to blastocyst development and quality (Yuan et al., 2016), which could impact implantation. It has been shown in mice that sperm relays epigenetic information to the oocyte during fertilization and influences pre-implantation embryo and offspring development (Sharma et al., 2016). The development of non-invasive biomarkers has driven extensive research in

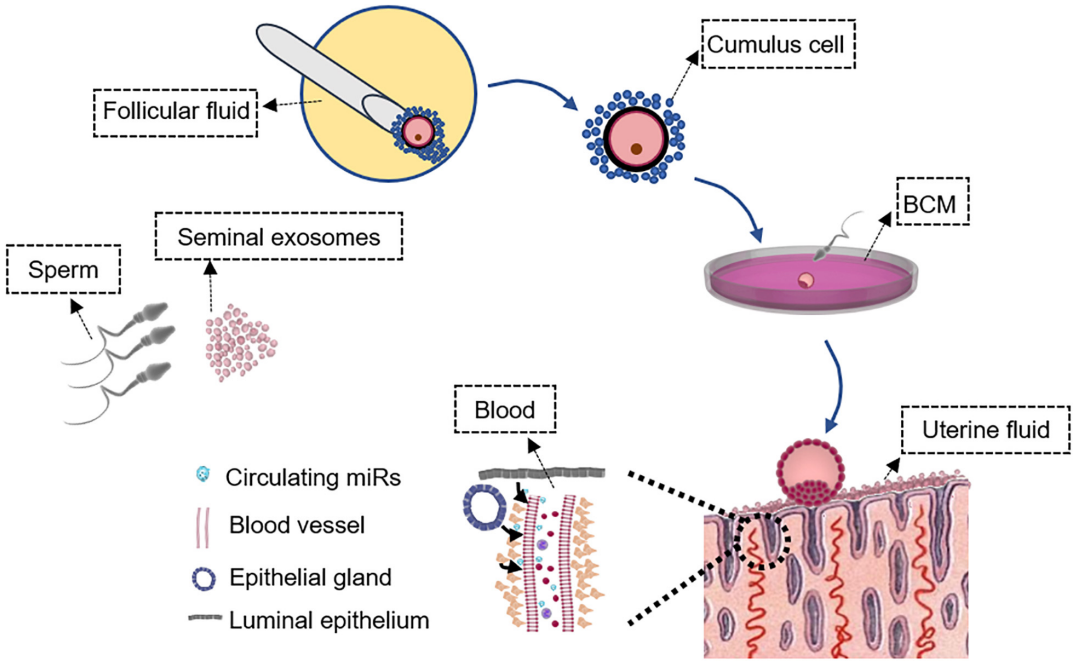

FIGURE 1 | Schematic of samples that can be collected non-invasively during *in vitro* fertilization (IVF) treatment. Characterization of the seminal exosome and sperm microRNA (miR) profiles could determine sperm quality to predict the potential of embryo development and IVF outcome. Analysis of miR expression in follicular fluid and cumulus cells may indicate oocyte and embryo quality, and implantation potential from an embryo's perspective. miR profiles in BCM also likely reflect embryo quality that may not be distinguished by morphology-based assessment. Endometrial cells release miRs in the blood and the expression levels of at least some endometrial miRs are reflected in the blood. Assessment of circulating miRs in the blood may predict endometrial receptivity and implantation outcome. Uterine fluid miR levels reflect "local" endometrial miR secretion and can be collected without compromising embryo transfer to provide information on endometrial receptivity. These samples are outlined. BCM, blastocyst culture medium.

this area with an overall aim to improve the success rate of implantation and IVF treatment.

CUMULUS CELLS AND FOLLICULAR FLUID

Cumulus cells are implicated in oocyte development and competence (Huang and Wells, 2010). In addition to interacting directly with the oocyte to facilitate maturation, cumulus cells are also bathed within the same follicular environment during oocyte maturation, thus may retain a footprint to reflect its quality and potential to form a viable embryo (**Figure 1**; Patrizio et al., 2007). It has been proven that cumulous cells are useful for non-invasive diagnosis of oocyte quality (Hamel et al., 2008; Devjak et al., 2016). Next-generation sequencing on human cumulus cells has revealed that miRs represent the major small RNA type, constituting as much as 71% of the total small RNAs (Xu et al., 2015). As a way of interaction, it has been shown that bovine cumulus cells and oocytes reciprocally affect the abundance of miRs in each cellular compartment (Abd El Naby, 2012), and these miRs readily control gene expression with extensive downstream functional implications. Gene expression studies on human cumulus cells have revealed transcripts that may be involved in oocyte maturation, implantation, and pregnancy with their regulatory miRs just beginning to be realized (Gasca et al., 2007; Hamel et al., 2008). During IVF treatment, cumulus cells are retrieved while still firmly attached to each oocyte, and as such, their collection can be sourced from individual oocytes and, thus provide an indication of the developmental potential for individual oocytes.

Follicular fluid is also collected during oocyte retrieval; however, unlike cumulus cells, follicular fluid normally collected during IVF stimulation is a pool from several oocytes, rather than a single oocyte to avoid multiple vaginal punctures. Despite this limitation, one study using pooled follicular fluid from individual patients has identified differences in miR expression between groups with different pregnancy outcomes (Scalici et al., 2016). This study screened five miRs and identified that hsa-miR-29a expression in the follicular fluid could predict pregnancy outcome with a specificity of 53.5% and has a higher discrimination power compared to prediction using embryo morphology scores (Scalici et al., 2016). Another two investigations collected follicular fluid from a single follicle and used microarrays to screen miRs that were able to predict the difference between good and bad quality blastocysts. Although hsa-miR-663b has been identified as a common miR that is inversely related to good quality blastocysts (Machtinger et al., 2017; Fu et al., 2018), the blastocyst quality discrimination method used in the two studies is based on routine morphological assessment. Therefore, the use of hsa-miR-663b as a marker of

good quality blastocysts can similarly be determined by routine morphological assessment and likely provides limited application potential to predict embryo implantation outcome. In a clinical IVF setting, generally, multiple oocytes are retrieved at one time, and it is likely that they differ in quality and potential to develop into viable blastocysts. This may limit the extensive application of follicular fluid as it cannot be used to evaluate miRs released by individual oocytes.

SEMINAL PLASMA AND SPERM

Defective sperm function is widely acknowledged as a major contributor to infertility. Under physiological conditions, the sperm acquires functional competence during their transit through the epididymis and female reproductive tract. Both biophysical and biochemical changes occur along this journey, eventually culminating in the ability of sperm to undergo an acrosome reaction, recognize the oocyte, and contribute to embryo development (Zhou et al., 2018). A number of recent studies in mice have provided evidence that uptake of miRs from the epididymal luminal environment endows the sperm with the capability to contribute to the early embryonic development and, thus, implantation upon delivery to the oocyte (Yuan et al., 2016; Conine et al., 2018, 2019). miR profile comparisons between mouse caput and cauda sperm have identified 27 miRs that are specifically enriched in cauda sperm, compared to caput sperm (Nixon et al., 2015; Sharma et al., 2018). Microinjection of cauda sperm-enriched miRs into caput-derived embryos rescue gene expression defects before implantation in mice (Conine et al., 2019). Further investigation has identified an epididymosome-dependent mechanism for the selective delivery of miRs into the sperm during their transit in the epididymis in mice (Reilly et al., 2016; Trigg et al., 2019; Zhou et al., 2019). In humans, differences in miR expression profiles have been recorded in both seminal plasma and sperm relative to different embryo qualities and pregnancy outcomes (Mokánszki et al., 2019; Abu-Halima et al., 2020; Xu et al., 2020). miR sequencing analysis on sperm samples grouped according to different embryo qualities has identified higher expression levels of hsa-miR-191 in the sperm group with better embryo developmental outcome (Xu et al., 2020). hsa-miR-19b-3p has a lower expression in sperm that is associated with a successful pregnancy outcome (Abu-Halima et al., 2020). Another recent study selected 11 spermatogenesis-related miRs and revealed that hsa-let-7a, hsa-miR-7-1-3p, hsa-miR-141, hsa-miR-200a, and hsa-miR-429 were significantly elevated, while hsa-miR-15b, hsa-miR-34b, and hsa-miR-122 were significantly downregulated in both seminal plasma and sperm of infertile male patients with impaired sperm production, compared to males with normal fertility (Mokánszki et al., 2019). Seminal plasma has been identified with an enriched population of epididymosome-like vesicles, namely, seminal exosomes (Vojtech et al., 2014). A limitation of using seminal exosomes is that they represent a mixed population of extracellular vesicles originating not only from the epididymis but also from the prostate and seminal vesicles (Rolland et al., 2013), Whether miR profiles in these vesicles correlate with sperm quality requires investigation. Nevertheless, seminal exosomes have been implicated in the transfer of cargo to sperm, which promotes their motility, ability to capacitate, and complete acrosomal exocytosis, therefore, affecting sperm quality (Tompkins et al., 2015). In addition, exosomes isolated from seminal plasma can modulate the immune response and gene expression changes in the female reproductive tract (Robertson and Sharkey, 2016; Bai et al., 2018), which eventually facilitate implantation and pregnancy in humans. Such functions are at least mediated via seminal exosome-carried miRs (Machtinger et al., 2016), and like epididymosomes, seminal exosomes carry distinctive profiles of miRs (Vojtech et al., 2014). Improved characterization of the seminal plasma and sperm miR profiles could not only be beneficial in terms of uncovering the causative basis of male gamete dysfunction but also for the provision of urgently needed biomarkers of sperm quality to reliably predict the outcome of IVF treatments.

SPENT BLASTOCYST CULTURE MEDIUM

In an IVF setting, a fertilized oocyte is generally cultured *in vitro* for up to 5–6 days to the blastocyst stage before transfer. Spent culture media can be collected during media change without affecting embryo quality. It has been demonstrated that over 96% of miRs present in the spent culture media originate from the trophectoderm and can be consistently detected after blastulation under IVF culture conditions (Capalbo et al., 2016). It is tempting to speculate that blastocyst-secreted miRs participate in the regulation of trophectoderm–endometrial luminal epithelial interactions therefore implantation. In keeping with this notion, it has been identified that embryos with different implantation outcomes (implanted versus non-implanted) secrete different profiles of miR into the culture medium (Cuman et al., 2015; Borges et al., 2016; Capalbo et al., 2016). Increased expression of hsa-miR-142-3p and decreased expression of hsa-miR-20a and hsa-miR-30c have been identified in non-implanted blastocyst culture medium (BCM), compared to implanted BCM (**Table 1**; Borges et al., 2016; Capalbo et al., 2016). Further, microarray screens have identified a list of miRs exclusively detected in either implanted or non-implanted BCM (**Table 1**; Cuman et al., 2015; Capalbo et al., 2016). miR profiles in the BCM also likely reflect embryo quality and overall IVF outcome, as summarized in **Table 1** (McCallie et al., 2010; Rosenbluth et al., 2014; Abu-Halima et al., 2020).

A previous study has proposed that while the pre-implantation embryo is in the uterine cavity, it packages regulatory miRs into extracellular vesicles (Ashary et al., 2018). They further propose that the packaged miRs are taken up by the endometrial luminal epithelial cells and alter their function to prepare for implantation. Incubation of primary human endometrial epithelial cells (HEECs) with BCM collected from embryos that were implanted increases their adhesive capacity to trophoblast cell line-formed spheroids (Cuman et al., 2013). Other notable examples include hsa-miR-661, which is exclusively secreted by blastocysts that fail to implant (Cuman et al., 2015).

TABLE 1 | Identified microRNAs (miRs) in blastocyst culture medium (BCM) with diagnostic potential.

Total number of miRs examined	miR expression	References
12 miRs	BCM from polycystic ovaries: Hsa-let-7a ↓, hsa-miR-24 ↓, hsa-miR-92 ↓, hsa-miR-93 ↓, hsa-miR-19a ↓, hsa-miR-19b ↓	McCallie et al., 2010
377 miRs	Non-implanted BCM: Hsa-miR-20a ↓, Hsa-miR-30c ↓	Capalbo et al., 2016
	Only detected in implanted BCM: Hsa-miR-220, hsa-miR-146b-3p, hsa-miR-512-3p, hsa-miR-34c, hsa-miR-375	
754 miRs	Failed IVF: Hsa-miR-191 ↑, hsa-miR-372 ↑, hsa-miR-645 ↑	Rosenbluth et al., 2014
7 miRs	Non-implanted BCM: Hsa-miR-142-3p ↑	Borges et al., 2016
784 miRs	Non-implanted group exclusively: Hsa-miR-374b-3p, hsa-miR-518c-3p, hsa-miR-126-3p, hsa-miR-361-5p,	Cuman et al., 2015
	hsa-miR-29b-2-5p, hsa-miR-516b-5p, hsa-miR-371a-5p, hsa-miR-372, hsa-miR-518a-3p, hsa-miR-149-5p, hsa-miR-571,	
	hsa-miR-943, hsa-miR-937-3p, hsa-miR-761, hsa-miR-106b-3p, hsa-miR-182-3p, hsa-miR-624, hsa-miR-661-5p,	
	hsa-miR-515-5p, hsa-let-7b-3p, hsa-miR-577, hsa-miR-1912	
	Implanted group exclusively: Hsa-miR-23a-3p, hsa-miR-570-3p, hsa-miR-485-3p, hsa-miR-572, hsa-miR-26b-5p,	
	hsa-miR-150-5p, hsa-miR-744-5p, hsa-miR-874, hsa-miR-24-2-5p, hsa-miR-300, hsa-miR-619, hsa-miR-208a,	
	hsa-miR-612, hsa-miR-26b-3p, hsa-miR-632, hsa-miR-362-3p, hsa-miR-543, hsa-miR-380-5p, hsa-miR-638	
372 miRs	High quality embryo: Hsa-miR-320a ↑, hsa-miR-15a-5p ↑, hsa-miR-21-5p ↓, hsa-miR-29a-3p ↓	Abu-Halima et al., 2020
	Negative pregnancy: Hsa-let-7a-5p ↑, hsa-miR-19b-3p ↓	

Secreted hsa-miR-661 from non-implanted BCM is taken up by HEECs and reduces their adhesion to trophoblast cell-formed spheroids (Cuman et al., 2015). A recent study also demonstrates that incubation of HEECs with BCM from embryos that implanted, compared to embryos that did not implant during IVF, leads to a substantial change in the expression of long non-coding RNAs in the HEECs (Takamura et al., 2019). PTENP1 is one of the most decreased long non-coding RNAs in HEECs after being treated with BCM from embryos that fail to implant (Takamura et al., 2019). Functionally, knockdown of PTENP1 impairs HEEC adhesion via a miR-dependent mechanism to downregulate gene targets essential for receptivity (Takamura et al., 2019).

The implanted and non-implanted embryos from which BCM was collected had an indistinguishable morphology based on currently available assessment of embryo quality. Thus, miRs in the BCM may serve as promising non-invasive biomarkers to improve the diagnostic accuracy of embryo quality and implantation potential. An obvious challenge to achieve this is to determine which cohorts of miRs are present in BCM samples that correlate with implantation outcome, in particular, regardless of embryo culture conditions. Although some miRs such as hsa-miR-19b-3p and hsa-miR-372 have been identified in at least two independent studies (**Table 1**), the comparison of secreted miRs in BCM with different implantation outcomes has demonstrated a generally inconsistent result among different studies (McCallie et al., 2010; Rosenbluth et al., 2014; Cuman et al., 2015; Borges et al., 2016; Capalbo et al., 2016; Abu-Halima et al., 2020). Contributing factors to this inconsistency include diverse embryo culture conditions in different IVF clinics, unstandardized protocols, manual effects on RNA isolation, and miR detection (Belandres et al., 2019). In addition, an obvious confounder of associating miRs in BCM with failed implantation outcome is the potential effects of the endometrium. A failed implantation group from which BCM was collected could be due to poor embryo quality, dysregulated endometrium, or altered receptivity window. The communication between an embryo and endometrium remains a "black box," and it is perhaps notable that not all secreted miRs are taken up by endometrial luminal epithelial cells to regulate implantation. For future diagnostic purposes, it is necessary to identify which miRs are taken up by endometrium and their actions on the endometrium. A panel of miRs will likely to be included, with the functional consequence of each individual miR on implantation being confirmed in ideally both humans (*in vitro*) and preclinical animal models (*in vivo*). Detailed functional studies have only covered a small proportion of miRs identified so far (**Table 2**; Chu et al., 2015; Cuman et al., 2015; Kang et al., 2015; Kottawatta et al., 2015; Vilella et al., 2015; Zhang et al., 2015; Cai et al., 2016; Chen et al., 2016; Zheng et al., 2017; Sirohi et al., 2018; Winship et al., 2018; Balaguer et al., 2019; Griffiths et al., 2019; Takamura et al., 2019).

BLOOD

MicroRNAs are also readily secreted into the blood. Circulating miRs are packaged in membrane-bound vesicles, attached to high-density lipoproteins or bound to RNA-binding proteins, which endow them with striking stability in the blood (Schwarzenbach et al., 2014). The human endometrium features a rich blood supply with the responsibility to

TABLE 2 | miRs that regulate embryo implantation.

miR	Phenotype	Target (s)	Affect implantation in animal model	References
Hsa-miR-200c	Overexpression of miR-200c in RL95-2 and Ishikawa cells impair receptive ability *in vitro*	FUT4↓	Yes (mouse)	Zheng et al., 2017
Hsa-miR-661	Secreted by non-implanted embryo and transferred to HEECs to affect their adhesive capacity *in vitro*	PVRL1↓	Not available	Cuman et al., 2015
	Overexpression of miR-661 in HEECs *in vitro* impairs adhesion	MDM2↓	Not available	Winship et al., 2018
Hsa-miR-181a	Inhibition of miR-181a compromises human endometrial stromal cell decidualization *in vitro*	KLF12↓	Yes (mouse)	Chu et al., 2015; Zhang et al., 2015
Hsa-miR-212	hCG stimulates miR-212 expression in Ishikawa cells to favor spheroid adhesion *in vitro*	OLFM1↓, CTBP1↓	Not available	Kottawatta et al., 2015
Hsa-miR-145	Overexpression of miR-145 in Ishikawa cells affects mouse embryo attachment *in vitro*	IGF1R↓	Not available	Kang et al., 2015
Hsa-miR-30d	Human endometrial secreted miR-30d is taken up by mouse pre-implantation embryo and increases embryo adhesion *in vitro*	*Itgb3*↑, *Itga7*↑, *Cdh5*↑	Yes (Mouse)	Vilella et al., 2015; Balaguer et al., 2019
	Overexpression of miR-30d in Ishikawa cells facilitates adhesion *in vitro*	*SNAI1*↓	Yes (Mouse)	Cai et al., 2016; Balaguer et al., 2019
Hsa-miR-125b	Overexpression of miR-125b in HEECs inhibits cell migration and invasion *in vitro*	MMP26↓	Yes (Mouse)	Chen et al., 2016
Hsa-miR-29c	Overexpression of miR-29c in HEECs impairs adhesion *in vitro*	COL4A1↓	Not available	Griffiths et al., 2019
Hsa-miR-590-3p	Overexpression of miR-590-3p in HEECs *in vitro* impairs adhesion	N/A	Not available	Takamura et al., 2019
Hsa-miR-140	Overexpression of miR-140 in RL95-2 endometrial epithelial cells impairs adhesion and spheroid outgrowth *in vitro*	N/A	Yes (Rat)	Sirohi et al., 2018

provide an optimal environment to promote receptivity and implantation (Farrer-Brown et al., 1970). Endometrial cells may secrete/transport a number of miRs to the tissue site of action by way of the blood, and studies suggest that endometrial expression levels of at least some miRs are reflected in the blood (Kresowik et al., 2014; Di Pietro et al., 2018). Circulating miRs in the blood may be able to predict endometrial receptivity and implantation. A previous study used whole blood and paired mid-secretory phase endometrial tissue to determine whether circulating miRs could distinguish fertile from recurrent implantation failure patients (Rekker et al., 2018). miR-30a-5p was identified as differentially expressed in whole blood between the two groups; however, this difference was not reflected in the paired endometrial tissue (Rekker et al., 2018). One possible explanation is that blood cells express miRs (Jickling et al., 2014), which may mask endometrial tissue-secreted miRs. Recent work using paired serum and mid-secretory phase endometrium investigated five miRs and identified a positive correlation of hsa-miR-31 expression levels between serum and endometrial tissue (Kresowik et al., 2014). Alternatively, extracellular miR expression levels do not necessarily reflect cellular expression levels. Whether miR biomarkers have critical functions in endometrial receptivity also needs to be determined experimentally, as differentially expressed circulating miRs between women with normal fertility and infertility may not all have functional relevance in receptivity or implantation. Functional studies of the identified circulating and cellular miRs in receptivity and implantation models could provide evidence to support their potential application as biomarkers and treatment targets. For example, hsa-miR-200c expression is increased in the serum of infertility and abortion patients, compared to healthy women (Zheng et al., 2017). Functional analysis using both human endometrial cell lines and a mouse model demonstrates that hsa-miR-200c overexpression impairs endometrial cell receptivity in both species (Zheng et al., 2017).

The obvious challenge to predict implantation outcome using miRs in the blood will be to distinguish the endometrial secreted miRs from miRs secreted by other tissues. Of note, the process of embryo implantation somewhat resembles that of cancer cell metastasis. Both processes share some of the cellular mechanisms in cell adhesion, invasion, and angiogenesis (Murray and Lessey, 1999). miRs such as hsa-miR-29c (Griffiths et al., 2019) and hsa-miR-125b (Chen et al., 2016) that are dysregulated in the endometrium from infertile women are also associated with gastric and endometrial cancers (Shang et al., 2012; Wang et al., 2019). Cancer cells releasing miRs into the blood may confound the detection of miRs secreted by the endometrium. In this regard, an important feature of the endometrium is that it regenerates itself at each menstrual cycle. The endometrium is only receptive to an implanting embryo within a very short window in the mid-secretory phase (Ashary et al., 2018). Such a functional switch is mediated by coordinated changes of miR expression (Vilella et al., 2015). These phase-dependent changes, in turn, may endow endometrial-secreted miRs with unique cycle-dependent expression fingerprints that can be used to distinguish from the background of other potential

tissue-secreted miRs. This theory is evidenced by a previous study comparing miR expression between the proliferative phase and mid-secretory phase in paired serum and endometrial tissue from fertile women. hsa-miR-31 has been identified as a potential biomarker that is elevated in both serum and endometrium in the mid-secretory phase, compared to the proliferative phase (Kresowik et al., 2014). It is also essential to investigate appropriate controls from different pathologies as comparative groups. The predictive application of blood miRs on implantation will likely be based on the multiple measurements of miR expression at different phases within a menstrual cycle.

Another challenge of using miR levels in the blood for biomarker purposes has been identified in cancer diagnosis. A previous study selected 79 solid cancer-circulating miR biomarkers and determined their expression levels in blood cells. Forty-six of the 79 miRs were highly expressed in the blood cells (Pritchard et al., 2012). Plasma isolated from the blood with different blood cell counts or hemolysis impacted the expression levels of select miRs (Pritchard et al., 2012). Inconsistency has also been observed between plasma and serum levels of miR between pregnant and non-pregnant patient groups after embryo transfer (Yang et al., 2018). To improve the accuracy of prediction, a panel of miRs is required, as has been proposed for cancer diagnosis (Madhavan et al., 2013). To achieve this, an investigation of miR levels from large cohorts of women with different etiologies of infertility and other pathologies is required for their potential use as biomarkers. We have previously identified a dysregulation of miR-processing machinery in the endometrium of a cohort of infertile patients, which would have an overall impact on miR secretion due to compromised miR processing within the cell (Loke et al., 2019). The miR secretion in this cohort may be different compared to other infertile cohorts caused by different etiologies. Identifying which miRs are responsible for ensuring endometrial receptivity is also required to determine whether the biomarkers may also be useful as treatment targets of dysregulated endometrial receptivity.

UTERINE FLUID

The uterine fluid is secreted by the human endometrium as an indirect approach to communicate with an embryo for the preparation of implantation. Compared to other body fluids, uterine fluid is a more "local" secretion and, thus, may provide direct information when assessing biomarkers for implantation. Detailed compositional analysis has revealed that uterine fluid contains miRs and proteins with changed profiles across the menstrual cycle (Scotchie et al., 2009; Ng et al., 2013). Functional analysis has proven that endometrial cells secreted miRs, such as hsa-miR-30d, that are taken up by the embryo via the trophectoderm and regulate adhesion *in vitro* (Vilella et al., 2015). Further investigation demonstrates that secreted miRs in the uterine fluid target an extensive of implantation-related genes (Ng et al., 2013). Of note, the miRs in the uterine fluid can be sourced from different endometrial cells and the blood. This can be determined via *in situ* hybridization on endometrial sections, like what has been done for protein via immunostaining (Hannan et al., 2010). Uterine fluid can be collected via either aspiration or lavage without compromising implantation (Hannan et al., 2012). To the best of our knowledge, however, most currently available studies on uterine fluid have focused on comparing the proteins between fertile and infertile patients (Hannan et al., 2010; Salamonsen et al., 2013). There are presently limited studies investigating the potential of using miRs in the uterine fluid as a diagnostic approach for implantation.

OVERALL CHALLENGES OF USING SECRETED MIRS TO PREDICT IMPLANTATION

Although miRs are highly desirable as non-invasive biomarkers to predict implantation, this field of research is somewhat confounded by a general inconsistency of miR expression levels across different studies. It has been identified that a number of factors including RNA isolation and detection systems can contribute to this inconsistency. Recently published work from one laboratory, which used different commercial kits to isolate RNA, demonstrated that the recovery of RNA was variable between the commercial kits (El-Khoury et al., 2016; Wright et al., 2020). In addition, the selection of endogenous controls to normalize the target miR expression levels directly affects the results, and such importance has been neglected by some studies. For miR normalization, an ideal endogenous control should be stably expressed in the body fluid with minimal biological variation, and the expression should not change with different implantation outcomes. It is known that in body fluids, the expression of some cellular endogenous controls may vary between different samples bringing deviation in normalization. It is an essential first step to compare the expression variability of a number of endogenous control candidates in a given body fluid system and confirm their stability. This has not been conducted in some studies and may have contributed to the variability of miR expression. A workflow has been proposed to identify the best normalization control (Schwarzenbach et al., 2015). All these steps introducing impact factors require standardization before a solid conclusion can be drawn.

Adding to this challenge is the observation that inherent differences between women, together with different IVF protocols, may lead to differential expression patterns of miR in the human endometrium. A microarray study has identified that luteal support following controlled ovarian stimulation has a profound influence on the miR profile in the endometrium (Zhao et al., 2012). Specifically, progesterone supplementation is associated with a significant increase in miR expression in the endometrium compared to a no steroid supplementation group following controlled ovarian stimulation (Zhao et al., 2012). The findings are in accordance with a previous report identifying differential expression patterns of miR between natural and stimulated IVF cycles (Sha et al., 2011). In addition, patients receiving the same IVF treatment who have different serum progesterone levels have been identified to have different miR expression patterns in the endometrial tissue collected 6 days

after oocyte retrieval (Li et al., 2011). Microarray analysis of the endometrium identified four miRs (hsa-miR-451, hsa-miR-424, hsa-miR-125b, and hsa-miR-30b) that were decreased in the high serum progesterone group (Li et al., 2011). The effects of controlled ovarian stimulation and luteal phase support need to be considered when comparing data from different studies.

CONCLUSION

Measurement of miRs in the samples that can be collected without compromising embryo transfer in the same menstrual cycle opens new perspectives for the diagnosis of embryo implantation potential. Unfortunately, our understanding of the mechanisms of how miR dysregulation impacts implantation and how this accordingly affects miR secretion remains far from complete. Interpretation of research findings is confounded by unstandardized assessment of miRs in a given body fluid. Resolving these questions would have a major impact on biomarker development and clinical practice for reproductive clinicians and scientists. This includes optimizing the selection of embryos for transfer during IVF, improvement of implantation success rates, and the minimization of multiple pregnancies. It is likely that a combination of samples that can be collected either non-invasively or relatively non-invasively, as summarized in this review, will be useful to assess implantation potential at different stages of conceptus establishment and development. This relies on research to find miR biomarkers related to implantation regulation and the development of new technologies to improve miR detection. A few microfluidic devices have been developed recently with a larger capacity to include more miRs and reduce analysis time. Improved diagnosis of embryo implantation could have a profound effect on psychological and financial well-being on women and couples undergoing IVF treatment.

AUTHOR CONTRIBUTIONS

Both authors made substantial contributions to the conception of this review and the critical appraisal of the literature summarized herein, wrote the manuscript, and approved the final version of this article before submission.

FUNDING

This work was supported by a project grant (APP1120689) and a senior research fellowship (#550905) from the National Health and Medical Research Council (NHMRC) of Australia to ED. WZ was supported by an Early Career Researcher Grant and a Department of Obstetrics and Gynaecology Innovation Grant (The University of Melbourne).

REFERENCES

Abd El Naby, W. S. H. (2012). Expression analysis of regulatory MicroRNA in bovine cumulus oocyte complex and preimplantation embryos. *Zygote* 21, 31–51. doi: 10.1017/s0967199411000566

Abu-Halima, M., Khaizaran, Z. A., Ayesh, B. M., Fischer, U., Khaizaran, S. A., Al-Battah, F., et al. (2020). MicroRNAs in combined spent culture media and sperm are associated with embryo quality and pregnancy outcome. *Fertil. Steril.* 113, 970.e2–980.e2.

Ashary, N., Tiwari, A., and Modi, D. (2018). Embryo implantation: war in times of love. *Endocrinology* 159, 1188–1198. doi: 10.1210/en.2017-03082

Bai, R., Latifi, Z., Kusama, K., Nakamura, K., Shimada, M., and Imakawa, K. (2018). Induction of immune-related gene expression by seminal exosomes in the porcine endometrium. *Biochem. Biophys. Res. Commun.* 495, 1094–1101. doi: 10.1016/j.bbrc.2017.11.100

Balaguer, N., Moreno, I., Herrero, M., Gonzáléz-Monfort, M., Vilella, F., and Simón, C. (2019). MicroRNA-30d deficiency during preconception affects endometrial receptivity by decreasing implantation rates and impairing fetal growth. *Am. J. Obstet. Gynecol.* 221, 46.e1-46.e16.

Belandres, D., Shamonki, M., and Arrach, N. (2019). Current status of spent embryo media research for preimplantation genetic testing. *J. Assist. Reprod. Genet.* 36, 819–826. doi: 10.1007/s10815-019-01437-6

Boomsma, C., Kavelaars, A., Eijkemans, M., Lentjes, E., Fauser, B., Heijnen, C., et al. (2009). Endometrial secretion analysis identifies a cytokine profile predictive of pregnancy in IVF. *Hum. Reprod.* 24, 1427–1435. doi: 10.1093/humrep/dep011

Borges, E. Jr., Setti, A. S., Braga, D. P., Geraldo, M. V., Figueira, R. D. C. S., and Iaconelli, A. Jr. (2016). miR-142-3p as a biomarker of blastocyst implantation failure-A pilot study. *JBRA Assist. Reprod.* 20, 200–205. doi: 10.5935/1518-0557.20160039

Bushati, N., and Cohen, S. M. (2007). microRNA functions. *Annu. Rev. Cell Dev. Biol.* 23, 175–205.

Cai, J. L., Liu, L. L., Hu, Y., Jiang, X. M., Qiu, H. L., Sha, A.-G., et al. (2016). Polychlorinated biphenyls impair endometrial receptivity in vitro via regulating mir-30d expression and epithelial mesenchymal transition. *Toxicology* 365, 25–34. doi: 10.1016/j.tox.2016.07.017

Capalbo, A., Ubaldi, F. M., Cimadomo, D., Noli, L., Khalaf, Y., Farcomeni, A., et al. (2016). MicroRNAs in spent blastocyst culture medium are derived from trophectoderm cells and can be explored for human embryo reproductive competence assessment. *Fertil. Steril.* 105, 225–235. doi: 10.1016/j.fertnstert.2015.09.014

Chachamovich, J. R., Chachamovich, E., Ezer, H., Fleck, M. P., Knauth, D., and Passos, E. P. (2010). Investigating quality of life and health-related quality of life in infertility: a systematic review. *J. Psychosom. Obstet. Gynaecol.* 31, 101–110. doi: 10.3109/0167482x.2010.481337

Chen, C., Zhao, Y., Yu, Y., Li, R., and Qiao, J. (2016). MiR-125b regulates endometrial receptivity by targeting MMP26 in women undergoing IVF-ET with elevated progesterone on HCG priming day. *Sci. Rep.* 6:25302.

Chu, B., Zhong, L., Dou, S., Wang, J., Li, J., Wang, M., et al. (2015). miRNA-181 regulates embryo implantation in mice through targeting leukemia inhibitory factor. *J. Mol. Cell Biol.* 7, 12–22. doi: 10.1093/jmcb/mjv006

Conine, C. C., Sun, F., Song, L., Rivera-Pérez, J. A., and Rando, O. J. (2018). Small RNAs gained during epididymal transit of sperm are essential for embryonic development in mice. *Dev. Cell* 46, 470–480. doi: 10.1016/j.devcel.2018.06.024

Conine, C. C., Sun, F., Song, L., Rivera-Pérez, J. A., and Rando, O. J. (2019). MicroRNAs absent in caput sperm are required for normal embryonic development. *Dev. Cell* 50, 7–8. doi: 10.1016/j.devcel.2019.06.007

Craciunas, L., Gallos, I., Chu, J., Bourne, T., Quenby, S., Brosens, J. J., et al. (2019). Conventional and modern markers of endometrial receptivity: a systematic review and meta-analysis. *Hum. Reprod. Upd.* 25, 202–223. doi: 10.1093/humupd/dmy044

Cui, W. (2010). Mother or nothing: the agony of infertility. *Bull. World Health Organ.* 88, 881–882. doi: 10.2471/blt.10.011210

Cuman, C., Menkhorst, E., Rombauts, L., Holden, S., Webster, D., Bilandzic, M., et al. (2013). Preimplantation human blastocysts release factors that differentially alter human endometrial epithelial cell adhesion and gene expression relative to IVF success. *Hum. Reprod.* 28, 1161–1171. doi: 10.1093/humrep/det058

Cuman, C., Van Sinderen, M., Gantier, M. P., Rainczuk, K., Sorby, K., Rombauts, L., et al. (2015). Human blastocyst secreted microRNA regulate endometrial

epithelial cell adhesion. *eBio Med.* 2, 1528–1535. doi: 10.1016/j.ebiom.2015.09.003

Devjak, R., Papler, T. B., Verdenik, I., Tacer, K. F., and Bokal, E. V. (2016). Embryo quality predictive models based on cumulus cells gene expression. *Balkan J. Med. Genet.* 19, 5–12. doi: 10.1515/bjmg-2016-0001

Di Pietro, C., Caruso, S., Battaglia, R., Iraci Sareri, M., La Ferlita, A., Strino, F., et al. (2018). MiR-27a-3p and miR-124-3p, upregulated in endometrium and serum from women affected by Chronic Endometritis, are new potential molecular markers of endometrial receptivity. *Am. J. Reprod. Immunol.* 80:e12858. doi: 10.1111/aji.12858

Díaz-Gimeno, P., Horcajadas, J. A., Martínez-Conejero, J. A., Esteban, F. J., Alamá, P., Pellicer, A., et al. (2011). A genomic diagnostic tool for human endometrial receptivity based on the transcriptomic signature. *Fertil. Steril.* 95, 50–60. doi: 10.1016/j.fertnstert.2010.04.063

El-Khoury, V., Pierson, S., Kaoma, T., Bernardin, F., and Berchem, G. (2016). Assessing cellular and circulating miRNA recovery: the impact of the RNA isolation method and the quantity of input material. *Sci. Rep.* 6:19529.

Farrer-Brown, G., Beilby, J., and Tarbit, M. (1970). The blood supply of the uterus: 1. *Arterial vasculature. J. Obstet. Gynaecol. Br. Common.* 77, 673–681. doi: 10.1111/j.1471-0528.1970.tb03592.x

Fu, J., Qu, R. G., Zhang, Y. J., Gu, R. H., Li, X., Sun, Y. J., et al. (2018). Screening of miRNAs in human follicular fluid reveals an inverse relationship between microRNA-663b expression and blastocyst formation. *Reprod. Biomed. Online* 37, 25–32. doi: 10.1016/j.rbmo.2018.03.021

Gardner, D. K., and Balaban, B. (2016). Assessment of human embryo development using morphological criteria in an era of time-lapse, algorithms and 'OMICS': is looking good still important? *Mol. Hum. Reprod.* 22, 704–718. doi: 10.1093/molehr/gaw057

Gardner, D. K., Lane, M., Stevens, J., Schlenker, T., and Schoolcraft, W. B. (2000). Blastocyst score affects implantation and pregnancy outcome: towards a single blastocyst transfer. *Fertil. Steril.* 73, 1155–1158. doi: 10.1016/s0015-0282(00)00518-5

Gasca, S., Pellestor, F., Assou, S., Loup, V., Anahory, T., Dechaud, H., et al. (2007). Identifying new human oocyte marker genes: a microarray approach. *Reprod. Biomed. Online* 14, 175–183. doi: 10.1016/s1472-6483(10)60785-7

Giorgetti, C., Terriou, P., Auquier, P., Hans, E., Spach, J. L., Salzmann, J., et al. (1995). Implantation: embryo score to predict implantation after in-vitro fertilization: based on 957 single embryo transfers. *Hum. Reprod.* 10, 2427–2431. doi: 10.1093/oxfordjournals.humrep.a136312

Griffiths, M., Van Sinderen, M., Rainczuk, K., and Dimitriadis, E. (2019). miR-29c overexpression and COL4A1 downregulation in infertile human endometrium reduces endometrial epithelial cell adhesive capacity in vitro implying roles in receptivity. *Sci. Rep.* 9:8644.

Hamel, M., Dufort, I., Robert, C., Gravel, C., Leveille, M. C., Leader, A., et al. (2008). Identification of differentially expressed markers in human follicular cells associated with competent oocytes. *Hum. Reprod.* 23, 1118–1127. doi: 10.1093/humrep/den048

Hannan, N. J., Nie, G., Rainzcuk, A., Rombauts, L., and Salamonsen, L. A. (2012). Uterine lavage or aspirate: which view of the intrauterine environment? *Reprod. Sci.* 19, 1125–1132. doi: 10.1177/1933719112443879

Hannan, N. J., Stephens, A. N., Rainczuk, A., Hincks, C., Rombauts, L. J., and Salamonsen, L. A. (2010). 2D-DiGE analysis of the human endometrial secretome reveals differences between receptive and nonreceptive states in fertile and infertile women. *J. Proteome Res.* 9, 6256–6264. doi: 10.1021/pr1004828

Huang, Z., and Wells, D. (2010). The human oocyte and cumulus cells relationship: new insights from the cumulus cell transcriptome. *Mol. Hum. Reprod.* 16, 715–725. doi: 10.1093/molehr/gaq031

Jickling, G. C., Ander, B. P., Zhan, X., Noblett, D., Stamova, B., and Liu, D. (2014). microRNA expression in peripheral blood cells following acute ischemic stroke and their predicted gene targets. *PLoS One* 9:e99283. doi: 10.1371/journal.pone.0099283

Kang, Y. J., Lees, M., Matthews, L. C., Kimber, S. J., Forbes, K., and Aplin, J. D. (2015). miR-145 suppresses embryo–epithelial juxtacrine communication at implantation by modulating maternal IGF1R. *J. Cell Sci.* 128, 804–814. doi: 10.1242/jcs.164004

Kottawatta, K. S., So, K. H., Kodithuwakku, S. P., Ng, E. H., Yeung, W. S., and Lee, K. F. (2015). MicroRNA-212 regulates the expression of olfactomedin 1 and C-terminal binding protein 1 in human endometrial epithelial cells to enhance spheroid attachment in vitro. *Biol. Reprod.* 93:109.

Kresowik, J. D., Devor, E. J., Van Voorhis, B. J., and Leslie, K. K. (2014). MicroRNA-31 is significantly elevated in both human endometrium and serum during the window of implantation: a potential biomarker for optimum receptivity. *Biol. Reprod.* 91:17.

Kropp, J., Salih, S. M., and Khatib, H. (2014). Expression of microRNAs in bovine and human pre-implantation embryo culture media. *Front Genet* 5:91. doi: 10.3389/fgene.2014.00091

Li, R., Qiao, J., Wang, L., Li, L., Zhen, X., Liu, P., et al. (2011). MicroRNA array and microarray evaluation of endometrial receptivity in patients with high serum progesterone levels on the day of hCG administration. *Reprod. Biol. Endocrinol.* 9:29. doi: 10.1186/1477-7827-9-29

Li, T., Greenblatt, E., and Chan, C. (2019). Isolation and profiling of extracellular vesicles in uterine fluid to determine novel markers of endometrial receptivity. *Fertil. Steril.* 112:e314. doi: 10.1016/j.fertnstert.2019.07.911

Loke, H., Rainczuk, K., and Dimitriadis, E. (2019). MicroRNA biogenesis machinery is dysregulated in the endometrium of infertile women suggesting a role in receptivity and infertility. *J. Histochem. Cytochem.* 67, 589–599. doi: 10.1369/0022155419854064

Machtinger, R., Laurent, L. C., and Baccarelli, A. A. (2016). Extracellular vesicles: roles in gamete maturation, fertilization and embryo implantation. *Hum. Reprod. Upd.* 22, 182–193.

Machtinger, R., Rodosthenous, R. S., Adir, M., Mansour, A., Racowsky, C., Baccarelli, A. A., et al. (2017). Extracellular microRNAs in follicular fluid and their potential association with oocyte fertilization and embryo quality: an exploratory study. *J. Assist. Reprod. Genet.* 34, 525–533. doi: 10.1007/s10815-017-0876-8

Madhavan, D., Cuk, K., Burwinkel, B., and Yang, R. (2013). Cancer diagnosis and prognosis decoded by blood-based circulating microRNA signatures. *Front. Genet.* 4:116. doi: 10.3389/fgene.2013.00116

McCallie, B., Schoolcraft, W. B., and Katz-Jaffe, M. G. (2010). Aberration of blastocyst microRNA expression is associated with human infertility. *Fertil. Steril.* 93, 2374–2382. doi: 10.1016/j.fertnstert.2009.01.069

Mokánszki, A., Molnár, Z., Varga Tóthné, E., Bodnár, B., Jakab, A., Bálint, B. L., et al. (2019). Altered microRNAs expression levels of sperm and seminal plasma in patients with infertile ejaculates compared with normozoospermic males. *Hum. Fertil.* [Epub ahead of print].

Murray, M. J., and Lessey, B. A. (1999). *Embryo Implantation, and Tumor Metastasis: Common Pathways of Invasion, and Angiogenesis, Semin Reprod Endocrinol.* New York, NY: Thieme Medical Publishers, 275–290.

Ng, Y. H., Rome, S., Jalabert, A., Forterre, A., Singh, H., Hincks, C. L., et al. (2013). Endometrial exosomes/microvesicles in the uterine microenvironment: a new paradigm for embryo-endometrial cross talk at implantation. *PLoS One* 8:e58502. doi: 10.1371/journal.pone.0058502

Nixon, B., Stanger, S. J., Mihalas, B. P., Reilly, J. N., Anderson, A. L., Tyagi, S., et al. (2015). The microRNA signature of mouse spermatozoa is substantially modified during epididymal maturation. *Biol. Reprod.* 93:91.

Norwitz, E. R., Schust, D. J., and Fisher, S. J. (2001). Implantation and the survival of early pregnancy. *N. Engl. J. Med.* 345, 1400–1408. doi: 10.1056/nejmra000763

Patrizio, P., Fragouli, E., Bianchi, V., Borini, A., and Wells, D. (2007). Molecular methods for selection of the ideal oocyte. *Reprod. Biomed. Online* 15, 346–353. doi: 10.1016/s1472-6483(10)60349-5

Paul, A. B., Sadek, S. T., and Mahesan, A. M. (2019). The role of microRNAs in human embryo implantation: a review. *J. Assist. Reprod. Genet.* 36, 179–187. doi: 10.1007/s10815-018-1326-y

Pritchard, C. C., Kroh, E., Wood, B., Arroyo, J. D., Dougherty, K. J., Miyaji, M. M., et al. (2012). Blood cell origin of circulating microRNAs: a cautionary note for cancer biomarker studies. *Cancer Prev. Res.* 5, 492–497. doi: 10.1158/1940-6207.capr-11-0370

Ralt, D., Goldenberg, M., Fetterolf, P., Thompson, D., Dor, J., Mashiach, S., et al. (1991). Sperm attraction to a follicular factor (s) correlates with human egg fertilizability. *Proc. Natl. Acad. Sci. U.S.A.* 88, 2840–2844. doi: 10.1073/pnas.88.7.2840

Reilly, J. N., McLaughlin, E. A., Stanger, S. J., Anderson, A. L., Hutcheon, K., Church, K., et al. (2016). Characterisation of mouse epididymosomes reveals a complex profile of microRNAs and a potential mechanism for modification of the sperm epigenome. *Sci. Rep.* 6, 1–15.

Rekker, K., Altmäe, S., Suhorutshenko, M., Peters, M., Martinez-Blanch, J. F., Codoñer, F. M., et al. (2018). A two-cohort RNA-seq study reveals changes in endometrial and blood miRNome in fertile and infertile women. *Genes* 9:574. doi: 10.3390/genes9120574

Robertson, S. A., and Sharkey, D. J. (2016). Seminal fluid and fertility in women. *Fertil. Steril.* 106, 511–519. doi: 10.1016/j.fertnstert.2016.07.1101

Rolland, A. D., Lavigne, R., Dauly, C., Calvel, P., Kervarrec, C., Freour, T., et al. (2013). Identification of genital tract markers in the human seminal plasma using an integrative genomics approach. *Hum. Reprod.* 28, 199–209. doi: 10.1093/humrep/des360

Rosenbluth, E. M., Shelton, D. N., Wells, L. M., Sparks, A. E., and Van Voorhis, B. J. (2014). Human embryos secrete microRNAs into culture media—a potential biomarker for implantation. *Fertil. Steril.* 101, 1493–1500. doi: 10.1016/j.fertnstert.2014.01.058

Salamonsen, L. A., Edgell, T., Rombauts, L. J., Stephens, A. N., Robertson, D. M., Rainczuk, A., et al. (2013). Proteomics of the human endometrium and uterine fluid: a pathway to biomarker discovery. *Fertil. Steril.* 99, 1086–1092. doi: 10.1016/j.fertnstert.2012.09.013

Scalici, E., Traver, S., Mullet, T., Molinari, N., Ferrieres, A., Brunet, C., et al. (2016). Circulating microRNAs in follicular fluid, powerful tools to explore in vitro fertilization process. *Sci. Rep.* 6:24976.

Schwarzenbach, H., Da Silva, A. M., Calin, G., and Pantel, K. (2015). Data normalization strategies for microRNA quantification. *Clin. Chem.* 61, 1333–1342. doi: 10.1373/clinchem.2015.239459

Schwarzenbach, H., Nishida, N., Calin, G. A., and Pantel, K. (2014). Clinical relevance of circulating cell-free microRNAs in cancer. *Nat. Rev. Clin. Oncol.* 11, 145–156. doi: 10.1038/nrclinonc.2014.5

Scotchie, J. G., Fritz, M. A., Mocanu, M., Lessey, B. A., and Young, S. L. (2009). Proteomic analysis of the luteal endometrial secretome. *Reprod. Sci.* 16, 883–893. doi: 10.1177/1933719109337165

Sha, A. G., Liu, J. L., Jiang, X. M., Ren, J. Z., Ma, C. H., Lei, W., et al. (2011). Genome-wide identification of micro-ribonucleic acids associated with human endometrial receptivity in natural and stimulated cycles by deep sequencing. *Fertil. Steril.* 96, 150–155. doi: 10.1016/j.fertnstert.2011.04.072

Shang, C., Lu, Y. M., and Meng, L. R. (2012). MicroRNA-125b down-regulation mediates endometrial cancer invasion by targeting ERBB2. *Med. Sci. Monit.* 18, BR149–BR155.

Sharma, U., Conine, C. C., Shea, J. M., Boskovic, A., Derr, A. G., Bing, X. Y., et al. (2016). Biogenesis and function of tRNA fragments during sperm maturation and fertilization in mammals. *Science* 351, 391–396. doi: 10.1126/science.aad6780

Sharma, U., Sun, F., Conine, C. C., Reichholf, B., Kukreja, S., Herzog, V. A., et al. (2018). Small RNAs are trafficked from the epididymis to developing mammalian sperm. *Dev. Cell* 46, 481–494. doi: 10.1016/j.devcel.2018.06.023

Sirohi, V. K., Gupta, K., Kumar, R., Shukla, V., and Dwivedi, A. (2018). Selective estrogen receptor modulator Ormeloxifene suppresses embryo implantation via inducing miR-140 and targeting insulin-like growth factor 1 receptor in rat uterus. *J. Steroid Biochem. Mol. Biol.* 178, 272–282. doi: 10.1016/j.jsbmb.2018.01.006

Takamura, M., Zhou, W., Rombauts, L., and Dimitriadis, E. (2019). The long noncoding RNA PTENP1 regulates human endometrial epithelial adhesive capacity in vitro: implications in infertility. *Biol. Reprod.* 102, 53–62. doi: 10.1093/biolre/ioz173

Tompkins, A. J., Chatterjee, D., Maddox, M., Wang, J., Arciero, E., Camussi, G., et al. (2015). The emergence of extracellular vesicles in urology: fertility, cancer, biomarkers and targeted pharmacotherapy. *J. Extracell. Vesicles* 4:23815. doi: 10.3402/jev.v4.23815

Trigg, N. A., Eamens, A. L., and Nixon, B. (2019). The contribution of epididymosomes to the sperm small RNA profile. *Reproduction* 157, R209–R223.

Vilella, F., Moreno-Moya, J. M., Balaguer, N., Grasso, A., Herrero, M., Martínez, S., et al. (2015). Hsa-miR-30d, secreted by the human endometrium, is taken up by the pre-implantation embryo and might modify its transcriptome. *Development* 142, 3210–3221. doi: 10.1242/dev.124289

Vojtech, L., Woo, S., Hughes, S., Levy, C., Ballweber, L., Sauteraud, R. P., et al. (2014). Exosomes in human semen carry a distinctive repertoire of small non-coding RNAs with potential regulatory functions. *Nucleic Acids Res.* 42, 7290–7304. doi: 10.1093/nar/gku347

Wang, L., Yu, T., Li, W., Li, M., Zuo, Q., Zou, Q., et al. (2019). The miR-29c-KIAA1199 axis regulates gastric cancer migration by binding with WBP11 and PTP4A3. *Oncogene* 38, 3134–3150. doi: 10.1038/s41388-018-0642-0

Wilcox, A. J., Weinberg, C. R., O'Connor, J. F., Baird, D. D., Schlatterer, J. P., Canfield, R. E., et al. (1988). Incidence of early loss of pregnancy. *N. Engl. J. Med.* 319, 189–194.

Winship, A., Ton, A., Van Sinderen, M., Menkhorst, E., Rainczuk, K., Griffiths, M., et al. (2018). Mouse double minute homologue 2 (MDM2) downregulation by miR-661 impairs human endometrial epithelial cell adhesive capacity. *Reprod. Fertil. Dev.* 30, 477–486. doi: 10.1071/rd17095

Wright, K., de Silva, K., Purdie, A. C., and Plain, K. M. (2020). Comparison of methods for miRNA isolation and quantification from ovine plasma. *Sci. Rep.* 10:825.

Xu, B., Zhang, Y. W., Tong, X. H., and Liu, Y. S. (2015). Characterization of microRNA profile in human cumulus granulosa cells: identification of microRNAs that regulate Notch signaling and are associated with PCOS. *Mol. Cell. Endocrinol.* 404, 26–36. doi: 10.1016/j.mce.2015.01.030

Xu, H., Wang, X., Wang, Z., Li, J., Xu, Z., Miao, M., et al. (2020). MicroRNA expression profile analysis in sperm reveals hsa-mir-191 as an auspicious omen of in vitro fertilization. *BMC Genomics* 21:165. doi: 10.1186/s12864-020-6570-8

Yang, Q., Gu, W. W., Gu, Y., Yan, N. N., Mao, Y. Y., Zhen, X. X., et al. (2018). Association of the peripheral blood levels of circulating microRNAs with both recurrent miscarriage and the outcomes of embryo transfer in an in vitro fertilization process. *J. Transl. Med.* 16:186.

Yuan, S., Schuster, A., Tang, C., Yu, T., Ortogero, N., Bao, J., et al. (2016). Sperm-borne miRNAs and endo-siRNAs are important for fertilization and preimplantation embryonic development. *Development* 143, 635–647. doi: 10.1242/dev.131755

Zhang, Q., Zhang, H., Jiang, Y., Xue, B., Diao, Z., Ding, L., et al. (2015). MicroRNA-181a is involved in the regulation of human endometrial stromal cell decidualization by inhibiting Krüppel-like factor 12. *Reprod. Biol. Endocrinol.* 13:23.

Zhao, Y., Zacur, H., Cheadle, C., Ning, N., Fan, J., and Vlahos, N. F. (2012). Effect of luteal-phase support on endometrial microRNA expression following controlled ovarian stimulation. *Reprod. Biol. Endocrinol.* 10:72. doi: 10.1186/1477-7827-10-72

Zheng, Q., Zhang, D., Yang, Y. U., Cui, X., Sun, J., Liang, C., et al. (2017). MicroRNA-200c impairs uterine receptivity formation by targeting FUT4 and α 1, 3-fucosylation. *Cell Death. Differ.* 24, 2161–2172. doi: 10.1038/cdd.2017.136

Zhou, W., De Iuliis, G. N., Dun, M. D., and Nixon, B. (2018). Characteristics of the epididymal luminal environment responsible for sperm maturation and storage. *Front. Endocrinol.* 9:59. doi: 10.3389/fendo.2018.00059

Zhou, W., Stanger, S. J., Anderson, A. L., Bernstein, I. R., De Iuliis, G. N., McCluskey, A., et al. (2019). Mechanisms of tethering and cargo transfer during epididymosome-sperm interactions. *BMC Biol.* 17:35. doi: 10.1186/s12915-019-0653-5

Conflict of Interest: The authors declare that the research was conducted in the absence of any commercial or financial relationships that could be construed as a potential conflict of interest.

frontiers in Cell and Developmental Biology

REVIEW
published: 28 January 2021
doi: 10.3389/fcell.2021.628339

Functional Non-coding RNA During Embryonic Myogenesis and Postnatal Muscle Development and Disease

Hongmei Luo[1,2†], *Wei Lv*[1,2†], *Qian Tong*[1,2], *Jianjun Jin*[1,2], *Zaiyan Xu*[1,3*] and *Bo Zuo*[1,2,4*]

[1] Key Laboratory of Swine Genetics and Breeding of the Ministry of Agriculture and Rural Affairs, Huazhong Agricultural University, Wuhan, China, [2] Key Laboratory of Agriculture Animal Genetics, Breeding and Reproduction of the Ministry of Education, Huazhong Agricultural University, Wuhan, China, [3] Department of Basic Veterinary Medicine, College of Veterinary Medicine, Huazhong Agricultural University, Wuhan, China, [4] The Cooperative Innovation Center for Sustainable Pig Production, Wuhan, China

OPEN ACCESS

Edited by:
Tomokazu Tomo Fukuda, Iwate University, Japan

Reviewed by:
XiuKai Cao, Yangzhou University, China
Constantinos Demonacos, The University of Manchester, United Kingdom

***Correspondence:**
Zaiyan Xu
xuzaiyan@mail.hzau.edu.cn
Bo Zuo
zuobo@mail.hzau.edu.cn

[†] *These authors have contributed equally to this work*

Specialty section:
This article was submitted to Cell Growth and Division, a section of the journal Frontiers in Cell and Developmental Biology

Received: *11 November 2020*
Accepted: *06 January 2021*
Published: *28 January 2021*

Citation:
Luo H, Lv W, Tong Q, Jin J, Xu Z and Zuo B (2021) Functional Non-coding RNA During Embryonic Myogenesis and Postnatal Muscle Development and Disease. Front. Cell Dev. Biol. 9:628339. doi: 10.3389/fcell.2021.628339

Skeletal muscle is a highly heterogeneous tissue that plays a crucial role in mammalian metabolism and motion maintenance. Myogenesis is a complex biological process that includes embryonic and postnatal development, which is regulated by specific signaling pathways and transcription factors. Various non-coding RNAs (ncRNAs) account for the majority of total RNA in cells and have an important regulatory role in myogenesis. In this review, we introduced the research progress in miRNAs, circRNAs, and lncRNAs related to embryonic and postnatal muscle development. We mainly focused on ncRNAs that regulate myoblast proliferation, differentiation, and postnatal muscle development through multiple mechanisms. Finally, challenges and future perspectives related to the identification and verification of functional ncRNAs are discussed. The identification and elucidation of ncRNAs related to myogenesis will enrich the myogenic regulatory network, and the effective application of ncRNAs will enhance the function of skeletal muscle.

Keywords: myogenesis, muscle disease, miRNAs, lncRNAs, circRNAs

INTRODUCTION

Skeletal muscle is a highly heterogeneous tissue that contains myofibers, the basement membrane, muscle satellite cells, immunocytes, and nerves, and plays a crucial role in locomotion, metabolism, and homeostasis. In mice and humans, this tissue represents ∼30–40% of the total body mass (Zierath and Hawley, 2004). The molecular regulation of the skeletal muscle during embryonic and postnatal development is complex. Many aspects of adult myogenesis resemble embryonic morphogenetic episodes (Bentzinger et al., 2012). In vertebrate embryos, the skeletal muscles of the trunk and limbs are derived from the paraxial mesoderm and first form a certain number of somites (Bentzinger et al., 2012). Somites undergo morphogenetic changes and differentiate into sclerotome and dermomyotome, and muscle progenitor cells (MPCs) delaminate from the surrounding of the dermomyotome under the regulation of the Shh, Notch, and Wnt signaling pathways (Grefte et al., 2007). At this stage Myf5 and Mrf4, independently of Pax3/7, regulate the entry of MPCs into the myogenic program. MPCs express Pax3 and Pax7 genes, and migrate to the limbs and trunk (Buckingham and Relaix, 2007). However, some MPCs give rise to

a subpopulation of postnatal muscle stem cells called satellite cells (SCs) (Gros et al., 2005). Both MPCs and SCs can give rise to myoblasts to complete myogenesis. The committed myoblast undergo proliferation, exit the cell cycle, express myogenic regulatory factors (MRFs), undergo morphological changes, fusing to form multinucleated myotubes. Finally, these myotubes are further fused into mature myofibers (Tajbakhsh, 2009) (**Figure 1**). Six1/4 and Pax3/7 are master regulators of MPCs but not SCs during early lineage specification, whereas Myf5 and MyoD commit MPCs and SCs to the myogenic program. MPCs and SCs expression of the terminal differentiation genes are performed by both myogenin (MyoG) and MyHC (Bentzinger et al., 2012). Skeletal muscle is composed of multinucleated contractile myofibers. Studies have shown that committed myoblasts align and fuse to generate small multinucleated myofibers during primary myogenesis in the embryo [from embryonic day 11 (E11)-E14.5]; during secondary myogenesis (from E14.5-to birth), the formation of myofibers containing hundreds of myonuclei are regulated *via* numerous signaling pathways and transcription factors (Sambasivan and Tajbakhsh, 2007).

SCs reside between the sarcolemma and basal lamina of myofibers (Mauro, 1961). SCs can serve as a pathway for skeletal muscle fiber growth after birth by activating myogenesis, repairing muscle fiber damage, or prolonging muscle fiber growth (Grounds and Yablonka-Reuveni, 1993). Under normal conditions, SCs express Pax7 and remain in a state of mitotic quiescence (Cheung and Rando, 2013). When muscles are stimulated or injured, SCs are immediately activated, proliferated, and differentiated like myoblasts. Finally, these cells fuse with the original myofibers or fuse with each other into myotubes and connect to the tail of old myofibers to form new myofibers (Zammit et al., 2006). This process is called postnatal muscle development (Relaix and Zammit, 2012). The SC population is a heterogeneous mixture of stem cells and committed progenitors (Le Grand and Rudnicki, 2007), and proliferates and divides into two daughter cells in an "asymmetric" pattern after activation (Kuang et al., 2007). Using chromosome orientation-fluorescence *in situ* hybridization in transgenic Tg:Pax7-nGFP mice, Rocheteau et al. (2012) demonstrated that all chromatids segregate asymmetrically in SCs. Cho and Doles used single cell RNA sequencing (scRNA-seq) to study the transcriptional diversity of freshly isolated skeletal muscle SCs and found the extensive transcriptional heterogeneity between individual SCs (Cho and Doles, 2017). Single-cell mass spectrometry revealed the heterogeneity of skeletal muscle SC in the activation of myogenesis *in vitro* and *in vivo* (Porpiglia et al., 2017).

Both embryonic myogenesis and postnatal skeletal muscle development is a highly regulated process; each step of the process is regulated by specific signaling pathways and transcription factors such as Sonic hedgehog (Shh), Notch, Wnt, and bone morphogenetic protein 4 (BMP4) (Jin et al., 2016), especially MRFs and post-transcriptional regulation by ncRNAs (Pauli et al., 2011; Zammit, 2017). The Encyclopedia of DNA Elements (Consortium) project showed that 80% of the eukaryotic genome is transcribed (Consortium, 2012), but <2% of total genomic sequences are transcribed into mature protein-coding RNAs, and the vast majority of transcripts are ncRNAs (Cheng et al., 2005). Various ncRNAs account for the majority of total RNA in cells. ncRNAs include tRNA, rRNA, eRNA, mitochondrial ncRNAs, micro (mi) RNAs, long non-coding (lnc) RNAs, circular (circ) RNAs, and PIWI-interacting RNAs (pi) RNAs (de Gonzalo-Calvo and Thum, 2018). Furthermore, ncRNAs are involved in diverse biological processes, and an increasing number of studies have shown that ncRNA-mediated epigenetic regulation plays an important role in myogenesis. In this review, we mainly focused on the importance of miRNAs, circRNAs, and lncRNAs in embryonic myogenesis and postnatal skeletal muscle development, and discussed their regulation of muscle disease. Finally, challenges and future perspectives in the identification of novel muscle-related ncRNAs were discussed.

miRNAs AND MYOGENESIS

miRNA and Embryonic Myogenesis

miRNAs are a class of small RNAs that are 20–24 nucleotides in length, and regulate the expression of target messenger RNAs (mRNAs) through base-pairing with the 3′ untranslated regions (3′UTRs) (Bartel, 2009). This interaction leads to inhibition of translation, mRNA cleavage, and transcript degradation (Bethune et al., 2012). This mechanism reportedly guides a diverse set of RNA-induced silencing complexes (RISC) to target mRNAs (Schraivogel and Meister, 2014). The biogenesis of most miRNAs depends on specific RNA processing enzymes, including Drosha and its essential cofactor DGCR8, Dicer (Bushati and Cohen, 2007). Dicer activity is essential for normal muscle development during embryogenesis, and Dicer muscle-specific mutants reduced muscle miRNAs and led to a decrease in myofiber development by reducing muscle mass and perinatal lethality in mice (O'Rourke et al., 2007). The role of miRNAs during embryogenesis was explored in zebrafish. Giraldez and colleagues generated maternal-zygotic Dicer (MZdicer) mutants that disrupted the Dicer ribonuclease III and double-stranded RNA-binding domains. MZdicer mutants displayed abnormal morphogenesis during gastrulation, somitogenesis, and heart development. Mutant embryos failed to process precursor miRNAs into mature miRNAs, but injecting preprocessed miRNAs restored gene silencing, indicating that miRNAs are essential for early embryogenesis (Giraldez et al., 2005). A growing number of studies have elucidated that miRNAs regulate various aspects of animal embryogenesis, with some miRNAs functioning in a tissue-specific manner.

MyomiRs are a muscle-enriched group of miRNAs, mainly composed of miR-1 and miR-133 families, including miR-1/miR-1-2/miR-206 and miR133a /miR-133b (Horak et al., 2016; Mok et al., 2017). Furthermore, miR-1 and miR-133 are potent repressors of non-muscle gene expression and cell fate during mouse and human embryonic stem cell differentiation (Ivey et al., 2008). In zebrafish, downregulation of miR-1 and miR-133 altered muscle gene expression and disrupted actin organization and sarcomere assembly during muscle differentiation (Mishima et al., 2009). During embryonic

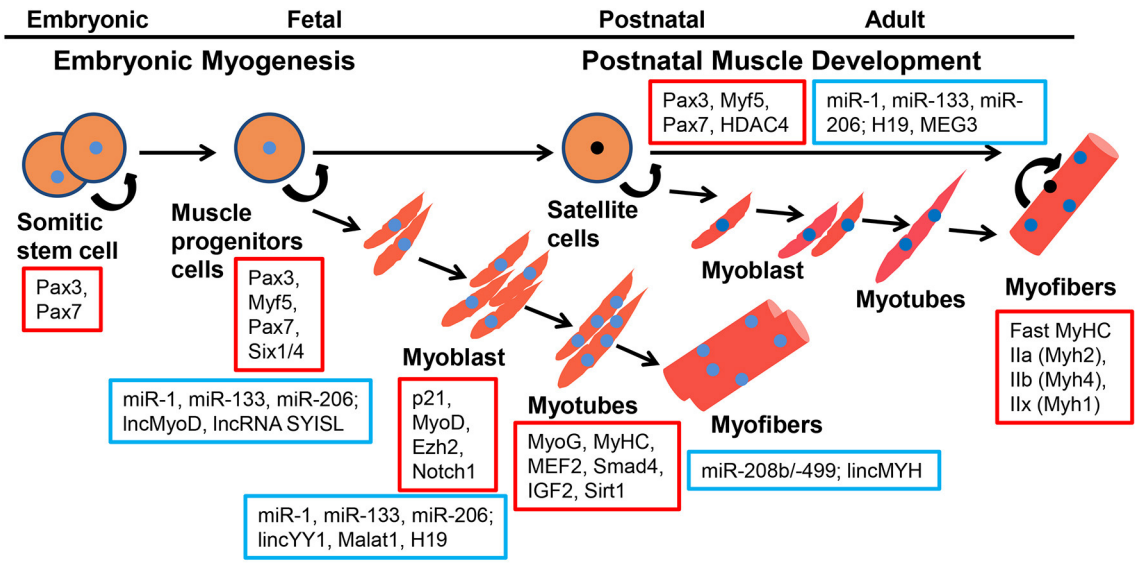

FIGURE 1 | Coding genes and ncRNAs regulate the process of embryonic and postnatal myogenesis. Coding genes are represented in red squares, ncRNAs are represented in blue squares.

myogenesis, miR-1 and miR-133 actively shaped gene expression patterns. Among the set of myomiRs, miR-206 was detected in somites of chick and mouse embryos (Sweetman et al., 2006). Sweetman et al. (2008) demonstrated that the ectopic expression of MRFs in the developing chicken neural tube induced the expression of distinct myomiRs such as miR-1 and miR-206, whereas the lack of *Myf-5* resulted in a loss of myomiR expression in developing somites. Their results indicated that myomiRs regulate myogenesis through MRFs. Additional gain- and loss-of-function experiments are needed to illustrate the role of myomiRs during myogenesis by affecting MRF expression. In *Xenopus laevis*, Vergara et al. examined the expression of miR-206 accompanying somitogenesis. Both knockdown and overexpression of miR-206 resulted in abnormal somite formation (Vergara et al., 2018). Conversely, miR-133 knockdown impaired myotome formation and growth, and the evolutionarily conserved miR-133 family mediated Gli3 silencing was critical for embryonic myogenesis (Mok et al., 2018). Other studies have specifically focused on the genetic analysis of myomiRs in a variety of model organisms, including flies, zebrafish, and mice (Sokol, 2012). MyomiRs are integrated into myogenic regulatory networks and, in turn, have widespread control of muscle gene expression.

In addition to myomiRs, several other miRNAs are involved in skeletal muscle embryonic development. For example, miR-196 reportedly acts upstream of Hoxb8 and Shh *in vivo* in the context of limb development, and primarily regulated the transcription of myogenesis (Hornstein et al., 2005). The zebrafish *Myf5* locus has an intronic miRNA, termed miR-3906 or miR-In300, which was found to impair fast muscle differentiation by targeting *Homer-1b* or *Dmrt2a*, respectively, in zebrafish embryos (Lin et al., 2013). miR-203 was transiently upregulated in chicken embryos on days 10 to 16 (E10–E16)c and was sharply downregulated and not expressed after E16 in the chicken embryonic skeletal muscle. Histological profiles and weight variations of embryo skeletal muscle revealed that miR-203 expression correlates with muscle embryonic development (Luo et al., 2014). Collectively, these results demonstrated the expression and function of myomiRs in skeletal embryonic myogenesis.

Functional Analysis of miRNAs During Postnatal Muscle Development

In recent years, a fraction of miRNAs has been detected in the skeletal muscle. Herein, we systematically summarized the functions and regulatory mechanisms of miRNAs (**Table 1**) during postnatal skeletal muscle development.

Several 100 miRNAs have been identified in plants, animals, and viruses by employing molecular cloning and bioinformatic approaches. In different tissues, miRNAs were found to downregulate gene expression by base-pairing with the 3′UTRs of target mRNAs; they also function this mechanism during myogenesis. For instance, miRNAs can influence proliferation *via* mRNAs coding regulators of the cell cycle. miR-27b is a functionally conserved miRNA that targets Pax3 to promote myoblast proliferation in mouse and goat (Crist et al., 2009; Ling et al., 2018). miR-195/497 is a positive regulator of SC quiescence by targeting Ccnd1 and Ccnd2 (Sato et al., 2014). The insulin-like growth factor (IGF) pathway, myocyte enhancer factor-2 (MEF2), and MRF factors play vital roles in myogenesis, miRNAs can regulate these pathways. For example, IGF-2, a critical regulator of skeletal myogenesis, is a direct and major target of miR-125b in both myocytes and regenerating muscles. miR-125b negatively modulated myoblast differentiation *in vitro* and muscle regeneration *in vivo* (Ge et al., 2011). MEF2A is a member of the MEF2 family of transcription factors, and miR-155 significantly suppressed the

TABLE 1 | Functions and regulatory mechanisms of miRNAs in postnatal skeletal muscle development.

miRNA	Functions	Mechanisms	Species	References
DmiR-1	Required for the dramatic post-mitotic growth of larval muscle	Targets twist	*Drosophila*	Sokol and Ambros, 2005
miR-1	Promotes myoblast proliferation and differentiation	Targets HDAC4	Mouse	Chen et al., 2006
	Maintains SCs quiescence and promotes self-renewal		Goat	Sui et al., 2020
miR-181	Required for skeletal myoblast terminal differentiation	Targets HoxA11	Mouse	Naguibneva et al., 2006
miR-214	Modulation of Hedgehog (Hh) signaling in somite cells, enhance slow-muscle cell types	Targets suppressor of fused [su(fu)]	Zebrafish	Flynt et al., 2007
	Promotes myoblast differentiation	Targets Ezh2	Mouse	Juan et al., 2009
miR-221/222	Inhibits proliferation and differentiation	Targets p27	Quail	Cardinali et al., 2009
miR-208b/-499	Activates slow and represses fast myofibers gene programs	Targets Sox6	Mouse	van Rooij et al., 2009
miR-27b	Promotes myoblast differentiation	Targets Pax3	Mouse	Crist et al., 2009
	Promotes myoblast proliferation and differentiation		Goat	Ling et al., 2018
	Promotes myoblast differentiation	Inhibits MDFI expression	Porcine	Hou et al., 2018
miR-206	Promotes myoblasts proliferation and differentiation	Targets Pax7	Mouse	Chen et al., 2010
miR-486	Promotes myoblast differentiation	Targets Pax7	Mouse	Dey et al., 2011
miR-155	Inhibits myoblast differentiation	Targets MEF2A	Mouse	Seok et al., 2011
miR-125b	Inhibits myoblast differentiation	Targets IGF2	Mouse	Ge et al., 2011
miR-26a	Promotes myoblast differentiation	Targets Smad1 and Smad4	Mouse	Dey et al., 2012
miR-489	Maintains SCs quiescence and regulates self-renewal	Post-transcriptionally suppresses the oncogene Dek	Mouse	Cheung et al., 2012
miR-31	Maintains SC quiescence	Sequesteres in mRNP granules together with Myf5 mRNAs.	Mouse	Crist et al., 2012
miR-23a	Inhibits myogenic differentiation	Targets fast myosin heavy chain (Myh) genes, including Myh 1, 2 and 4	Mouse	Cornu et al., 2012
miR-128a	Negatively regulates myoblast proliferation and myotubes hypertrophy	Regulates IRS1/Akt insulin signaling	Mouse	Motohashi et al., 2013
miR-675-3p/-5p	Promotes myoblast differentiation and regeneration	Targets Smad transcription factors	Mouse	Dey et al., 2014
miR-146b	Promotes myogenic differentiation	Targets Smad4, Notch1, and Hmga2	Mouse	Khanna et al., 2014
miR-195/497	Maintains SCs quiescence	Targets Ccnd1 and Ccnd2	Mouse	Sato et al., 2014
miR-186	Inhibits myoblast differentiation	Targets myogenin	Mouse	Antoniou et al., 2014
miR-30a	Promotes myogenesis by increasing apoptosis and altering somite morphology	Targets Six1	Zebrafish	O'Brien et al., 2014
miR-431	Promotes differentiation and regeneration of old skeletal muscle	Targets Smad4	Mouse and human	Lee et al., 2015
miR-15b/miR-23b/miR-106b/miR-503	Pitx2-miRNA pathway regulates myoblast proliferation	Targets CyclinD1 and CyclinD2	Mouse	Lozano-Velasco et al., 2015
miR-20a/20b	Promotes myoblast differentiation and represses myoblast proliferation	Targets E2F transcription factor 1 (E2F1)	Chicken	Luo et al., 2016
miR-29a	Promotes SCs proliferation	Targets FGF2	Mouse	Galimov et al., 2016
miR-17-92	Promotes myoblast proliferation but inhibits myotubes formation	Targets ENH1	Mouse	Qiu et al., 2016
miR-34c	Inhibits myoblast proliferation and promotes differentiation	A regulatory loop with Notch1	Mouse	Hou et al., 2017

(Continued)

TABLE 1 | Continued

miRNA	Functions	Mechanisms	Species	References
miR-139	Promotes SCs differentiation	Targets DHFR	Bovine	Zhou et al., 2018
miR-708	Activates SCs and regulates self-renewal	Antagonizes Tensin3 to inhibit FAK activation	Mouse	Baghdadi et al., 2018
miR-487b-3p	Suppresses the proliferation and differentiation of myoblast	Targets IRS1	Goat	Wang et al., 2018
miR-17/19	Promotes myoblast differentiation	miR-17 targets Ccnd2, Jak1 and Rhoc, miR-19 complement miR-17	Mouse	Kong et al., 2019
miR-208b	Promotes myoblast proliferation, inhibits differentiation	Targets the E-protein family member TCF12	Mouse	Fu et al., 2020
	Stimulates fast-to-slow fiber conversion and oxidative metabolism programmers	Targets FNIP1		
miR-9-5p	Inhibits the proliferation and differentiation of SCs	Targets IGF2BP3	Chicken	Yin et al., 2020

expression of MEF2A, repressing skeletal muscle differentiation (Seok et al., 2011). MRFs, including Myf5, MyoD, Myf6, and myogenin, regulate skeletal muscle differentiation, where myogenin plays a critical role in regulating the final stage of muscle differentiation. Antoniou et al. (2014) predicted that six miRNAs (miR-182, miR-186, miR-135, miR-491, miR-329, and miR-96) bind the myogenin 3′-UTR, but only miR-186 is a novel post-transcriptional regulator of myogenin during skeletal myogenesis. Recently, Fu et al. showed that miR-208b targeted the E-protein family member TCF12 to promote mouse myoblast proliferation and inhibit their differentiation. Meanwhile, miR-208b stimulated fast-to-slow fiber conversion and oxidative metabolism process by targeting FNIP1, thereby regulating postnatal muscle development (Fu et al., 2020). Several miRNAs are reportedly present in muscle cells and their modulating influence on myogenesis is likely to be overly complex. Some miRNAs target the same transcriptional networks in different species (**Supplementary Table 1**).

cicrRNA DURING MYOGENESIS

cicrRNA and Embryonic Myogenesis

With the advent of high-throughput sequencing and novel bioinformatic tools, thousands of circRNAs were discovered and their abundance and function were recorded (Salzman et al., 2012; Memczak et al., 2013). circRNAs are characterized by a covalently closed ring structure without 3′ and 5′ ends and are generated by precursor mRNA back-splicing of exons. Typically, the expression levels of circRNAs are low, often exhibiting cell- and tissue-specific patterns in eukaryotes (Li et al., 2018c). Increasing evidence has demonstrated that circRNAs participate in many steps of gene expression by acting as miRNA sponges, miRNA decoy, RNA-binding proteins (RBPs), as well as mediating RNA translation and protein interaction. Several studies have demonstrated that circRNAs possess coding capabilities (Panda et al., 2017). Owing to the non-linear conformation of circRNAs and lack of polyadenylated [poly (A)] tails, very few circRNAs can be identified by RNA-seq, but circRNAs are readily detectable in ribosomal RNA-depleted RNA-seq datasets (Greco et al., 2018). One microarray analysis found that 581 circRNAs were differentially regulated between C2C12 myoblasts and myotubes (Chen et al., 2018a). However, their roles remain to be explored. Notably, circRNAs may play a vital role in myogenesis. Fan et al. (2015) developed a single-cell universal poly(A)-independent RNA sequencing (SUPeR-seq) method to sequence both polyadenylated and non-polyadenylated RNAs from individual cells, discovering 2,891 circRNAs and 913 novel linear transcripts in mouse preimplantation embryos. This research is crucial to decipher functional regulators of circRNAs during early mammalian embryonic development. An increasing number of databases have suggested that skeletal muscle is one of the tissues enriched in circRNAs (Cheng et al., 2005; Li et al., 2017).

circSVIL, an exonic circular, was differentially expressed in chicken skeletal muscle at E11, E16, and post-hatching day 1 (P1) (Ouyang et al., 2018b). circSVIL functions as miR-203 sponges and upregulates levels of *c-JUN* and *MEF2C*, thereby promoting the proliferation and differentiation of myoblasts (Ouyang et al., 2018a). circFGFR2, generated by exon 3–6 of the *FGFR2* gene, was differentially expressed during chicken embryo skeletal muscle development (Chen et al., 2018b). circFGFR2 directly targeted miR-133a-5p and miR-29b-1-5p and further eliminated the inhibitory effects of the two miRNAs on myoblast proliferation and differentiation (Chen et al., 2018b). The circRNA sequencing data of bovine skeletal muscle tissue demonstrated that circFUT10 was highly (but differentially) expressed in embryonic and adult skeletal muscle tissues. Reportedly, circFUT10 regulated myoblast differentiation and cell survival by directly binding to miR-133a and inhibiting miR-133a activity (Li et al., 2018b). circFUT10 may target myomiRs to regulate embryonic myogenesis. The expression level of circSNX29 was considerably higher in the bovine embryonic skeletal muscle than in adult skeletal muscle. circSNX29 directly interacted with miR-744 and efficiently reversed the suppression of Wnt5a and calcium/calmodulin–dependent protein kinase II delta (CaMKIIδ) (Peng et al., 2019). In bovine, enhancing circFUT10 or circSNX29 expression may emerge as a potential

TABLE 2 | Functions and regulatory mechanisms of circRNAs in skeletal muscle development.

circRNA	Functions	Mechanisms	Species	References
circLMO7	Inhibits myoblast differentiation and promotes myogenesis	miR-378a-3p sponge	Bovine	Wei et al., 2016
circ-ZNF609	Promotes myoblast proliferation	Protein encoding	Human	Legnini et al., 2017
circRBFOX2	Promotes myoblast proliferation	mir-206 sponge	Chicken	Ouyang et al., 2018b
circFGFR4	Promotes myoblast differentiation and apoptosis	miR-107 sponge	Bovine	Li et al., 2018a
circ-Zfp609	Inhibits myoblast differentiation	miR-194-5p sponge	Mouse	Wang et al., 2019b
circHIPK3	Promotes myoblast proliferation and myogenesis	miR-30a-3p sponge	Chicken	Chen et al., 2019
	Promotes myoblast differentiation	miR-124 and miR-379 sopnge	Mouse	Yao et al., 2020
circ-FoxO3	Inhibits myoblast differentiation	miR-138-5p sponge	Mouse	Li et al., 2019b
circTitin (circTTN)	Promotes proliferation and differentiation of bovine primary myoblast	miR-432 sponge	Bovine	Wang et al., 2019a
circTMTC1	Inhibits chicken SMSC differentiation	miR-128-3p sponge	Chicken	Shen et al., 2019
CDR1as (ciRS-7)	Promotes myogenic differentiation	miR-7 sponge	Goat	Li et al., 2019a
circHUWE1	Facilitates myoblast proliferation, inhibits apoptosis and differentiation	miR-29b sponge	Bovine	Yue et al., 2020a
circSamd4	Promotes myogenic differentiation	Associates with PUR proteins	Mouse	Pandey et al., 2020
circINSR	Promotes proliferation and reduces apoptosis of bovine embryonic myoblast	miR-34a sponge	Bovine	Shen et al., 2020

target in breeding strategies attempting to control muscle development. Overall, circRNAs play a role in regulating the myoblast cycle and development by acting as miRNA binding sites to facilitate the regulation of gene expression during myogenesis (Zhang et al., 2018a). In Duroc pigs, Hong et al. (2019) performed RNase R+RNA-seq in three distinct stages of embryonic skeletal muscle development (33, 65, and 90 days prenatal) to identify circRNAs and found that many circRNAs were specifically expressed at different embryonic stages. Collectively, these findings are helpful for further research on circRNAs in myogenesis.

circRNAs Regulating Postnatal Muscle Development

Here, we summarized the current research progress on the role of circRNAs in postnatal myogenesis (**Table 2**).

Interestingly, almost all circRNAs can act as miRNA sponges to regulate the transcription and splicing of target genes. For example, circHIPK3 promoted the proliferation and differentiation of chicken myoblast cells by sponging miR-30a-3p binding to MEF2C (Chen et al., 2019). circHIPK3 can promote the differentiation of C2C12 myoblasts as a sponge of miR-124 and miR-379 (Yao et al., 2020). circINSR promoted proliferation and reduced apoptosis of bovine embryonic myoblasts by sponging miR-34a (Shen et al., 2020). Some circRNAs can be translated into proteins in the post-transcriptional regulation of muscle development. circ-ZNF609 specifically regulated mouse and human myoblast proliferation. circ-ZNF609 can be translated into a protein in a splicing-dependent and cap-independent manner when ectopically expressed (Legnini et al., 2017). circZfp609, the mouse homolog of circ-ZNF609, can sponge miR-194-5p to sequester its inhibition on BCLAF1 to repress myogenic differentiation (Wang et al., 2019b). Recently, researchers have shown that circSamd4, which is conserved between humans and mice, has a positive function in skeletal muscle differentiation by associating with PURA and PURB, two repressors of myogenesis that inhibit transcription of the myosin heavy chain (MHC) protein family (Pandey et al., 2020). This illustrated the protein interaction mechanism of circRNAs.

lncRNAs IN MYOGENESIS

Role of lncRNAs in Regulating Embryonic Myogenesis

lncRNAs were originally considered as genomic transcription "noise" and account for a large proportion of total ncRNAs (Kapranov et al., 2007; Struhl, 2007). With weak or no protein-coding potential, lncRNAs are a class of RNA more than 200 nucleotides in length, possessing complex spatial structures and diverse functions (Derrien et al., 2012). Several lncRNAs are transcribed by RNA polymerase II (Pol II) from genomic loci with similar chromatin states to mRNAs; they are often 5′-capped, spliced, polyadenylated, with the absence of a translated open reading frame (ORF) (Quinn and Chang, 2016). lncRNAs are ubiquitous in organisms and are cell-type-specific, with poor evolutionary conservation among different species (Engreitz et al., 2016). Numerous studies have shown that lncRNAs are involved in the regulation of gene expression, epigenetics, cell differentiation, apoptosis, metabolism, signal transduction, and immune response (Mattick, 2005; Zhang et al., 2019).

Interestingly, emerging studies have also demonstrated that some lncRNAs can encode micropeptides shorter than 100 amino acids to exert micropeptide-mediated functions (Anderson et al., 2015). Many computational pipelines developed from poly (A) RNA-seq in different cells can identify new lncRNAs, and several studies have shown that lncRNAs participate in embryo myogenesis.

H19 was one of the earliest known examples of imprinted lncRNAs that did not contain any conserved ORFs between mice and humans (Brannan et al., 1990). H19 is strongly repressed after birth in all mouse tissues, but it remains expressed in the skeletal muscle and heart in adults, suggesting an important function in these muscles (Poirier et al., 1991). Gabory and colleagues found that the H19 gene participates as a *trans* regulator in the fine-tuning of this imprinted gene network (IGN) in the mouse embryo (Gabory et al., 2009). This is the first *in vivo* evidence of a functional role for H19. Pauli et al. (2012) performed a time-series of RNA-seq experiments at eight stages during early zebrafish embryo development and observed that lncRNAs were particularly numerous during very early embryo development. *In situ* hybridization showed that lncRNAs are expressed in narrower time windows and are specifically enriched in early-stage embryos. Whole-mount *in situ* hybridization showed that lncIRS1 was expressed in the forming somites in the HH10 chick embryo, controlled IRS1 protein levels, and further activated the IGF-1 signaling pathway by functioning as ceRNA to sponge miR-15a, miR-15b-5p, and miR-15c-5p (Li et al., 2019c). Regarding lncRNAs in embryonic myogenesis, a review by Bouckenheimer et al. summarized their expression patterns and roles during early human embryo development and in pluripotent stem cells (PSCs). Importantly, abundant public mRNA sequencing (mRNA-seq) data have been used to illustrate the large number of lncRNAs expressed during embryo development (Bouckenheimer et al., 2016). These results support the notion that lncRNAs are part of dynamic changes in transcript expression occurring during mammalian early embryo development, including myogenesis. Sweta et al. suggested that lncRNAs are important for mesodermal specification and further differentiation, development, and functions of mesodermal derivatives, including *lncRNA Evx1as*, *lncRNA HoxBlinc*, *and yylncT* (Sweta et al., 2019). During embryonic development, the musculature of the adult body is derived from the mesoderm. Accordingly, these lncRNAs may function early myogenesis. However, insufficient evidence is available. Collectively, a better understanding of lncRNAs that can regulate the development of skeletal muscle will open potential avenues for their efficacious production, and enhance our knowledge regarding embryonic myogenesis development.

Functions and Mechanisms of lncRNAs in Postnatal Muscle Development

Numerous lncRNAs have been detected in skeletal muscle, but only a small fraction of lncRNAs have been characterized. Recent reports have indicated lncRNAs exert functional roles through multiple mechanisms, including transcription activation, molecular sponge activity, competitive binding, mRNA translation, and protein stability. Studies have shown that numerous lncRNAs interact with miRNAs to facilitate myogenesis. We displayed a known pattern of lncRNAs during skeletal muscle development (**Figure 2**; **Supplementary Table 2**).

Notably, functions of lncRNAs are associated with their subcellular location and microenvironment (Chen, 2016). linc-YY1 activated gene expression *in trans* by interacting with YY1 and removing the YY1/PRC2 complex from target promoters such as Myh and Troponin, thus promoting muscle differentiation and regeneration (Zhou et al., 2015). SYISL interacted with Ezh2, the core component of PRC2, to regulate the expression of p21 and muscle-specific genes such as MyoG, MCK, and Myh4, leading to the promotion of myoblast proliferation and inhibition of myogenic differentiation (Jin et al., 2018). In the nucleus, lncRNAs can also bind to transcription factors or RBPs to influence transcription activation. For instance, lncRNA SRA promoted differentiation as a coregulator of MyoD, along with RNA helicase p68/p72 (Caretti et al., 2006; Hube et al., 2011). linc-RAM, which is induced by MyoD, interacts with MyoD, and supports the assembly of the MyoD-Baf60c-Brg complex to promote muscle growth and regeneration (Yu et al., 2017).

Most lncRNAs in the cytoplasm act as ceRNAs with miRNAs, such as lncMD1 (Cesana et al., 2011; Legnini et al., 2014), lnc-mg (Zhu et al., 2017; Du et al., 2019), and lnc-MAR1 (Zhang et al., 2018b). Recently, Li reported that 2310043L19Rik (lnc-231) inhibited differentiation and promoted proliferation of myoblasts as ceRNA to target miR-125a-5p, thereby inhibiting the function of E2F3 mRNA (Li et al., 2020b). Conversely, H19 can act as a molecular scaffold to recruit TDP43 to promoters of MyoD and activate transcription, thereby promoting porcine SC differentiation (Li et al., 2020a). Furthermore, some lncRNAs can give rise to functional micropeptides. A conserved lncRNA, LINC00961/5430416O09Rik, which is localized on the late endosome/lysosome and encodes a polypeptide of 90 amino acids termed small regulatory polypeptide of amino acid response (SPAR), interacted with lysosomal v-ATPase to negatively regulate mammalian target of rapamycin complex 1 (mTORC1) activation, as well as skeletal muscle regeneration (Matsumoto et al., 2017; Tajbakhsh, 2017). Myoregulin (MLN) and dwarf open reading frame (DWORF) are micropeptide-encoded tissue-specific putative lncRNAs, located at the sarcoplasmic reticulum membrane (Ivey et al.), and can directly bind SERCA; MLN inhibits SERCA activity and hinders the uptake of Ca^{2+} into the SR. However, DWORF increases SERCA activity by reducing exercise performance and Ca^{2+} uptake into the SR (Anderson et al., 2015; Nelson et al., 2016). As the sequence length of lncRNAs is larger than that of miRNAs and circRNAs, they function diverse mechanisms and play extensive roles in life processes.

Previous studies have focused on the function of ncRNAs in the nucleus and cytoplasm. Mitochondria are important organelles and the main energy metabolism sites in cells (Nunnari and Suomalainen, 2012). The roles of ncRNAs in mitochondria have become a new biology research topic (Bandiera et al., 2011). Barrey et al. for the first time demonstrated the presence of pre-miRNA and miRNA in the human mitochondria isolated

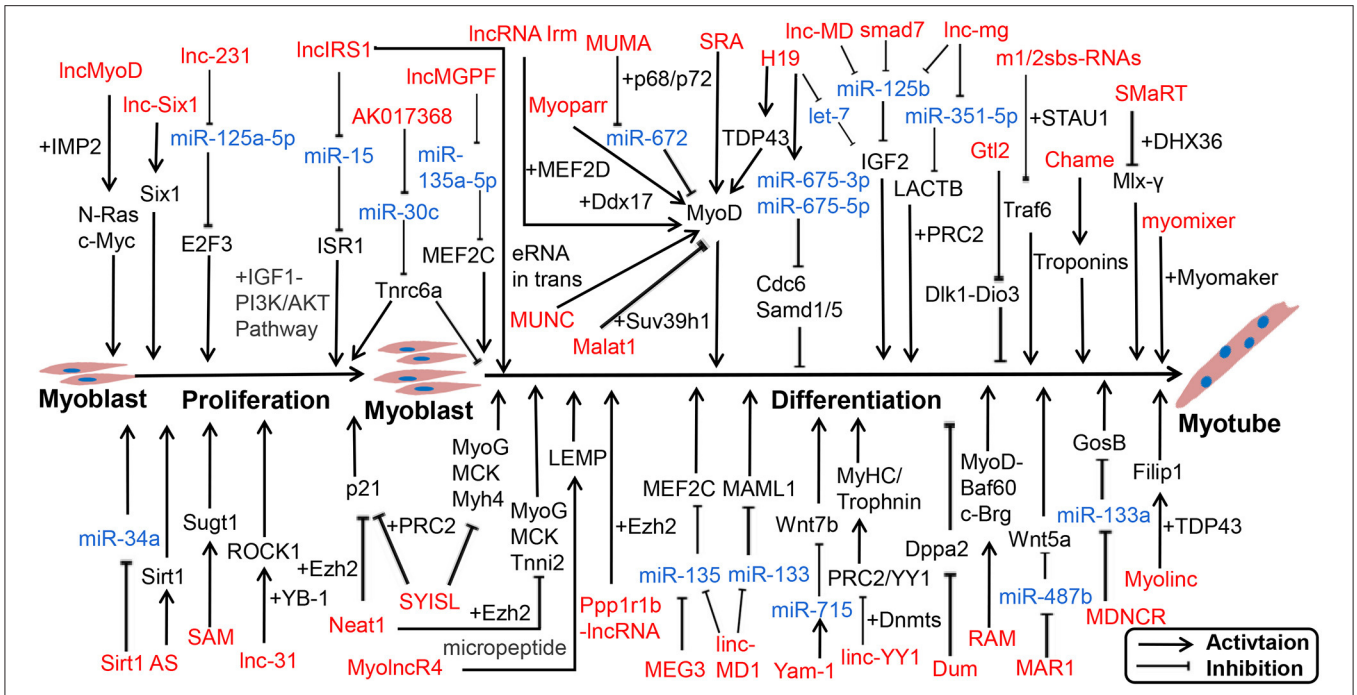

FIGURE 2 | lncRNA-miRNA-gene network regulates proliferation and differentiation of myoblast. lncRNAs are represented in red, miRNAs are represented in blue.

from skeletal muscular cells (Barrey et al., 2011). The muscle-specific miR-1 is able to stimulate mitochondrial translation of multiple mtDNA-encoded transcripts, while repressing its nuclear DNA-encoded targets in the cytoplasm (Zhang et al., 2014). Some lncRNAs generated from the mammalian mitochondrial genome or located in mitochondria have been identified. Rackham et al. (2011) identified three lncRNAs generated from the mitochondrial genome named lncND5 RNA, lncND6 RNA and lncCytb RNA. Ro et al. reported that the mouse and human mitochondrial genomes encodes abundant small RNAs and named mitochondrial genome-encoded small RNAs (mitosRNAs), which may play an important regulatory role in the control of mitochondrial gene expression (Ro et al., 2013). The regulation mechanism and function of mitochondrial ncRNAs in myogenesis remain to be further explored.

As mentioned above, ncRNAs play an important role in regulating myogenesis during embryonic and adult stages. Crosstalk between miRNA-circRNA-lncRNA appears to be common in muscle development. lncRNAs can inhibit the function of miRNA through sequence-specific binding, whereas circRNAs can act as molecular sponges for miRNAs to regulate target mRNAs related to myogenesis. Further insights into postnatal skeletal muscle development will illustrate complex and dynamic regulatory networks.

ncRNAs IN MUSCLE DISEASE

Skeletal muscle is a complex tissue in mammals, and skeletal muscle diseases are known to occur owing to physiological and pathological factors. Common skeletal muscle diseases include atrophy (Cohen et al., 2015), Duchenne muscular dystrophy (DMD) (Matsumura et al., 1994), and hypertrophy (Walters, 2017). Several reports have suggested that ncRNAs may play a functional role in muscle disease and could be potentially exploited as therapeutic tools. The impact of ncRNA dysregulation in muscle disease reported in recent years is depicted in **Figure 3**.

An understanding of how ncRNAs regulate skeletal muscle functions and disease can provide novel therapeutic targets for the prevention and treatment of muscle pathologies in metabolic diseases. Two muscle-specific ubiquitin ligases, MAFbx/Atrogin-1 and muscle RING-finger 1 (MuRF1), are prominently induced during muscle atrophy and mediate atrophy-associated protein degradation (Sacheck et al., 2007). Blocking the expression of these two ubiquitin ligases affords protection against muscle atrophy. Wada and colleagues reported that miR-23a suppressed the translation of both MAFbx/Atrogin-1 and MuRF1 in a 3′-UTR-dependent manner. Ectopic expression of miR-23a was sufficient to protect the muscle from atrophy both *in vitro* and *in vivo* (Wada et al., 2011). Direct interactions were identified between miR-376c-3p and the 3′ UTR of Atrogin-1, leading to repression of Atrogin-1, and thereby induction of eIF3f protein levels in both human and mouse skeletal muscle cells (Shin et al., 2020). Reportedly, lncRNA Pvt1 is upregulated during muscle atrophy by blocking c-Myc phosphorylation and degradation. Functionally, Pvt1 affects mitochondrial respiration and morphology, thereby affecting muscle atrophy and myofiber size *in vivo* (Alessio et al., 2019). In addition to affecting myogenesis during embryonic and postnatal development, muscle disease is affected by

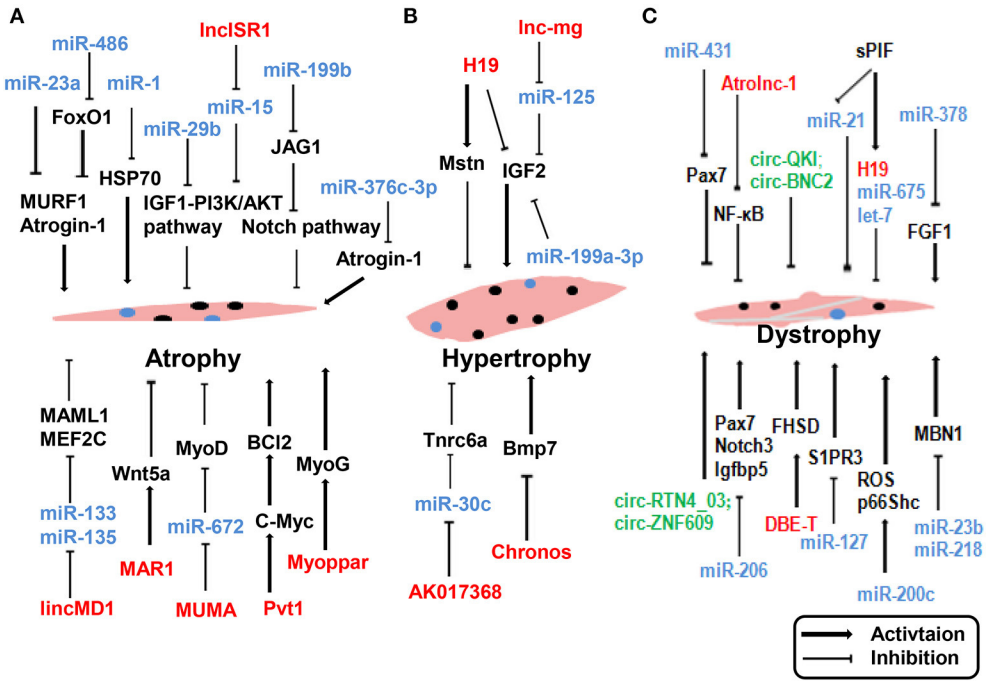

FIGURE 3 | ncRNAs regulate muscle atrophy **(A)**, hypertrophy **(B)**, and dystrophy **(C)**. lncRNAs are represented in red, miRNAs are represented in blue, circRNAs are represented in green. Myoblast, black nuclei; satlliate cells, blue nuclei.

miR-206. Loss of miR-206 accelerated and exacerbated the dystrophic phenotype in mdx mice by suppressing Pax7, Notch3, and Igfbp5 (Liu et al., 2012). In contrast, several lncRNAs are known to affect the pathological status of skeletal muscle dystrophy. lncRNA Atrolnc-1 was abundantly expressed in skeletal muscle and markedly increased in atrophying muscle. Atrolnc-1 strongly binds to ABIN-1, inhibits NF-κB signaling, and causes protein degradation in muscle cells (Sun et al., 2018). H19 can influence muscle hypertrophy by regulating the expression of Mstn and IGF2 (Martinet et al., 2016). Neppl and colleagues observed that lncRNA Chronos was expressed in muscles. Inhibition of Chronos induced myofiber hypertrophy both *in vitro* and *in vivo* through the epigenetic modulation of Bmp7 signaling (Neppl et al., 2017). Knockdown of lncRNA AK017368 promoted muscle hypertrophy *in vivo*. Notably, lncRNA AK017368 promoted proliferation and inhibited differentiation of myoblasts by competing with Tnrc6a for miR-30c (Liang et al., 2018).

Furthermore, circRNAs are associated with muscle disease. The dystrophy gene was among the first genes identified to generate circRNAs in skeletal muscle (Surono et al., 1999). Legnini et al. analyzed data from both normal and dystrophic human myoblasts and identified circ-QKI and circ-BNC2 upregulated during *in vitro* differentiation, and downregulated in the DMD conditions, which is consistent with the notion that dystrophic cells have altered progression into the differentiation process (Legnini et al., 2017). Song et al. identified 197 differentially expressed circRNAs between mdx mice and C57 mice by microarray analysis. A circRNA/miRNA interaction network was predicted by bioinformatic approaches (Song et al., 2020). These studies described the expression pattern of circRNAs and indicated that circRNAs may play pivotal roles in the pathophysiological mechanisms of DMD.

CONCLUSION AND FUTURE PERSPECTIVE

The discovery of ncRNAs has remarkably broadened our understanding of epigenetic regulation. Most researchers have used overexpression or inhibition of ncRNA function to explore their mechanisms during myogenesis; moreover, some ncRNAs have been well-investigated using *in vivo* mouse models. Several reports have revealed ncRNA functions in skeletal muscle development and disease and can be developed as novel biomarkers or targets for improving muscular abilities and therapeutic strategies.

Despite improvements in our knowledge regarding the role of ncRNAs in myogenesis, detailed identification and verification of ncRNAs still encounter several obstacles, including the following:

1) several techniques have been used to identify ncRNAs, including ncRNA microarray analysis and sequencing methods based on poly (A) sequencing, especially next-generation sequencing (NGS). The limitations of NGS on the identification of ncRNAs and its regulatory mechanisms need to be addressed as non-poly (A) forms of ncRNAs

such as circRNAs are often ignored. Furthermore, there are a variety of ncRNA databases available, such as miRBase, TargetScan, ribosomal RNA-depleted RNA-seq datasets, lncRNA Database v2.0, and Linc2GO. We need to determine a systematic identification approach to combine ncRNA data generated from different methodologies.

2) Most known miRNAs and circRNAs demonstrate cytoplasmic localization, whereas lncRNAs are present in both the nucleoli and cytoplasm. Furthermore, nuclear miRNA-directed gene regulation constitutes a departure from the prevailing view of miRNA functions (Roberts, 2014), which requires different experimental schemes to identify functional ncRNAs. Fang et al. developed PIRCh-seq, a method that enables a comprehensive survey of chromatin-associated ncRNAs in a histone modification-specific manner (Fang et al., 2019). PIRCh-seq significantly reduces the influence of nascent transcripts and more precisely reveals relationships between chromatin and its associated ncRNAs than other sequencing methods. More recently, ribosome profiling, droplet digital PCR, and NanoString Technologies nCounter assays have uncovered the functions of ncRNAs (Chen, 2020).
3) Current experiments need to be based on the million-cell scale, and their accuracy does not support the single-cell level experiment. The current omics research field has been transformed from mixed sample research to single-cell level research. Single-cell sequencing technology has revealed the existence of cellular heterogeneity and related molecular mechanisms in detail. For some precious cell samples or embryonic samples, rigorous validation experiments are needed.
4) The mechanism of ncRNAs has been assessed *via* RIP, ChIRP, CHART, or GRID. One limitation of these probe approaches is that their efficacy is based on the size and location of ncRNAs. In recent years, many studies have reported that ncRNAs play biological functions through exosomes mediating intercellular communication (Romancino et al., 2013). Exosomes have been described as 40–100 nm vesicles that are secreted by a broad range of cell types and have been identified in diverse body fluids (Raposo and Stoorvogel, 2013). Exosomes have classically double membrane structure containing rich source of proteins, lipids, mRNAs and miRNA biological ingredients (Chevillet et al., 2014). The proteomic analysis of C2C12 myoblast and myotube exosome-like vesicles showed that exosomes could regulate muscle development (Forterre et al., 2014b). Myotube-derived exosomal miRNAs downregulate Sirtuin1 in myoblasts during muscle cell differentiation (Forterre et al., 2014a). Hudson et al. found that the expression of miR-23a in exosomes was altered, which weakened its inhibitory effect on target genes MuRf1 and atrogin-1, and leaded to muscle atrophy (Hudson et al., 2014). Mesenchymal-stem-cell-derived exosomes had low concentrations of muscle-repair-related cytokines and a number of repair-related miRNAs such as miR-494 to promote myogenesis and angiogenesis *in vitro* (Nakamura et al., 2015). There is growing evidence indicating active function of lncRNAs and circRNAs in exosomes (Yue et al., 2020b). Bioactive lncARSR (lncRNA Activated in RCC with Sunitinib Resistance) could be incorporated into exosomes and transmitted to sensitive cells, thus disseminating sunitinib resistance (Qu et al., 2016). H19 can be transferred from carcinoma-associated fibroblasts (CAFs) to colorectal cancer cells (CRCs) through exosomes, and acts as a competing endogenous RNA sponge for miR-141 in CRCs, promoting the stemness and chemoresistance of CRCs (Ren et al., 2018). However, the ncRNAs of exosomes related to myogenesis needs more in-depth analysis.
5) The functional interaction maps for a majority of characteristic ncRNAs with DNA or transcription factors, except for some well-studied cases, remain largely unknown. One crucial issue hindering the progression of this field is the limitations of RNA-DNA binding interaction technology and the lack of an ncRNAs-DNA-protein international database. Addressing these issues would significantly enhance our understanding of mechanisms that dictate ncRNAs association with myogenesis.

Furthermore, the identification of functional ncRNAs to improve muscle development remains a challenge that needs to be resolved. A major hindrance for most applications is the tissue delivery and distribution of ncRNAs for efficacy (Kaemmerer, 2018). For example, miRNAs function by integrating with complexes (RISC), which impedes their crossing of membranes; lncRNAs have low conservation between species, and their length and higher structure are complex. Currently, the most commonly used gene delivery methods for RNA-based therapeutics are recombinant viral systems such as adenovirus, lentivirus, and adeno-associated viruses (AAVs), which are employed either to inhibit or overexpress miRNAs, circRNAs, and lncRNAs (Sweta et al., 2019). Furthermore, the potential toxicity of the viral vectors should be determined to reduce negative impacts on the receptor. In addition to the delivery system for viral vectors, gene editing technology, antisense oligonucleotides (ASOs), and RNA interference (RNAi)-mediated approaches have also been reported. In recent years, the CRISPR/Cas9 system has been used as an efficient gene editing tool to investigate the function of ncRNAs. However, gene editing technology has presented off-target effects and ethical disputes. In contrast, the ASO technology has fewer off-target effects than the small RNA-mediated approach and the CRISPR/Cas9 system (Bennett and Swayze, 2010). To realize the full potential of ncRNAs as biomarkers or therapeutic targets against muscle, validation studies are warranted using both *in vitro* and *in vivo* systems to illustrate the integrated network of myogenesis.

AUTHOR CONTRIBUTIONS

HL and WL wrote the manuscript and selected the literature. BZ and ZX proposed the topic, wrote the manuscript, and corrected and gave suggestions to improve the manuscript. HL, WL, QT, JJ, ZX, and BZ reviewed the manuscript and prepared tables and figures. All authors read and approved the final manuscript.

FUNDING

This work was financially supported by the Key R&D projects of Hubei Province (2020BBB069), the National Key Project of Transgenic Research (Grant 2016ZX08006-002), the National Natural Science Foundation of China (Grant 31900448), the Agricultural Innovation Fund of Hubei Province (2016-620-000-001-043), the Fundamental Research Funds for the Central Universities (Program 2662018PY045), and the China Postdoctoral Science Foundation (Program 590319103).

ACKNOWLEDGMENTS

We would like to thank Editage (www.editage.com) for English language editing.

SUPPLEMENTARY MATERIAL

The Supplementary Material for this article can be found online at: https://www.frontiersin.org/articles/10.3389/fcell.2021.628339/full#supplementary-material

REFERENCES

Alessio, E., Buson, L., Chemello, F., Peggion, C., Grespi, F., Martini, P., et al. (2019). Single cell analysis reveals the involvement of the long non-coding RNA Pvt1 in the modulation of muscle atrophy and mitochondrial network. *Nucleic Acids Res.* 47, 1653–1670. doi: 10.1093/nar/gkz007

Anderson, D. M., Anderson, K. M., Chang, C. L., Makarewich, C. A., Nelson, B. R., McAnally, J. R., et al. (2015). A micropeptide encoded by a putative long noncoding RNA regulates muscle performance. *Cell* 160, 595–606. doi: 10.1016/j.cell.2015.01.009

Antoniou, A., Mastroyiannopoulos, N. P., Uney, J. B., and Phylactou, L. A. (2014). miR-186 inhibits muscle cell differentiation through myogenin regulation. *J. Biol. Chem.* 289, 3923–3935. doi: 10.1074/jbc.M113.507343

Baghdadi, M. B., Firmino, J., Soni, K., Evano, B., Di Girolamo, D., Mourikis, P., et al. (2018). Notch-induced miR-708 antagonizes satellite cell migration and maintains quiescence. *Cell Stem Cell* 23, 859–868 e855. doi: 10.1016/j.stem.2018.09.017

Bandiera, S., Ruberg, S., Girard, M., Cagnard, N., Hanein, S., Chretien, D., et al. (2011). Nuclear outsourcing of RNA interference components to human mitochondria. *PLoS ONE* 6:e20746. doi: 10.1371/journal.pone.0020746

Barrey, E., Saint-Auret, G., Bonnamy, B., Damas, D., Boyer, O., and Gidrol, X. (2011). Pre-microRNA and mature microRNA in human mitochondria. *PLoS ONE* 6:e20220. doi: 10.1371/journal.pone.0020220

Bartel, D. P. (2009). MicroRNAs: target recognition and regulatory functions. *Cell* 136, 215–233. doi: 10.1016/j.cell.2009.01.002

Bennett, C. F., and Swayze, E. E. (2010). RNA targeting therapeutics: molecular mechanisms of antisense oligonucleotides as a therapeutic platform. *Annu. Rev. Pharmacol. Toxicol.* 50, 259–293. doi: 10.1146/annurev.pharmtox.010909.105654

Bentzinger, C. F., Wang, Y. X., and Rudnicki, M. A. (2012). Building muscle: molecular regulation of myogenesis. *Cold Spring Harb. Perspect. Biol.* 4:a008342. doi: 10.1101/cshperspect.a008342

Bethune, J., Artus-Revel, C. G., and Filipowicz, W. (2012). Kinetic analysis reveals successive steps leading to miRNA-mediated silencing in mammalian cells. *EMBO Rep.* 13, 716–723. doi: 10.1038/embor.2012.82

Bouckenheimer, J., Assou, S., Riquier, S., Hou, C., Philippe, N., Sansac, C., et al. (2016). Long non-coding RNAs in human early embryonic development and their potential in ART. *Hum. Reprod. Update* 23, 19–40. doi: 10.1093/humupd/dmw035

Brannan, C. I., Dees, E. C., Ingram, R. S., and Tilghman, S. M. (1990). The product of the H19 gene may function as an RNA. *Mol. Cell. Biol.* 10, 28–36. doi: 10.1128/MCB.10.1.28

Buckingham, M., and Relaix, F. (2007). The role of Pax genes in the development of tissues and organs: Pax3 and Pax7 regulate muscle progenitor cell functions. *Annu. Rev. Cell Dev. Biol.* 23, 645–673. doi: 10.1146/annurev.cellbio.23.090506.123438

Bushati, N., and Cohen, S. M. (2007). microRNA functions. *Annu. Rev. Cell Dev. Biol.* 23, 175–205. doi: 10.1146/annurev.cellbio.23.090506.123406

Cardinali, B., Castellani, L., Fasanaro, P., Basso, A., Alema, S., Martelli, F., et al. (2009). Microrna-221 and microrna-222 modulate differentiation and maturation of skeletal muscle cells. *PLoS ONE* 4:e7607. doi: 10.1371/journal.pone.0007607

Caretti, G., Schiltz, R. L., Dilworth, F. J., Di Padova, M., Zhao, P., Ogryzko, V., et al. (2006). The RNA helicases p68/p72 and the noncoding RNA SRA are coregulators of MyoD and skeletal muscle differentiation. *Dev. Cell* 11, 547–560. doi: 10.1016/j.devcel.2006.08.003

Cesana, M., Cacchiarelli, D., Legnini, I., Santini, T., Sthandier, O., Chinappi, M., et al. (2011). A long noncoding RNA controls muscle differentiation by functioning as a competing endogenous RNA. *Cell* 147, 358–369. doi: 10.1016/j.cell.2011.09.028

Chen, B., Yu, J., Guo, L., Byers, M. S., Wang, Z., Chen, X., et al. (2019). Circular RNA circHIPK3 promotes the proliferation and differentiation of chicken myoblast cells by sponging miR-30a-3p. *Cells* 8:177. doi: 10.3390/cells8020177

Chen, J. F., Mandel, E. M., Thomson, J. M., Wu, Q., Callis, T. E., Hammond, S. M., et al. (2006). The role of microRNA-1 and microRNA-133 in skeletal muscle proliferation and differentiation. *Nat. Genet.* 38, 228–233. doi: 10.1038/ng1725

Chen, J. F., Tao, Y., Li, J., Deng, Z., Yan, Z., Xiao, X., et al. (2010). microRNA-1 and microRNA-206 regulate skeletal muscle satellite cell proliferation and differentiation by repressing Pax7. *J. Cell Biol.* 190, 867–879. doi: 10.1083/jcb.200911036

Chen, L. L. (2016). Linking long noncoding RNA localization and function. *Trends Biochem. Sci.* 41, 761–772. doi: 10.1016/j.tibs.2016.07.003

Chen, L. L. (2020). The expanding regulatory mechanisms and cellular functions of circular RNAs. *Nat. Rev. Mol. Cell Biol.* 21, 475–490. doi: 10.1038/s41580-020-0243-y

Chen, R., Jiang, T., Lei, S., She, Y., Shi, H., Zhou, S., et al. (2018a). Expression of circular RNAs during C2C12 myoblast differentiation and prediction of coding potential based on the number of open reading frames and N6-methyladenosine motifs. *Cell Cycle* 17, 1832–1845. doi: 10.1080/15384101.2018.1502575

Chen, X., Ouyang, H., Wang, Z., Chen, B., and Nie, Q. (2018b). A novel circular RNA generated by FGFR2 gene promotes myoblast proliferation and differentiation by sponging miR-133a-5p and miR-29b-1-5p. *Cells* 7:199. doi: 10.3390/cells7110199

Cheng, J., Kapranov, P., Drenkow, J., Dike, S., Brubaker, S., Patel, S., et al. (2005). Transcriptional maps of 10 human chromosomes at 5-nucleotide resolution. *Science* 308, 1149–1154. doi: 10.1126/science.1108625

Cheung, T. H., Quach, N. L., Charville, G. W., Liu, L., Park, L., Edalati, A., et al. (2012). Maintenance of muscle stem-cell quiescence by microRNA-489. *Nature* 482, 524–528. doi: 10.1038/nature10834

Cheung, T. H., and Rando, T. A. (2013). Molecular regulation of stem cell quiescence. *Nat. Rev. Mol. Cell Biol.* 14, 329–340. doi: 10.1038/nrm3591

Chevillet, J. R., Kang, Q., Ruf, I. K., Briggs, H. A., Vojtech, L. N., Hughes, S. M., et al. (2014). Quantitative and stoichiometric analysis of the microRNA content of exosomes. *Proc. Natl. Acad. Sci. U.S.A.* 111, 14888–14893. doi: 10.1073/pnas.1408301111

Cho, D. S., and Doles, J. D. (2017). Single cell transcriptome analysis of muscle satellite cells reveals widespread transcriptional heterogeneity. *Gene* 636, 54–63. doi: 10.1016/j.gene.2017.09.014

Cohen, S., Nathan, J. A., and Goldberg, A. L. (2015). Muscle wasting in disease: molecular mechanisms and promising therapies. *Nat. Rev. Drug Discov.* 14, 58–74. doi: 10.1038/nrd4467

Consortium, E. P. (2012). An integrated encyclopedia of DNA elements in the human genome. *Nature* 489, 57–74. doi: 10.1038/nature11247

Cornu, J. N., Terrasa, J. B., Cussenot, O., Haab, F., and Lukacs, B. (2012). Evolution of the landscape of surgical management of prostate cancer in France: the case of radical prostatectomy. *Eur. Urol.* 62, 735–736. doi: 10.1016/j.eururo.2012.06.053

Crist, C. G., Montarras, D., and Buckingham, M. (2012). Muscle satellite cells are primed for myogenesis but maintain quiescence with sequestration of Myf5 mRNA targeted by microRNA-31 in mRNP granules. *Cell Stem Cell* 11, 118–126. doi: 10.1016/j.stem.2012.03.011

Crist, C. G., Montarras, D., Pallafacchina, G., Rocancourt, D., Cumano, A., Conway, S. J., et al. (2009). Muscle stem cell behavior is modified by microRNA-27 regulation of Pax3 expression. *Proc. Natl. Acad. Sci. U.S.A.* 106, 13383–13387. doi: 10.1073/pnas.0900210106

de Gonzalo-Calvo, D., and Thum, T. (2018). Circulating non-coding RNAs as biomarkers to predict and monitor the response to exercise: chances and hurdles. *Eur. Heart J.* 39:3552. doi: 10.1093/eurheartj/ehy457

Derrien, T., Johnson, R., Bussotti, G., Tanzer, A., Djebali, S., Tilgner, H., et al. (2012). The GENCODE v7 catalog of human long noncoding RNAs: analysis of their gene structure, evolution, and expression. *Genome Res.* 22, 1775–1789. doi: 10.1101/gr.132159.111

Dey, B. K., Gagan, J., and Dutta, A. (2011). miR-206 and−486 induce myoblast differentiation by downregulating Pax7. *Mol. Cell. Biol.* 31, 203–214. doi: 10.1128/MCB.01009-10

Dey, B. K., Gagan, J., Yan, Z., and Dutta, A. (2012). miR-26a is required for skeletal muscle differentiation and regeneration in mice. *Genes Dev.* 26, 2180–2191. doi: 10.1101/gad.198085.112

Dey, B. K., Pfeifer, K., and Dutta, A. (2014). The H19 long noncoding RNA gives rise to microRNAs miR-675-3p and miR-675-5p to promote skeletal muscle differentiation and regeneration. *Genes Dev.* 28, 491–501. doi: 10.1101/gad.234419.113

Du, J., Zhang, P., Zhao, X., He, J., Xu, Y., Zou, Q., et al. (2019). MicroRNA-351-5p mediates skeletal myogenesis by directly targeting lactamase-beta and is regulated by lnc-mg. *FASEB J.* 33, 1911–1926. doi: 10.1096/fj.201701394RRR

Engreitz, J. M., Haines, J. E., Perez, E. M., Munson, G., Chen, J., Kane, M., et al. (2016). Local regulation of gene expression by lncRNA promoters, transcription and splicing. *Nature* 539, 452–455. doi: 10.1038/nature20149

Fan, X., Zhang, X., Wu, X., Guo, H., Hu, Y., Tang, F., et al. (2015). Single-cell RNA-seq transcriptome analysis of linear and circular RNAs in mouse preimplantation embryos. *Genome Biol.* 16:148. doi: 10.1186/s13059-015-0706-1

Fang, J., Ma, Q., Chu, C., Huang, B., Li, L., Cai, P., et al. (2019). PIRCh-seq: functional classification of non-coding RNAs associated with distinct histone modifications. *Genome Biol.* 20:292. doi: 10.1186/s13059-019-1880-3

Flynt, A. S., Li, N., Thatcher, E. J., Solnica-Krezel, L., and Patton, J. G. (2007). Zebrafish miR-214 modulates Hedgehog signaling to specify muscle cell fate. *Nat. Genet.* 39, 259–263. doi: 10.1038/ng1953

Forterre, A., Jalabert, A., Berger, E., Baudet, M., Chikh, K., Errazuriz, E., et al. (2014a). Proteomic analysis of C2C12 myoblast and myotube exosome-like vesicles: a new paradigm for myoblast-myotube cross talk? *PLoS ONE* 9:e84153. doi: 10.1371/journal.pone.0084153

Forterre, A., Jalabert, A., Chikh, K., Pesenti, S., Euthine, V., Granjon, A., et al. (2014b). Myotube-derived exosomal miRNAs downregulate Sirtuin1 in myoblasts during muscle cell differentiation. *Cell Cycle* 13, 78–89. doi: 10.4161/cc.26808

Fu, L., Wang, H., Liao, Y., Zhou, P., Xu, Y., Zhao, Y., et al. (2020). miR-208b modulating skeletal muscle development and energy homoeostasis through targeting distinct targets. *RNA Biol.* 17, 743–754. doi: 10.1080/15476286.2020.1728102

Gabory, A., Ripoche, M. A., Le Digarcher, A., Watrin, F., Ziyyat, A., Forne, T., et al. (2009). H19 acts as a trans regulator of the imprinted gene network controlling growth in mice. *Development* 136, 3413–3421. doi: 10.1242/dev.036061

Galimov, A., Merry, T. L., Luca, E., Rushing, E. J., Mizbani, A., Turcekova, K., et al. (2016). MicroRNA-29a in adult muscle stem cells controls skeletal muscle regeneration during injury and exercise downstream of fibroblast growth factor-2. *Stem Cells* 34, 768–780. doi: 10.1002/stem.2281

Ge, Y., Sun, Y., and Chen, J. (2011). IGF-II is regulated by microRNA-125b in skeletal myogenesis. *J. Cell Biol.* 192, 69–81. doi: 10.1083/jcb.201007165

Giraldez, A. J., Cinalli, R. M., Glasner, M. E., Enright, A. J., Thomson, J. M., Baskerville, S., et al. (2005). MicroRNAs regulate brain morphogenesis in zebrafish. *Science* 308, 833–838. doi: 10.1126/science.1109020

Greco, S., Cardinali, B., Falcone, G., and Martelli, F. (2018). Circular RNAs in muscle function and disease. *Int. J. Mol. Sci.* 19:3454. doi: 10.3390/ijms19113454

Grefte, S., Kuijpers-Jagtman, A. M., Torensma, R., and Von den Hoff, J. W. (2007). Skeletal muscle development and regeneration. *Stem Cells Dev.* 16, 857–868. doi: 10.1089/scd.2007.0058

Gros, J., Manceau, M., Thome, V., and Marcelle, C. (2005). A common somitic origin for embryonic muscle progenitors and satellite cells. *Nature* 435, 954–958. doi: 10.1038/nature03572

Grounds, M. D., and Yablonka-Reuveni, Z. (1993). Molecular and cell biology of skeletal muscle regeneration. *Mol. Cell Biol. Hum. Dis. Ser.* 3, 210–256. doi: 10.1007/978-94-011-1528-5_9

Hong, L., Gu, T., He, Y., Zhou, C., Hu, Q., Wang, X., et al. (2019). Genome-Wide Analysis Of Circular RNAs mediated ceRNA regulation in porcine embryonic muscle development. *Front. Cell Dev. Biol.* 7:289. doi: 10.3389/fcell.2019.00289

Horak, M., Novak, J., and Bienertova-Vasku, J. (2016). Muscle-specific microRNAs in skeletal muscle development. *Dev. Biol.* 410, 1–13. doi: 10.1016/j.ydbio.2015.12.013

Hornstein, E., Mansfield, J. H., Yekta, S., Hu, J. K., Harfe, B. D., McManus, M. T., et al. (2005). The microRNA miR-196 acts upstream of Hoxb8 and Shh in limb development. *Nature* 438, 671–674. doi: 10.1038/nature04138

Hou, L., Xu, J., Jiao, Y., Li, H., Pan, Z., Duan, J., et al. (2018). MiR-27b promotes muscle development by inhibiting MDFI expression. *Cell. Physiol. Biochem.* 46, 2271–2283. doi: 10.1159/000489595

Hou, L., Xu, J., Li, H., Ou, J., Jiao, Y., Hu, C., et al. (2017). MiR-34c represses muscle development by forming a regulatory loop with Notch1. *Sci. Rep.* 7:9346. doi: 10.1038/s41598-017-09688-y

Hube, F., Velasco, G., Rollin, J., Furling, D., and Francastel, C. (2011). Steroid receptor RNA activator protein binds to and counteracts SRA RNA-mediated activation of MyoD and muscle differentiation. *Nucleic Acids Res.* 39, 513–525. doi: 10.1093/nar/gkq833

Hudson, M. B., Woodworth-Hobbs, M. E., Zheng, B., Rahnert, J. A., Blount, M. A., Gooch, J. L., et al. (2014). miR-23a is decreased during muscle atrophy by a mechanism that includes calcineurin signaling and exosome-mediated export. *Am. J. Physiol. Cell Physiol.* 306, C551–558. doi: 10.1152/ajpcell.00266.2013

Ivey, K. N., Muth, A., Arnold, J., King, F. W., Yeh, R. F., Fish, J. E., et al. (2008). MicroRNA regulation of cell lineages in mouse and human embryonic stem cells. *Cell Stem Cell* 2, 219–229. doi: 10.1016/j.stem.2008.01.016

Jin, J. J., Lv, W., Xia, P., Xu, Z. Y., Zheng, A. D., Wang, X. J., et al. (2018). Long noncoding RNA SYISL regulates myogenesis by interacting with polycomb repressive complex 2. *Proc. Natl. Acad. Sci. U.S.A.* 115, E9802–E9811. doi: 10.1073/pnas.1801471115

Jin, W., Peng, J., and Jiang, S. (2016). The epigenetic regulation of embryonic myogenesis and adult muscle regeneration by histone methylation modification. *Biochem. Biophys. Rep.* 6, 209–219. doi: 10.1016/j.bbrep.2016.04.009

Juan, A. H., Kumar, R. M., Marx, J. G., Young, R. A., and Sartorelli, V. (2009). Mir-214-dependent regulation of the polycomb protein Ezh2 in skeletal muscle and embryonic stem cells. *Mol. Cell* 36, 61–74. doi: 10.1016/j.molcel.2009.08.008

Kaemmerer, W. F. (2018). How will the field of gene therapy survive its success? *Bioeng. Transl. Med.* 3, 166–177. doi: 10.1002/btm2.10090

Kapranov, P., Cheng, J., Dike, S., Nix, D. A., Duttagupta, R., Willingham, A. T., et al. (2007). RNA maps reveal new RNA classes and a possible function for pervasive transcription. *Science* 316, 1484–1488. doi: 10.1126/science.1138341

Khanna, N., Ge, Y., and Chen, J. (2014). MicroRNA-146b promotes myogenic differentiation and modulates multiple gene targets in muscle cells. *PLoS ONE* 9:e100657. doi: 10.1371/journal.pone.0100657

Kong, D., He, M., Yang, L., Zhou, R., Yan, Y. Q., Liang, Y., et al. (2019). MiR-17 and miR-19 cooperatively promote skeletal muscle cell differentiation. *Cell. Mol. Life Sci.* 76, 5041–5054. doi: 10.1007/s00018-019-03165-7

Kuang, S., Kuroda, K., Le Grand, F., and Rudnicki, M. A. (2007). Asymmetric self-renewal and commitment of satellite stem cells in muscle. *Cell* 129, 999–1010. doi: 10.1016/j.cell.2007.03.044

Le Grand, F., and Rudnicki, M. A. (2007). Skeletal muscle satellite cells and adult myogenesis. *Curr. Opin. Cell Biol.* 19, 628–633. doi: 10.1016/j.ceb.2007.09.012

Lee, K. P., Shin, Y. J., Panda, A. C., Abdelmohsen, K., Kim, J. Y., Lee, S. M., et al. (2015). miR-431 promotes differentiation and regeneration of old skeletal muscle by targeting Smad4. *Genes Dev.* 29, 1605–1617. doi: 10.1101/gad.263574.115

Legnini, I., Di Timoteo, G., Rossi, F., Morlando, M., Briganti, F., Sthandier, O., et al. (2017). Circ-ZNF609 is a circular RNA that can be translated and functions in myogenesis. *Mol. Cell* 66, 22–37 e29. doi: 10.1016/j.molcel.2017.02.017

Legnini, I., Morlando, M., Mangiavacchi, A., Fatica, A., and Bozzoni, I. (2014). A feedforward regulatory loop between HuR and the long noncoding RNA linc-MD1 controls early phases of myogenesis. *Mol. Cell* 53, 506–514. doi: 10.1016/j.molcel.2013.12.012

Li, C., Li, X., Yao, Y., Ma, Q., Ni, W., Zhang, X., et al. (2017). Genome-wide analysis of circular RNAs in prenatal and postnatal muscle of sheep. *Oncotarget* 8, 97165–97177. doi: 10.18632/oncotarget.21835

Li, H., Wei, X., Yang, J., Dong, D., Hao, D., Huang, Y., et al. (2018a). circFGFR4 promotes differentiation of myoblasts via binding miR-107 to relieve its inhibition of Wnt3a. *Mol. Ther. Nucleic Acids* 11, 272–283. doi: 10.1016/j.omtn.2018.02.012

Li, H., Yang, J., Wei, X., Song, C., Dong, D., Huang, Y., et al. (2018b). CircFUT10 reduces proliferation and facilitates differentiation of myoblasts by sponging miR-133a. *J. Cell. Physiol.* 233, 4643–4651. doi: 10.1002/jcp.26230

Li, J., Zhao, W., Li, Q., Huang, Z., Shi, G., and Li, C. (2020a). Long non-coding RNA H19 Promotes porcine satellite cell differentiation by interacting with TDP43. *Genes* 11:259. doi: 10.3390/genes11030259

Li, L., Chen, Y., Nie, L., Ding, X., Zhang, X., Zhao, W., et al. (2019a). MyoD-induced circular RNA CDR1as promotes myogenic differentiation of skeletal muscle satellite cells. *Biochim. Biophys. Acta Gene Regul. Mech.* 1862, 807–821. doi: 10.1016/j.bbagrm.2019.07.001

Li, R., Li, B., Shen, M., Cao, Y., Zhang, X., Li, W., et al. (2020b). LncRNA 2310043L19Rik inhibits differentiation and promotes proliferation of myoblast by sponging miR-125a-5p. *Aging* 12, 5625–5639. doi: 10.18632/aging.102905

Li, X., Li, C., Liu, Z., Ni, W., Yao, R., Xu, Y., et al. (2019b). Circular RNA circ-FoxO3 inhibits myoblast cells differentiation. *Cells* 8:616. doi: 10.3390/cells8060616

Li, X., Yang, L., and Chen, L. L. (2018c). The biogenesis, functions, and challenges of circular RNAs. *Mol. Cell* 71, 428–442. doi: 10.1016/j.molcel.2018.06.034

Li, Z., Cai, B., Abdalla, B. A., Zhu, X., Zheng, M., Han, P., et al. (2019c). LncIRS1 controls muscle atrophy via sponging miR-15 family to activate IGF1-PI3K/AKT pathway. *J. Cachexia Sarcopenia Muscle* 10, 391–410. doi: 10.1002/jcsm.12374

Liang, T., Zhou, B., Shi, L., Wang, H., Chu, Q., Xu, F., et al. (2018). lncRNA AK017368 promotes proliferation and suppresses differentiation of myoblasts in skeletal muscle development by attenuating the function of miR-30c. *FASEB J.* 32, 377–389. doi: 10.1096/fj.201700560rr

Lin, C. Y., Chen, J. S., Loo, M. R., Hsiao, C. C., Chang, W. Y., and Tsai, H. J. (2013). MicroRNA-3906 regulates fast muscle differentiation through modulating the target gene homer-1b in zebrafish embryos. *PLoS ONE* 8:e70187. doi: 10.1371/journal.pone.0070187

Ling, Y. H., Sui, M. H., Zheng, Q., Wang, K. Y., Wu, H., Li, W. Y., et al. (2018). miR-27b regulates myogenic proliferation and differentiation by targeting Pax3 in goat. *Sci. Rep.* 8:3909. doi: 10.1038/s41598-018-22262-4

Liu, N., Williams, A. H., Maxeiner, J. M., Bezprozvannaya, S., Shelton, J. M., Richardson, J. A., et al. (2012). microRNA-206 promotes skeletal muscle regeneration and delays progression of Duchenne muscular dystrophy in mice. *J. Clin. Invest.* 122, 2054–2065. doi: 10.1172/JCI62656

Lozano-Velasco, E., Vallejo, D., Esteban, F. J., Doherty, C., Hernandez-Torres, F., Franco, D., et al. (2015). A Pitx2-microRNA pathway modulates cell proliferation in myoblasts and skeletal-muscle satellite cells and promotes their commitment to a myogenic cell fate. *Mol. Cell. Biol.* 35, 2892–2909. doi: 10.1128/MCB.00536-15

Luo, W., Li, G., Yi, Z., Nie, Q., and Zhang, X. (2016). E2F1-miR-20a-5p/20b-5p auto-regulatory feedback loop involved in myoblast proliferation and differentiation. *Sci. Rep.* 6:27904. doi: 10.1038/srep27904

Luo, W., Wu, H., Ye, Y., Li, Z., Hao, S., Kong, L., et al. (2014). The transient expression of miR-203 and its inhibiting effects on skeletal muscle cell proliferation and differentiation. *Cell Death Dis.* 5:e1347. doi: 10.1038/cddis.2014.289

Martinet, C., Monnier, P., Louault, Y., Benard, M., Gabory, A., and Dandolo, L. (2016). H19 controls reactivation of the imprinted gene network during muscle regeneration. *Development* 143, 962–971. doi: 10.1242/dev.131771

Matsumoto, A., Pasut, A., Matsumoto, M., Yamashita, R., Fung, J., Monteleone, E., et al. (2017). mTORC1 and muscle regeneration are regulated by the LINC00961-encoded SPAR polypeptide. *Nature* 541, 228–232. doi: 10.1038/nature21034

Matsumura, K., Tome, F. M., Collin, H., Leturcq, F., Jeanpierre, M., Kaplan, J. C., et al. (1994). Expression of dystrophin-associated proteins in dystrophin-positive muscle fibers (revertants) in Duchenne muscular dystrophy. *Neuromuscul. Disord.* 4, 115–120. doi: 10.1016/0960-8966(94)90002-7

Mattick, J. S. (2005). The functional genomics of noncoding RNA. *Science* 309, 1527–1528. doi: 10.1126/science.1117806

Mauro, A. (1961). Satellite cell of skeletal muscle fibers. *J. Biophys. Biochem. Cytol.* 9, 493–495. doi: 10.1083/jcb.9.2.493

Memczak, S., Jens, M., Elefsinioti, A., Torti, F., Krueger, J., Rybak, A., et al. (2013). Circular RNAs are a large class of animal RNAs with regulatory potency. *Nature* 495, 333–338. doi: 10.1038/nature11928

Mishima, Y., Abreu-Goodger, C., Staton, A. A., Stahlhut, C., Shou, C., Cheng, C., et al. (2009). Zebrafish miR-1 and miR-133 shape muscle gene expression and regulate sarcomeric actin organization. *Genes Dev.* 23, 619–632. doi: 10.1101/gad.1760209

Mok, G. F., Lozano-Velasco, E., Maniou, E., Viaut, C., Moxon, S., Wheeler, G., et al. (2018). miR-133-mediated regulation of the Hedgehog pathway orchestrates embryo myogenesis. *Development* 145:dev159657. doi: 10.1242/dev.159657

Mok, G. F., Lozano-Velasco, E., and Munsterberg, A. (2017). microRNAs in skeletal muscle development. *Semin. Cell Dev. Biol.* 72, 67–76. doi: 10.1016/j.semcdb.2017.10.032

Motohashi, N., Alexander, M. S., Shimizu-Motohashi, Y., Myers, J. A., Kawahara, G., and Kunkel, L. M. (2013). Regulation of IRS1/Akt insulin signaling by microRNA-128a during myogenesis. *J. Cell Sci.* 126(Pt 12), 2678–2691. doi: 10.1242/jcs.119966

Naguibneva, I., Ameyar-Zazoua, M., Polesskaya, A., Ait-Si-Ali, S., Groisman, R., Souidi, M., et al. (2006). The microRNA miR-181 targets the homeobox protein Hox-A11 during mammalian myoblast differentiation. *Nat. Cell Biol.* 8, 278–284. doi: 10.1038/ncb1373

Nakamura, Y., Miyaki, S., Ishitobi, H., Matsuyama, S., Nakasa, T., Kamei, N., et al. (2015). Mesenchymal-stem-cell-derived exosomes accelerate skeletal muscle regeneration. *FEBS Lett.* 589, 1257–1265. doi: 10.1016/j.febslet.2015.03.031

Nelson, B. R., Makarewich, C. A., Anderson, D. M., Winders, B. R., Troupes, C. D., Wu, F., et al. (2016). A peptide encoded by a transcript annotated as long noncoding RNA enhances SERCA activity in muscle. *Science* 351, 271–275. doi: 10.1126/science.aad4076

Neppl, R. L., Wu, C. L., and Walsh, K. (2017). lncRNA Chronos is an aging-induced inhibitor of muscle hypertrophy. *J. Cell Biol.* 216, 3497–3507. doi: 10.1083/jcb.201612100

Nunnari, J., and Suomalainen, A. (2012). Mitochondria: in sickness and in health. *Cell* 148, 1145–1159. doi: 10.1016/j.cell.2012.02.035

O'Brien, J. H., Hernandez-Lagunas, L., Artinger, K. B., and Ford, H. L. (2014). MicroRNA-30a regulates zebrafish myogenesis through targeting the transcription factor Six1. *J. Cell Sci.* 127(Pt 10), 2291–2301. doi: 10.1242/jcs.143677

O'Rourke, J. R., Georges, S. A., Seay, H. R., Tapscott, S. J., McManus, M. T., Goldhamer, D. J., et al. (2007). Essential role for Dicer during skeletal muscle development. *Dev. Biol.* 311, 359–368. doi: 10.1016/j.ydbio.2007.08.032

Ouyang, H., Chen, X., Li, W., Li, Z., Nie, Q., and Zhang, X. (2018a). Circular RNA circSVIL promotes myoblast proliferation and differentiation by sponging miR-203 in chicken. *Front. Genet.* 9:172. doi: 10.3389/fgene.2018.00172

Ouyang, H., Chen, X., Wang, Z., Yu, J., Jia, X., Li, Z., et al. (2018b). Circular RNAs are abundant and dynamically expressed during embryonic muscle development in chickens. *DNA Res.* 25, 71–86. doi: 10.1093/dnares/dsx039

Panda, A. C., Grammatikakis, I., Munk, R., Gorospe, M., and Abdelmohsen, K. (2017). Emerging roles and context of circular RNAs. *Wiley Interdiscip. Rev. RNA* 8:e1386. doi: 10.1002/wrna.1386

Pandey, P. R., Yang, J. H., Tsitsipatis, D., Panda, A. C., Noh, J. H., Kim, K. M., et al. (2020). circSamd4 represses myogenic transcriptional activity of PUR proteins. *Nucleic Acids Res.* 48, 3789–3805. doi: 10.1093/nar/gkaa035

Pauli, A., Rinn, J. L., and Schier, A. F. (2011). Non-coding RNAs as regulators of embryogenesis. *Nat. Rev. Genet.* 12, 136–149. doi: 10.1038/nrg2904

Pauli, A., Valen, E., Lin, M. F., Garber, M., Vastenhouw, N. L., Levin, J. Z., et al. (2012). Systematic identification of long noncoding RNAs expressed during zebrafish embryogenesis. *Genome Res.* 22, 577–591. doi: 10.1101/gr.133009.111

Peng, S., Song, C., Li, H., Cao, X., Ma, Y., Wang, X., et al. (2019). Circular RNA SNX29 sponges miR-744 to regulate proliferation and differentiation of myoblasts by activating the Wnt5a/Ca(2+) signaling pathway. *Mol. Ther. Nucleic Acids* 16, 481–493. doi: 10.1016/j.omtn.2019.03.009

Poirier, F., Chan, C. T., Timmons, P. M., Robertson, E. J., Evans, M. J., and Rigby, P. W. (1991). The murine H19 gene is activated during embryonic stem cell differentiation *in vitro* and at the time of implantation in the developing embryo. *Development* 113, 1105–1114.

Porpiglia, E., Samusik, N., Ho, A. T. V., Cosgrove, B. D., Mai, T., Davis, K. L., et al. (2017). High-resolution myogenic lineage mapping by single-cell mass cytometry. *Nat. Cell Biol.* 19, 558–567. doi: 10.1038/ncb3507

Qiu, H., Liu, N., Luo, L., Zhong, J., Tang, Z., Kang, K., et al. (2016). MicroRNA-17-92 regulates myoblast proliferation and differentiation by targeting the ENH1/Id1 signaling axis. *Cell Death Differ.* 23, 1658–1669. doi: 10.1038/cdd.2016.56

Qu, L., Ding, J., Chen, C., Wu, Z. J., Liu, B., Gao, Y., et al. (2016). Exosome-transmitted lncARSR promotes sunitinib resistance in renal cancer by acting as a competing endogenous RNA. *Cancer Cell* 29, 653–668. doi: 10.1016/j.ccell.2016.03.004

Quinn, J. J., and Chang, H. Y. (2016). Unique features of long non-coding RNA biogenesis and function. *Nat. Rev. Genet.* 17, 47–62. doi: 10.1038/nrg.2015.10

Rackham, O., Shearwood, A. M., Mercer, T. R., Davies, S. M., Mattick, J. S., and Filipovska, A. (2011). Long noncoding RNAs are generated from the mitochondrial genome and regulated by nuclear-encoded proteins. *RNA* 17, 2085–2093. doi: 10.1261/rna.029405.111

Raposo, G., and Stoorvogel, W. (2013). Extracellular vesicles: exosomes, microvesicles, and friends. *J. Cell Biol.* 200, 373–383. doi: 10.1083/jcb.201211138

Relaix, F., and Zammit, P. S. (2012). Satellite cells are essential for skeletal muscle regeneration: the cell on the edge returns centre stage. *Development* 139, 2845–2856. doi: 10.1242/dev.069088

Ren, J., Ding, L., Zhang, D., Shi, G., Xu, Q., Shen, S., et al. (2018). Carcinoma-associated fibroblasts promote the stemness and chemoresistance of colorectal cancer by transferring exosomal lncRNA H19. *Theranostics* 8, 3932–3948. doi: 10.7150/thno.25541

Ro, S., Ma, H. Y., Park, C., Ortogero, N., Song, R., Hennig, G. W., et al. (2013). The mitochondrial genome encodes abundant small noncoding RNAs. *Cell Res.* 23, 759–774. doi: 10.1038/cr.2013.37

Roberts, T. C. (2014). The MicroRNA biology of the mammalian nucleus. *Mol. Ther. Nucleic Acids* 3:e188. doi: 10.1038/mtna.2014.40

Rocheteau, P., Gayraud-Morel, B., Siegl-Cachedenier, I., Blasco, M. A., and Tajbakhsh, S. (2012). A subpopulation of adult skeletal muscle stem cells retains all template DNA strands after cell division. *Cell* 148, 112–125. doi: 10.1016/j.cell.2011.11.049

Romancino, D. P., Paterniti, G., Campos, Y., De Luca, A., Di Felice, V., d'Azzo, A., et al. (2013). Identification and characterization of the nano-sized vesicles released by muscle cells. *FEBS Lett.* 587, 1379–1384. doi: 10.1016/j.febslet.2013.03.012

Sacheck, J. M., Hyatt, J. P., Raffaello, A., Jagoe, R. T., Roy, R. R., Edgerton, V. R., et al. (2007). Rapid disuse and denervation atrophy involve transcriptional changes similar to those of muscle wasting during systemic diseases. *FASEB J.* 21, 140–155. doi: 10.1096/fj.06-6604com

Salzman, J., Gawad, C., Wang, P. L., Lacayo, N., and Brown, P. O. (2012). Circular RNAs are the predominant transcript isoform from hundreds of human genes in diverse cell types. *PLoS ONE* 7:e30733. doi: 10.1371/journal.pone.0030733

Sambasivan, R., and Tajbakhsh, S. (2007). Skeletal muscle stem cell birth and properties. *Semin. Cell Dev. Biol.* 18, 870–882. doi: 10.1016/j.semcdb.2007.09.013

Sato, T., Yamamoto, T., and Sehara-Fujisawa, A. (2014). miR-195/497 induce postnatal quiescence of skeletal muscle stem cells. *Nat. Commun.* 5:4597. doi: 10.1038/ncomms5597

Schraivogel, D., and Meister, G. (2014). Import routes and nuclear functions of Argonaute and other small RNA-silencing proteins. *Trends Biochem. Sci.* 39, 420–431. doi: 10.1016/j.tibs.2014.07.004

Seok, H. Y., Tatsuguchi, M., Callis, T. E., He, A., Pu, W. T., and Wang, D. Z. (2011). miR-155 inhibits expression of the MEF2A protein to repress skeletal muscle differentiation. *J. Biol. Chem.* 286, 35339–35346. doi: 10.1074/jbc.M111.273276

Shen, X., Liu, Z., Cao, X., He, H., Han, S., Chen, Y., et al. (2019). Circular RNA profiling identified an abundant circular RNA circTMTC1 that inhibits chicken skeletal muscle satellite cell differentiation by sponging miR-128-3p. *Int. J. Biol. Sci.* 15, 2265–2281. doi: 10.7150/ijbs.36412

Shen, X., Zhang, X., Ru, W., Huang, Y., Lan, X., Lei, C., et al. (2020). circINSR promotes proliferation and reduces apoptosis of embryonic myoblasts by sponging miR-34a. *Mol. Ther. Nucleic Acids* 19, 986–999. doi: 10.1016/j.omtn.2019.12.032

Shin, Y. J., Kwon, E. S., Lee, S. M., Kim, S. K., Min, K. W., Lim, J. Y., et al. (2020). A subset of microRNAs in the Dlk1-Dio3 cluster regulates age-associated muscle atrophy by targeting Atrogin-1. *J. Cachexia Sarcopenia Muscle* 11, 1336–1350. doi: 10.1002/jcsm.12578

Sokol, N. S. (2012). The role of microRNAs in muscle development. *Curr. Top. Dev. Biol.* 99, 59–78. doi: 10.1016/B978-0-12-387038-4.00003-3

Sokol, N. S., and Ambros, V. (2005). Mesodermally expressed Drosophila microRNA-1 is regulated by Twist and is required in muscles during larval growth. *Genes Dev.* 19, 2343–2354. doi: 10.1101/gad.1356105

Song, Z., Liu, Y., Fang, X., Xie, M., Ma, Z., Zhong, Z., et al. (2020). Comprehensive analysis of the expression profile of circRNAs and their predicted protein-coding ability in the muscle of mdx mice. *Funct. Integr. Genomics* 20, 397–407. doi: 10.1007/s10142-019-00724-w

Struhl, K. (2007). Transcriptional noise and the fidelity of initiation by RNA polymerase II. *Nat. Struct. Mol. Biol.* 14, 103–105. doi: 10.1038/nsmb0207-103

Sui, M., Zheng, Q., Wu, H., Zhu, L., Ling, Y., Wang, L., et al. (2020). The expression and regulation of miR-1 in goat skeletal muscle and satellite cell during muscle growth and development. *Anim. Biotechnol.* 31, 455–462. doi: 10.1080/10495398.2019.1622555

Sun, L., Si, M., Liu, X., Choi, J. M., Wang, Y., Thomas, S. S., et al. (2018). Long-noncoding RNA Atrolnc-1 promotes muscle wasting in mice with chronic kidney disease. *J. Cachexia Sarcopenia Muscle* 9, 962–974. doi: 10.1002/jcsm.12321

Surono, A., Takeshima, Y., Wibawa, T., Ikezawa, M., Nonaka, I., and Matsuo, M. (1999). Circular dystrophin RNAs consisting of exons that were skipped by alternative splicing. *Hum. Mol. Genet.* 8, 493–500. doi: 10.1093/hmg/8.3.493

Sweetman, D., Goljanek, K., Rathjen, T., Oustanina, S., Braun, T., Dalmay, T., et al. (2008). Specific requirements of MRFs for the expression of muscle specific microRNAs, miR-1, miR-206 and miR-133. *Dev. Biol.* 321, 491–499. doi: 10.1016/j.ydbio.2008.06.019

Sweetman, D., Rathjen, T., Jefferson, M., Wheeler, G., Smith, T. G., Wheeler, G. N., et al. (2006). FGF-4 signaling is involved in mir-206 expression in developing somites of chicken embryos. *Dev. Dyn.* 235, 2185–2191. doi: 10.1002/dvdy.20881

Sweta, S., Dudnakova, T., Sudheer, S., Baker, A. H., and Bhushan, R. (2019). Importance of long non-coding RNAs in the development and disease of skeletal muscle and cardiovascular lineages. *Front. Cell Dev. Biol.* 7:228. doi: 10.3389/fcell.2019.00228

Tajbakhsh, S. (2009). Skeletal muscle stem cells in developmental vs. regenerative myogenesis. *J. Intern. Med* 266, 372–389. doi: 10.1111/j.1365-2796.2009.02158.x

Tajbakhsh, S. (2017). lncRNA-encoded polypeptide SPAR(s) with mTORC1 to regulate skeletal muscle regeneration. *Cell Stem Cell* 20, 428–430. doi: 10.1016/j.stem.2017.03.016

van Rooij, E., Quiat, D., Johnson, B. A., Sutherland, L. B., Qi, X., Richardson, J. A., et al. (2009). A family of microRNAs encoded by myosin genes governs myosin expression and muscle performance. *Dev. Cell* 17, 662–673. doi: 10.1016/j.devcel.2009.10.013

Vergara, H. M., Ramirez, J., Rosing, T., Nave, C., Blandino, R., Saw, D., et al. (2018). miR-206 is required for changes in cell adhesion that drive muscle cell morphogenesis in *Xenopus laevis*. *Dev. Biol.* 438, 94–110. doi: 10.1016/j.ydbio.2018.03.021

Wada, S., Kato, Y., Okutsu, M., Miyaki, S., Suzuki, K., Yan, Z., et al. (2011). Translational suppression of atrophic regulators by microRNA-23a integrates resistance to skeletal muscle atrophy. *J. Biol. Chem.* 286, 38456–38465. doi: 10.1074/jbc.M111.271270

Walters, J. (2017). Muscle hypertrophy and pseudohypertrophy. *Pract. Neurol.* 17, 369–379. doi: 10.1136/practneurol-2017-001695

Wang, J., Tan, J., Qi, Q., Yang, L., Wang, Y., Zhang, C., et al. (2018). miR-487b-3p suppresses the proliferation and differentiation of myoblasts by targeting IRS1 in skeletal muscle myogenesis. *Int. J. Biol. Sci.* 14, 760–774. doi: 10.7150/ijbs.25052

Wang, X., Cao, X., Dong, D., Shen, X., Cheng, J., Jiang, R., et al. (2019a). Circular RNA TTN acts as a miR-432 sponge to facilitate proliferation and differentiation of myoblasts via the IGF2/PI3K/AKT signaling pathway. *Mol. Ther. Nucleic Acids* 18, 966–980. doi: 10.1016/j.omtn.2019.10.019

Wang, Y., Li, M., Wang, Y., Liu, J., Zhang, M., Fang, X., et al. (2019b). A Zfp609 circular RNA regulates myoblast differentiation by sponging miR-194-5p. *Int. J. Biol. Macromol.* 121, 1308–1313. doi: 10.1016/j.ijbiomac.2018.09.039

Wei, X., Li, H., Zhang, B., Li, C., Dong, D., Lan, X., et al. (2016). miR-378a-3p promotes differentiation and inhibits proliferation of myoblasts by targeting HDAC4 in skeletal muscle development. *RNA Biol.* 13, 1300–1309. doi: 10.1080/15476286.2016.1239008

Yao, R., Yao, Y., Li, C., Li, X., Ni, W., Quan, R., et al. (2020). Circ-HIPK3 plays an active role in regulating myoblast differentiation. *Int. J. Biol. Macromol.* 155, 1432–1439. doi: 10.1016/j.ijbiomac.2019.11.119

Yin, H., He, H., Shen, X., Zhao, J., Cao, X., Han, S., et al. (2020). miR-9-5p inhibits skeletal muscle satellite cell proliferation and differentiation by targeting IGF2BP3 through the IGF2-PI3K/Akt signaling pathway. *Int. J. Mol. Sci.* 21:1655. doi: 10.3390/ijms21051655

Yu, X., Zhang, Y., Li, T., Ma, Z., Jia, H., Chen, Q., et al. (2017). Long non-coding RNA Linc-RAM enhances myogenic differentiation by interacting with MyoD. *Nat. Commun.* 8:14016. doi: 10.1038/ncomms14016

Yue, B., Wang, J., Ru, W., Wu, J., Cao, X., Yang, H., et al. (2020a). The circular RNA circHUWE1 sponges the miR-29b-AKT3 axis to regulate myoblast development. *Mol. Ther. Nucleic Acids* 19, 1086–1097. doi: 10.1016/j.omtn.2019.12.039

Yue, B., Yang, H., Wang, J., Ru, W., Wu, J., Huang, Y., et al. (2020b). Exosome biogenesis, secretion and function of exosomal miRNAs in skeletal muscle myogenesis. *Cell Prolif.* 53:e12857. doi: 10.1111/cpr.12857

Zammit, P. S. (2017). Function of the myogenic regulatory factors Myf5, MyoD, Myogenin and MRF4 in skeletal muscle, satellite cells and regenerative myogenesis. *Semin. Cell Dev. Biol.* 72, 19–32. doi: 10.1016/j.semcdb.2017.11.011

Zammit, P. S., Partridge, T. A., and Yablonka-Reuveni, Z. (2006). The skeletal muscle satellite cell: the stem cell that came in from the cold. *J. Histochem. Cytochem.* 54, 1177–1191. doi: 10.1369/jhc.6R6995.2006

Zhang, P., Xu, H., Li, R., Wu, W., Chao, Z., Li, C., et al. (2018a). Assessment of myoblast circular RNA dynamics and its correlation with miRNA during myogenic differentiation. *Int. J. Biochem. Cell Biol.* 99, 211–218. doi: 10.1016/j.biocel.2018.04.016

Zhang, X., Wang, W., Zhu, W., Dong, J., Cheng, Y., Yin, Z., et al. (2019). Mechanisms and functions of long non-coding RNAs at multiple regulatory levels. *Int. J. Mol. Sci.* 20:5573. doi: 10.3390/ijms20225573

Zhang, X., Zuo, X., Yang, B., Li, Z., Xue, Y., Zhou, Y., et al. (2014). MicroRNA directly enhances mitochondrial translation during muscle differentiation. *Cell* 158, 607–619. doi: 10.1016/j.cell.2014.05.047

Zhang, Z. K., Li, J., Guan, D., Liang, C., Zhuo, Z., Liu, J., et al. (2018b). A newly identified lncRNA MAR1 acts as a miR-487b sponge to promote skeletal muscle differentiation and regeneration. *J. Cachexia Sarcopenia Muscle* 9, 613–626. doi: 10.1002/jcsm.12281

Zhou, L., Sun, K., Zhao, Y., Zhang, S., Wang, X., Li, Y., et al. (2015). Linc-YY1 promotes myogenic differentiation and muscle regeneration through an interaction with the transcription factor YY1. *Nat. Commun.* 6:10026. doi: 10.1038/ncomms10026

Zhou, S., Li, S., Zhang, W., Tong, H., Li, S., and Yan, Y. (2018). MiR-139 promotes differentiation of bovine skeletal muscle-derived satellite cells by regulating DHFR gene expression. *J. Cell. Physiol.* 234, 632–641. doi: 10.1002/jcp.26817

Zhu, M., Liu, J., Xiao, J., Yang, L., Cai, M., Shen, H., et al. (2017). Lnc-mg is a long non-coding RNA that promotes myogenesis. *Nat. Commun.* 8:14718. doi: 10.1038/ncomms14718

Zierath, J. R., and Hawley, J. A. (2004). Skeletal muscle fiber type: influence on contractile and metabolic properties. *PLoS Biol.* 2:e348. doi: 10.1371/journal.pbio.0020348

Conflict of Interest: The authors declare that the research was conducted in the absence of any commercial or financial relationships that could be construed as a potential conflict of interest.

frontiers in Cell and Developmental Biology

ORIGINAL RESEARCH
published: 04 February 2021
doi: 10.3389/fcell.2021.607332

The BMP2 Signaling Axis Promotes Invasive Differentiation of Human Trophoblasts

Jiali You[1,2†], Wei Wang[1†], Hsun-Ming Chang[2], Yuyin Yi[2], Hongjin Zhao[2], Hua Zhu[2], Yu Sun[1], Minyue Tang[1], Chunyan Wang[1], Yimiao Sang[1], Guofang Feng[1], Shaobing Cheng[3], Peter C. K. Leung[2] and Yi-Min Zhu[1]**

[1] Department of Reproductive Endocrinology, School of Medicine, Women's Hospital, Zhejiang University, Hangzhou, China, [2] Department of Obstetrics and Gynaecology, BC Children's Hospital Research Institute, University of British Columbia, Vancouver, BC, Canada, [3] Department of Colorectal Surgery, School of Medicine, The First Affiliated Hospital, Zhejiang University, Hangzhou, China

OPEN ACCESS

Edited by:
Linjun Hong,
South China Agricultural University, China

Reviewed by:
Eva Dimitriadis,
University of Melbourne, Australia
Suk-Won Jin,
Gwangju Institute of Science and Technology, South Korea

***Correspondence:**
Peter C. K. Leung
peter.leung@ubc.ca
Yi-Min Zhu
zhuyim@zju.edu.cn

† These authors have contributed equally to this work

Specialty section:
This article was submitted to Cell Growth and Division, a section of the journal Frontiers in Cell and Developmental Biology

Received: 16 September 2020
Accepted: 11 January 2021
Published: 04 February 2021

Citation:
You J, Wang W, Chang H-M, Yi Y, Zhao H, Zhu H, Sun Y, Tang M, Wang C, Sang Y, Feng G, Cheng S, Leung PCK and Zhu Y-M (2021) The BMP2 Signaling Axis Promotes Invasive Differentiation of Human Trophoblasts. Front. Cell Dev. Biol. 9:607332. doi: 10.3389/fcell.2021.607332

Embryo implantation and trophoblast invasion are principal limiting factors of pregnancy establishment. Aberrant embryo development or improper trophoblast differentiation and invasion may lead to various unfavorable pregnancy-related outcomes, including early pregnancy loss (EPL). Our clinical data show that the serum BMP2 levels were significantly increased during the first trimester of pregnancy and that the serum and BMP2 expression levels were lower in women with EPL than in women with normal early pregnancies. Moreover, we observed that BMP2 was expressed in oocytes and trophoblast cells of cleaved embryos and blastocysts prior to implantation in both humans and mice. Exogenous BMP2 promoted embryonic development by enhancing blastocyst formation and hatching in mice. LncRNA NR026833.1 was upregulated by BMP2 and promoted SNAIL expression by competitively binding to miR-502-5p. SNAIL induced MMP2 expression and promoted cell invasion in primary extravillous trophoblast cells. BMP2 promotes the invasive differentiation of mouse trophoblast stem cells by downregulating the expression of TS cell marker and upregulating the expression of trophoblast giant cell marker and labyrinthine/spongiotrophoblast marker. Our findings provide significant insights into the regulatory roles of BMP2 in the development of the placenta, which may give us a framework to explore new therapeutic strategies to pregnancy-related complications.

Keywords: BMP2, early pregnancy loss, trophoblast invasion, trophoblast differentiation, embryo development, lncRNA

INTRODUCTION

Implantation of a competent blastocyst into a receptive uterus is key for the establishment of pregnancy. Upon implantation, the outer monolayer of the blastocyst, consisting of trophectodermal (TE) cells, generates the first trophoblast lineages, which develop into diverse trophoblast cell types (Bianchi et al., 1993). Additionally, the inner cell mass (ICM) of the blastocyst develops into the second bilaminar extraembryonic tissue that gives rise to the embryo proper in mice and humans (Gardner, 1982; Stirparo et al., 2018). With the process of epithelial-mesenchymal transition (EMT), some TE cells develop into cytotrophoblast cells to form cell columns connecting

to the endometrium. Extravillous trophoblasts (EVTs) are derived from cytotrophoblast cells in the anchoring columns under the influence of growth factors and cytokines derived from many cells, including decidual macrophages, uterine NK cells and stromal cells. After migration from the attached embryo, these highly invasive EVTs appropriately invade the uterine epithelium and uterine spiral arteries, a process that is indispensable for proper placentation and successful establishment of mammalian pregnancy (Wehrum et al., 2011; Gupta et al., 2016). In humans, the occurrence of EVT invasion in the endometrial stroma and myometrium (inner third) is critical for developing definitive maternal-fetal circulation and successful pregnancy (Cakmak and Taylor, 2011). Aberrant trophoblast (EVT or syncytiotrophoblast) differentiation or improper trophoblast invasion may lead to various unfavorable pregnancy-related outcomes, including early pregnancy loss (EPL), preeclampsia, intrauterine growth restriction, and choriocarcinoma (Brosens et al., 2011).

Given the complexity of embryo implantation and early placental development, it is likely that many mechanisms are involved in the pathophysiology of EPL. In the specimens obtained from EPL, the trophoblastic shell is thin and fragmented, and trophoblast infiltration around the lumen of the endometrial vessels and decidua is reduced. Placentation failure can be a primary event, as a result of a major chromosomal abnormality, or can be a secondary event as a result of early fetal demise due to a major developmental abnormality. Previous studies have shown that the degree of placentation defects and trophoblast apoptosis is increased in EPL, independent of the presence or absence of a chromosomal abnormality (Greenwold et al., 2003; Hempstock et al., 2003). Hence, a comprehensive understanding of the molecular mechanisms underlying trophoblast invasion is essential for improving the diagnosis and treatment of EPL.

As the largest subfamily of the transforming growth factor β (TGF-β) superfamily, bone morphogenetic proteins (BMPs) are essential promoting factors for organogenesis, including placental development (Shimasaki et al., 2004). Among the BMP members, BMP2 is detected in the murine endometrium during the period of decidualization and pregnancy establishment. The spatiotemporal expression of BMP2, which is correlated with mouse embryo implantation at the maternal-fetal interface, suggests that BMP2 plays an important role in the regulation of embryo implantation and early placentation (Ying and Zhao, 2000; Paria et al., 2001). In mice, conditional depletion of *Bmp2* in the uterus showed that the uterine stroma is incapable of undergoing decidualization to support further placental development, leading to sterility (Lee et al., 2007). Similarly, conditional depletion of the type II receptor for BMP2 (*Bmpr2*) in the mouse uterus resulted in fetal growth retardation and severe hemorrhage at the implantation sites, which subsequently caused fetal demise and placental abruption (Nagashima et al., 2013). Furthermore, the proinvasive effects of BMP2 have been reported in the EMT-related carcinogenesis of various cancers including breast, colon, gastric, and pancreatic cancers (Clement et al., 2005; Kang et al., 2010; Chen et al., 2011; Kim et al., 2015; Yang et al., 2015). Our previous studies revealed that BNP2 is expressed at a high level in primary human EVT cells and that BMP2 promotes the cell invasion of human trophoblast cells (Zhao et al., 2018a,b, 2020). Despite the essential role of BMP2 in the regulation of human trophoblast invasion, the precise molecular mechanisms by which BMP2 regulates trophoblast invasion remain largely unknown. Furthermore, the results obtained from conditional ablation of *Bmp2* in the uterus have indicated the critical role of BMP2 in regulating the transformation of the uterine stroma during embryo implantation in the mouse (Lee et al., 2007). However, it is unclear whether BMP2 is involved in the development of fetoplacental connections and the pathogenesis of EPL. The objective of this study was to use clinical samples and *in vitro* functional studies with human and mouse cells to investigate the expression, functional role and underlying molecular mechanisms of BMP2 in the regulation of trophoblast differentiation and invasion. Additionally, we aimed to obtain comprehensive information on the involvement of BMP2 in the pathogenesis of EPL (pregnancy loss at 5–8 weeks) and identify a therapeutic target for this pregnancy complication.

MATERIALS AND METHODS

Subjects and Samples Collection

From October 2017 to April 2018, fifty healthy non-pregnant (Non-P) women were recruited as the control group; fifty pregnant women with a diagnosis of EPL attending Women's Hospital, School of Medicine, Zhejiang University, Hangzhou, Zhejiang, China, were recruited as the study group. These pregnant women had vaginal bleeding and/or lower abdominal pain for the first time in the previous few days (0–2 days). The diagnosis of EPL was based on the clinical history, clinical examination, and transvaginal ultrasound (TVU) results. In cases where pregnancy structures (a gestational sac without fetal heart rate) were identified by TVU, the final diagnosis of EPL was made. Inclusion criteria were a gestational age between 5 and 8 weeks (based on the first day of the last menstrual period) and no history of recurrent spontaneous abortions, chromosomal abnormalities, endocrine diseases, anatomical abnormalities of the genital tract, infections, immunological diseases, trauma, internal diseases, or any chemical agent intake before their elective terminations; fifty age-matched women with a normal pregnancy (NP) who were undergoing terminations of pregnancy for psychological reasons at the same gestational age were designated the control pregnancy group. Blood samples were collected in EDTA-containing tubes (BD, Franklin Lakes, NJ, United States) and serum was isolated within 1 h by centrifugation at 1,900 × g for 10 min at 4°C to remove blood cells, and then at 16,000 × g for 10 min at 4°C to remove additional cellular nucleic acids attached to cell debris. Samples were stored at −80°C prior to analysis. Placental villous tissues were taken through the cervix during dilatation and aspiration according to strict clinical procedures. Embryos with arrested development or poor preimplantation morphology (zygotes, 4-cell stage, 8–16-cell stage, morulas, and blastocysts) that cannot to be used for transfer from assisted reproductive technology (IVF) patients were collected. Informed consent was obtained from each woman for the use of blood

samples, placental villous tissue, and embryos, and the study was approved by the Ethical Review Committee of Women's Hospital, Zhejiang University School of Medicine. All the samples were stored at −80℃ or fixed in 4% formaldehyde until use.

Measurement of BMP2 and MMP2 Activity

The BMP2 levels were quantified using a commercially available ELISA kit (Quantikine, BMP2 Immunoassay, R&D Systems, MN, United States). The MMP2 activity was measured using a commercially available ELISA kit (Quantikine, MMP2 Immunoassay, R&D Systems). All samples were assayed according to the manufacturer's instructions and were tested in duplicate by personnel blinded to each patient group. The optical density of each well was determined using a microplate reader at an absorbance of 450 nm. No interference and no cross-reactivity were expected based on the manufacturer's instructions. The minimum detectable dose (MDD) of BMP2 ELISA ranged from 4.3 to 29 pg/mL. The mean MDD was 11 pg/mL. The dynamic range of BMP2 ELISA ranged from 62.5 to 4,000 pg/mL. The mean MDD of MMP2 was 28.8 pg/mL. The dynamic range of MMP2 ELISA ranged from 28.2 to 43,070 pg/mL.

First-Strand cDNA Synthesis and qPCR

Total RNA was extracted using TRIzol reagent (Life Technologies) following the manufacturer's instructions. RNA concentrations were measured by absorbance at a 260 nm wavelength using a NanoDrop 2,000 Spectrophotometer (Thermo Fisher Scientific). Reverse transcription was performed using a QuantiTect Reverse Transcription Kit (QIAGEN), and 1 μg of total RNA was used according to the manufacturer's instructions.

Real-time PCR was performed using the ABI Prism 7,300 sequencing detection system (PerkinElmer Applied Biosystems) in a 96-well microplate. In total, the 25 μl real-time PCR system contained 12.5 μl of SYBR Green qPCR MasterMix (Applied Biosystems), 7.5 μl of a diluted primer mixture (300 nM), and 5 μl of diluted cDNA template (25 ng RNA input). The primer sequences for real-time PCR are listed in **Supplementary Data 1**. The real-time PCR conditions were optimized as follows: 50°C for 2 min and 95°C for 10 min, followed by 40 cycles at 95°C for 15 s and 55°C for 1 min. The nucleotide sequences of the resultant PCR products were confirmed by sequencing. The relative mRNA expression levels were determined using the $2^{-\Delta\Delta CT}$ method. The mRNA and lncRNA expression levels were standardized to the endogenous GAPDH expression level.

Western Blot Analysis

Cell extraction buffer (Life Technologies) was used to extract the entire cell lysate according to the manufacturer's instructions. The protein lysates (30 μg) were electrophoresed on 8% SDS-polyacrylamide gels and transferred to a nitrocellulose membrane (Amersham Pharmacia Biotech). The membranes were immunoblotted with specific primary antibodies against BMP2, SNAIL, and MMP2 (listed in **Supplementary Data 2**) overnight at 4°C. The signals were detected with an enhanced chemiluminescence system (Amersham Pharmacia Biotech) after incubation with an HRP-conjugated secondary antibody (Santa Cruz Biotechnology). To standardize the levels of the protein loaded into each lane, the blots were reprobed with a polyclonal antibody directed against human α-tubulin. All primary antibodies used in this study are listed in **Supplementary Data 2**.

Immunohistochemistry

Placental villous tissues were fixed in 4% formaldehyde and embedded in paraffin for sectioning. The placenta sections were deparaffinized and rehydrated before antigen retrieval with Dako antigen retrieval reagent (pH, 6.0). The sections were incubated with antibodies against BMP2 (1:50) at 4°C overnight following endogenous peroxidase blocking. A universal Dako-labeled streptavidin biotin-HRP system (Universal LSAB_Kit/HRP) was used for primary antibody detection. PBS containing rabbit IgG1 isotype (Abcam, ab172730, Cambridge, MA, United States) was used as a negative control and the concentration of the antibody used in IHC was 10 μg/ml. The sections were then exposed to a chromogen reaction (0.05% diaminobenzidine and 3% H_2O_2) and counterstained with Harris hematoxylin (Sigma). The signals were observed under a light microscope (Leica).

Primary Human EVT Isolation and Culture

Thirty first-trimester human placentas (5–8 weeks gestation) were collected from women undergoing elective termination of pregnancy. Primary human EVT cells were isolated from chorionic villous explants as previously described and cultured at 37°C in a humidified 5% CO_2/air atmosphere (Li et al., 2014). Briefly, the placenta villi tips were finely minced and cultured for 3–4 days in flasks with DMEM (Life Technologies) supplemented with 10% (vol/vol) FBS, 100 U/mL penicillin, and 100 μg/mL streptomycin. Non-attached pieces were removed and attached villous tissue fragments were cultured for another 10–14 days to allow for EVT outgrowth. EVT cells were subsequently separated from villous explants by trypsinization. Percoll gradient centrifugation, negative magnetic cell sorting using an antibody against classical major histocompatibility complex molecules and *in vitro* culture on a matrix-coated growth surface. The cells were fixed and probed with a specific antibody against cytokeratin-7 (EMD Millipore; MAB3554; Billerica, MA, United States) (10 μg/mL diluted at 1:100) followed by probing with a fluorescein isothiocyanate-conjugated secondary antibody or DAPI counterstaining. Next, we counted the number that was stained by cytokeratin-7 and DAPI. Only cultures showing more than 99% positive staining for cytokeratin-7 (**Supplementary Figure 1**) were used in this study. In general, cytotrophoblasts outgrow from villi onto Matrigel differentiate into EVT. Each experiment performed with primary EVT cells was replicated with cells from five different placentas. This study was approved by the Ethical Review Committee of Women's Hospital, Zhejiang University School of Medicine, and all women provided informed written consent.

Small-Interfering RNA Transfection

ON-TARGETplus siRNA (Thermo Fisher Scientific) targeting the target gene was transfected into primary EVTs or mouse trophoblast stem (TS) cells using Lipofectamine RNAiMAX Reagent (Life Technologies). The cells transfected with ON-TARGETplus control siRNA were used as a negative control in these studies.

Matrigel-Coated Transwell Invasion Assay

Primary human EVT cell invasiveness was examined using the Corning Biocoat Growth Factor Reduced Matrigel Invasion Chamber (pore size, 8 μm; catalog no. 354483) according to the guidelines for use. Briefly, primary EVT cells were pretreated with vehicle control or BMP2 (25 ng/mL) for 20 min. Then, each insert was seeded with 5×10^4 cells suspended in 250 μL vehicle/BMP2-containing DMEM supplemented with 0.1% (vol/vol) FBS, and 750 μL DMEM supplemented with 10% (vol/vol) FBS was added to the lower chamber. At the end of the experiment, non-invading cells were removed from the upper side of the membrane, and cells on the lower side were fixed in cold methanol for 20 min before they were stained with 0.1% crystal violet for 20 min. Membranes were cut out from the transwell inserts using a scalpel and mounted on glass slides with Cytoseal mounting medium. Cells on the lower aspect of the mounted membranes were viewed and photographed under a Nikon Eclipse 80i microscope. For quantification, the numbers of stained cells in five selected areas (top, middle, bottom, left, and right) were manually counted. Mean values from at least five independent experiments, each duplicated, were used in statistics.

Luciferase Reporter Assay

Potential binding sites were predicted using the TargetScan database. The linear form of NR026833.1 or the 3′-UTR of SNAIL containing the binding site of miR-502-5p or mutated was cloned downstream of the Renilla luciferase gene in the dual luciferase plasmid pmirGLO vector (Promega) to construct the pmirGLO-NR026833.1 vector or pmirGLO- SNAIL-3′UTR vector. Briefly, EVT cells (1×10^5 cells/well) were added to a 24-well plate for transfection. With the addition of 20 pmol of miR-502-5p mimics or negative control mimics, 0.8 μg of pmirGLO- NR026833.1 vector, pmirGLO-SNAIL-3′UTR vector or pmirGLO vector, were co-transfected into cells using Lipoimax (Invitrogen). Overexpression of miR-502-5p mimics after transfection in the cells was assessed by qPCR. After transfection for 48 h, the cells were harvested, and luciferase activities were measured using the Dual-Luciferase Reporter Assay System (Promega, Madison, WI, United States). Luciferase activity was measured as firefly luciferase/renilla luciferase ratio.

Oligonucleotide Transfection, miR Assay, and lncRNA Assay

The transient transfection was carried out when the cultured cells reached 60–70% confluence. si-RNA, si-LncRNA, miRNA mimic and their related control oligonucleotide were designed and synthesized by RiboBio (Guangzhou, China). All the transfection procedures were performed using the final concentration of 60 nM of miRNA mimics, 100 nM of miRNA inhibitor or si-LncRNA. LipoRNAi Max (Invitrogen, Carlsbad, CA, United States) was used as the transfection medium according to the manufacturer's instructions.

Superovulation and Embryo Collection

Female ICR mice (6–8 weeks; Shanghai SLAC Laboratory Animal Co., Ltd., Shanghai, China) were intraperitoneally injected with 10 IU of pregnant mare serum gonadotropin (PMSG; Ningbo Second Hormone Factory, Ningbo, China), followed by a 10 IU injection of human chorionic gonadotropin (hCG; Ningbo Second Hormone Factory, Ningbo, China) 48 h after PMSG injection. Female mice were mated with male ICR mice (8–10 weeks; Shanghai SLAC Laboratory Animal Co., Ltd.) after the hCG injection. Mouse embryos were collected from female ICR mice if a vaginal plug was present. A total of 30 female mice were used for superovulation and three mice were used in each stage of the immunofluorescence experiment (a total of 21 female mice). The processes of blastocyst formation and hatching were observed using microscopy. Six independent experiments ($n = 6$) were performed, resulting in a total of 110 embryos in the control group and 111 embryos in the BMP2-treatment group (a total of 9 female mice). Unfertilized oocytes were collected from the ampulla of the oviducts at 14 h after hCG injection without mating. Zygotes were obtained from the ampulla of the oviducts of plug-positive females at 18 h post-hCG injection. Cumulus cells were dispersed with 0.3 mg/mL hyaluronidase. Other preimplantation mouse embryos were collected at 42–45 h (the 2-cell stage), 52–55 h (the 4-cell stage), 65–68 h (the 8-cell stage), and 93–96 h (the blastocyst stage) after hCG injection. Embryos were flushed from the oviducts and uterus using M2 medium (M7167, Sigma-Aldrich). All experimental procedures were performed in accordance with the guidelines of the Guide for the Care and Use of Laboratory Animals and approved by the Animal Ethics Committee of Zhejiang University for animal experiments.

Embryo Immunofluorescence

The embryos were washed three times with phosphate-buffered saline (PBS) containing 0.5% bovine serum albumin (BSA, Sigma-Aldrich) and fixed in 4% paraformaldehyde for 30 min. Fixed embryos were washed three times in PBS containing 0.5% BSA, used immediately, or stored at 4°C in embryo storage buffer (PBS + 0.9% sodium azide) for up to 1 week. Fixed embryos were permeabilized with 0.01% Triton X-100 for 30 min and washed three times with PBS containing 0.5% BSA before being blocked in a 5% BSA/PBS solution for 1 h. Embryos were incubated with a primary antibody against BMP2 at a 1:500 dilution in 5% BSA/PBS overnight at 4°C. Finally, these embryos were washed three times for 20 min in 0.5% BSA/PBS containing 0.05% Tween 20 (0.5% BSA/PBST) and incubated with a fluorescein isothiocyanate-conjugated secondary antibody (1:200, Invitrogen, Carlsbad, CA, United States) for 1 h. The nuclei were stained with 1 mg/mL 40′, 6′-diamidino-2-phenylindole (DAPI, Sigma-Aldrich) for 10 min. Embryos at the 8-cell stage were chosen as negative controls.

Images were taken on an Olympus FV1000 confocal microscope and processed using Adobe Photoshop. The same experiment was independently repeated three times, each time in triplicate, and 20–30 embryos of different developmental stages were examined each time.

Embryo Culture

To study the role of BMP2 in preimplantation embryo development and zona hatching (complete escape of the blastocyst from its zona pellucida) *in vitro*, two-cell embryos on day 2 (08:30–09:00 h) were recovered and pooled from several mice in M2 medium (M7167, Sigma-Aldrich). The embryos were washed three times in KSOM medium. Embryos were cultured in groups in microdrops (50 μl) of Whitten's medium under light oil in an atmosphere of 5% CO_2/95% air at 37°C for 72 h in the presence or absence of BMP2 (100 ng/ml). BMP2 was added when the cultures were started. The embryos were observed every 24 h to monitor their development. Each experiment was repeated six times with the exception of numerous replicates of controls included in each experimental repetition.

Mouse TS Cell Culture and Differentiation Induction

The mouse TS cells line was kindly donated by Dr. Haibin Wang from the Chinese Academy of Sciences (Beijing, China). Mouse trophoblast stem cells (TS cells) that were established from mouse 3.5 days postcoitum blastocysts or the extraembryonic ectoderms of 6.5 days postcoitum embryos can either self-renew or differentiate into distinct trophoblastic cell populations, including invasive mouse trophoblastic giant cells (Tanaka et al., 1998; Uy et al., 2002). Briefly, TS cells were maintained and propagated in 25 ng/mL fibroblast growth factor 4 (FGF4) culture medium supplemented with 1 mg/mL heparin (Sigma-Aldrich) and composed of 30% TS medium (RPMI 1640 supplemented with 20% FBS, 50 mg/mL penicillin/streptomycin, 2 mM L-glutamine, 1 mM sodium pyruvate, and additional additives, including 50 mM β-mercaptoethanol) and 70% mouse embryonic fibroblast (MEF) conditioned medium. Differentiation of the mouse TS cells was induced by the removal of FGF4, heparin, and MEF-conditioned medium for 7 days.

Statistical Analysis

All statistical analyses were performed using SPSS 16.0 (SPSS, Chicago, IL, United States) and GraphPad Prism 5.0 (GraphPad Software, Inc., San Diego, CA, United States). Data are presented as the mean ± SD from at least five independent experiments. Differences between groups were determined by Student's *t*-test or one-way analysis of variance, and statistical significance was defined as $P < 0.05$. Differences in the rates of development and hatching between the protease treatment groups and the control group were analyzed by a χ^2-test. $P < 0.05$ was defined as statistically significant.

TABLE 1 | Clinical and biochemical characteristics of the women included in this study.

	Non-pregnacy (Non-P, $n = 50$)	Normal pregnancy (NP, $n = 50$)	Early pregnancy loss (EPL, $n = 50$)
Age (year)	28.04 ± 3.14	28.06 ± 4.65	28.92 ± 3.48
Gestational age (day)	–	47.06 ± 4.99	48.76 ± 4.18
Serum β-HCG (IU/mL)	–	38,427.18 ± 41,159.79[a]	22,510.28 ± 30,457.91[a]
Serum BMP2 (pg/mL)	36.28 ± 13.82[b]	51.02 ± 18.77[bc]	43.16 ± 16.35[c]

Data are presented as the means ± SD. [a]$P < 0.05$; [b]$P < 0.001$; [c]$P < 0.05$.

RESULTS

Decreased Serum Levels of BMP2 Are Associated With EPL

To investigate the functional role of BMP2 during early pregnancy in humans, we first examined the serum levels of BMP2 by recruiting three groups of women, including healthy non-pregnant (Non-P) women, women with NP and women with EPL. The clinical and biochemical characteristics of the women included in this study are shown in **Table 1**. Women in all three groups ($n = 50$ in each group) were of similar age. Women in the NP group had a similar gestational age to those in the EPL group (47.06 ± 4.99 days vs. 48.76 ± 4.18 days, respectively, $P > 0.05$). Maternal serum β-HCG levels were significantly higher in the NP group than in the EPL group (38,427.18 ± 41,159.79 IU/mL vs. 22,510.28 ± 30,457.91 IU/mL, respectively, $P < 0.05$). Compared with Non-P women, women with NPs had significantly higher serum BMP2 levels (36.28 ± 13.82 pg/mL vs. 51.02 ± 18.77 pg/mL, respectively, $P < 0.001$) (**Table 1** and **Figure 1A**). Notably, subjects in the NP group had higher serum BMP2 levels than those in the EPL group (51.02 ± 18.77 pg/mL vs. 43.16 ± 16.35 pg/mL, respectively, $P < 0.05$) (**Table 1** and **Figure 1A**).

The Expression of BMP2 Is Higher in Women With Normal Early Pregnancies Than in Those With EPL

Although the expression of BMP2 at the maternal-fetal interface has been reported (Paria et al., 2001), whether BMP2 is expressed in human embryos remains to be elucidated. We thus used immunostaining analysis to examine the expression and localization of BMP2 in human preimplantation embryos. As shown in **Figure 1B**, immunostaining for BMP2 was observed in all embryos analyzed at different stages of development. At the zygote and 4-cell stages, BMP2 was mainly expressed around the nucleus, and BMP2 was mainly localized in the cytoplasm from the 8-cell stage of embryos. Notably, strong cytoplasmic BMP2 staining was observed in the trophectoderm, the cell layer from which the trophoblast differentiates (**Figure 1B**). Nonetheless, BMP2 was also expressed in the ICM that gives rise to the definitive structures of the fetus (**Figure 1B**). Given that the

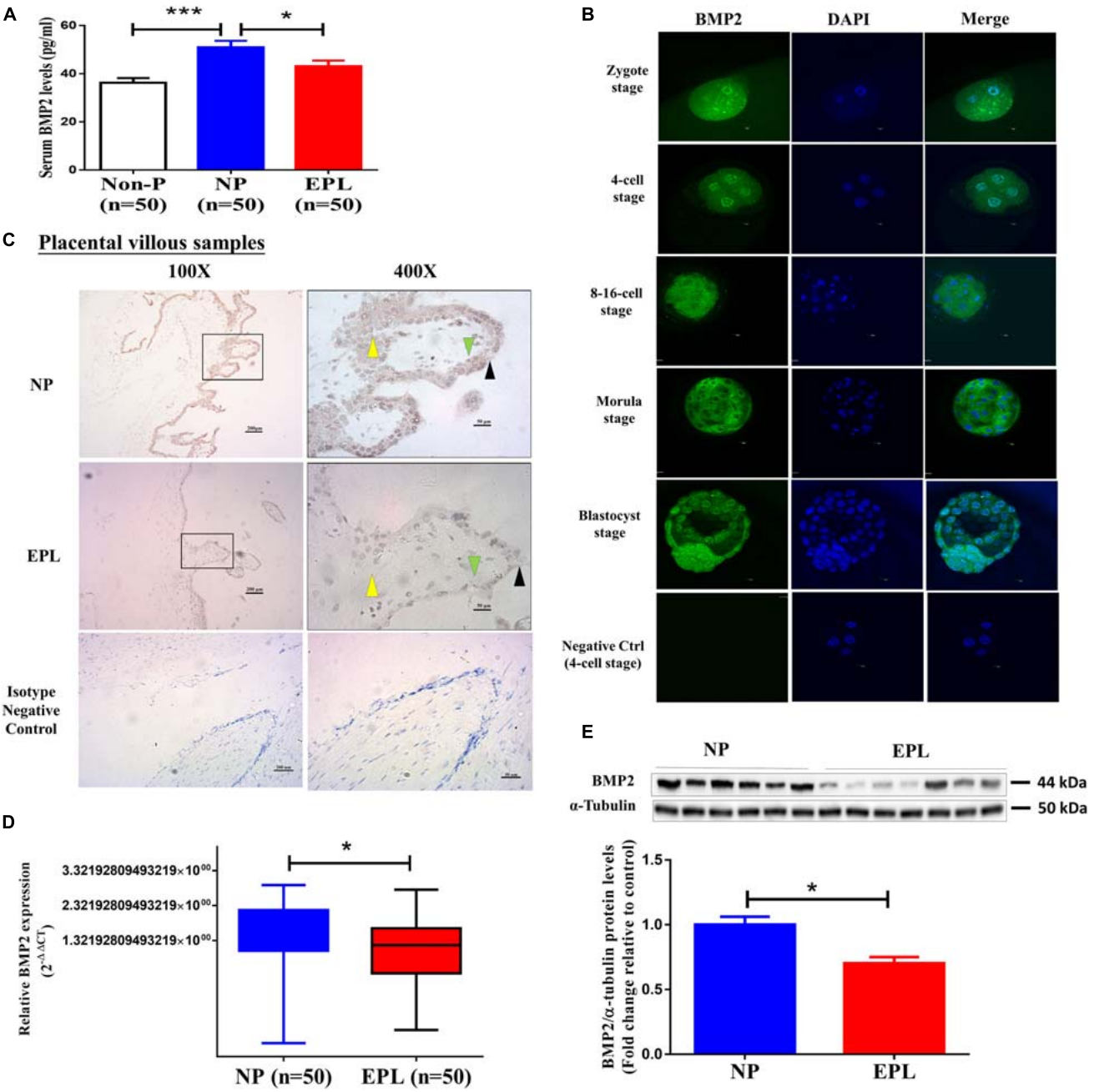

FIGURE 1 | BMP2 expression in women with normal early pregnancies and EPL. **(A)** Comparison of the circulating BMP2 levels in non-pregnant (Non-P) women (n = 50), normal early pregnant women (NP, n = 50) and women with EPL (n = 50). The serum samples collected from these women were measured using ELISA. **(B)** The expression and localization of BMP2 in human preimplantation embryos. Human preimplantation embryos, including the zygote, 4-cell, 8-16-cell, morula and blastocyst stages, were fixed and probed with a specific antibody against human BMP2 followed by probing with a fluorescein isothiocyanate-conjugated secondary antibody or DAPI counterstaining. PBS without primary antibody was used as a negative control. The images were detected using confocal microscopy. **(C)** Expression and localization of BMP2 in first-trimester human placental villus tissues obtained from women with NPs and EPL. The images were detected using immunohistochemistry staining. PBS containing rabbit IgG1 isotype was used as a negative control. Stronger brown cytoplasmic staining of BMP2 was detected in the cell column EVTs (yellow arrowheads), syncytiotrophoblasts (black arrowheads) and CTBs (green arrowheads) of the placental villous tissues obtained from women with NPs (scale bar 1/4 200 mm in 100 × images and scale bar 1/4 50 mm in 400 × images). **(D,E)** The mRNA **(D)** and protein **(E)** levels of BMP2 in villous tissue obtained from women with NPs (n = 50) and EPL (n = 50) were examined using RT-qPCR and western blot analyses, respectively. The relative amounts of mRNA were calculated using the $2^{-\Delta\Delta Ct}$ method and normalized to that of the internal control gene *GAPDH*. The relative amounts of protein were normalized to that of the internal control α-tubulin. Differences between groups were determined by either Student's t-test or one-way analysis of variance (*$P < 0.05$, ***$P < 0.001$).

serum BMP2 levels were decreased in women with EPL, we next compared the expression of BMP2 in placental villous tissues obtained from women with NPs and those from women with EPL using immunohistochemistry. As shown in **Figure 1C**, the results revealed that the immunohistochemical staining for BMP2 was significantly decreased in the cytoplasm of cell column EVT, syncytiotrophoblastic (synCTB) and cytotrophoblastic (CTB) cells in the villous tissues obtained from women with EPL. Similarly, the mRNA and protein levels of BMP2 were reduced in cell lysates of the villous tissues obtained from women with EPL (**Figures 1D,E** and **Supplementary Figure 2**).

BMP2 Upregulates MMP2 Expression, Increases MMP2 Activity and Promotes Cell Invasion in Primary Human EVT Cells

We further used primary human EVT cells isolated from first-trimester human placental villous tissues (normal pregnancies in women who were undergoing elective surgical termination at the gestational age of 5–8 weeks) to investigate the cellular activity of BMP2. To examine the bioactivity of exogenous BMP2, we treated primary EVT cells with 25 ng/mL BMP2 for 12 h, and the results showed that BMP2 significantly increased the mRNA levels of the inhibitor of differentiation (Id) proteins, ID1, ID2, and ID3 (**Supplementary Figure 3**). Using the Matrigel-coated transwell invasion assay and CCK-8 assay, we found that treatment of primary human EVT cells for 72 h with 25 ng/mL recombinant human BMP2 (BMP2) significantly increased cell invasion without affecting cell viability, indicating that BMP2 promotes cell invasion in primary human EVT cells (**Figure 2A**). Furthermore, the Gene Set Enrichment Analysis obtained from the gene sequencing results revealed that a high expression level of BMP2 was correlated with the EMT-related signaling pathway (**Figure 2B**). Matrix metalloproteases (MMPs), especially MMP2 and MMP9 are two gelatinases that are expressed in EVT cells and are associated with EMT-mediated trophoblast invasion during first-trimester pregnancy (Shimonovitz et al., 1994; Isaka et al., 2003). To investigate the effect of BMP2 on the expression of MMP2 and MMP9, we treated primary EVT cells with 25 ng/mL BMP2 for 12 or 24 h. The results showed that BMP2 significantly increased the mRNA and protein levels of MMP2 in primary EVT cells (**Figures 2C,D**). Moreover, treatment of primary EVT cells with 25 ng/mL BMP2 for 24 h increased MMP2 activity in the conditioned medium of cultured cells (**Figure 2E**). However, BMP2 did not have such effects on the expression of MMP9 and other MMPs (**Supplementary Figure 4**). These results indicate that BMP2 promotes cell invasion, most likely, by upregulating the expression of MMP2 in primary EVT cells.

SNAIL Mediates the BMP2-Induced Upregulation of MMP2 and Increase in Cell Invasion in Primary Human EVT Cells

The SNAIL protein is a prototypical EMT-inducing transcription factor that has been shown to mediate activin A-induced upregulation of MMP2 (Li et al., 2015). We thus investigated whether SNAIL plays a regulatory role in the BMP2-induced upregulation of MMP2 and increase in cell invasion. Using a siRNA-mediated knockdown approach, we found that the targeted depletion of SNAIL downregulated the mRNA and protein levels up to 80–90% (**Figures 3A,B**). Notably, SNAIL knockdown completely reversed the BMP2-induced upregulation of MMP2 expression (**Figures 3A,B**). Similarly, SNAIL knockdown completely abolished BMP2-induced increases in cell invasion (**Figure 3C** and **Supplementary Figure 5**). These results indicate that SNAIL is the main transcription factor that mediates the BMP2-induced trophoblast cell invasion. To further investigate the functional role of MMP2 in trophoblast invasion, we used siRNA-mediated knockdown approaches. The results showed that knockdown of MMP2 significantly decreased cell invasion in primary EVT cells (**Figure 3D**).

MiR-502-5p Suppresses the Expression of SNAIL and Decreases SNAIL-Mediated Cell Invasion in Primary Human EVT Cells

To investigate the molecular mechanisms by which BMP2 regulates the expression of SNAIL, we performed bioinformatics analysis using TargetScan[1]. The results showed that the 3′ UTR of SNAIL mRNA contains a putative binding site of miR-502-5p. We thus treated primary EVT cells with 25 nM miR-NC (as a negative control) or 25 nM miR-502-5p mimic for 24 h, and the transfection efficiency was examined using RT-qPCR (**Figure 4A**). The results showed that transfection with miR-502-5p mimic significantly increased miR-502-5p level up to 40 folds (**Figure 4A**). Notably, the results showed that the miR-502-5p mimic significantly decreased the mRNA and protein levels of SNAIL (**Figures 4B,C**). To further confirm that SNAIL is the target of miR-502-5p, we cloned the SNAIL 3′ UTR sequence into a luciferase reporter construct (designated SNAIL 3′-UTR-WT) and mutated the putative miR-502-5p binding site (designated SNAIL 3′-UTR-MUT) (**Figure 4D**). Primary human EVT cells were transfected for 24 h with SNAIL 3′-UTR-WT or SNAIL 3′-UTR-MUT along with 25 nM miR-NC or 25 nM miR-502-5p mimic, and the luciferase activities of the cells were detected using a dual-luciferase assay. As shown in **Figure 4D**, compared with miR-NC, the miR-502-5p mimic significantly decreased the luciferase activity of SNAIL 3′-UTR-WT. However, the miR-502-5p mimic had no significant influence on the luciferase activity of the SNAIL 3′-UTR-MUT. Notably, the inhibition of miR-502-5p using the miR-502-5p inhibitor abolished the suppressive effect induced by the SNAIL knockdown (**Figure 4E** and **Supplementary Figure 6**). These results indicate that SNAIL is a direct target of miR-502-5p in primary EVT cells.

ALK2 or ALK3 Mediates the BMP2-Induced Upregulation of SNAIL and MMP2 Expression in Primary Human EVT Cells

To date, three type I receptors (ALK2, ALK3, and ALK6) have been implicated in BMP-induced SMAD1/5/8 phosphorylation

[1]http://www.targetscan.org/vert_50/

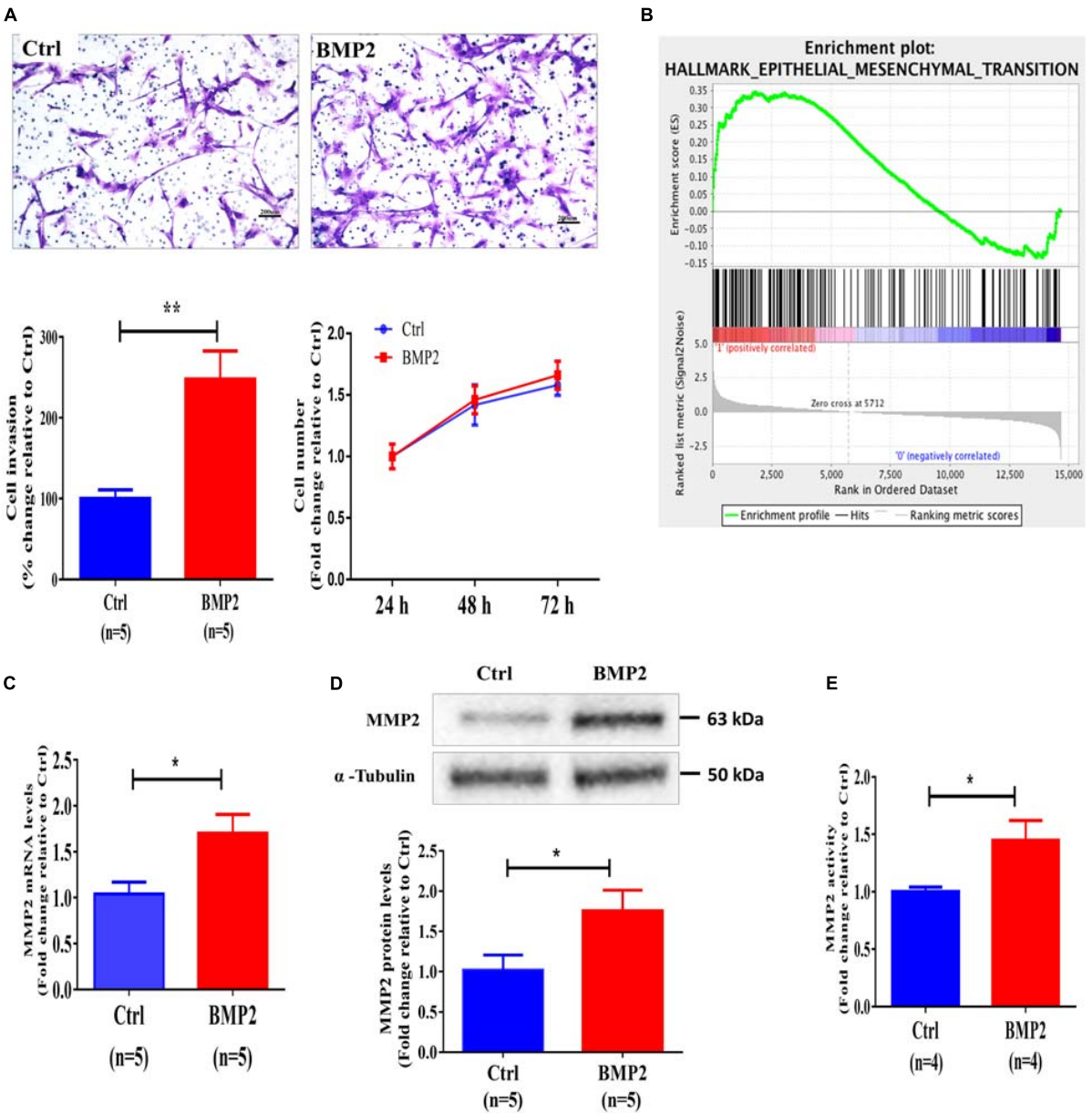

FIGURE 2 | BMP2 upregulates MMP2 expression and promotes cell invasion in primary human EVT cells. **(A)** Primary human EVT cells were treated with a vehicle control (Ctrl) or 25 ng/mL BMP2 for 72 h, and cell invasion was examined using the Matrigel-coated transwell invasion assay. A representative image of the assay (scale bar represents 200 μm) and quantitative results are shown separately. Primary human EVT cells were seeded in 24-well plates, and the cells were treated every 24 h (24, 48 and 72 h) with Ctrl or 25 ng/mL BMP2 for a total of 72 h. Cell viability was determined using a CCK-8 assay. **(B)** The correlation between BMP2 treatment and the EMT signaling pathway sing the gene set enrichment analysis plot. **(C,D)** Primary human EVT cells were treated for 12 h **(C)** or 24 h **(D)** with Ctrl or 25 ng/mL BMP2 and the mRNA **(C)** and protein **(D)** levels of MMP2 were examined using RT-qPCR and western blot analyses, respectively. GAPDH and α-tubulin were used to normalize the RT-qPCR and western blot results, respectively. **(E)** Primary human EVT cells were treated for 24 h with Ctrl or 25 ng/mL BMP2 and MMP2 activity was examined using ELISA. The results are expressed as the mean ± SEM of five independent experiments ($n = 5$, $^{*}P < 0.05$, $^{**}P < 0.01$). Differences between groups were determined by Student's *t*-test.

(Miyazono et al., 2001). To determine whether ALK2, ALK3 or ALK6 are required for BMP15-induced SMAD1/5/8 activation, primary EVT cells were treated with BMP2 in the presence or absence of 0.5 μM DMH-1 (a selective inhibitor of ALK2/3) (Yu et al., 2008). As shown in **Figures 5A,B**, treatment of primary EVT cells with DMH-1 completely abolished BMP2-induced increases in the mRNA levels of SNAIL and MMP2. Similarly, treatment of primary EVT cells with DMH-1 completely abolished BMP2-induced increases in the protein levels of SNAIL and MMP2 (**Figures 5C,D**). These results indicate that ALK2 or ALK3, but not ALK6, is required for the upregulation of SNAIL and MMP2 induced by BMP2 in primary EVT cells.

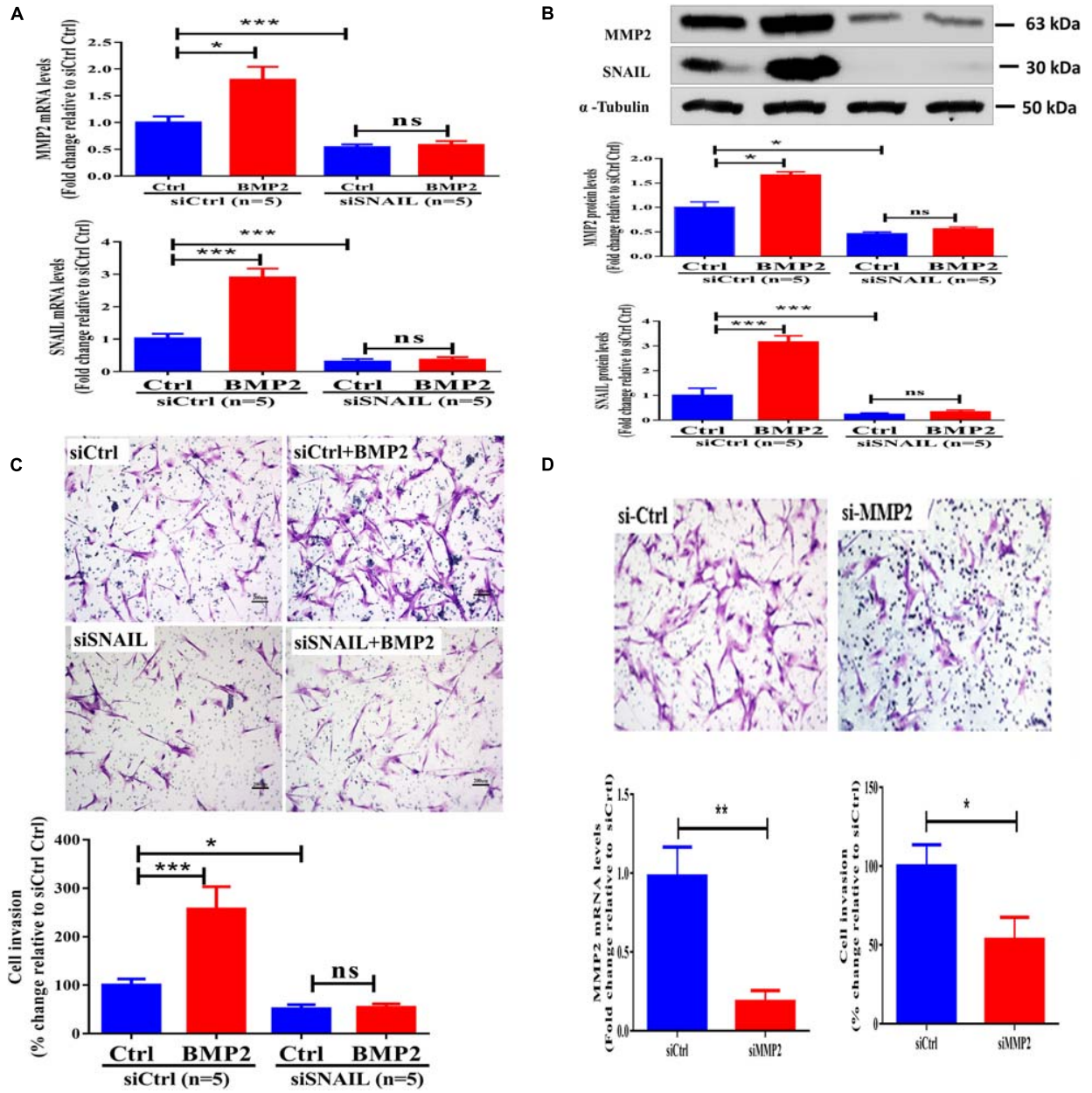

FIGURE 3 | SNAIL mediates the BMP2-induced upregulation of MMP2 and the increase in cell invasion of primary human EVT cells. **(A,B)** Primary human EVT cells were transfected with 25 nM control siRNA (siCtrl) or 25 nM SNAIL-specific siRNA (siSNAIL) for 48 h, and the cells were treated with Ctrl or 25 ng/mL BMP2 for an additional 12 h **(A)** or 24 h **(B)**. The mRNA **(A)** and protein **(B)** levels of MMP2 and SNAIL were examined using the RT-qPCR and western blot results, respectively. **(C)** Primary human EVT cells were transfected with 25 nM siCtrl or 25 nM siSNAIL for 24 h, and the cells were treated with Ctrl or 25 ng/mL BMP2 for an additional 48 h. Cell invasion was examined using the Matrigel-coated transwell invasion assay. **(D)** Primary human EVT cells were transfected with 25 nM siCtrl or 25 nM siMMP2 for 24 h. The mRNA levels of MMP2 and cell invasion was examined using RT-qPCR and Matrigel-coated transwell invasion assay, respectively. The results are expressed as the mean ± SEM of five independent experiments ($n = 5$, $^{*}P < 0.05$; $^{***}P < 0.001$; NS, no significant difference). Differences between groups were determined by one-way analysis of variance.

NR026833.1 Induces SNAIL Expression and Promotes Cell Invasion in Primazry Human EVT Cells

To further identify the regulatory networks of mRNAs, miRNAs, and lncRNAs, we treated primary human EVT cells (isolated from villous tissues obtained from three women with NPs) with 25 ng/mL BMP2 and performed high-throughput second-generation sequencing analysis. A total of 633 mRNAs (370 upregulated and 263 downregulated), 121 miRNAs (54 upregulated and 67 downregulated), and 908 lncRNAs (555 upregulated and 353 downregulated) were differentially

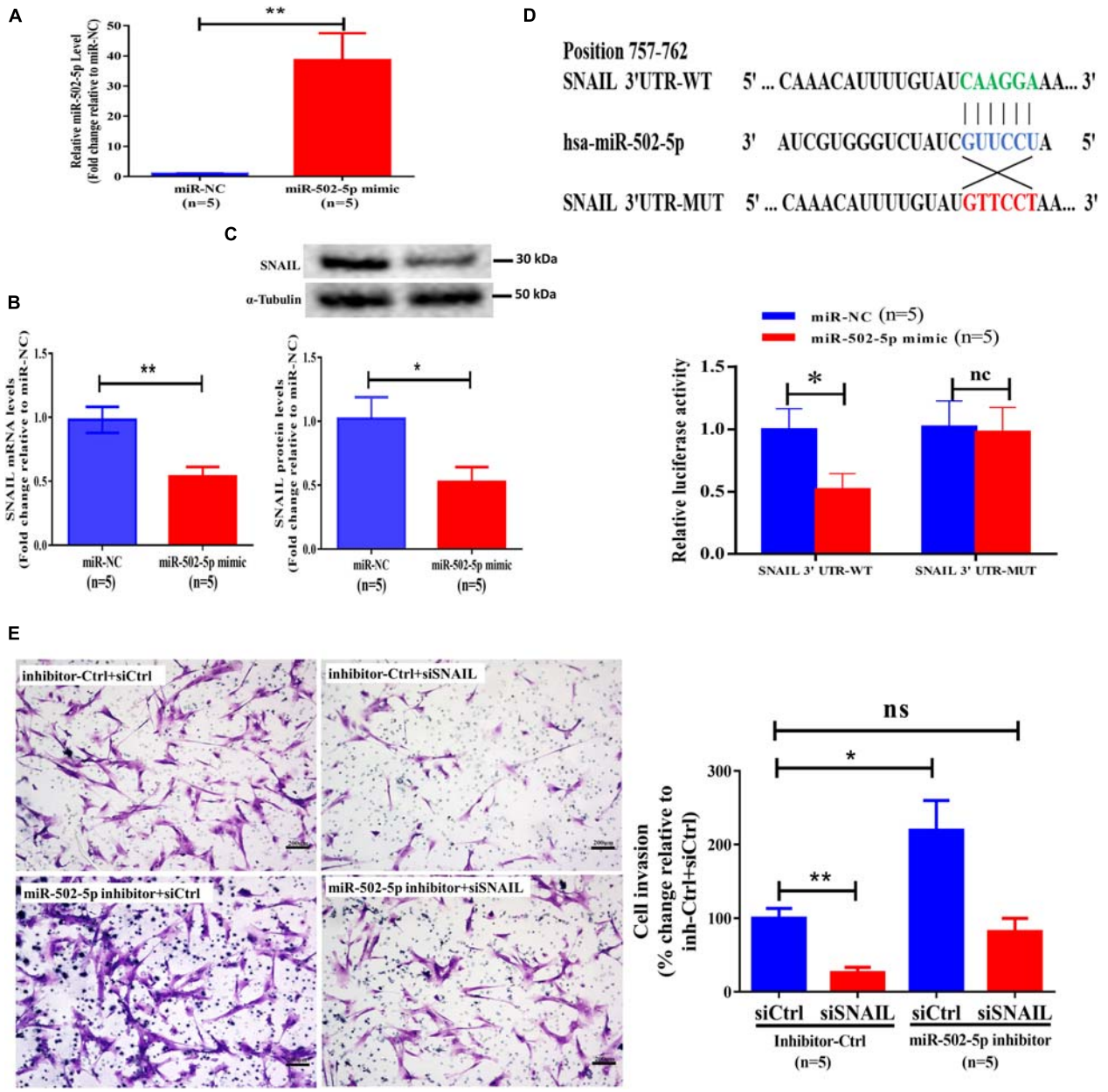

FIGURE 4 | MiR-502-5p suppresses SNAIL expression and decreases SNAIL-mediated cell invasion in primary human EVT cells. **(A–C)** Primary human EVT cells were transfected for 24 h with 25 nM miR-NC (as a negative control) or 25 nM miR-502-5p mimic, and the miR-505-5p levels **(A)** were examined using RT-qPCR. The mRNA **(B)** and protein **(C)** levels of SNAIL were examined using RT-qPCR and western blot analyses, respectively. **(D)** Primary human EVT cells were transfected for 24 h with 3′-UTR SNAIL-luciferase reporter (SNAIL 3′-UTR-WT) or 3′-UTR SNAIL mutant-luciferase reporter (SNAIL 3′-UTR-MUT) along with 25 nM miR-NC or 25 nM miR-502-5p mimic. The luciferase activities of cells were detected using a dual-luciferase assay. **(E)** Primary human EVT cells were cotransfected with 25 nM miRNA inhibitor negative control (inhibitor Ctrl) or 25 nM miR-502-5p inhibitor for 24 h as well as 25 nM siCtrl or 25 nM siSNAIL for 24 h. Cell invasion was examined using the Matrigel-coated transwell invasion assay. The results are expressed as the mean ± SEM of five independent experiments ($n = 5$, $^*P < 0.05$; $^{**}P < 0.001$; NS, no significant difference). Differences between groups were determined by Student's *t*-test or one-way analysis of variance.

expressed in the BMP2-treated group. Hierarchical clustering was performed to show the differential expression patterns of these mRNAs, miRNAs, and lncRNAs (**Figure 6**). Moreover, eight lncRNAs were selected for validation using RT-qPCR, and all these lncRNAs were upregulated by BMP2 according to the sequencing analysis (**Supplementary Figure 7**). Among these deregulated lncRNAs, NR026833.1 was upregulated up to 10-fold after BMP2 treatment (**Figure 7A**). Indeed, the results obtained from the correlation analysis showed that there was a positive correlation between the relative mRNA levels of BMP2 and those of NR026833.1 in villous tissues obtained from women with NPs (**Figure 7B**, $n = 50$). Intriguingly, the expression levels of

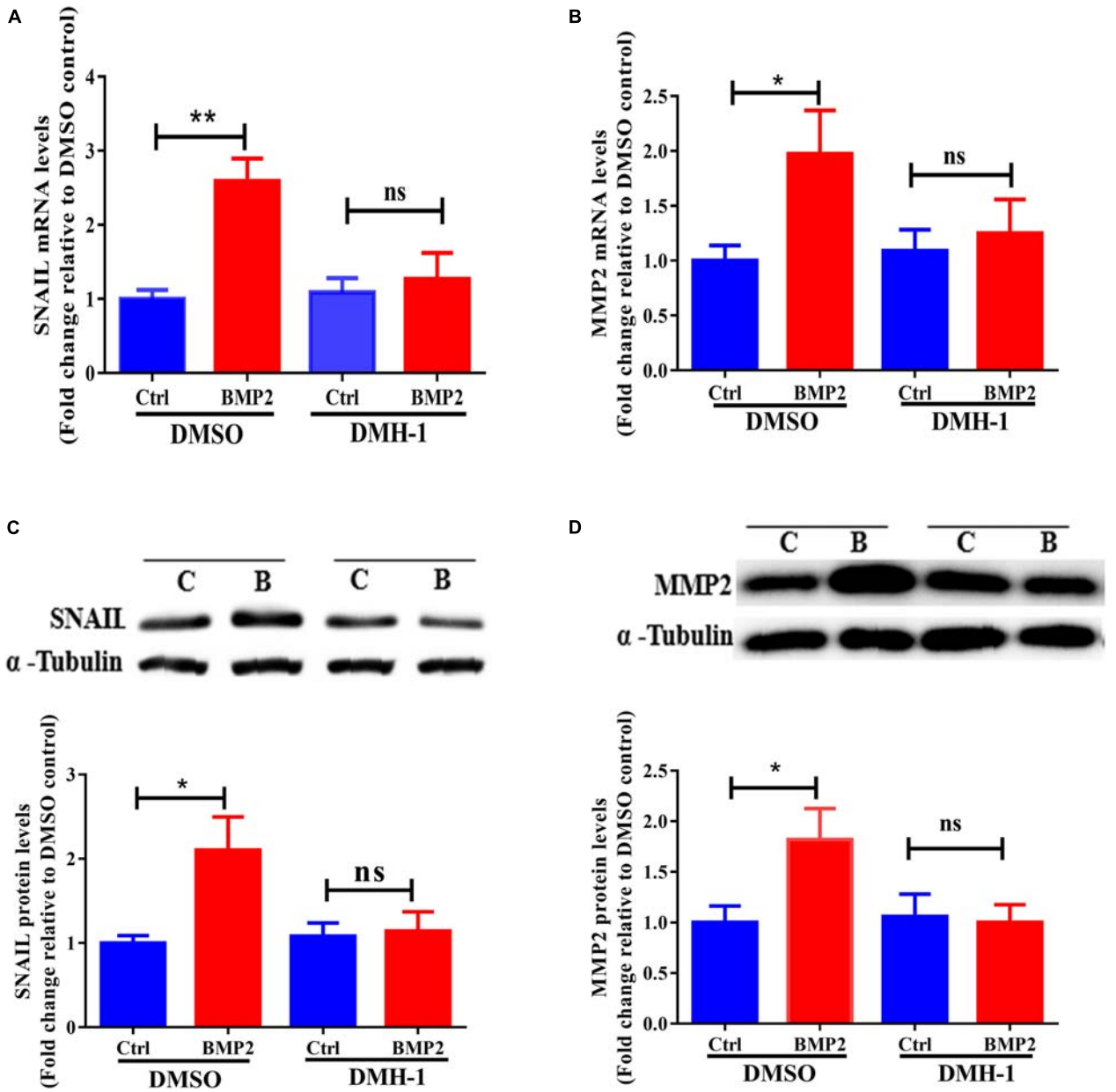

FIGURE 5 | ALK2 or ALK3 mediates BMP2-induced upregulation of SNAIL and MMP2 in primary EVT cells. **(A,B)** Primary human EVT cells were pretreated with vehicle control or DMH-1 (0.5 μM) for 60 min and the cells were treated with Ctrl or 25 ng/mL BMP2 for an additional 12 h. The mRNA levels of SNAIL **(A)** and MMP2 **(B)** were examined using RT-qPCR. **(C,D)**, Primary human EVT cells were pretreated with vehicle control or DMH-1 (0.5 μM) for 60 min and the cells were treated with Ctrl or 25 ng/mL BMP2 for an additional 24 h. The protein levels of SNAIL **(C)** and MMP2 **(D)** were examined using western blot analysis. The results are expressed as the mean ± SEM of four independent experiments ($n = 4$, $^*P < 0.05$; NS, no significant difference). Differences between groups were determined by one-way analysis of variance.

NR026833.1 in the villous tissues obtained from women with NPs ($n = 50$) were significantly higher than those from women with EPL (**Figure 7C**, $n = 50$), indicating that NR026833.1 could play a functional role in early pregnancy. Our *in vitro* experiments showed that NR026833.1 knockdown significantly downregulated SNAIL expression at the transcriptional and translational levels (**Figures 7D,E**) and decreased cell invasion (**Figure 7F**) in primary EVT cells.

NR026833.1 Binds to miR-502-5p and Promotes Cell Invasion in Primary Human EVT Cells

The NR026833.1 gene is located at chromosome 2 and has 3,463 nucleotides. To investigate the molecular mechanisms by which NR026833.1 regulates trophoblast invasion, we examined the localization of this lncRNA because the cellular activities

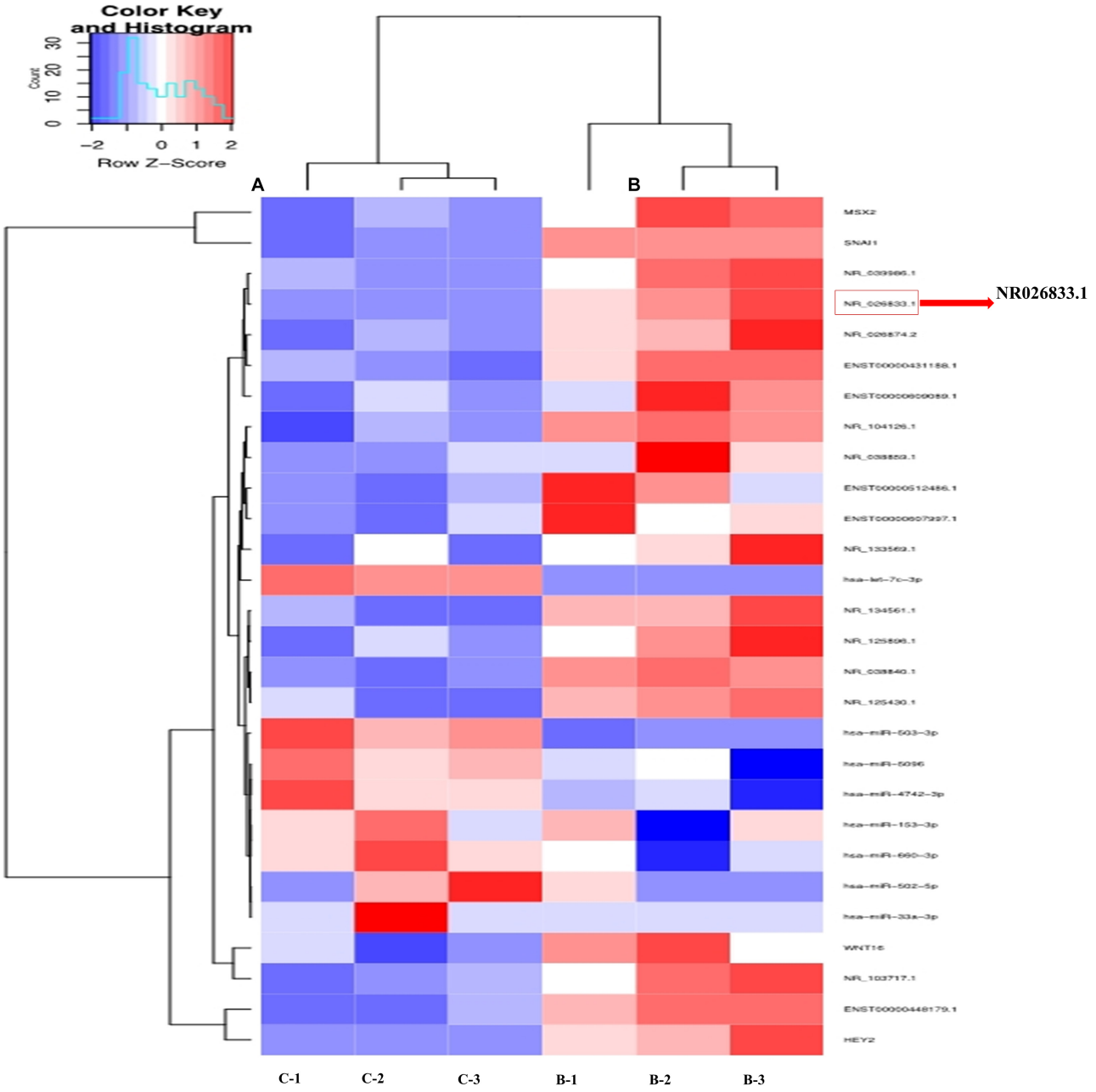

FIGURE 6 | Hierarchical clustering analysis of lncRNA and microRNA expression in primary human EVT cells treated with Ctrl (n = 3) or 25 ng/mL BMP2 (n = 3). Each row represents one type of RNA, and each column represents a sample **(A)** Ctrl; **(B)** BMP2 treatment). The color scale shown at the top illustrates the relative RNA expression level; red represents high expression, and blue represents low expression.

of lncRNAs are dependent on their subcellular distribution. Using cytoplasmic and nuclear RNA fractions combined with FISH analysis, we observed that NR026833.1 was preferentially localized in the cytoplasm of primary human EVT cells (**Figure 8A**). Studies have shown that cytoplasmic lncRNAs can directly bind to miRNAs and serve as microRNA sponges or competitive endogenous RNAs (ceRNAs) to block associations with target mRNAs (Zhou et al., 2014). Based on these studies and our sequencing results, we hypothesized that NR026833.1 has target sites against miR-502-5p and that NR026833.1 regulates trophoblast invasion by binding to miR-502-5p. To test this hypothesis, we constructed luciferase vectors by cloning wild-type NR026833.1 (NR026833.1 WT) and mutant NR026833.1 (NR026833.1 MUT). Using dual-luciferase assays, we found that transfection of the NR026833.1 WT together with the miR-502-5p mimic but not the NR026833.1 MUT with the miR-502-5p mimic significantly decreased the luciferase activity of primary EVT cells (**Figure 8B**).

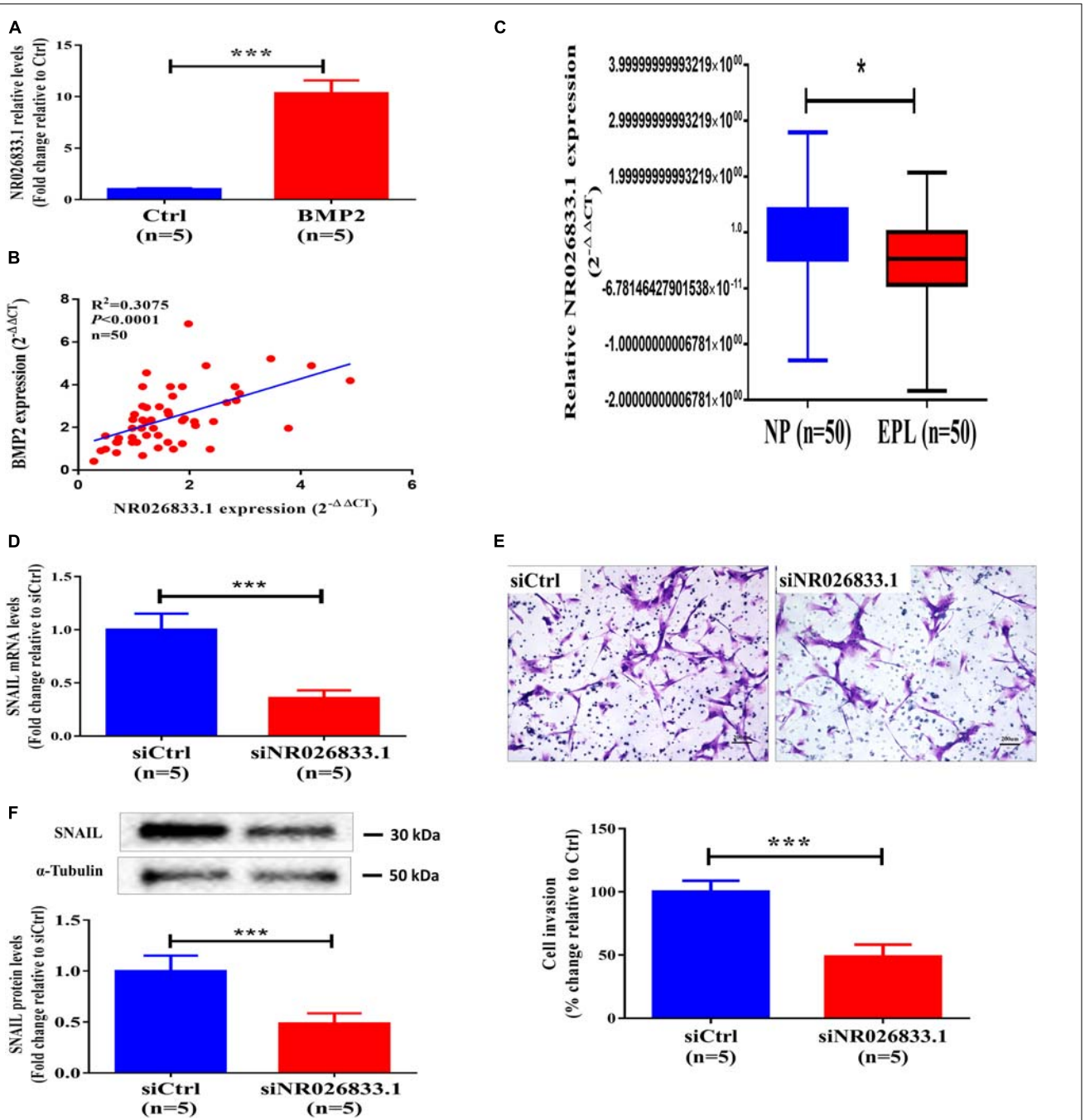

FIGURE 7 | NR026833.1 induces SNAIL expression and promotes cell invasion in primary human EVT cells. **(A)** Primary human EVT cells were treated with Ctrl or 25 ng/mL BMP2 for 12 h, and the levels of NR026833.1 were examined using RT-qPCR. **(B)** Correlation of the relative mRNA levels of BMP2 and those of NR026833.1 in villous tissues obtained from women with NPs (n = 50). **(C)** The relative levels of NR026833.1 in villous tissue obtained from women with NPs (n = 50) and EPL (n = 50) were examined using RT-qPCR. **(D,E)** Primary human EVT cells were transfected with 25 nM siCtrl or 25 nM NR026833.1-specific siRNA (si NR026833.1) for 48 h, and the mRNA **(E)** and protein **(F)** levels of SNAIL were examined using RT-qPCR and western blot analyses, respectively. **(F)** Primary human EVT cells were transfected with 25 nM siCtrl or 25 nM si NR026833.1 for 48 h. Cell invasion was examined using a Matrigel-coated transwell invasion assay. The results are expressed as the mean ± SEM of at least five independent experiments (*P < 0.05; ***P < 0.001). Differences between groups were determined by Student's t-test.

Additionally, transfection with the miR-502-5p mimic but not miR-NC significantly suppressed cell invasion in primary EVT cells (**Figure 8C**). Notably, overexpression of NR026833.1 (OE- NR026833.1) increased cell invasion and reversed the miR-502-5p mimic-induced suppression of cell invasion in primary EVT cells (**Figure 8D**). These results indicate that NR026833.1 promotes trophoblast invasion by interacting with miR-502-5p.

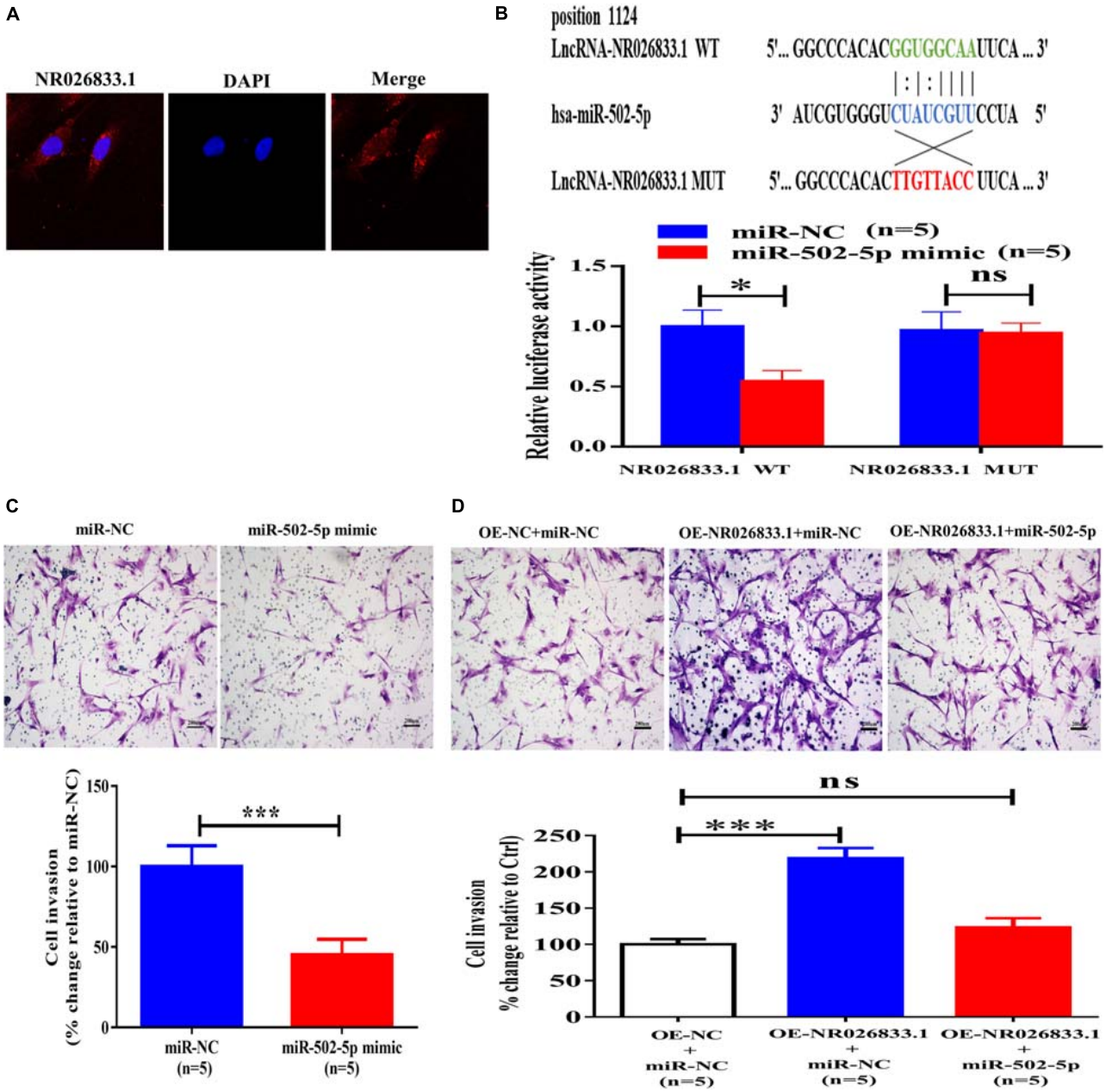

FIGURE 8 | NR026833.1 binds to miR-502-5p and promotes cell invasion in primary human EVT cells. **(A)** Localization of NR026833.1 (red) in primary human EVT cells using immunostaining. DAPI staining (blue) was used to determine the location of the nuclei. **(B)** Primary human EVT cells were transfected for 24 h with an NR026833.1-luciferase reporter (NR026833.1-WT) or an NR026833.1 mutant-luciferase reporter (NR026833.1-MUT) along with 25 nM miRNA-NC or 25 nM miR-502-5p mimic. The luciferase activities of the cells were detected using a dual-luciferase assay. **(C)** Primary human EVT cells were transfected for 24 h with 25 nM miR-NC or 25 nM miR-502-5p mimic, and cell invasion was examined using a Matrigel-coated transwell invasion assay. **(D)** Primary human EVT cells were transfected for 24 h with miR-NC plus overexpression vector negative control (OE-NC), miR-NC plus overexpression NR026833.1 (OE-NR026833.1) or miR-502-5p mimic plus OE-NR026833.1, and cell invasion was examined using a Matrigel-coated transwell invasion assay. The results are expressed as the mean ± SEM of five independent experiments ($n = 5$, $^{*}P < 0.05$; $^{***}P < 0.001$; NS, no significant difference). Differences between groups were determined by Student's *t*-test.

BMP2 Promotes the Development of Mouse Preimplantation Embryos

To compare embryonic development in humans and mice, we further investigated the expression, localization and functional roles of BMP2 in mouse embryos at the corresponding stages. Using the fluorescence analysis, we observed that BMP2 is expressed in the mouse oocyte and preimplantation embryo at all stages, including the zygotes, 2-cell embryos, 4-cell embryos, 8-cell embryos, morula and blastocysts (**Figure 9A**). Specifically, BMP2 is primarily localized in the cytoplasm (**Figure 9A**). Similar

TABLE 2 | Effects of BMP2 on the developmental potential of 2-cell mouse embryos.

		48 h	72 h	
		No. of blastocyst (%)	No. of blastocyst (%)	No. of blastocyst hatching (%)
Control	110[a]	51 (46.4)	95 (86.4)	53 (48.2)
BMP2	111[a]	74 (66.7)*	101 (91)	79 (71.2)*
P-value		0.002	0.278	0.002

[a]*Number of embryos that were examined.*
**P < 0.05 compared with Control.*

to that in humans, BMP2 in mice is localized at the perinuclear area at the 2-cell stage. Additionally, BMP2 is expressed in both the trophectoderm and ICM (mainly in trophectoderm cells) at the blastocyst stage. To examine the roles of BMP2, we cultured superovulated 2-cell stage mouse embryos with 100 ng/mL BMP2 for up to 72 h. The results showed that BMP2 significantly promoted blastocyst formation at 48 h and embryo hatching at 72 h (**Figure 9B** and **Table 2**).

BMP2 Promotes the Invasive Differentiation of Mouse TS Cells

To investigate the role of BMP2 in the regulation of trophoblast cell differentiation and invasion, we used mouse TS cells (established from 3.5 days postcoitus (dpc) blastocysts) to mimic the process of trophoblast differentiation *in vivo*. Our *in vitro* studies showed that BMP2 treatment promptly decreased the expression of the TS cell marker Eomes during the first 3 days of cell differentiation (**Figure 8A**). BMP2 increased the expression of the labyrinthine/spongiotrophoblast (SpT) cell marker Tpbpa and the trophoblast giant cell (TGC) marker Ctsq during the last 3 days of cell differentiation (**Figure 10A**). Specifically, after BMP2 treatment, the number of undifferentiated TS cells (a colony with tightly packed cells characteristic, yellow arrowheads) was decreased, while the number of differentiated TS cells (a typical TGC morphology, blue arrowheads) (**Figure 10B**). These results indicated that recombinant BMP2 promotes TS cell differentiation. Similar to the results in humans, BMP2 promoted cell invasion without affecting cell proliferation in mouse stem cells (**Figure 10C**). Additionally, BMP2 increased the expression of SNAIL and MMP2 at the transcriptional and translational levels in mouse TS cells (**Figure 10D**). Moreover, BMP2 significantly increased the MMP2 activity in the conditioned medium of cultured cells (**Figure 10D**). These results indicate that BMP2 promotes the invasive differentiation of mouse trophoblasts.

DISCUSSION

Trophoblast differentiation and invasion are critical for early embryo development and subsequent implantation, and any dysregulation of the key regulators in this process may lead to an unsuccessful pregnancy. Members of the TGF-β superfamily are involved in the regulation of embryo implantation and trophoblast invasion (Cheng et al., 2013; Li et al., 2014). Additionally, studies have shown that members of the BMP subfamily induce differentiation of cells to the trophoblast lineage (Xu et al., 2002; Lichtner et al., 2013). Our previous study also showed that BMP2 promotes human trophoblast cell invasion by upregulating EMT-associated markers (Zhao et al., 2018a,b, 2020). In this follow-up study, we further investigated the function and molecular mechanisms by which BMP2 regulates the process of embryo development and trophoblast differentiation. Information obtained from clinical samples showed that the serum BMP2 levels were significantly increased during the first trimester of pregnancy. Given that elevated peripheral BMP2 levels are associated with the development of placental tissue during the first trimester, trophoblast cells are one of the sources of the circulating BMP2. Additionally, the serum BMP2 levels were significantly reduced and the BMP2 expression levels were downregulated in villous tissues obtained from women with EPL, indicating that BMP2 is a principal factor for placentation in humans. Moreover, we provided the first data showing that BMP2 is expressed in the human oocyte and trophoblast cells of cleavage embryos and blastocysts prior to implantation. However, all the human embryos used in this study were embryos developing slowly or with arrested development and those with poor-quality embryo morphology. These embryos were selected not to be used for embryo transfer during assisted reproductive technology. Therefore, the expression level of BMP2 in these embryos could be different from those in the normal developed embryos. Previous studies have shown that embryo implantation promotes endometrium decidualization (Paria et al., 2001; Sharma et al., 2016). Taken together, previous studies and our results indicate that BMP2 secreted by endometrial cells and trophoblast cells may mediate their cooperation during placentation in an autocrine/paracrine manner, which is essential for early pregnancy maintenance.

In this study, the gene set enrichment analysis plot indicated a significant correlation between BMP2 and the EMT signaling pathway. EMT is a fundamental process of cell shape change that forms extravillous and interstitial cytotrophoblasts with mesenchymal characteristics during placental development (Kokkinos et al., 2010). MMPs have been reported to be related to the invasive ability of trophoblasts, which are capable of digesting collagen IV, a major component of the basement membrane (Seval et al., 2004). A previous study showed that MMP2 and MMP9 were localized at the placental bed, primarily in EVT cells during early pregnancy, and were involved in the regulation of trophoblast invasion (Ma et al., 2015). Specifically, MMP2 is expressed at a peak level, which is closely associated with invasive potential at the implantation site during the first trimester of pregnancy (Shimonovitz et al., 1994; Isaka et al., 2003; Bai et al., 2005; Jones et al., 2006). Notably, we found that BMP2 promoted trophoblast invasion by upregulating expression of MMP2 but not expression of MMP9. In the trophoblast cells obtained from a gestational placenta at 6–8 weeks, MMP2 is a key regulator of trophoblast invasion (Staun-Ram et al., 2004). Consistent with these results, our *in vitro* experiments confirmed that BMP2 plays

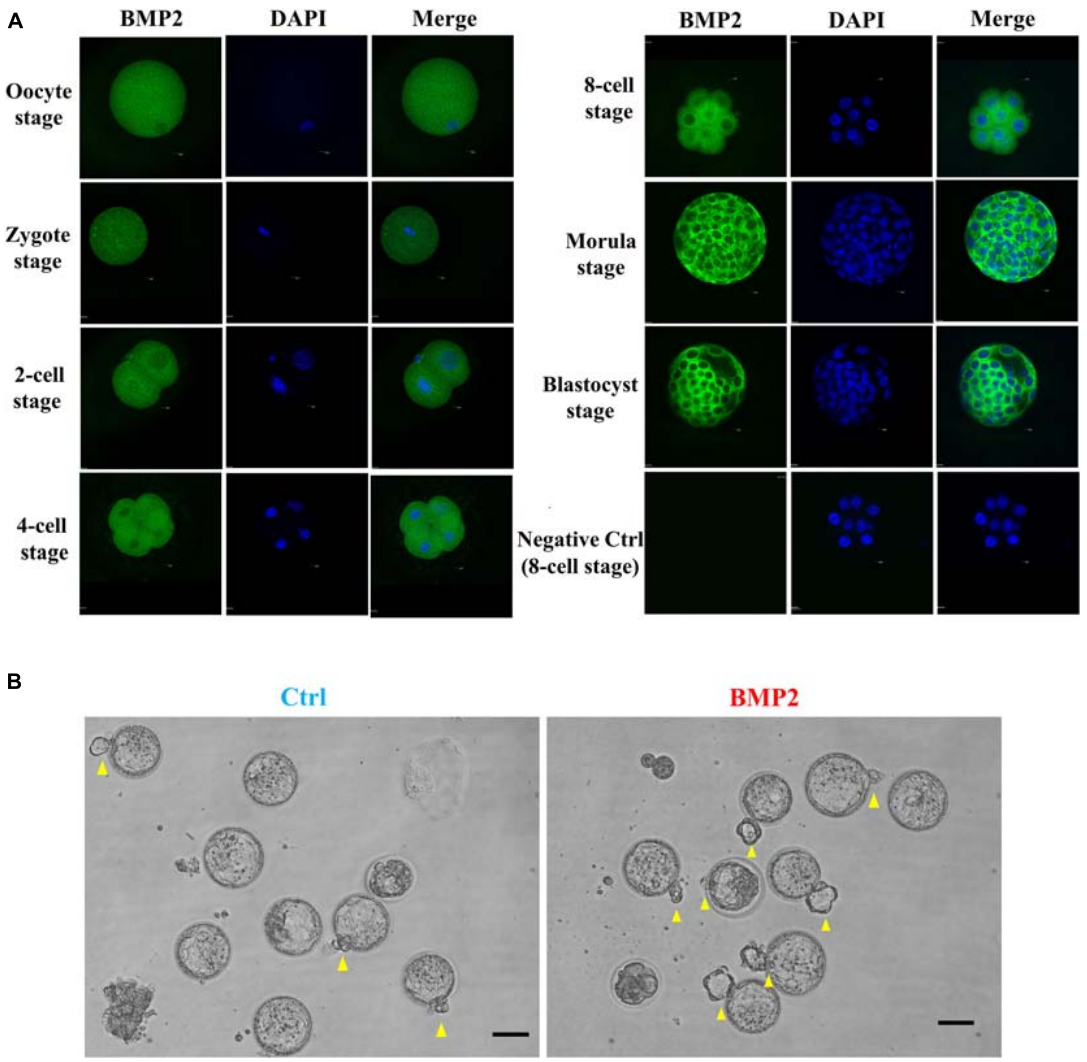

FIGURE 9 | BMP2 promotes the development of mouse preimplantation embryos. **(A)** The expression and localization of BMP2 in mouse preimplantation embryos. Mouse preimplantation embryos, including the oocyte, zygote, 2-cell, 4-cell, 8-cell, morula and blastocyst stages, were fixed and probed with a specific antibody against mouse BMP2 followed by probing with a fluorescein isothiocyanate-conjugated secondary antibody or DAPI counterstaining. The images were detected using confocal microscopy. **(B)** BMP2 accelerates the processes of blastocyst formation and hatching. Mouse 2-cell embryos were cultured in HTF medium with Ctrl or 100 ng/mL BMP2 for 72 h. The processes of blastocyst formation and hatching (yellow arrowheads) were detected with microscopic observation. Six independent experiments (n = 6) were performed, and similar results were obtained (the total number of embryos in the control group was 110 and that in the BMP2 group was 111). The scale bars represent 50 μm.

a key role in regulating trophoblast invasion by upregulating MMP2 expression through SNAIL.

In the present study, our functional studies revealed that BMP2 has a regulatory role in the promotion of trophoblast invasion in primary EVT cells. Using whole-genome sequencing, we identified certain differentially expressed mRNAs, miRNAs and lncRNAs that are associated with BMP2-induced trophoblast invasion. Many studies have demonstrated the involvement of miRNAs and lncRNAs in the regulation of trophoblast function and placental development in humans (McAninch et al., 2017; Hayder et al., 2018). LncRNAs are defined as RNAs longer than 200 nucleotides in length and do not produce a protein product. Here, we showed that BMP2 prominently induces the upregulation of NR026833.1, a lncRNA expressed in primary human EVT cells. Indeed, the expression levels of BMP2 were positively correlated with those in human villous tissue. Clinical data also showed that the expression levels of NR026833.1 were significantly reduced in villous tissues obtained from women with EPL compared to those obtained from women with NPs, indicating that this lncRNA has a role in early placentation. Our experiments further demonstrated that NR026833.1 knockdown decreased cell invasion, whereas NR026833.1 overexpression increased cell invasion in primary EVT cells. LncRNA can serve as a miRNA sponge to sequester and saturate the cellular pool of miRNA, thereby operating as a competitive inhibitor to suppress the

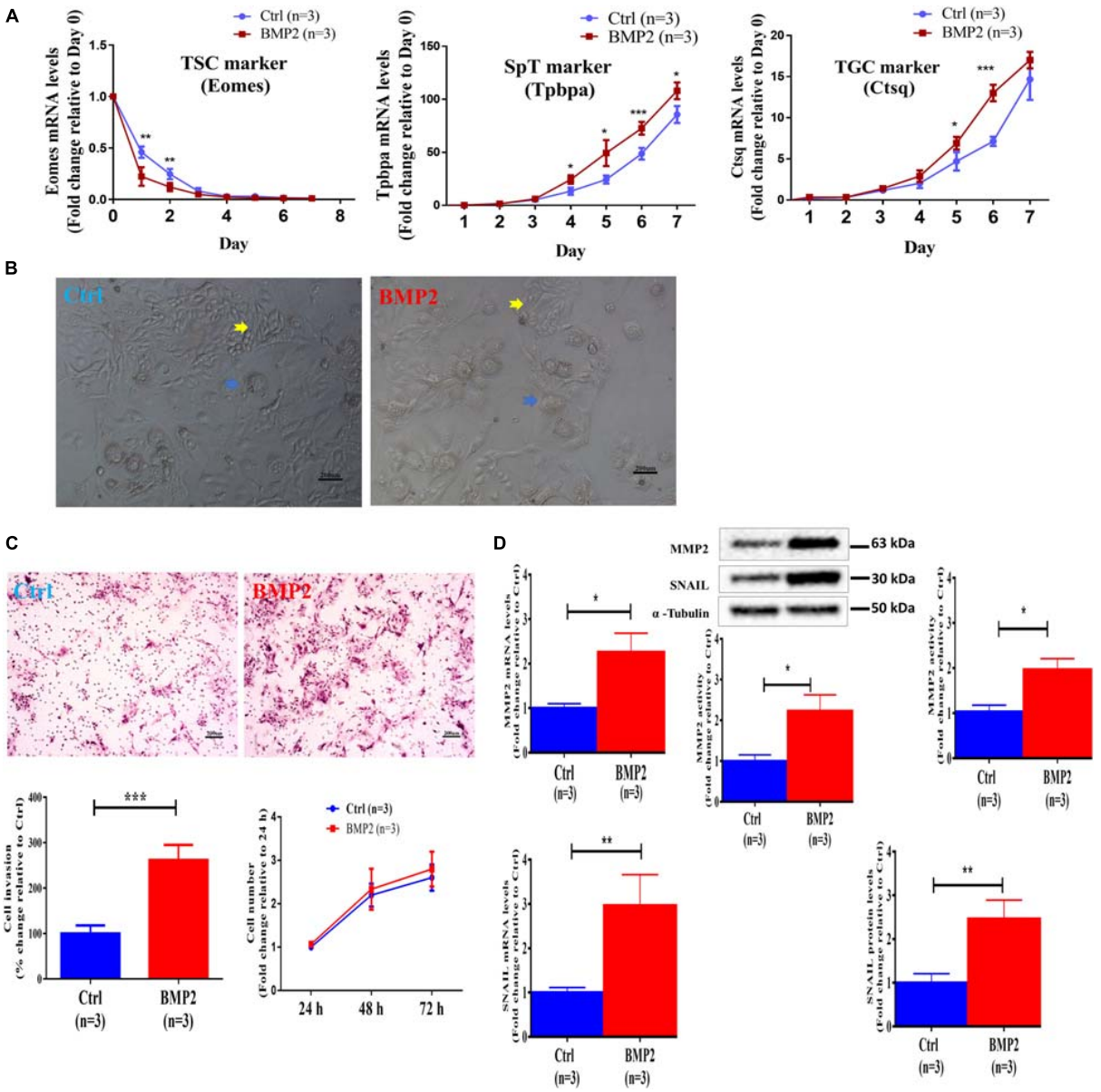

FIGURE 10 | BMP2 promotes the invasive differentiation of mouse TS cells. **(A)** TS cells were treated with Ctrl or 100 ng/mL BMP2 every 24 h for up to 7 days, and three cell marker genes, including *Eomes* (TS cell marker), *Tpbpa* (SpT marker) and *Ctsq* (TGC marker), were examined using RT-qPCR. **(B)** TS cells were treated with Ctrl or 100 ng/mL BMP2 for 4 days, and cell images were detected with microscopic observation. Undifferentiated TS cells showed a colony with characteristic tightly packed cells (yellow arrowheads), while differentiated TS cells showed a typical TGC morphology (blue arrowheads). These differentiated TS cells showed a flattened appearance and increased cell, nuclei and perinuclear granule sizes (blue arrowheads). The scale bars represent 200 μm. **(C)** TS cells were treated with Ctrl or 100 ng/mL BMP2 every 24 h for a total of 72 h, and cell invasion was examined using a Matrigel-coated transwell invasion assay. Cell viability was determined using a CCK-8 assay. **(D)** TS cells were treated for 12 or 24 h with Ctrl or 100 ng/mL BMP2, and the mRNA (12 h) and protein (24 h) levels of MMP2 and SNAIL were examined using RT-qPCR and western blot analyses, respectively. TS cells were treated for 24 h with Ctrl or 100 ng/mL BMP2, and the MMP2 activity was examined using ELISA. GAPDH and α-tubulin were used to normalize the RT-qPCR and western blot results, respectively. The results are expressed as the mean ± SEM of three independent experiments ($n = 3$, $^{*}P < 0.05$, $^{**}P < 0.01$ and $^{***}P < 0.001$). Differences between groups were determined by Student's *t*-test or one-way analysis of variance.

binding of miRNA to its mRNA targets (Bak and Mikkelsen, 2014). We further confirmed that NR026833.1 was preferentially localized in the cytoplasm of primary human EVT cells and that there was a binding site in NR026833.1 for miR-502-5p, a miRNA that was also expressed in primary human EVT cells. Notably, the miR-502-5p mimic abolished the cell invasion-promoting effect caused by NR026833.1 overexpression. These results indicate that NR026833.1 may serve as an intracellular sponge for miR-502-5p and may abolish the miR-502-5p-induced suppression of cell invasion. MiRNAs are classified as

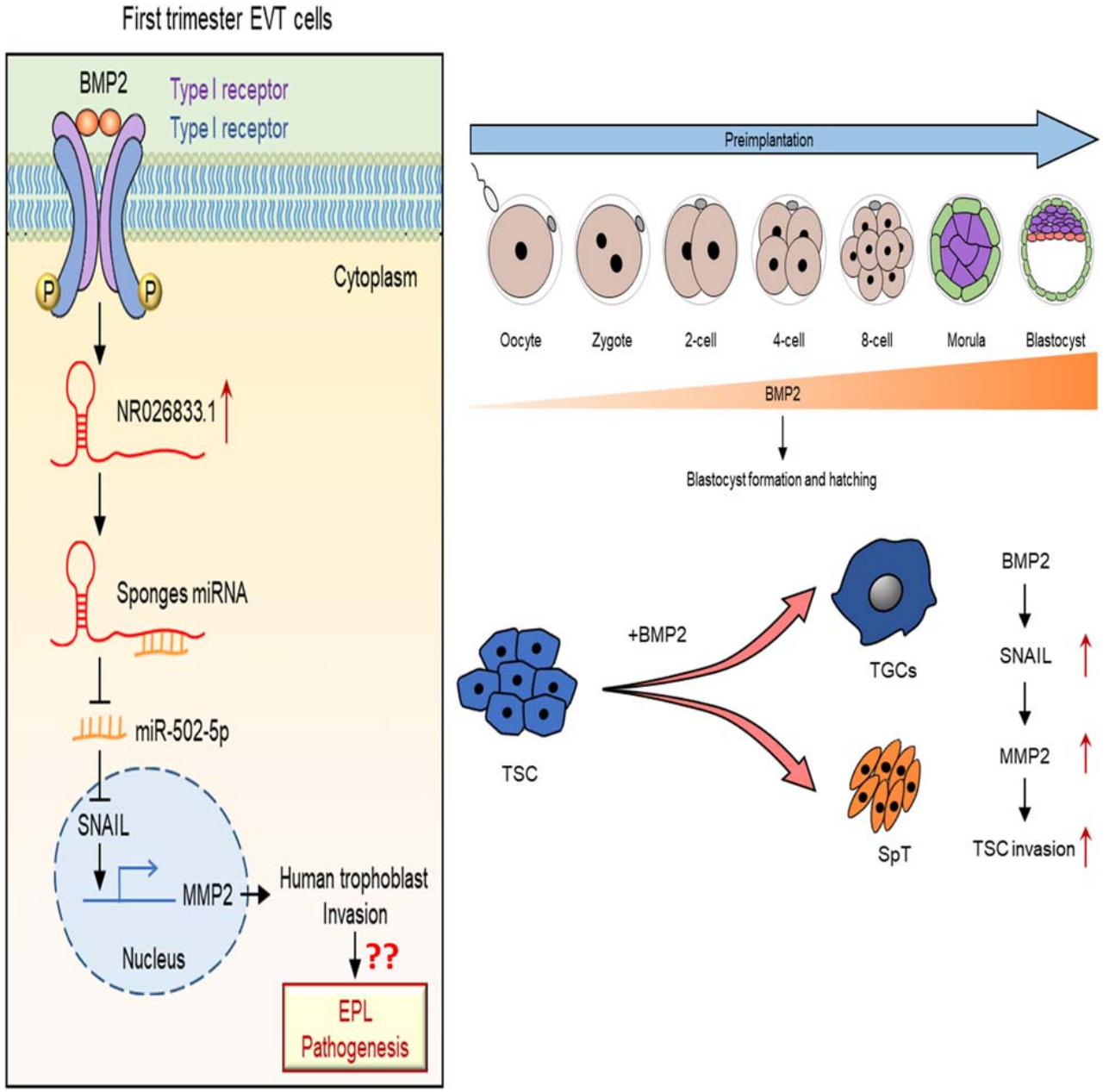

FIGURE 11 | A **s**chematic diagram of the regulatory role of the BMP2/NR026833.1/SNAIL/MMP2 signaling axis in promoting the invasive differentiation of trophoblasts. Left panel figure. LncRNA NR026833.1 is upregulated by BMP2 and promotes the expression of SNAIL (target gene of miR-502-5p) by acting as a decoy to competitively bind to miR-502-5p. The upregulation of SNAIL further acts as a transcription factor that induces the production of MMP2, which in turn promotes cell invasion in primary EVT cells. Right panel figure. In humans and mice, BMP2 is expressed in the oocyte and all embryo stages (especially the trophectoderm). Exogenous BMP2 enhances embryonic development by increasing blastocyst formation and hatching. Additionally, BMP2 promotes the invasive differentiation of TS cells by upregulating the expression of SNAIL and MMP2.

endogenous small non-coding RNAs that negatively modulate gene expression by binding to specific mRNAs and promoting their degradation or translational repression (Bartel, 2004). Using bioinformatics analysis and luciferase reporter assays, we identified a putative binding site of the 3′ UTR of SNAIL mRNA that specifically matched miR-502-5p, indicating that SNAIL is the target of this trophoblast-derived miRNA. Our study further revealed that transfection with the miR-502-5p mimic suppressed the expression of SNAIL at the transcriptional and translational levels and that inhibition of miR-502-5p reversed the siSNAIL-mediated decrease in cell invasion. SNAIL is a prototypical EMT-inducing transcription factor that is essential for trophoblast invasion (Blechschmidt et al., 2007). Using the siRNA-mediated inhibition approach,

we showed that SNAIL knockdown decreased basal and BMP2-induced cell invasion in primary EVT cells. These findings suggest that in human primary EVT cells, miR-502-5p acts to suppress cell invasion by binding to the EMT-related transcription factor SNAIL and that the BMP2-induced increase in NR026833.1 promotes the expression of SNAIL by competitively binding to (and suppressing the effect of) miR-502-5p.

Improper trophectoderm differentiation is associated with arrested preimplantation development and defective embryo implantation, leading to early pregnancy failure (Roberts and Fisher, 2011; Pfeffer and Pearton, 2012). Because of ethical issues, we utilized mouse embryos to investigate the effects of BMP2 on embryo development and trophoblast invasion. The results showed that BMP2 is expressed in the mouse oocyte and during all embryo stages, including 2, 4, and 8-cell embryos as well as morula and blastocysts (mainly in the trophectoderm cells). Intriguingly, exogenous BMP2 promoted embryonic development by enhancing blastocyst formation and hatching in mice. In line with our results, a previous study showed that several BMP2 receptor genes, including Bmpr1a, are expressed in the extraembryonic ectoderm (ExE) (Kishigami and Mishina, 2005). *In situ* hybridization studies in mice demonstrated that the expression of BMP2 in the uterus was spatiotemporally correlated with embryo implantation, suggesting that BMP2 plays a critical role during embryo implantation and early placentation (Paria et al., 2001). Additionally, we used mouse TS cells to examine the roles of BMP2 in the regulation of trophoblast cell differentiation and invasion. Our results showed that treatment with BMP2 promoted trophoblast differentiation by downregulating the expression of Eomes (TS cell marker) and upregulating the expression of Ctsq (TGC marker) and Tpbpa (SpT marker) in mouse TS cells. Additionally, exogenous BMP2 promoted cell invasion without affecting cell proliferation. Similar to the results in primary human EVT cells, the BMP2-induced increase in cell invasion is most likely through the upregulation of SNAIL and MMP2 expression in mouse TS cells (**Figure 9**). These findings suggest that the stimulatory effect of BMP2 on the invasive potential of trophoblasts most likely occurs at a very early stage of placentation. However, one question has been raised regarding the cause and effect of BMP2 and EPL in humans. Indeed, it is difficult to draw a conclusion whether changes in the levels of BMP2 are a cause or effect of the pregnancy loss in humans. Future studies aimed at addressing this issue will be of great interest.

CONCLUSION

In conclusion, our findings provide significant insights into the molecular biology of embryo-maternal interactions, underscoring the importance of BMP2 in promoting blastocyst implantation and placental development. These processes are essential for successful pregnancy and fetal development and growth. Notably, our study reveals a new regulatory pathway in which BMP2 induces a miR502-5p/SNAIL/MMP2 signaling axis via NR026833.1 upregulation (**Figure 11**). This advance in knowledge will provide us a framework to explore new diagnostic and therapeutic strategies for pregnancy-related complications.

DATA AVAILABILITY STATEMENT

The original contributions presented in the study are included in the article/**Supplementary Material**, further inquiries can be directed to the corresponding author/s.

ETHICS STATEMENT

The studies involving human participants were reviewed and approved by the Ethical Review Committee of Women's Hospital, Zhejiang University School of Medicine. The patients/participants provided their written informed consent to participate in this study. The animal study was reviewed and approved by the Ethical Review Committee of Women's Hospital, Zhejiang University School of Medicine.

AUTHOR CONTRIBUTIONS

Y-MZ and PL designed the research. JY and WW performed the research and analyzed the data. JY and H-MC wrote the manuscript. JY, HZha, HZhu, YS, and MT collected first trimester human placental villi. CW, YS, GF, and SC analyzed and interpreted the data. Y-MZ and PL revised the manuscript. All authors were involved in interpreting the data and approved the final article.

FUNDING

This work was supported by the National Key R&D Program of China (2018YFC1003200), the National Science and Technology Pillar Program during the 13th Five-year Plan Period (No.2016YFC1000302), the National Natural Science Foundation of China (81900461), the Zhejiang Provincial Natural Science Foundation of China (LQ19H160022 and LQ20H040010), and the Science and Technology Project of Zhejiang Province (LGF19H040017). This work was also supported by the CIHR Foundation Scheme Grant (No. 143317).

SUPPLEMENTARY MATERIAL

The Supplementary Material for this article can be found online at: https://www.frontiersin.org/articles/10.3389/fcell.2021.607332/full#supplementary-material

Supplementary Figure 1 | The purity of EVT cell cultures was verified by immunocytochemical staining for cytokeratin-7. DAPI was used to stain the cell nuclei.

Supplementary Figure 2 | A whole image of western blot showing the location of BMP2 (molecular weight: 44 kDa).

Supplementary Figure 3 | BMP2 upregulates the expression of ID1, ID2, and ID3 in primary human EVT cells. Primary human EVT cells were treated for 12 h with Ctrl or 25 ng/mL BMP2 and the mRNA levels of ID1, ID2, and ID3 were examined using RT-qPCR. GAPDH was used to normalize the RT-qPCR results. The results are expressed as the mean ± SEM of five independent experiments ($n = 5$, $^{***}P < 0.001$). Differences between groups were determined by Student's *t*-test.

Supplementary Figure 4 | Primary human EVT cells were treated for 12 h with Ctrl or 25 ng/mL BMP2 and the mRNA levels of MMP9 **(A)** and MMP1/3/7/10/11/12/14/15/16/17/21/23/24/25/28 **(B)** were examined using RT-qPCR. The results are expressed as the mean ± SEM of five independent experiments ($n = 5$, NS, no significant difference). Differences between groups were determined by Student's *t*-test.

Supplementary Figure 5 | SNAIL mediates the BMP2-induced upregulation of MMP2 and the increase in cell invasion of primary human EVT cells. Primary human EVT cells were transfected with 25 nM siCtrl or 25 nM siSNAIL for 24 h, and the cells were treated with Ctrl or 25 ng/mL BMP2 for an additional 48 h. Cell invasion was examined using the Matrigel-coated transwell invasion assay.

Supplementary Figure 6 | MiR-502-5p suppresses SNAIL expression and decreases SNAIL-mediated cell invasion in primary human EVT cells. Primary human EVT cells were cotransfected with 25 nM miRNA inhibitor negative control (inhibitor Ctrl) or 25 nM miR-502-5p inhibitor for 24 h as well as 25 nM siCtrl or 25 nM siSNAIL for 24 h. Cell invasion was examined using the Matrigel-coated transwell invasion assay.

Supplementary Figure 7 | (A,B) Volcano plot of the *P*-values as a function of weighted fold-change for lncRNAs in primary human EVT cells treated with BMP2. Gray dots represent lncRNAs not significantly differentially expressed (fold change < 1; $P > 0.05$) and red and green dots represent lncRNAs that are significantly differentially expressed (fold change ≥ 1; $P < 0.05$). **(C)** Primary human EVT cells were treated for 24 h with Ctrl or 25 ng/mL BMP2 and the relative levels of various lncRNA were examined using RT-qPCR.

Supplementary Data 1 | The list of primers sequence.

Supplementary Data 2 | The list of antibodies used in this study.

REFERENCES

Bai, S. X., Wang, Y. L., Qin, L., Xiao, Z. J., Herva, R., and Piao, Y. S. (2005). Dynamic expression of matrix metalloproteinases (MMP-2, -9 and -14) and the tissue inhibitors of MMPs (TIMP-1, -2 and -3) at the implantation site during tubal pregnancy. *Reproduction* 129, 103–113. doi: 10.1530/rep.1.00283

Bak, R. O., and Mikkelsen, J. G. (2014). miRNA sponges: soaking up miRNAs for regulation of gene expression. *Wiley Interdiscip. Rev. RNA* 5, 317–333. doi: 10.1002/wrna.1213

Bartel, D. P. (2004). MicroRNAs: genomics, biogenesis, mechanism, and function. *Cell* 116, 281–297.

Bianchi, D. W., Wilkins-Haug, L. E., Enders, A. C., and Hay, E. D. (1993). Origin of extraembryonic mesoderm in experimental animals: relevance to chorionic mosaicism in humans. *Am. J. Med. Genet.* 46, 542–550. doi: 10.1002/ajmg.1320460517

Blechschmidt, K., Mylonas, I., Mayr, D., Schiessl, B., Schulze, S., Becker, K. F., et al. (2007). Expression of E-cadherin and its repressor snail in placental tissue of normal, preeclamptic and HELLP pregnancies. *Virchows Arch.* 450, 195–202. doi: 10.1007/s00428-006-0343-x

Brosens, I., Pijnenborg, R., Vercruysse, L., and Romero, R. (2011). The "great obstetrical syndromes" are associated with disorders of deep placentation. *Am. J. Obstet. Gynecol.* 204, 193–201. doi: 10.1016/j.ajog.2010.08.009

Cakmak, H., and Taylor, H. S. (2011). Implantation failure: molecular mechanisms and clinical treatment. *Hum. Reprod. Update* 17, 242–253. doi: 10.1093/humupd/dmq037

Chen, X., Liao, J., Lu, Y., Duan, X., and Sun, W. (2011). Activation of the PI3K/Akt pathway mediates bone morphogenetic protein 2-induced invasion of pancreatic cancer cells Panc-1. *Pathol. Oncol. Res.* 17, 257–261. doi: 10.1007/s12253-010-9307-1

Cheng, J. C., Chang, H. M., and Leung, P. C. (2013). Transforming growth factor-beta1 inhibits trophoblast cell invasion by inducing Snail-mediated down-regulation of vascular endothelial-cadherin protein. *J. Biol. Chem.* 288, 33181–33192. doi: 10.1074/jbc.m113.488866

Clement, J. H., Raida, M., Sanger, J., Bicknell, R., Liu, J., Naumann, A., et al. (2005). Bone morphogenetic protein 2 (BMP-2) induces in vitro invasion and in vivo hormone independent growth of breast carcinoma cells. *Int. J. Oncol.* 27, 401–407.

Gardner, R. L. (1982). Investigation of cell lineage and differentiation in the extraembryonic endoderm of the mouse embryo. *J. Embryol. Exp. Morphol.* 68, 175–198.

Greenwold, N., Jauniaux, E., Gulbis, B., Hempstock, J., Gervy, C., and Burton, G. J. (2003). Relationship among maternal serum endocrinology, placental karyotype, and intervillous circulation in early pregnancy failure. *Fertil. Steril.* 79, 1373–1379. doi: 10.1016/s0015-0282(03)00364-9

Gupta, S. K., Malhotra, S. S., Malik, A., Verma, S., and Chaudhary, P. (2016). Cell signaling pathways involved during invasion and syncytialization of trophoblast cells. *Am. J. Reprod. Immunol.* 75, 361–371. doi: 10.1111/aji.12436

Hayder, H., O'Brien, J., Nadeem, U., and Peng, C. (2018). MicroRNAs: crucial regulators of placental development. *Reproduction* 155, R259–R271.

Hempstock, J., Jauniaux, E., Greenwold, N., and Burton, G. J. (2003). The contribution of placental oxidative stress to early pregnancy failure. *Hum. Pathol.* 34, 1265–1275. doi: 10.1016/j.humpath.2003.08.006

Isaka, K., Usuda, S., Ito, H., Sagawa, Y., Nakamura, H., Nishi, H., et al. (2003). Expression and activity of matrix metalloproteinase 2 and 9 in human trophoblasts. *Placenta* 24, 53–64. doi: 10.1053/plac.2002.0867

Jones, R. L., Findlay, J. K., Farnworth, P. G., Robertson, D. M., Wallace, E., and Salamonsen, L. A. (2006). Activin A and inhibin A differentially regulate human uterine matrix metalloproteinases: potential interactions during decidualization and trophoblast invasion. *Endocrinology* 147, 724–732. doi: 10.1210/en.2005-1183

Kang, M. H., Kim, J. S., Seo, J. E., Oh, S. C., and Yoo, Y. A. (2010). BMP2 accelerates the motility and invasiveness of gastric cancer cells via activation of the phosphatidylinositol 3-kinase (PI3K)/Akt pathway. *Exp. Cell Res.* 316, 24–37. doi: 10.1016/j.yexcr.2009.10.010

Kim, B. R., Oh, S. C., Lee, D. H., Kim, J. L., Lee, S. Y., Kang, M. H., et al. (2015). BMP-2 induces motility and invasiveness by promoting colon cancer stemness through STAT3 activation. *Tumour Biol.* 36, 9475–9486. doi: 10.1007/s13277-015-3681-y

Kishigami, S., and Mishina, Y. (2005). BMP signaling and early embryonic patterning. *Cytokine Growth Fact. Rev.* 16, 265–278. doi: 10.1016/j.cytogfr.2005.04.002

Kokkinos, M. I., Murthi, P., Wafai, R., Thompson, E. W., and Newgreen, D. F. (2010). Cadherins in the human placenta–epithelial-mesenchymal transition (EMT) and placental development. *Placenta* 31, 747–755. doi: 10.1016/j.placenta.2010.06.017

Lee, K. Y., Jeong, J. W., Wang, J., Ma, L., Martin, J. F., Tsai, S. Y., et al. (2007). Bmp2 is critical for the murine uterine decidual response. *Mol. Cell Biol.* 27, 5468–5478. doi: 10.1128/mcb.00342-07

Li, Y., Klausen, C., Cheng, J. C., Zhu, H., and Leung, P. C. (2014). Activin A, B, and AB increase human trophoblast cell invasion by up-regulating N-cadherin. *J. Clin. Endocrinol. Metab.* 99, E2216–E2225.

Li, Y., Klausen, C., Zhu, H., and Leung, P. C. (2015). Activin A increases human trophoblast invasion by inducing SNAIL-mediated MMP2 Up-regulation through ALK4. *J. Clin. Endocrinol. Metab.* 100, E1415–E1427.

Lichtner, B., Knaus, P., Lehrach, H., and Adjaye, J. (2013). BMP10 as a potent inducer of trophoblast differentiation in human embryonic and induced pluripotent stem cells. *Biomaterials* 34, 9789–9802. doi: 10.1016/j.biomaterials.2013.08.084

Ma, M. Z., Chu, B. F., Zhang, Y., Weng, M. Z., Qin, Y. Y., Gong, W., et al. (2015). Long non-coding RNA CCAT1 promotes gallbladder cancer development via negative modulation of miRNA-218-5p. *Cell Death Dis.* 6:e1583. doi: 10.1038/cddis.2014.541

McAninch, D., Roberts, C. T., and Bianco-Miotto, T. (2017). Mechanistic insight into long noncoding RNAs and the placenta. *Int. J. Mol. Sci.* 18:1371. doi: 10.3390/ijms18071371

Miyazono, K., Kusanagi, K., and Inoue, H. (2001). Divergence and convergence of TGF-beta/BMP signaling. *J. Cell Physiol.* 187, 265–276. doi: 10.1002/jcp.1080

Nagashima, T., Li, Q., Clementi, C., Lydon, J. P., DeMayo, F. J., and Matzuk, M. M. (2013). BMPR2 is required for postimplantation uterine function and pregnancy maintenance. *J. Clin. Invest.* 123, 2539–2550. doi: 10.1172/jci65710

Paria, B. C., Ma, W., Tan, J., Raja, S., Das, S. K., Dey, S. K., et al. (2001). Cellular and molecular responses of the uterus to embryo implantation can be elicited by locally applied growth factors. *Proc. Natl. Acad. Sci. U.S.A.* 98, 1047–1052. doi: 10.1073/pnas.98.3.1047

Pfeffer, P. L., and Pearton, D. J. (2012). Trophoblast development. *Reproduction* 143, 231–246.

Roberts, R. M., and Fisher, S. J. (2011). Trophoblast stem cells. *Biol. Reprod.* 84, 412–421.

Seval, Y., Akkoyunlu, G., Demir, R., and Asar, M. (2004). Distribution patterns of matrix metalloproteinase (MMP)-2 and -9 and their inhibitors (TIMP-1 and TIMP-2) in the human decidua during early pregnancy. *Acta Histochem.* 106, 353–362. doi: 10.1016/j.acthis.2004.07.005

Sharma, S., Godbole, G., and Modi, D. (2016). Decidual control of trophoblast invasion. *Am. J. Reprod. Immunol.* 75, 341–350. doi: 10.1111/aji.12466

Shimasaki, S., Moore, R. K., Otsuka, F., and Erickson, G. F. (2004). The bone morphogenetic protein system in mammalian reproduction. *Endocr. Rev.* 25, 72–101. doi: 10.1210/er.2003-0007

Shimonovitz, S., Hurwitz, A., Dushnik, M., Anteby, E., Geva-Eldar, T., and Yagel, S. (1994). Developmental regulation of the expression of 72 and 92 kd type IV collagenases in human trophoblasts: a possible mechanism for control of trophoblast invasion. *Am. J. Obstet. Gynecol.* 171, 832–838. doi: 10.1016/0002-9378(94)90107-4

Staun-Ram, E., Goldman, S., Gabarin, D., and Shalev, E. (2004). Expression and importance of matrix metalloproteinase 2 and 9 (MMP-2 and -9) in human trophoblast invasion. *Reprod. Biol. Endocrinol.* 2:59.

Stirparo, G. G., Boroviak, T., Guo, G., Nichols, J., Smith, A., and Bertone, P. (2018). Correction: integrated analysis of single-cell embryo data yields a unified transcriptome signature for the human pre-implantation epiblast *Development* 08:145. doi: 10.1242/dev.158501

Tanaka, S., Kunath, T., Hadjantonakis, A. K., Nagy, A., and Rossant, J. (1998). Promotion of trophoblast stem cell proliferation by FGF4. *Science* 282, 2072–2075. doi: 10.1126/science.282.5396.2072

Uy, G. D., Downs, K. M., and Gardner, R. L. (2002). Inhibition of trophoblast stem cell potential in chorionic ectoderm coincides with occlusion of the ectoplacental cavity in the mouse. *Development* 129, 3913–3924.

Wehrum, M. J., Buhimschi, I. A., Salafia, C., Thung, S., Bahtiyar, M. O., Werner, E. F., et al. (2011). Accreta complicating complete placenta previa is characterized by reduced systemic levels of vascular endothelial growth factor and by epithelial-to-mesenchymal transition of the invasive trophoblast. *Am. J. Obstet. Gynecol.* 204:411.

Xu, R. H., Chen, X., Li, D. S., Li, R., Addicks, G. C., Glennon, C., et al. (2002). BMP4 initiates human embryonic stem cell differentiation to trophoblast. *Nat. Biotechnol.* 20, 1261–1264. doi: 10.1038/nbt761

Yang, Y., Yang, C., and Zhang, J. (2015). C23 protein meditates bone morphogenetic protein-2-mediated EMT via up-regulation of Erk1/2 and Akt in gastric cancer. *Med. Oncol.* 32:76.

Ying, Y., and Zhao, G. Q. (2000). Detection of multiple bone morphogenetic protein messenger ribonucleic acids and their signal transducer, Smad1, during mouse decidualization. *Biol. Reprod.* 63, 1781–1786. doi: 10.1095/biolreprod63.6.1781

Yu, P. B., Hong, C. C., Sachidanandan, C., Babitt, J. L., Deng, D. Y., Hoyng, S. A., et al. (2008). Dorsomorphin inhibits BMP signals required for embryogenesis and iron metabolism. *Nat. Chem. Biol.* 4, 33–41. doi: 10.1038/nchembio.2007.54

Zhao, H. J., Chang, H. M., Zhu, H., Klausen, C., Li, Y., and Leung, P. C. K. (2018a). Bone morphogenetic protein 2 promotes human trophoblast cell invasion by inducing activin A production. *Endocrinology* 159, 2815–2825. doi: 10.1210/en.2018-00301

Zhao, H. J., Klausen, C., Li, Y., Zhu, H., Wang, Y. L., and Leung, P. C. K. (2018b). Bone morphogenetic protein 2 promotes human trophoblast cell invasion by upregulating N-cadherin via non-canonical SMAD2/3 signaling. *Cell Death Dis.* 9:174.

Zhao, H. J., Klausen, C., Zhu, H., Chang, H. M., Li, Y., and Leung, P. C. K. (2020). Bone morphogenetic protein 2 promotes human trophoblast cell invasion and endothelial-like tube formation through ID1-mediated upregulation of IGF binding protein-3. *FASEB J.* 34, 3151–3164. doi: 10.1096/fj.201902168rr

Zhou, X., Gao, Q., Wang, J., Zhang, X., Liu, K., and Duan, Z. (2014). Linc-RNA-RoR acts as a "sponge" against mediation of the differentiation of endometrial cancer stem cells by microRNA-145. *Gynecol. Oncol.* 133, 333–339. doi: 10.1016/j.ygyno.2014.02.033

Conflict of Interest: The authors declare that the research was conducted in the absence of any commercial or financial relationships that could be construed as a potential conflict of interest.

frontiers in Cell and Developmental Biology

ORIGINAL RESEARCH
published: 16 February 2021
doi: 10.3389/fcell.2021.641891

Integrated Characterization of lncRNA-Immune Interactions in Prostate Cancer

Wei Hu[1†], Yanru Wang[2†], Zhixiao Fang[1], Wei He[2] and Shengli Li[1*]*

[1] Institute of Translational Medicine, Shanghai General Hospital, Shanghai Jiao Tong University School of Medicine, Shanghai, China, [2] Department of Nuclear Medicine, Huadong Hospital Affiliated to Fudan University, Shanghai, China

Prostate cancer is among the top mortality factors in male around the world. Long non-coding RNAs (lncRNAs) have been shown to play crucial roles in tumor biology and immunology. However, lncRNA-immune interactions have not yet examined in prostate cancer. Here, we performed integrated analysis to characterize lncRNA-immune interactions in prostate cancer through multidimensional aspects, including immune-related hallmarks, tumor immunogenomic signatures, immune-related biological processes, immune cells, and immune checkpoints. We dissected the dysregulation of lncRNAs and their clinical relevance in prostate cancer, such as RP11-627G23.1 and RP11-465N4.5. Immune-related hallmarks took up the major parts among top significant lncRNA-hallmark interactions. Our analysis revealed that TGF-β signaling pathway was the most frequent to associate with lncRNAs, which is a signature of immune response in cancer. In addition, immune response and its regulation were the most closely connected immunological processes with lncRNA, implying the regulatory roles of lncRNAs on immune response in prostate cancer. We found that memory resting $CD4^+$ T cells were the most lncRNA-correlated immune cell. LINC00861 was found to be potentially intervening targets of immunotherapy for prostate cancer patients, which was significantly associated with PD-1 and CTLA4. Collectively, we offered a handy resource to investigate regulatory roles of lncRNAs on tumor immunology and the development of clinical utility of lncRNAs in prostate cancer.

Keywords: long non-coding RNA, immune checkpoint, immunotherapy, prostate cancer, tumor immunology

OPEN ACCESS

Edited by:
Li Meng,
The Chinese University of Hong Kong, China

Reviewed by:
Meng Zhou,
Wenzhou Medical University, China
Chunjie Jiang,
University of Pennsylvania, United States

****Correspondence:***
Wei He
heweixu@hotmail.com
Shengli Li
shengli.li@shsmu.edu.cn

† These authors have contributed equally to this work

Specialty section:
This article was submitted to Cell Growth and Division, a section of the journal Frontiers in Cell and Developmental Biology

Received: *15 December 2020*
Accepted: *28 January 2021*
Published: *16 February 2021*

Citation:
Hu W, Wang Y, Fang Z, He W and Li S (2021) Integrated Characterization of lncRNA-Immune Interactions in Prostate Cancer. Front. Cell Dev. Biol. 9:641891. doi: 10.3389/fcell.2021.641891

INTRODUCTION

Prostate cancer is the most common malignancy in male, especially in Western World (Ferlay et al., 2015; Ku et al., 2019; Siegel et al., 2020). Despite substantial advances in diagnosis and therapeutics in prostate cancer, it still ranks the first cause of cancer mortality of male in the United States, which caused 33,330 deaths in 2020 statistics (Siegel et al., 2020). Studies regarding molecular alterations of prostate cancer offered mounts of potential diagnostic and therapeutic targets, with non-coding RNAs playing important roles (Ku et al., 2019).

Transcriptome diversity and their connections with critical biological processes have been investigated in multiple cancer types, among which non-coding RNAs took a large part

Abbreviations: lncRNA, long non-coding RNA; TCGA, The Cancer Genome Atlas; PRAD, Prostate Adenocarcinoma; GDC: Genomic Data Commons; TIME: tumor immune microenvironment; ICB: immune checkpoint blockade; CAFs: carcinoma-associated fibroblasts; Tregs: regulatory T cells.

(Kahles et al., 2018; Hua et al., 2019; Li et al., 2019). Long non-coding RNAs (lncRNAs) are >200 nt RNA molecules with limited protein-coding capability, which have been once considered as transcriptional noises (Du et al., 2013; Cech and Steitz, 2014; Iyer et al., 2015). Studies have shown that lncRNAs exert their biological functions through various ways, including miRNA sponges (Hansen et al., 2013; Yuan et al., 2014; Marchese et al., 2017), decoys to bind proteins (Carpenter et al., 2013; Qian et al., 2016), scaffolds or guides to regulate protein-protein or protein-DNA interactions (Engreitz et al., 2013; Lee et al., 2016). LncRNAs have been shown to play important roles in human cancers (Iyer et al., 2015; Niknafs et al., 2016; Li S. et al., 2018; Li Z. et al., 2018), including prostate cancer (Hua et al., 2018, 2019). In particular, down-regulation of UCA1 (urothelial carcinoma associated 1) inhibited proliferation of prostate cancer cells by modulating MYO6 through sponging miR-143 (Yu et al., 2020). Tumor immune microenvironment (TIME) is among the key factors impacting the treatment response, especially immunotherapy (Fridman et al., 2017; Mouw et al., 2017; Thorsson et al., 2018). The infiltrated abundance of cytotoxic and helper T lymphocytes within tumor microenvironment has shown prognostic and clinical implications in multiple cancer types (Fridman et al., 2017). A variety of immunogenomic features have been shown to contribute to influencing TIME, including tumor mutation burden and DNA damage repair defects (Bryant et al., 2017; Vitkin et al., 2019). Among genitourinary malignancies, prostate cancer shows unique TIME profiles with different features of infiltrated immune cell populations and immunogenomic features (Dallos and Drake, 2018; Vitkin et al., 2019). Through integrated analysis of lncRNA and immune features across 33 different cancer types, Li Y. et al. (2020) demonstrated that lncRNAs were closely interacted with immune-related pathways and infiltrated immune cells in cancer. However, the landscape of aberrant lncRNAs and their interactions with immune features in prostate cancer have not been characterized.

In the present study, we dissected the dysregulation of lncRNAs in prostate cancer and their clinical relevance. To comprehensively characterize lncRNA-immune interactions in prostate cancer, we assessed the associations between lncRNA expression and various immune features, including immune-related hallmarks, tumor immunogenomic signatures, immune-related biological processes, tumor infiltrated immune cells, and immune checkpoints. Our analysis revealed close connections between prostate cancer (PRAD) differential lncRNAs and these immune features in prostate cancer and suggested the potential clinical utility of lncRNAs in immunotherapy for patients with prostate cancer.

MATERIALS AND METHODS

Differential Expression Analysis

The read count profiles of genes in 18 The Cancer Genome Atlas (TCGA) cohorts with more than five paired adjacent normal samples were retrieved from the Genomic Data Commons (GDC) data portal[1] (Grossman et al., 2016). Raw read counts were normalized to FPKM units (Fragments Per Kilobase of transcript per Million mapped reads). Raw read count matrices were then subject to DESeq2 (Love et al., 2014) for differential expression analysis of long non-coding genes. Genes with fold change >1.5 and false discovery rate (FDR) (Benjamini–Hochberg corrected *P*-value) <0.05 were considered to be significantly expressed in tumor samples.

Risk Evaluation and Survival Analysis

Expression levels of individual differential lncRNAs across all prostate cancer samples were used to investigate the relations between expression variations and patient prognosis. The Cox univariate proportional hazards regression model was adopted to determine risk lncRNAs in prostate cancer. For each lncRNA, all patients were dichotomized into high- and low-expression groups using the median expression level as cut-off. The Kaplan–Meier algorithm was further utilized to compare overall survival times between the two groups as described in previous study (Li et al., 2017, 2019). Differences of overall survival times were estimated by using the log rank test.

Calculation of Gene Set Scores

The hallmark gene sets were first obtained from the Molecular Signature Database (MSigDB) (Liberzon et al., 2015). Then, the hallmark scores in each sample were calculated based on Gene Set Variation Analysis (GSVA) (Hänzelmann et al., 2013). Specifically, the GSVA algorithm was employed to evaluate the variation of hallmark activities over each sample in an unsupervised manner by utilizing expression profiles of genes annotated in corresponding hallmarks. Finally, the activity score of each hallmark was assigned to each sample.

Enrichment of lncRNAs in Biological Features

To evaluate the enrichment of individual lncRNAs in specific biological features, the correlations between individual lncRNAs and genes of biological features were first calculated by Spearman's correlation. LncRNA-gene pairs with $|Rs| > 0.3$ and FDR < 0.05 were considered as significant correlated pairs. For each lncRNA, Fisher's exact test and hypergeometric test was employed to estimate the difference of significant pairs between interested features and the others across 50 hallmarks and 95 immune-related biological processes, respectively. LncRNA-hallmark pairs with OR > 1 and FDR < 0.05 were considered as significantly enriched pairs. The corresponding lncRNAs were assigned to significant paired biological features as highly associated lncRNAs.

Estimation of Immune Cell Abundance in Tumor Samples

For each sample, the CIBERSORT (Newman et al., 2015) algorithm was employed to evaluate the relative immune cell abundance from gene expression profiles. In particular, immune-cell-type gene expression was deconvolved based on predefined

[1] https://portal.gdc.cancer.gov/

immune cell signatures. In this study, the LM22 immune cell signature was adopted. These immune cells were validated to differentially express in one certain leukocyte population compared to all other hematopoietic cell types. Specifically, LM22 signature includes 22 different immune cell types, i.e., "B cells naive," "B cells memory," "Plasma cells," "T cells CD8," "T cells CD4 naive," "T cells CD4 memory resting," "T cells CD4 memory activated," "T cell follicular helper," "T cells regulatory (Tregs)," "NK cells resting," "NK cells activated," "Monocytes," "Macrophages M0," "Macrophages M1," "Macrophages M2," "Dendritic cells resting," "Dendritic cells activated," "Mast cells resting," "Mast cells activated," "Eosinophils," and "Neutrophils." The correlation between expression level of each lncRNA and abundance of immune cells was then calculated to determine immune cell-related lncRNAs in prostate cancer.

Statistical Analysis and Plots

All statistical calculation and plots in this study were performed in R environment[2]. Unless specially stated, a statistical test with *P*-value or FDR < 0.05 was considered as significant.

RESULTS

Characterization of lncRNA Dysregulation and Clinical Relevance in Prostate Cancer

To systematically investigate dysregulation of lncRNAs in prostate cancer, we retrieved gene expression matrix from TCGA PRAD cohort, including 499 tumor and 52 paired adjacent normal prostate samples. All lncRNAs annotated in GENCODE (release v22) were extracted from the obtained expression matrix of PRAD. In total, 13,676 lncRNAs were detected with expression of no less than 0.1 FPKM in at least one PRAD sample. Various expression cut-offs were used to examine the expression distributions of lncRNAs across PRAD samples. Despite universal low expression, lncRNAs were extensively expressed in PRAD samples. In particular, an average of 32.1% lncRNAs were detected in more than 90% samples and 22.7% lncRNAs were expressed in less than 10% samples (**Supplementary Figure 1A**). On average, 29.5% lncRNAs exhibited expression levels more than 0.1 FPKM, and 7.78% lncRNAs expressed more than 1 FPKM (**Supplementary Figure 1B**). Differential expression analysis was further performed, wherein 1,421 down-regulated and 2,517 up-regulated lncRNAs were identified in prostate cancer samples (**Figure 1A** and **Supplementary Table 1**). Most of PRAD differential lncRNAs were identified differential expression in multiple cancer types with over three quarters show differential expression in 4–10 cancer types (**Supplementary Figure 1C** and **Supplementary Table 2**). Across 18 different cancer types, 77 lncRNAs were exclusively differentially expressed in PRAD cohort. For example, RP11-328K15.1 showed no significant differential expression in multiple cancer types except PRAD (**Figure 1B**), which might indicate specific biological functions in the tumor biology of prostate cancer. To further investigate the clinical relevance of PRAD differential lncRNAs, associations between lncRNA expression and patient survival time were assessed by Cox regression analysis. The expression level of most differential lncRNAs were negatively associated with prognosis of PRAD patients, wherein seven lncRNAs were associated with good prognosis, such as RP1-278O22.1, while 128 lncRNAs were associated with bad prognosis, such as RP5-1142A6.9 (**Figure 1C** and **Supplementary Table 3**). Higher expression level of RP11-627G23.1 ($P = 0.0039$, log rank test) and RP11-465N4.5 ($P = 0.0058$, log rank test) were significantly associated with decreased survival of patients with PRAD (**Figure 1D**). Similarly, the expression level of most differential lncRNAs were also negatively associated with disease-free survival of PRAD patients (**Supplementary Figure 2**). Our results demonstrated that lncRNAs play important roles in PRAD and could be potential prognosis biomarkers.

PRAD Differential lncRNAs Were Closely Associated With Biological Hallmarks

To further explore the major biological functions that differential lncRNAs might impact, we estimated the associations between 50 biological hallmarks and individual lncRNAs. Overall, differential lncRNAs tend to be more positively associated with biological hallmarks (**Figure 2A**), wherein the distribution of correlation index is relatively balanced associated in the immune hallmarks and less than one fifth exhibited significant correlations (**Supplementary Figure 3A** and **Supplementary Table 4**). We next performed enrichment analysis to examine lncRNAs that were exclusively correlated with some hallmarks than others (see section "Materials and Methods"). In total, 24,096 significant lncRNA-hallmark pairs were identified. Immune-related hallmarks showed relatively balanced distribution of highly associated lncRNA numbers among individual hallmarks, whereas other types exhibited larger number of associated lncRNAs in specific biological hallmarks (**Supplementary Figure 3B** and **Supplementary Table 5**). The most significantly enriched lncRNA-hallmark pair is between CTD-3247F14.2 and "TNFA signaling via NFKB." The observation showed that CTD-3247F14.2 was prone to correlate with genes involved in "TNFA signaling via NFKB" than those in other hallmarks, indicated potential regulatory roles of CTD-3247F14.2 for "TNFA signaling via NFKB" in prostate cancer. Among the top 10 lncRNA-hallmark pairs, six are immune-related biological hallmarks, such as "allograft rejection" (**Figure 2B**). In addition, LINC00664 was exclusively significantly enriched in "E2F targets," which is a proliferation-related hallmark. Among significant lncRNA-hallmark pairs, a subset of lncRNAs showed exclusively enrichment in most immune hallmarks. The majority of these lncRNAs were also enriched in the process of epithelial-mesenchymal transition, indicating potential lncRNA-mediated metastasis via immune processes (**Figure 2C**). Although cancer-related signaling and proliferative hallmarks showed the most associated lncRNAs, immune-related hallmarks hold almost

[2]https://www.r-project.org/

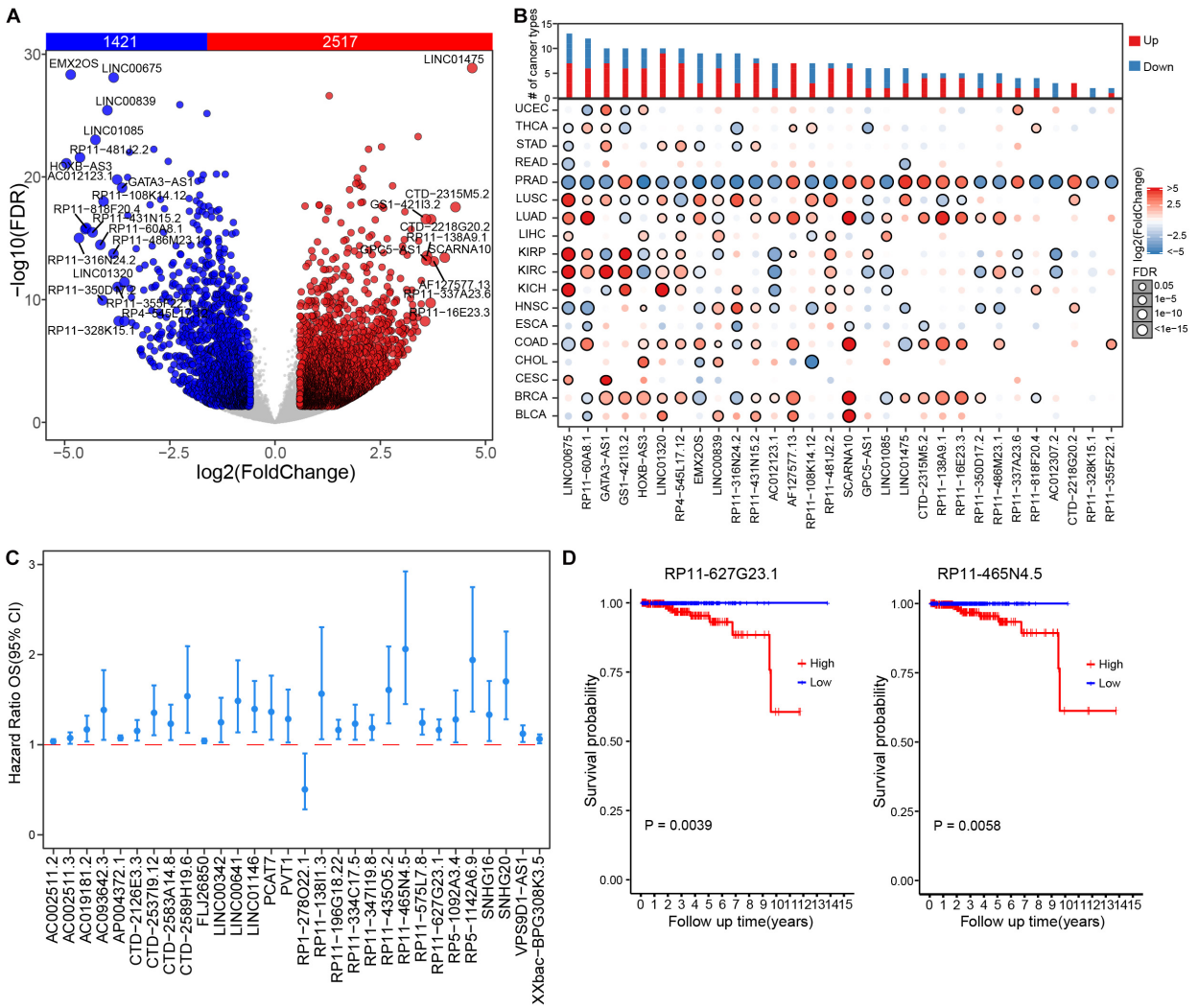

FIGURE 1 | Dysregulation and clinical relevance of lncRNAs in prostate cancer. **(A)** Volcano plot shows the expression difference of lncRNA in prostate cancer samples compared to those paired adjacent normal samples. **(B)** The expression changes of top 30 differential lncRNAs of prostate cancer across 18 TCGA cancer types. **(C)** The survival risk assessment of differential lncRNAs, showing top significant lncRNAs (FPKM > 1) in univariate regression analysis. **(D)** Kaplan–Meier curve of RP11-627G23.1 and RP11-465N4.5 in PRAD cohort.

half of the top significant enriched lncRNA-hallmark pairs (**Supplementary Table 5**).

LncRNAs Showed Extensive Association With Immunogenomic Signatures in PRAD

It is observed that a considerable portion of significantly enriched lncRNA-hallmark pairs were related to immune hallmarks, we next examined the associations between lncRNAs and immunogenomic signatures. Relative activities of 26 tumor immunogenomic signatures were retrieved from a previous study (Thorsson et al., 2018), which were utilized to assess the associations between lncRNAs and immunogenomic signatures in prostate cancer (see section "Materials and Methods"). The majority (21 in 26) of immunogenomic signatures have significantly associated lncRNAs, wherein most lncRNAs were positively associated with corresponding immunogenomic signatures (**Figure 3A** and **Supplementary Table 6**). "TGF-β response," "stromal fraction," "leukocyte fraction," and "lymphocyte infiltration signature score" have larger number of associated lncRNAs (more than 300 lncRNAs). Besides some differential lncRNAs that were shared among distinct immunogenomic signatures, considerable proportions of lncRNAs were exclusively associated with individual immunogenomic signatures. In particular, almost half of "TGF-β response"-associated lncRNAs were specifically positive associated with "TGF-β response" (**Figure 3B**). Additionally, a subset of differential lncRNAs were exclusively negative associated with "wound healing" activity. Specifically, "TGF-β response" showed much higher activity in RP11-166D19.1-high PRAD samples than those in RP11-166D19.1-low PRAD samples

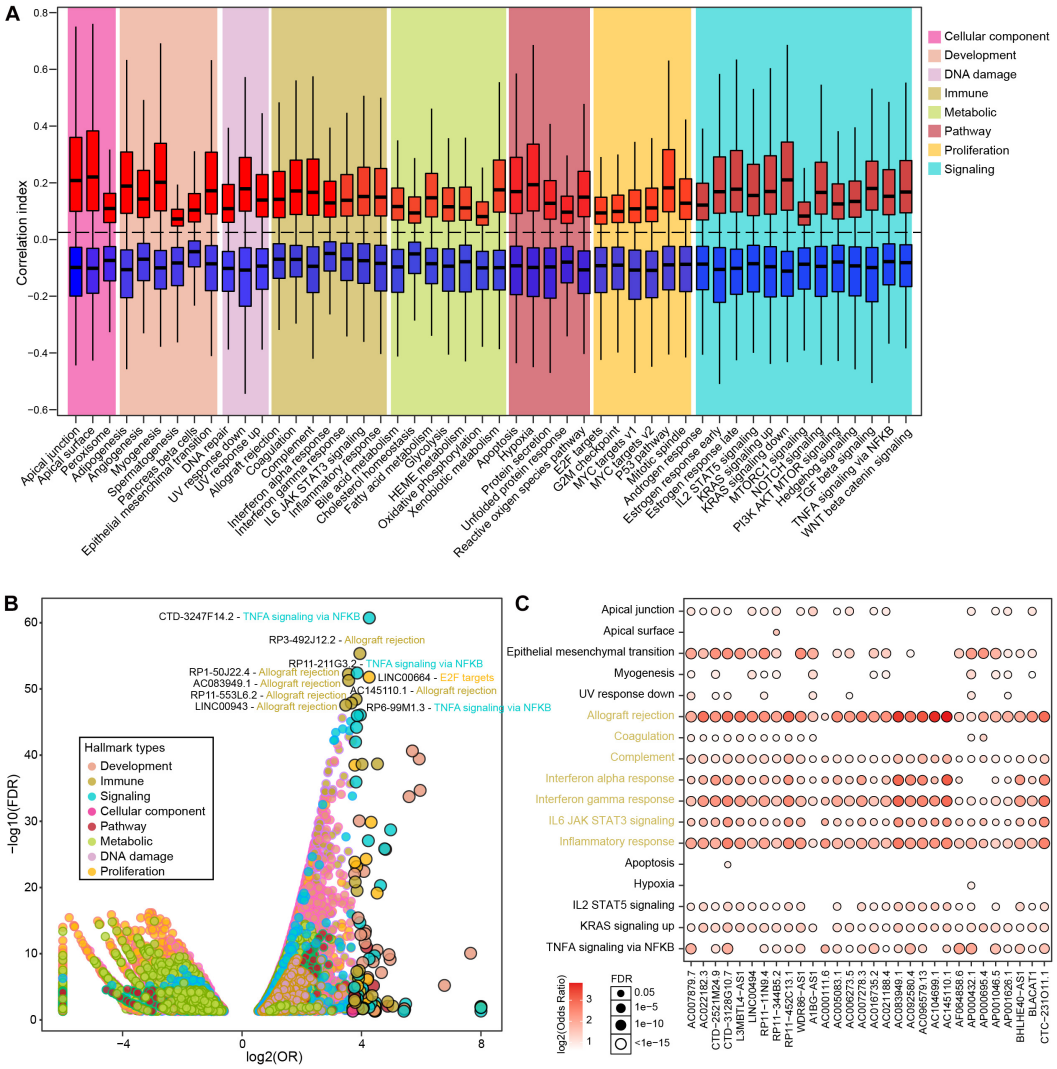

FIGURE 2 | The correlations between PRAD differential lncRNAs and various hallmarks. **(A)** Boxplots show correlation indexes of positively and negatively correlated lncRNAs in each type of hallmark. **(B)** Bubble plot shows the enrichment of lncRNA-hallmark pairs in cancer hallmarks. **(C)** A subset of lncRNAs that were significantly enriched in immune-related hallmarks.

(P < 2E-16, **Figure 3C**). Prostate cancer samples with higher level of FAM201A exhibited significantly lower level of "TGF-β response" activity (P = 2.7E-12, **Figure 3D**). In collection, our analysis suggested lncRNAs as markers of activity levels of immunogenomic signatures in prostate cancer.

LncRNAs Were Frequently Connected With Immune-Related Biological Processes in Prostate Cancer

We next explored the connections between lncRNAs and immune-related biological processes in prostate cancer. Totally, 38 immune-related processes were found to be significantly enriched by multiple lncRNAs in PRAD samples, such as "Regulation of immune response," "Regulation of immune system process," and "Immune system development" (**Figure 4A** and **Supplementary Table 7**). The most parts of differential lncRNAs potentially regulate immune response and immune system. In addition, differential lncRNAs were also found to be connected with cellular immunity, such as "Regulation of lymphocyte mediated immunity," "leukocyte mediated immunity," and "lymphocyte mediated immunity." Prostate cancer samples with low level of CTD-2521M24.9 showed significantly lower activity level of immune response (P < 2E-16, **Figure 4B**). High expression level of CTD-2521M24.9 indicated high activity levels of immune system development (P < 2E-16, **Figure 4C**). Interestingly, different lncRNAs could regulate the same immune-related processes through modulating diverse genes (**Figure 4D**). For example, AC006273.5 was found to regulate "Immune response" by modulating CD40 and TMEM173, whereas A1BG-AS1 could potentially regulate "Immune response" through CD40, ELF4,

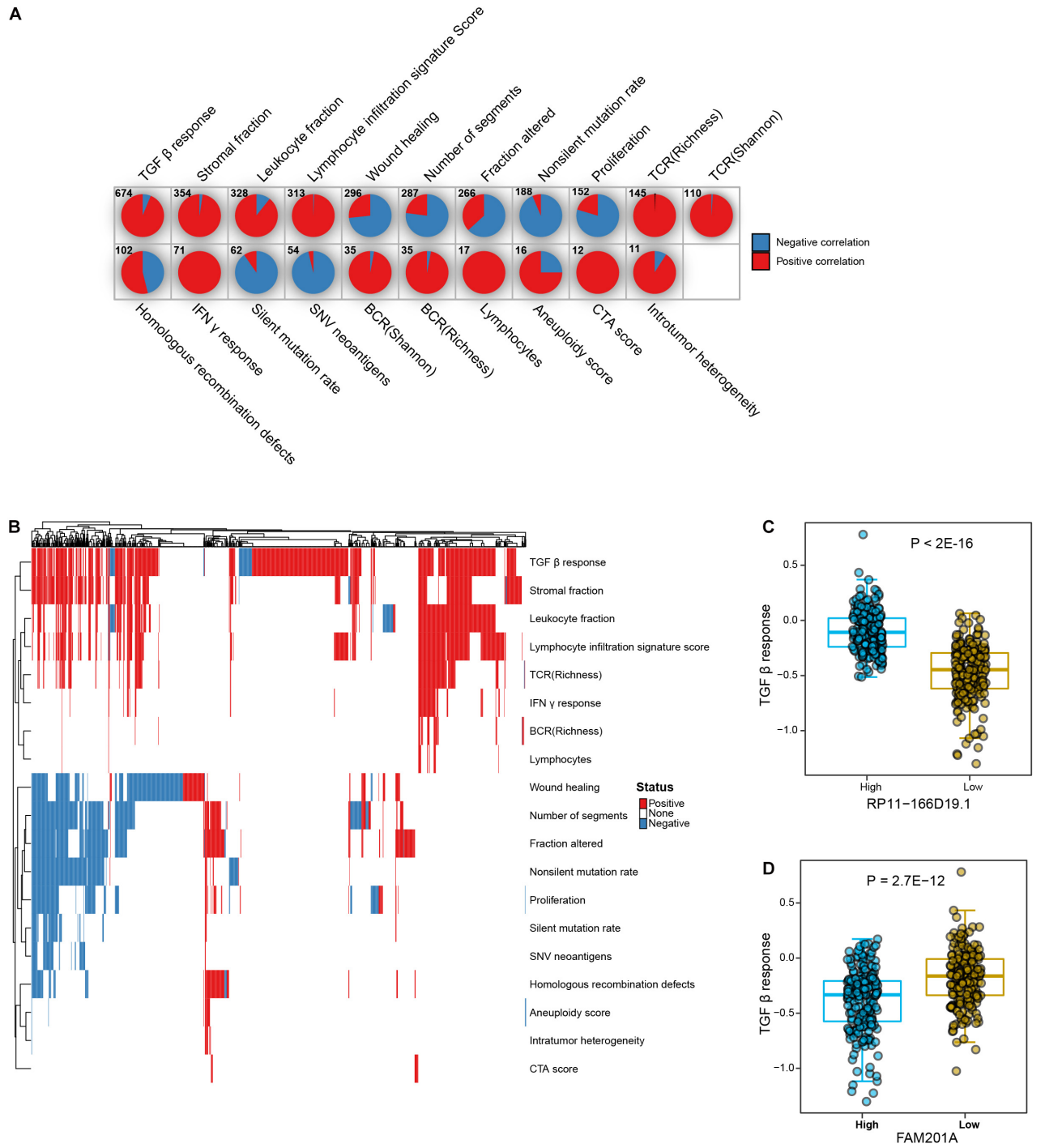

FIGURE 3 | Associations between lncRNAs and tumor immune signature. **(A)** Pie charts show the numbers of significant positively and negatively correlated lncRNAs in each type of immunogenomic signatures. **(B)** Heatmap shows the landscape of significant correlated lncRNAs across different immunogenomic signatures. **(C)** Comparison of TGF-β response scores between high and low expression level of RP11-166D19.1 in PRAD samples. **(D)** Comparison of TGF-β response scores between high and low expression level of FAM201A in PRAD samples.

NLRP1, MR1, and TMEM173. Furthermore, some lncRNAs exclusively regulate individual immune processes though the same genes. For example, LINC00654 were found to regulate "Immunological synapse formation" through DLG1, CORO1A, DOCK2, PRF1, and EPHB1. In summary, these observations demonstrated that lncRNAs were frequently connected with immune-related biological processes in prostate cancer.

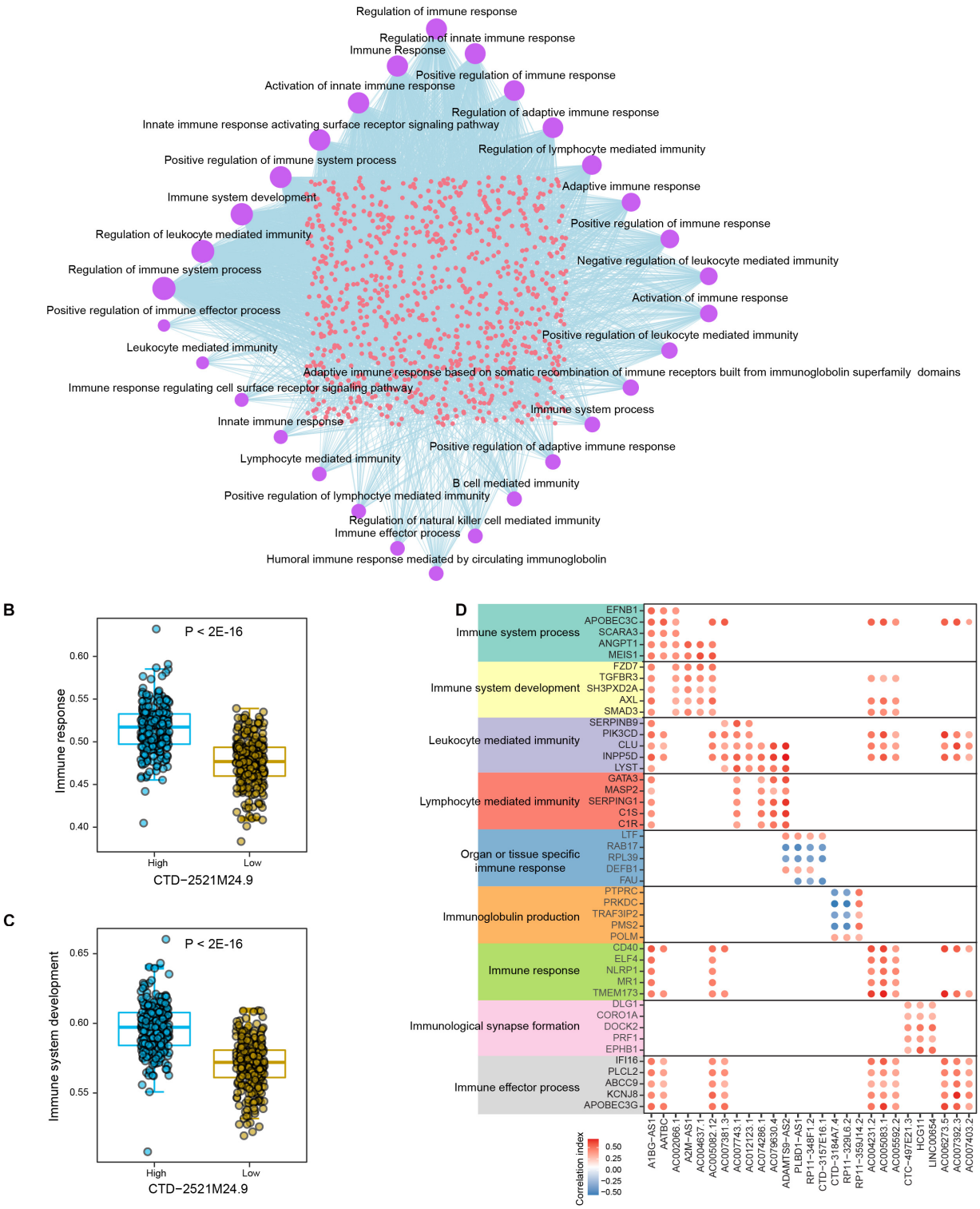

FIGURE 4 | The crosstalk between lncRNAs and immune-related biological processes in PRAD. **(A)** Network shows the connections between differential lncRNAs and top significant immune-related biological processes in PRAD. Circle sizes indicate the numbers of significantly enriched lncRNAs for individual immune-related biological processes. **(B)** Comparison of immune response activities between high and low expression levels of CTD-2521M24.9. **(C)** Comparison of immune system development activities between high and low expression levels of CTD-2521M24.9. **(D)** Points show the correlations between lncRNAs and representative genes in individual immune-related biological processes.

Interactions Between lncRNAs and Infiltrated Immune Cells and Immune Checkpoints Suggest Novel Therapeutic Strategy for Immunotherapy in Prostate Cancer

Studies on tumor immunology have proposed various therapeutic strategies for tumor patients, among which immune checkpoint blockade (ICB) therapy showed promising clinical benefits in multiple solid tumor types. Among significant lncRNA-immune cell interactions, memory resting $CD4^+$ T cells were found to interact with the most differential lncRNAs, most of which were positively correlated (**Figure 5A** and **Supplementary Table 8**). In particular, cancer samples with high expression level of MAGI2-AS3 showed significantly higher infiltrated abundance of memory resting $CD4^+$ T cells than those with low expression (P < 2E-16, **Figure 5B**). High expression of CTD-3184A7.4 indicated significantly lower level of infiltrated memory resting $CD4^+$ T cell in prostate cancer (P = 8.3E-10, **Figure 5C**). To further explore the associations between lncRNAs and immune checkpoints in prostate cancer, we estimated the correlations between the expression levels of lncRNAs and immune checkpoint genes. Most of PRAD differential lncRNAs were found to be significantly positively correlated with immune checkpoint gene expression (**Figure 5D** and **Supplementary Table 9**). Some lncRNAs are positively associated with most immune checkpoint genes, such as LINC00861 and CTD-2521M24.9, while some are negative correlated with most of these genes, such as RP3-325F22.5, BMPR1B-AS1, LINC00665, and RP11-44B19.1. Specifically, LINC00861 was the most positively related to PD1 (P < 2E-16, **Figure 5E**), CTLA4 (P < 2E-16, **Figure 5F**) and TIGIT, and CTD-2521M24.9 was the most positively related to PD-L1; in contrast, LINC00665, RP3325F22.5, BMPR1B-AS1, and RP11-44B19.1 were the most negatively correlated to PD1, PD-L1, CTLA4, and TIGIT. Moreover, a Sankey diagram was employed to describe the connections between lncRNAs, immune cells and actionable immune checkpoints, with a subset of lncRNAs was closely related to the immune cells and actionable immune checkpoints (**Supplementary Figure 4**). These observations implied that LINC00861 might regulate the expression of PD-1 and CTLA4, actionable targets of ICB therapy or be efficient biomarker for their abundance in prostate cancer. Collectively, these results suggested that lncRNAs might be utilized to modulate activity of immune cells or levels of immune checkpoints to promote immunotherapy for patients with prostate cancer.

DISCUSSION

To comprehensively characterize the lncRNA-immune interactions in prostate cancer, our study explored the relations between lncRNAs and biological hallmarks, tumor immunogenomic signatures, immune-related biological processes, infiltrated immune cells, and immune checkpoints. Our study unveiled frequent interactions between PRAD differential lncRNAs and multiple immune features.

Our analysis presented comprehensive characterization of lncRNA dysregulation and clinical relevance in prostate cancer. We identified prostate cancer-specific dysregulated lncRNAs and prognostic lncRNAs, such as RP11-627G23.1 and RP11-465N4.5. We revealed the close associations between differential lncRNAs and biological hallmarks. Although immune-related hallmarks were not enriched of the largest number of lncRNAs, they took up approximately half of top significant lncRNA-hallmark associations. Allograft rejection is the top lncRNA-related cancer hallmarks, indicating the potential roles of dysregulated lncRNAs in organ transplantation. For example, in renal transplantation, oncogenic lncRNA-ATB is significantly overexpressed in acute rejection patients and regulates renal cell proliferation and cyclosporine A-mediated apoptosis (Qiu et al., 2017). The important roles of lncRNA-mediated innate and adaptive immune responses have been highlighted in recent years, especially in cancer immunity (Yu et al., 2018; Denaro et al., 2019; Wu et al., 2020). A subset of lncRNAs enriched in most immune hallmarks suggests their potential roles in modulating cancer immunity to facilitate cancer progression. For example, lncRNA cox-2 facilitates the polarization of M2 macrophages and therefore induces the malignant phenotypes of hepatocellular carcinoma cells and angiogenesis (Ye et al., 2018). As another example, FOXC1-mediated LINC00301 triggers malignant potential of non-small cell lung cancer cells and modulates the Tregs and $CD8^+$ T cell populations by activating TGF-β signaling (Sun C.-C. et al., 2020).

Besides immune-related hallmarks, we also involved tumor immunogenomic signatures, immune-related biological processes, tumor infiltrated immune cells, and immune checkpoints. These features reflect immunological activities from diverse aspects in tumor samples (Grivennikov et al., 2010; Chen and Mellman, 2017; Greten and Grivennikov, 2019). In particular, tumor immunogenomic signatures represent genomic variations that were induced by or could induce immune reprogramming (Thorsson et al., 2018). Moreover, TGF-β signaling contributes to malignancy of cancer cells and immunosuppressive microenvironment, thus thwarting cancer immunotherapy (Colak and ten Dijke, 2017; Batlle and Massagué, 2019). A large amount of lncRNAs was related to TGF-β response in prostate cancer, suggesting their profound implication in TGF-β-mediated immune processes. For example, TGF-β1-simulated lncRNA DNM3OS induces transformation of prostate stromal cells by targeting miR-29a/29b/COL3A1 and miR-361/TGFβ1 axes (Wang et al., 2019). As another example, the therapeutic efficiency of PSMA-targeted human CAR T cells are enhanced upon TGF-β insensitivity in the treatment of prostate cancer (Kloss et al., 2018). Furthermore, stromal fraction is the second frequent lncRNA-related immune feature, profoundly implicating in cancer development and immunity (Tyekucheva et al., 2017; De Jaeghere et al., 2019; Ahn and Kim, 2020). For example, lncRNA H19 derived from carcinoma-associated fibroblasts (CAFs) contributes to the stemness and chemoresistance of colorectal cancer by targeting miR-141 (Ren et al., 2018). As another example, lncRNA-CAF induce transition from normal fibroblasts to CAFs by stabling IL-33,

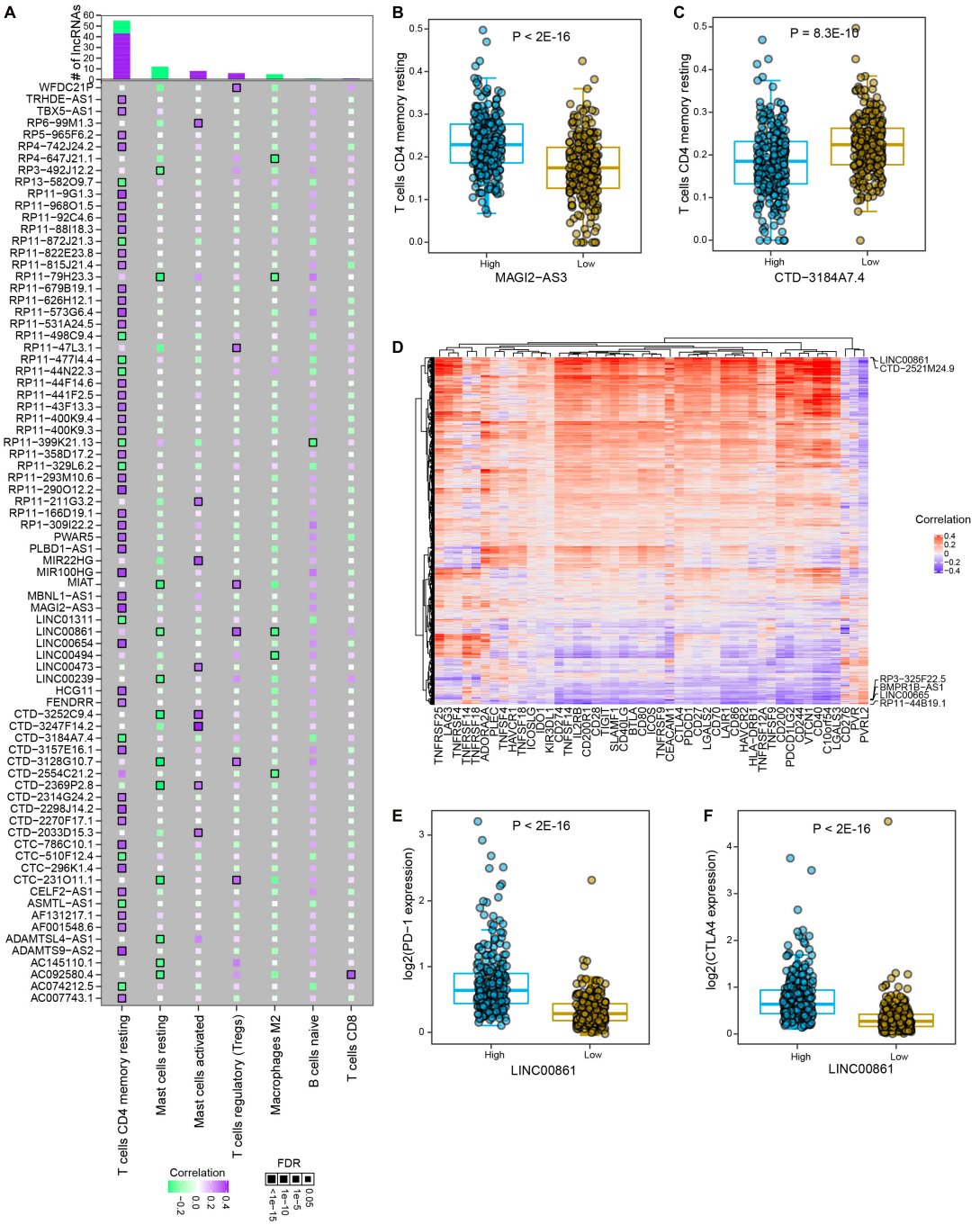

FIGURE 5 | The interactions between PRAD differential lncRNAs and major immune cells and immune checkpoint genes. **(A)** The correlations between significant differential lncRNAs and major immune cell types. Colors indicate correlation coefficients and diamond sizes represent FDR values. **(B)** Comparison of relative abundance of memory resting T cells between high and low expression levels of MAGI2-AS3 in PRAD samples. **(C)** Comparison of relative abundance of memory resting T cells between high and low expression levels of CTD-3184A7.4 in PRAD samples. **(D)** Heatmap shows the correlations between the expression of immune checkpoint genes and differential lncRNAs. **(E)** Comparison of PD-1 expression between high and low LINC00861 expression levels in PRAD samples. **(F)** Comparison of CTLA4 expression between high and low LINC00861 expression levels in PRAD samples.

thereby leading to development of oral squamous cell carcinoma (Ding et al., 2018).

The activities of immune cells and abundance of immune checkpoints were crucial factors that affect the outcomes of immunotherapy for tumor patients (Cha et al., 2020; Jafari et al., 2020; Zhou et al., 2020). Our analysis found that a large number of lncRNAs were significantly associated with memory resting $CD4^+$ T cells, such as MAGI2-AS3 and CTD-3184A7.4.

Memory $CD4^+$ T cell is a subset of T cell population that sustains in the absence of antigen and prepares for rapid immune response upon repeat antigen exposure (Hope et al., 2019). It has been shown that central memory $CD4^+$ T cells in peripheral blood are associated with clinical response of PD-1 antibody therapy in melanoma patients. Our observations indicated that these lncRNAs might be able to modulate the activities of memory resting $CD4^+$ T cells. Overexpression of MAGI2-AS3 or knockdown of CTD-3184A7.4 may activate memory resting $CD4^+$ T cells to enhance immune response against tumor cells. Interestingly, MAGI2-AS3 has been widely studied in cancers, while these studies mainly focused in regulating cancer cells themselves (Liu et al., 2019; Li D. et al., 2020). Our results point out that various lncRNA could have immune regulatory role other than their influence on cancer cells. In addition, the close connection between lncRNAs and immune checkpoints has been revealed, suggesting a profound implication of lncRNA in immune checkpoint regulation. For example, LncRNA KCNQ1OT1 inhibits the cytotoxicity of $CD8^+$ T cells and promotes the malignant ability of prostate cancer cells by targeting miR-15a/PD-L1 axis (Chen et al., 2020). As another example, lncAMPC activates LIF/LIFR/Jak1/STAT3 pathway to stable PD-L1 and metastasis-associated genes, thereby contributing to metastasis and immunosuppression in prostate cancer (Zhang et al., 2020). Of note, in prostate cancer, LINC00861 was closely associated with T cells regulatory, macrophages M2 and mast cells resting as well as a series of immune checkpoints, including PD1, PD-L1, and CTLA4. These evidence indicates a LINC00861-mediated tumor immune response beyond its reported regulation of malignant potential on cancer cells (Liu et al., 2021). Further experimental validation is needed to confirm the regulatory functions of the immune-related lncRNAs and select the most efficacious lncRNAs to boost the antitumor immune response. We believe that intervention of immune response through lncRNAs will be promising therapeutics for patients with prostate cancer.

CONCLUSION

In conclusion, our study facilitated the understanding of lncRNA-immune interactions and provided a valuable resource of immune-related lncRNAs in prostate cancer. These lncRNAs could be potential biomarkers for immune cells or immune-related activities in prostate cancer. Because tumor immunity has major impacts on cancer progression, many immune-related lncRNAs can predict prognosis and immunotherapy of cancers (Zhou et al., 2017, 2018; Sun J. et al., 2020; Zhou et al., 2020). Therefore, these lncRNAs could be potentially utilized to predict and even modulate immune cell activities or immune checkpoint abundance to benefit immunotherapy for patients with prostate cancer.

DATA AVAILABILITY STATEMENT

The datasets presented in this study can be found in online repositories. The names of the repository/repositories and accession number(s) can be found in the article/ **Supplementary Material**.

ETHICS STATEMENT

The patient data we used were acquired as publicly available datasets that were collected with patients' informed consent.

AUTHOR CONTRIBUTIONS

SL designed the study and wrote the manuscript. SL and WHe supervised the project. WHu, YW, and SL collected the data resource. WHu and SL performed the data analysis. WHu, YW, WHe, and ZF reviewed the manuscript. All authors read and approved the final manuscript.

FUNDING

This study was supported by Shanghai General Hospital Startup Funding (02.06.01.20.06).

ACKNOWLEDGMENTS

We gratefully acknowledge contributions from TCGA Research Network.

SUPPLEMENTARY MATERIAL

The Supplementary Material for this article can be found online at: https://www.frontiersin.org/articles/10.3389/fcell.2021.641891/full#supplementary-material

REFERENCES

Ahn, Y.-H., and Kim, J. S. (2020). Long non-coding RNAs as regulators of interactions between cancer-associated fibroblasts and cancer cells in the tumor microenvironment. *Int. J. Mol. Sci.* 21:7484. doi: 10.3390/ijms21207484

Batlle, E., and Massagué, J. (2019). Transforming growth factor-β signaling in immunity and cancer. *Immunity* 50, 924–940. doi: 10.1016/j.immuni.2019.03.024

Bryant, G., Wang, L., and Mulholland, D. J. (2017). Overcoming oncogenic mediated tumor immunity in prostate cancer. *Int. J. Mol. Sci.* 18:1542. doi: 10.3390/ijms18071542

Carpenter, S., Aiello, D., Atianand, M. K., Ricci, E. P., Gandhi, P., Hall, L. L., et al. (2013). A long noncoding RNA mediates both activation and repression of immune response genes. *Science* 341, 789–792. doi: 10.1126/science.1240925

Cech, T. R., and Steitz, J. A. (2014). The noncoding RNA revolution-trashing old rules to forge new ones. *Cell* 157, 77–94. doi: 10.1016/j.cell.2014.03.008

Cha, H. R., Lee, J. H., and Ponnazhagan, S. (2020). Revisiting immunotherapy: a focus on prostate cancer. *Cancer Res.* 80, 1615–1623. doi: 10.1158/0008-5472.CAN-19-2948

Chen, D. S., and Mellman, I. (2017). Elements of cancer immunity and the cancer-immune set point. *Nature* 541, 321–330. doi: 10.1038/nature21349

Chen, Q.-H., Li, B., Liu, D.-G., Zhang, B., Yang, X., and Tu, Y.-L. (2020). LncRNA KCNQ1OT1 sponges miR-15a to promote immune evasion and malignant progression of prostate cancer via up-regulating PD-L1. *Cancer Cell Int.* 20:394. doi: 10.1186/s12935-020-01481-8

Colak, S., and ten Dijke, P. (2017). Targeting TGF-β signaling in cancer. *Trends Cancer* 3, 56–71.

Dallos, M. C., and Drake, C. G. (2018). Blocking PD-1 / PD-L1 in genitourinary malignancies to immunity and beyond. *Cancer J.* 24, 20–30.

De Jaeghere, E. A., Denys, H. G., and De Wever, O. (2019). Fibroblasts fuel immune escape in the tumor microenvironment. *Trends Cancer* 5, 704–723. doi: 10.1016/j.trecan.2019.09.009

Denaro, N., Merlano, M. C., and Lo Nigro, C. (2019). Long noncoding RNAs as regulators of cancer immunity. *Mol. Oncol.* 13, 61–73. doi: 10.1002/1878-0261.12413

Ding, L., Ren, J., Zhang, D., Li, Y., Huang, X., Hu, Q., et al. (2018). A novel stromal lncRNA signature reprograms fibroblasts to promote the growth of oral squamous cell carcinoma via LncRNA-CAF/interleukin-33. *Carcinogenesis* 39, 397–406. doi: 10.1093/carcin/bgy006

Du, Z., Fei, T., Verhaak, R. G. W., Su, Z., Zhang, Y., Brown, M., et al. (2013). Integrative genomic analyses reveal clinically relevant long noncoding RNAs in human cancer. *Nat. Struct. Mol. Biol.* 20, 908–913. doi: 10.1038/nsmb.2591

Engreitz, J. M., Pandya-Jones, A., McDonel, P., Shishkin, A., Sirokman, K., Surka, C., et al. (2013). The Xist lncRNA exploits three-dimensional genome architecture to spread across the X chromosome. *Science* 341:1237973. doi: 10.1126/science.1237973

Ferlay, J., Soerjomataram, I., Dikshit, R., Eser, S., Mathers, C., Rebelo, M., et al. (2015). Cancer incidence and mortality worldwide: sources, methods and major patterns in GLOBOCAN 2012. *Int. J. Cancer* 136, E359–E386. doi: 10.1002/ijc.29210

Fridman, W. H., Zitvogel, L., Sautès-Fridman, C., and Kroemer, G. (2017). The immune contexture in cancer prognosis and treatment. *Nat. Rev. Clin. Oncol.* 14, 717–734. doi: 10.1038/nrclinonc.2017.101

Greten, F. R., and Grivennikov, S. I. (2019). Inflammation and cancer: triggers, mechanisms, and consequences. *Immunity* 51, 27–41. doi: 10.1016/j.immuni.2019.06.025

Grivennikov, S. I., Greten, F. R., and Karin, M. (2010). Immunity, inflammation, and cancer. *Cell* 140, 883–899. doi: 10.1016/j.cell.2010.01.025

Grossman, R. L., Heath, A. P., Ferretti, V., Varmus, H. E., Lowy, D. R., Kibbe, W. A., et al. (2016). Toward a shared vision for cancer genomic data. *N. Engl. J. Med.* 375, 1109–1112.

Hansen, T. B., Jensen, T. I., Clausen, B. H., Bramsen, J. B., Finsen, B., Damgaard, C. K., et al. (2013). Natural RNA circles function as efficient microRNA sponges. *Nature* 495, 384–388. doi: 10.1038/nature11993

Hänzelmann, S., Castelo, R., and Guinney, J. (2013). GSVA: gene set variation analysis for microarray and RNA-Seq data. *BMC Bioinformatics* 14:7. doi: 10.1186/1471-2105-14-7

Hope, J. L., Stairiker, C. J., Bae, E.-A., Otero, D. C., and Bradley, L. M. (2019). Striking a balance-cellular and molecular drivers of memory T cell development and responses to chronic stimulation. *Front. Immunol.* 10:1595. doi: 10.3389/fimmu.2019.01595

Hua, J. T., Ahmed, M., Guo, H., Zhang, Y., Chen, S., Soares, F., et al. (2018). Risk SNP-Mediated promoter-enhancer switching drives prostate cancer through lncRNA PCAT19. *Cell* 174, 564–575.e18. doi: 10.1016/j.cell.2018.06.014

Hua, J. T., Chen, S., and He, H. H. (2019). Landscape of noncoding RNA in prostate cancer. *Trends Genet.* 35, 840–851. doi: 10.1016/j.tig.2019.08.004

Iyer, M. K., Niknafs, Y. S., Malik, R., Singhal, U., Sahu, A., Hosono, Y., et al. (2015). The landscape of long noncoding RNAs in the human transcriptome. *Nat. Genet.* 47, 199–208. doi: 10.1038/ng.3192

Jafari, S., Molavi, O., Kahroba, H., Hejazi, M. S., Maleki-Dizaji, N., Barghi, S., et al. (2020). Clinical application of immune checkpoints in targeted immunotherapy of prostate cancer. *Cell. Mol. Life Sci.* 77, 3693–3710. doi: 10.1007/s00018-020-03459-1

Kahles, A., Lehmann, K. V., Toussaint, N. C., Hüser, M., Stark, S. G., Sachsenberg, T., et al. (2018). Comprehensive analysis of alternative splicing across tumors from 8,705 patients. *Cancer Cell* 34, 211–224.e6. doi: 10.1016/j.ccell.2018.07.001

Kloss, C. C., Lee, J., Zhang, A., Chen, F., Melenhorst, J. J., Lacey, S. F., et al. (2018). Dominant-Negative TGF-β receptor enhances PSMA-Targeted human CAR T cell proliferation and augments prostate cancer eradication. *Mol. Ther.* 26, 1855–1866. doi: 10.1016/j.ymthe.2018.05.003

Ku, S. Y., Gleave, M. E., and Beltran, H. (2019). Towards precision oncology in advanced prostate cancer. *Nat. Rev. Urol.* 16, 645–654. doi: 10.1038/s41585-019-0237-8

Lee, S., Kopp, F., Chang, T.-C., Sataluri, A., Chen, B., Sivakumar, S., et al. (2016). Noncoding RNA NORAD regulates genomic stability by sequestering PUMILIO proteins. *Cell* 164, 69–80. doi: 10.1016/j.cell.2015.12.017

Li, D., Wang, J., Zhang, M., Hu, X., She, J., Qiu, X., et al. (2020). LncRNA MAGI2-AS3 is regulated by BRD4 and promotes gastric cancer progression via maintaining ZEB1 overexpression by sponging miR-141/200a. *Mol. Ther. Nucleic Acids* 19, 109–123. doi: 10.1016/j.omtn.2019.11.003

Li, S., Hu, Z., Zhao, Y., Huang, S., and He, X. (2019). Transcriptome-Wide analysis reveals the landscape of aberrant alternative splicing events in liver cancer. *Hepatology* 69, 359–375.

Li, S., Li, Y., He, X., Zheng, Q., Huang, S., Zhao, J., et al. (2018). exoRBase: a database of circRNA, lncRNA and mRNA in human blood exosomes. *Nucleic Acids Res.* 46, D106–D112. doi: 10.1093/nar/gkx891

Li, T., Li, S., Chen, D., Chen, B., Yu, T., Zhao, F., et al. (2017). Transcriptomic analyses of RNA-binding proteins reveal eIF3c promotes cell proliferation in hepatocellular carcinoma. *Cancer Sci.* 108, 877–885. doi: 10.1111/cas.13209

Li, Y., Jiang, T., Zhou, W., Li, J., Li, X., Wang, Q., et al. (2020). Pan-cancer characterization of immune-related lncRNAs identifies potential oncogenic biomarkers. *Nat. Commun.* 11:1000. doi: 10.1038/s41467-020-14802-2

Li, Z., Zhang, J., Liu, X., Li, S., Wang, Q., Di Chen, et al. (2018). The LINC01138 drives malignancies via activating arginine methyltransferase 5 in hepatocellular carcinoma. *Nat. Commun.* 9:1572.

Liberzon, A., Birger, C., Thorvaldsdóttir, H., Ghandi, M., Mesirov, J. P., and Tamayo, P. (2015). The molecular signatures database hallmark gene set collection. *Cell Syst.* 1, 417–425.

Liu, H., Zhang, L., Ding, X., and Sui, X. (2021). LINC00861 inhibits the progression of cervical cancer cells by functioning as a ceRNA for miR?513b?5p and regulating the PTEN/AKT/mTOR signaling pathway. *Mol. Med. Rep.* 23. doi: 10.3892/mmr.2020.11662

Liu, Q., Liu, S., Wang, X., Zhang, J., and Liu, K. (2019). LncRNA MAGI2-AS3 is involved in cervical squamous cell carcinoma development through CDK6 up-regulation. *Infect. Agent. Cancer* 14:37. doi: 10.1186/s13027-019-0238-5

Love, M. I., Huber, W., and Anders, S. (2014). Moderated estimation of fold change and dispersion for RNA-seq data with DESeq2. *Genome Biol.* 15:550.

Marchese, F. P., Raimondi, I., and Huarte, M. (2017). The multidimensional mechanisms of long noncoding RNA function. *Genome Biol.* 18:206. doi: 10.1186/s13059-017-1348-2

Mouw, K. W., Goldberg, M. S., Konstantinopoulos, P. A., and D'Andrea, A. D. (2017). DNA damage and repair biomarkers of immunotherapy response. *Cancer Discov.* 7, 675–693. doi: 10.1158/2159-8290.CD-17-0226

Newman, A. M., Liu, C. L., Green, M. R., Gentles, A. J., Feng, W., Xu, Y., et al. (2015). Robust enumeration of cell subsets from tissue expression profiles. *Nat. Methods* 12, 453–457. doi: 10.1038/nmeth.3337

Niknafs, Y. S., Han, S., Ma, T., Speers, C., Zhang, C., Wilder-Romans, K., et al. (2016). The lncRNA landscape of breast cancer reveals a role for DSCAM-AS1 in breast cancer progression. *Nat. Commun.* 7:12791. doi: 10.1038/ncomms12791

Qian, P., He, X. C., Paulson, A., Li, Z., Tao, F., Perry, J. M., et al. (2016). The Dlk1-Gtl2 locus preserves LT-HSC function by inhibiting the PI3K-mTOR pathway to restrict mitochondrial metabolism. *Cell Stem Cell* 18, 214–228. doi: 10.1016/j.stem.2015.11.001

Qiu, J., Chen, Y., Huang, G., Zhang, Z., Chen, L., and Na, N. (2017). Transforming growth factor-β activated long non-coding RNA ATB plays an important role in acute rejection of renal allografts and may impacts the postoperative pharmaceutical immunosuppression therapy. *Nephrology (Carlton)* 22, 796–803. doi: 10.1111/nep.12851

Ren, J., Ding, L., Zhang, D., Shi, G., Xu, Q., Shen, S., et al. (2018). Carcinoma-associated fibroblasts promote the stemness and chemoresistance of colorectal cancer by transferring exosomal lncRNA H19. *Theranostics* 8, 3932–3948. doi: 10.7150/thno.25541

Siegel, R. L., Miller, K. D., and Jemal, A. (2020). Cancer statistics, 2020. *CA Cancer J. Clin.* 70, 7–30. doi: 10.3322/caac.21590

Sun, C.-C., Zhu, W., Li, S.-J., Hu, W., Zhang, J., Zhuo, Y., et al. (2020). FOXC1-mediated LINC00301 facilitates tumor progression and triggers an immune-suppressing microenvironment in non-small cell lung cancer by regulating the HIF1α pathway. *Genome Med.* 12:77. doi: 10.1186/s13073-020-00773-y

Sun, J., Zhang, Z., Bao, S., Yan, C., Hou, P., Wu, N., et al. (2020). Identification of tumor immune infiltration-associated lncRNAs for improving prognosis and immunotherapy response of patients with non-small cell lung cancer. *J. Immunother. Cancer* 8:e000110. doi: 10.1136/jitc-2019-000110

Thorsson, V., Gibbs, D. L., Brown, S. D., Wolf, D., Bortone, D. S., Ou Yang, T. H., et al. (2018). The immune landscape of cancer. *Immunity* 48, 812–830.e14. doi: 10.1016/j.immuni.2018.03.023 ,

Tyekucheva, S., Bowden, M., Bango, C., Giunchi, F., Huang, Y., Zhou, C., et al. (2017). Stromal and epithelial transcriptional map of initiation progression and metastatic potential of human prostate cancer. *Nat. Commun.* 8:420. doi: 10.1038/s41467-017-00460-4

Vitkin, N., Nersesian, S., Siemens, D. R., and Koti, M. (2019). The tumor immune contexture of prostate cancer. *Front. Immunol.* 10:603. doi: 10.3389/fimmu.2019.00603

Wang, R., Zhang, M., Ou, Z., He, W., Chen, L., Zhang, J., et al. (2019). Long noncoding RNA DNM3OS promotes prostate stromal cells transformation via the miR-29a/29b/COL3A1 and miR-361/TGFβ1 axes. *Aging (Albany N.Y.)* 11, 9442–9460. doi: 10.18632/aging.102395

Wu, M., Fu, P., Qu, L., Liu, J., and Lin, A. (2020). Long noncoding RNAs, new critical regulators in cancer immunity. *Front. Oncol.* 10:550987. doi: 10.3389/fonc.2020.550987

Ye, Y., Xu, Y., Lai, Y., He, W., Li, Y., Wang, R., et al. (2018). Long non-coding RNA cox-2 prevents immune evasion and metastasis of hepatocellular carcinoma by altering M1/M2 macrophage polarization. *J. Cell. Biochem.* 119, 2951–2963. doi: 10.1002/jcb.26509

Yu, W.-D., Wang, H., He, Q.-F., Xu, Y., and Wang, X.-C. (2018). Long noncoding RNAs in cancer-immunity cycle. *J. Cell. Physiol.* 233, 6518–6523. doi: 10.1002/jcp.26568

Yu, Y., Gao, F., He, Q., Li, G., and Ding, G. (2020). lncRNA UCA1 functions as a ceRNA to promote prostate cancer progression via sponging miR143. *Mol. Ther. Nucleic Acids* 19, 751–758. doi: 10.1016/j.omtn.2019.11.021

Yuan, J h, Yang, F., Wang, F., Ma, J. z, Guo, Y. j, Tao, Q. f, et al. (2014). A long noncoding RNA activated by TGF-β promotes the invasion-metastasis cascade in hepatocellular carcinoma. *Cancer Cell* 25, 666–681. doi: 10.1016/j.ccr.2014.03.010

Zhang, W., Shi, X., Chen, R., Zhu, Y., Peng, S., Chang, Y., et al. (2020). Novel long non-coding RNA lncAMPC promotes metastasis and immunosuppression in prostate cancer by stimulating LIF/LIFR expression. *Mol. Ther.* 28, 2473–2487. doi: 10.1016/j.ymthe.2020.06.013

Zhou, M., Zhang, Z., Bao, S., Hou, P., and Yan, C. (2020). Computational recognition of lncRNA signature of tumor-infiltrating B lymphocytes with potential implications in prognosis and immunotherapy of bladder cancer. *Brief. Bioinform.* bbaa047. doi: 10.1093/bib/bbaa047

Zhou, M., Zhang, Z., Zhao, H., Bao, S., Cheng, L., and Sun, J. (2018). An immune-related six-lncRNA signature to improve prognosis prediction of glioblastoma multiforme. *Mol. Neurobiol.* 55, 3684–3697. doi: 10.1007/s12035-017-0572-9

Zhou, M., Zhao, H., Xu, W., Bao, S., Cheng, L., and Sun, J. (2017). Discovery and validation of immune-associated long non-coding RNA biomarkers associated with clinically molecular subtype and prognosis in diffuse large B cell lymphoma. *Mol. Cancer* 16:16. doi: 10.1186/s12943-017-0580-4

Conflict of Interest: The authors declare that the research was conducted in the absence of any commercial or financial relationships that could be construed as a potential conflict of interest.

frontiers in Cell and Developmental Biology

MINI REVIEW
published: 11 March 2021
doi: 10.3389/fcell.2021.646326

Placenta-Derived MicroRNAs in the Pathophysiology of Human Pregnancy

Peng Xu[1†], Yeling Ma[2,3†], Hongyu Wu[2,3] and Yan-Ling Wang[2,3,4]*

[1] School of Life Science, Shanxi University, Taiyuan, China, [2] State Key Laboratory of Stem Cell and Reproductive Biology, Institute of Zoology; Institute for Stem Cell and Regeneration, Chinese Academy of Sciences, Beijing, China, [3] Beijing Institute for Stem Cell and Regenerative Medicine, Beijing, China, [4] University of Chinese Academy of Sciences, Beijing, China

In placental mammals, reproductive success, and maternal-fetal health substantially depend on a well-being placenta, the interface between the fetus and the mother. Disorders in placental cells are tightly associated with adverse pregnancy outcomes including preeclampsia (PE), fetal growth restriction, etc. MicroRNAs (miRNAs) represent small non-coding RNAs that regulate post-transcriptional gene expression and are integral to a wide range of healthy or diseased cellular proceedings. Numerous miRNAs have been detected in human placenta and increasing evidence is revealing their important roles in regulating placental cell behaviors. Recent studies indicate that placenta-derived miRNAs can be released to the maternal circulation via encapsulating into the exosomes, and they potentially target various maternal cells to provide a hormone-like means of intercellular communication between the mother and the fetus. These placental exosome miRNAs are attracting more and more attention due to their differential expression in pregnant complications, which may provide novel biomarkers for prediction of the diseases. In this review, we briefly summarize the current knowledge and the perspectives of the placenta-derived miRNAs, especially the exosomal transfer of placental miRNAs and their pathophysiological relevance to PE. The possible exosomal-miRNA-targeted strategies for diagnosis, prognosis or therapy of PE are highlighted.

Keywords: placenta, miRNA, exosome, pregnancy, preeclampsia

OPEN ACCESS

Edited by:
Li Meng,
The Chinese University of Hong Kong, China

Reviewed by:
Hamed Mirzaei,
Kashan University of Medical Sciences, Iran
Yingshi Ouyang,
Magee-Womens Research Institute, United States

****Correspondence:***
Yan-Ling Wang
wangyl@ioz.ac.cn

† These authors have contributed equally to this work

Specialty section:
This article was submitted to Cell Growth and Division, a section of the journal Frontiers in Cell and Developmental Biology

Received: *26 December 2020*
Accepted: *22 February 2021*
Published: *11 March 2021*

Citation:
Xu P, Ma Y, Wu H and Wang Y-L (2021) Placenta-Derived MicroRNAs in the Pathophysiology of Human Pregnancy. Front. Cell Dev. Biol. 9:646326. doi: 10.3389/fcell.2021.646326

INTRODUCTION

The placenta is a transient organ that plays a central role in maternal and fetal health during pregnancy (Anin et al., 2004). Serving as the interface between the fetal and maternal environments, human placenta performs many critical functions throughout the gestation, such as exchange of gases, nutrients and waste products between the mother and the growing fetus (Cross, 1998). Human placenta is also an endocrine gland that modulates maternal physiological and metabolic events and provides an immune-protective milieu in which the semi-allogenic fetus can develop (Regnault et al., 2002). Human placenta develops from the trophectoderm, the outer layer of the pre-implantation embryo. Highly proliferative, undifferentiated primitive cytotrophoblast (CTB) cells that are derived from the trophectoderm give rise to differentiated trophoblast cells, mainly including villous syncytiotrophoblast (STB), cytotrophoblast (CTB), and extravillous trophoblast (EVT; Ji et al., 2013). Defects in placental development, especially the dysregulation of trophoblast differentiation, are

tightly associated with fetal loss and pregnant complications, such as preeclampsia (PE), and fetal growth restriction (FGR; Knofler et al., 2019).

MicroRNAs (miRNAs) are endogenous, small non-coding single-stranded RNAs, on average 22nt in length, which can regulate gene expression primarily through post-transcriptional repression or messenger RNA degradation in a sequence-specific manner (Bartel, 2009). Most miRNAs are transcribed as precursors (either pri-miRNA or pre-mRNA) before capping and polyadenylation, and their biogenesis requires several enzymes, including Drosha, DGCR8, Dicer, and Argonaute (Ago) 2 (Donker et al., 2007). In recent years, the remarkable roles of miRNAs in cellular proceedings under healthy or diseased conditions have been increasingly recognized (Aghdam et al., 2019; Mirzaei and Hamblin, 2020; Sadri Nahand et al., 2020; Davoodvandi et al., 2021; Razavi et al., 2021). In particular, several studies have shown that knocking out the key enzymes in the miRNA processing results in embryonic arrest or even embryonic death (Bernstein et al., 2003; Alisch et al., 2007; Suh et al., 2010), indicating the significance of miRNAs in the regulation of pregnant process.

Human placenta is a transient organ with fast development characteristics and transcriptome diversity. By far, over 1000 mature miRNAs are identified in human genomes (Friedlander et al., 2014), among which more than 600 miRNAs have been found in human placenta (Mouillet et al., 2015), and a series of differential miRNAs have been demonstrated in the placentas from complicated pregnancies including PE (Pineles et al., 2007; Ura et al., 2014; Xu et al., 2014). In addition, *in vitro* and *in vivo* studies have revealed the vital roles of these placenta-derived miRNAs in the regulation of trophoblast cell behaviors and the occurrence of PE (Xu et al., 2014; Awamleh and Han, 2020; Dong et al., 2020). In addition to the intracellular silencing functions, an attractive feature of the placenta-derived miRNAs is their capability of releasing to the maternal circulation via being encapsulated into the exosomes, and thus potentially targeting various maternal cells to provide a hormone-like means of intercellular communication between the mother and the fetus (Chen et al., 2012).

In this article, we briefly summarize the current knowledge of the placenta-derived miRNAs, especially the exosomal transfer of placental miRNAs and their pathophysiological relevance to PE. The miRNA-targeted promising strategies for the diagnosis, prognosis or therapy of PE are highlighted.

EXPRESSION AND FUNCTION OF PLACENTA-DERIVED MIRNAS DURING PREGNANCY

Placental development is a complicated process during which various subtypes of cells dynamically differentiate and interact with each other throughout gestation (Ji et al., 2013). The expression timing and cellular localization of miRNAs may change along gestation, indicating their time-dependent, and/or cell-type-dependent working mechanisms in the placenta. This point has been well-reflected in many studies. For instance, the higher expression of placental miR-18a at early gestation, as well as its specific localization in invasive EVTs are in consistence with its functions to regulate trophoblast cell invasion through targeting TGF-β/Smad2 signaling (Xu et al., 2020). The hypoxia-induced miRNA, miR-210, is transcribed in various subtypes of placental trophoblasts at early gestation in human beings and mice. It participates in modulating trophoblast cell proliferation, invasion, apoptosis, syncytialization, and angiogenesis by targeting various genes (Anton et al., 2013; Wang H. et al., 2020). Deficiency in miR-210 leads to failure in the response of the placenta to maternal hypoxia, especially at early fetal growth stage (Bian et al., 2020).

To date, emerging evidence has demonstrated the significance of miRNAs as regulators of various cell behaviors in human placenta. For instance, let-7a, miR-377, miR-675, miR-145, and miR-518b, etc., are involved in the regulation of trophoblast cell proliferation (Forbes et al., 2012; Gao et al., 2012; Doridot et al., 2013; Liu et al., 2018), miR-34a, miR-29b, miR-376c, miR-195, miR-210, and many others have roles in modulating trophoblast cell differentiation toward the invasive pathway (Pang et al., 2010; Fu et al., 2013; Li et al., 2013; Luo et al., 2014; Wu et al., 2016). The placental steroidogenesis can be regulated by miR-210, miR-518c, and miR-22 (Ishibashi et al., 2012; Shao et al., 2017), and the mitochondrial respiration activities and apoptosis of placental cells are associated with miR-210 and miR-195 (Wang et al., 2018; Anton et al., 2019). However, these functional outcomes are vastly based on *in vitro* studies using various cell models, and the relevant *in vivo* evidence using genetically manipulated mouse models has been largely lacking.

Among the placenta-derived miRNAs, there exists a placenta-specific miRNA cluster termed the chromosome 19 miRNA cluster (C19MC). The C19MC is the largest cluster of miRNAs in the human genome, and contains 46 highly homologous miRNA genes within a ∼100 kb genomic region (Bortolin-Cavaille et al., 2009). The miRNAs in this cluster are predominantly expressed in the primate placenta and some fetal tissues as well as various tumor cells (Bentwich et al., 2005; Zhang et al., 2008; Setty et al., 2020). During pregnancy, they are highly expressed in placental trophoblasts, and released into maternal circulation which are eliminated after delivery (Luo et al., 2009; Donker et al., 2012). Although the full repertoire of the biological actions of C19MCs remains to be established, a recent study by Mouillet et al. (2020) have proved the roles of one of the C19MC members, miR-519d-3p, in promoting trophoblast cell proliferation and decreasing cell migration abilities. In addition, C19MC miRNAs are detected in embryonic stem (ES) cells, and their expression drops considerably when ES cells begin to differentiate, indicating their roles in the maintenance of the undifferentiated status (Stadler et al., 2010). Several members of C19MC miRNAs, such as miR-519, miR-517a, and miR-517c, also exhibit tumor-suppressive activity via triggering cell senescence (Marasa et al., 2010) or inhibiting cell proliferation (Liu et al., 2013).

SECRETION AND FUNCTION OF PLACENTAL MIRNAS IN EXOSOMES

Exosomes are small extracellular vesicles of endocytic origin (van der Pol et al., 2016). They can be released by many cells and

are found in body fluids, including peripheral blood, lymph, and milk, etc. (Akers et al., 2013). The significance of exosomes in the progression, diagnosis and treatment of various diseases have been suggested (Asgarpour et al., 2020; Ghaemmaghami et al., 2020; Hashemian et al., 2020; Nahand et al., 2020). Interestingly, during pregnancy, the number of exosomes in maternal plasma appears to be significantly increased from the first trimester (Sarker et al., 2014), and reaches a maximum level at term (Jin and Menon, 2018). It is estimated that the concentration of exosomes in maternal peripheral blood is 20-fold higher than non-pregnant control (Sabapatha et al., 2006), and returns to non-pregnant levels within 48 h of delivery (Salomon et al., 2014). In pregnant complication such as PE, the level of maternal circulating exosome is progressively higher than normal pregnant controls (Chiarello et al., 2018).

Exosomes contain multifaceted cargoes, including proteins, lipids, DNAs, mRNAs, miRNAs, LncRNAs, tRNA, and tRNA associated fragments (Sarker et al., 2014; Jeppesen et al., 2019). The selective sorting of miRNAs into exosomes is attributed to the help of specific RNA-binding proteins, such as hnRNPA2B1 and Ago-2. Other membrane proteins including Caveolin-1 and Neural Sphingomyelinase 2 are also involved in this process (Groot and Lee, 2020). The observations by Valadi et al. (2007) first demonstrated the mechanisms of genetic exchange between different cells by the exosome transfer of miRNAs. Later on, Luo et al. (2009) indicated the extracellular release of placental miRNAs via exosomes into maternal blood. By far, accumulating studies have identified many exosome-packaged placental miRNAs and their release into extracellular compartments and maternal blood (Kambe et al., 2014; Ouyang et al., 2014; Mitchell et al., 2015; Chang et al., 2017; Chiarello et al., 2018; Zhao et al., 2018; Czernek and Duchler, 2020; Li et al., 2020; Yadava et al., 2020; Yang et al., 2020; Wang Y. et al., 2020). The placental exosomal miRNAs may target other cells at the feto-maternal interface in paracrine manner (Takahashi et al., 2017; Wang Y. et al., 2020), or transfer to maternal recipient cells and play endocrine functions (Kambe et al., 2014; Zhao et al., 2018; Ma et al., 2020). What's more, bidirectional trafficking of exosomal miRNAs between the placenta and the fetal compartment has been suggested (Chang et al., 2017;

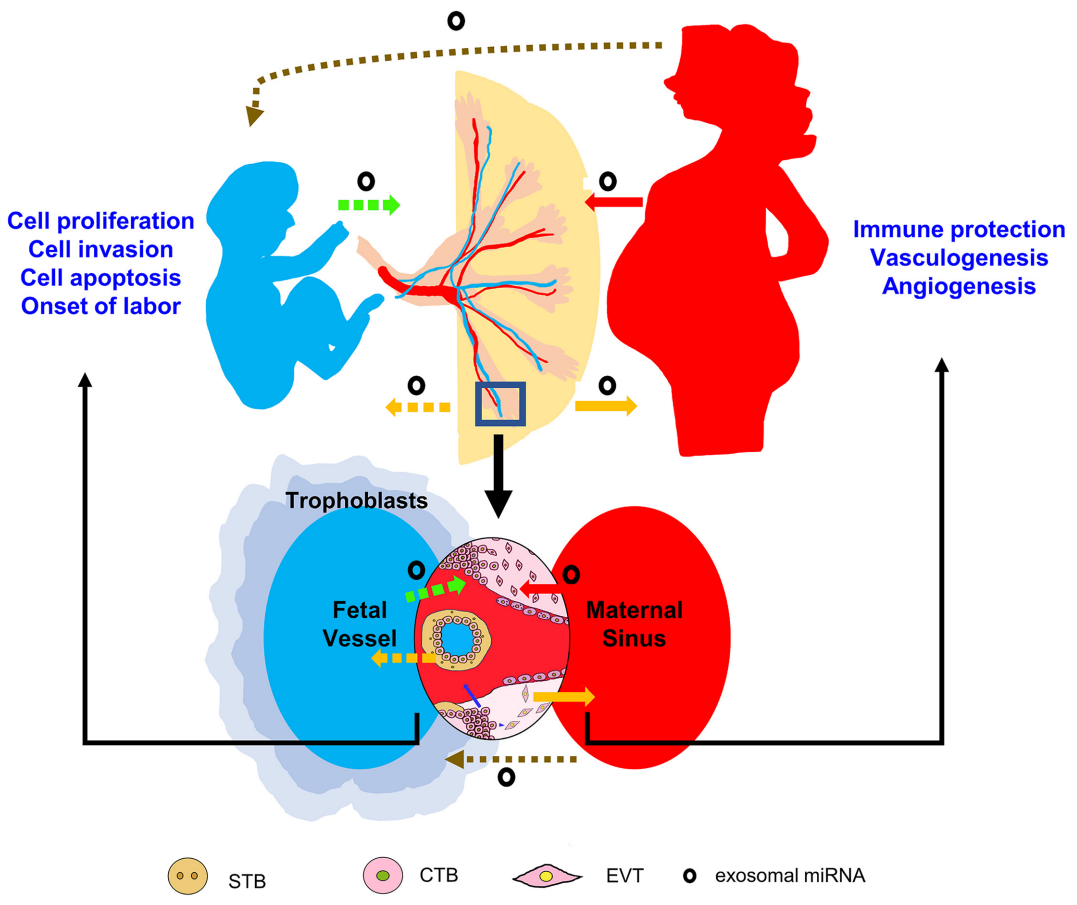

FIGURE 1 | Potential trafficking routes and working mechanisms of exosomal miRNAs during pregnancy. Placenta-derived exosomal miRNAs may be delivered to maternal or fetal circulation, and affect various cell events in targeting organs. The mother or fetus-derived exosomal miRNAs may also traffic to the placenta to regulate placental development. Note the dashed lines indicate the uncertainty of evidence by far, the blue arrow indicates endocrine manner and the blue arrow head indicates paracrine manner.

Shen et al., 2018; Yang et al., 2019; Yadava et al., 2020; Wang D. et al., 2020). We summarize the recognition of the placental exosomal miRNAs in **Figure 1**, and example some representative studies as below:

1) The placenta-derived exosomal miRNAs transfer to the maternal circulation and modulate maternal immune cells to protect the fetus from the maternal immune attacks. *In vivo* and *in vitro* studies have demonstrated the dramatical repression of PRKG1 expression in maternal NK cells by exosomal miR-517-3p (Kambe et al., 2014), and the downregulation of IL-24 and thus the suppression in the proliferative capacity and anti-inflammatory effect of macrophage by exosomal miR-203a-3p (Ma et al., 2020). In cattle, the placental exosome-derived bta-miR-499 inhibits the activation of NF-κB via Lin288/let-7 axis, thereby attenuates the inflammatory responses and forms an immune-tolerant microenvironment in the uterus. Inhibition of miR-499 lead to inflammatory deregulation and increased risk of pregnancy failure (Zhao et al., 2018).
2) Trophoblast cell behaviors can be regulated by exosomal miRNAs derived from the neighboring or distant placental cells. Exosomal miR-520c-3p of villous CTB origin can inhibit cell invasiveness via downregulating CD44 expression levels in targeted EVT cells (Takahashi et al., 2017). *In vivo* and *in vitro* results indicate the roles of placental exosomal miR-15a-5p in suppressing trophoblast cell proliferation, invasion, and apoptosis through downregulating CDK1 expression and hampering PI3K/AKT signaling, which is closely associated with PE progression (Wang Y. et al., 2020).
3) The placenta-derived exosomal miRNAs may regulate fetal vasculogenesis and angiogenesis. A study from Shen et al. (2018) showed the downregulation of eNOS expression in human umbilical vein endothelial cells by exosomal miR-155 of placenta origin, indicating the potential delivery of placental miRNAs to the fetal part. However, *ex vivo* or *in vivo* evidence that supports the transfer of placental exosomes from the placenta to the fetus remains largely lacking.
4) A potential mode of exosomal miRNAs-mediated fetus-to-placenta signaling has been suggested. For instance, miR-133b in human umbilical cord mesenchymal stem cell (MSC)-derived exosomes boosts trophoblast cell proliferation, migration, and invasion via targeting SGK1 gene (Wang D. et al., 2020). Exosomal miR-146a-5p and miR-548e-5p derived from amniotic fluid-MSCs exert anti-inflammatory effects on human trophoblast cells, and their dysregulation are associated with the occurrence of preterm birth (Yang et al., 2019). Umbilical artery-derived miR-15b-5p can be delivered to the placenta, and can repress the expression levels of Aplein and cytokines including IL-1, IL-6, IL-8, and TNF-α, and thus is believed to play roles in the onset of labor (Yadava et al., 2020). In addition to target trophoblast cells, the maternal and umbilical cord blood-derived exosomes can effectively influence endothelial cells, which is closely associated with the encapsulation of miRNAs into the exosomes (Jia et al., 2018). In pigs, miR-150 in umbilical cord blood-derived exosomes exhibits a pro-angiogenic effect by stimulating the proliferation and migration of endothelial cells. A reduced expression of this exosomal miRNA leads to intrauterine growth restriction of the fetus (Luo et al., 2018). However, more evidence from appropriate *in vivo* models are needed to clarify the working mechanisms of exosome transfer from the fetus to the placenta.

CLINICAL IMPLICATIONS OF THE PLACENTA-DERIVED MIRNAS FOR PE

Exploring the Pathogenesis of PE Using Placenta-Derived miRNAs

Preeclampsia has long been the leading cause of maternal and fetal morbidity and mortality, affecting approximately 2–7% of pregnancies. It is defined as the sudden onset of hypertension after the 20th week of gestation in pregnant women who had no preexisting hypertension, accompanied by significant proteinuria or multi-system symptoms, such as pulmonary oedema, seizures, or oliguria (Sibai, 2003). A well-accepted theory is that defects in placenta development, especially the dysregulation of trophoblastic behaviors, are predominant causes of the disease.

Great efforts have been put to identify genes or signaling pathways that are associated with the deregulation of trophoblast differentiation and the development of PE (Ji et al., 2013; Staff, 2019). A great number of differential miRNAs in PE placentas have been screened, and a series of *in vivo* and *in vitro* results have demonstrated the participation of these aberrantly expressed miRNAs in PE-associated placental defects (Pang et al., 2010; Ji et al., 2013; Anton et al., 2019; Xu et al., 2020).

For PE, a big challenge is the discrepancy between the key pathophysiological changes that are initiated well before the 20th week of gestation and the clinical symptoms that are not manifested until after that. Therefore, a critical thought is whether these differential placental miRNAs really contribute to the pathological change of PE or they are just the consequences of the disorder at late gestation (Baker and Delles, 2013). As stated above, placental miRNAs can be released to maternal circulation during pregnancy in pregnant women (Luo et al., 2009). Identification of the differential miRNAs in maternal blood at early-to-mid gestation in PE patients may provide valuable hints of the pathophysiological placental factors (Gunel et al., 2011). Our previous results have revealed several miRNAs (including miR-376c, miR-18a, miR-19b1, miR-92a1, miR-210, and miR-195) that exhibit significantly aberrant concentrations in the plasma of PE patients from gestational weeks 15–19 to term. These miRNAs in the placenta potentially contribute to compromised cell differentiation and functional homeostasis (Fu et al., 2013; Xu et al., 2014; Wang et al., 2018). However, results of genetic manipulation of these small RNAs in mice are lacking. Knocking down of miR-210 leads to relatively weak influence on fetal development (Krawczynski et al., 2016;

TABLE 1 | A brief summary of the differential exosomal miRNAs in the plasma from PE patients.

Exosomal miRNAs	Gestational weeks	Sample size	Method	Changes in PE plasma	Diagnostic capability	References
miR-885-5p	11–14 weeks	Selection cohort: PE (n = 19) and control (n = 14); Validation cohort: PE (n = 8) and control (n = 8)	NGS and qRT-PCR	↑	–	Sandrim et al., 2016
miR-136	<20-week gestation	PE (n = 20) and control (n = 23)	qRT-PCR	↑	AUC = 1.00, Sen = 95.00%, Spe = 100.00%	Motawi et al., 2018
miR-494	<20-week gestation	PE (n = 20) and control (n = 23)	qRT-PCR	↑	AUC = 0.87, Sen = 86.00%, Spe = 95.00%	Motawi et al., 2018
miR-495	<20-week gestation	PE (n = 20) and control (n = 23)	qRT-PCR	↑	AUC = 0.94, Sen = 90.00%, Spe = 83.00%	Motawi et al., 2018
miR-153-3p	Term	PE (n = 20) and control (n = 23)	Taqman qPCR	↑	–	Li et al., 2020
miR-222-3p	Term	PE (n = 20) and control (n = 23)	Taqman qPCR	↓	–	Li et al., 2020
miR-224-5p	Term	PE (n = 20) and control (n = 23)	Taqman qPCR	↓	–	Li et al., 2020
miR-325	Term	PE (n = 20) and control (n = 23)	Taqman qPCR	↑	–	Li et al., 2020
	–	PE (n = 20) and control (n = 23)	qRT-PCR	↑	–	Wang Y. et al., 2020
miR-342-3p	Term	PE (n = 20) and control (n = 23)	Taqman qPCR	↑	–	Li et al., 2020
miR-532-5p	Term	PE (n = 20) and control (n = 23)	Taqman qPCR	↓	–	Li et al., 2020
miR-653-5p	Term	PE (n = 20) and control (n = 23)	Taqman qPCR	↑	–	Li et al., 2020
miR-203a-3p	–	PE (n = 36) and control (n = 30)	qRT-PCR	↓	–	Ma et al., 2020
miR-134	<13-week gestation	PE (n = 4) and control (n = 5)	miRNA array	↑	–	Devor et al., 2020
miR-196b	26–40 weeks	PE (n = 4) and control (n = 5)	miRNA array	↓	–	Devor et al., 2020
miR-302c	26–40 weeks	PE (n = 4) and control (n = 5)	miRNA array	↑	–	Devor et al., 2020
miR-346	26–40 weeks	PE (n = 4) and control (n = 5)	miRNA array	↑	–	Devor et al., 2020
miR-376c	<13-week gestation	PE (n = 4) and control (n = 5)	miRNA array	↑	–	Devor et al., 2020
miR-486-3p	<13-week gestation	PE (n = 4) and control (n = 5)	miRNA array	↑	–	Devor et al., 2020
miR-590-5p	<13-week gestation	PE (n = 4) and control (n = 5)	miRNA array	↑	–	Devor et al., 2020
miR-618	26–40 weeks	PE (n = 4) and control (n = 5)	miRNA array	↑	–	Devor et al., 2020
miR-155	Term	PE (n = 10) and control (n = 10)	qRT-PCR	↑	–	Shen et al., 2018
miR-486-1-5p	The whole gestation	PE (n = 15) and control (n = 32)	NGS	↑	–	Salomon et al., 2017
	–	PE (n = 20) and control (n = 10)	qRT-PCR	↑	–	Wang Y. et al., 2020
miR-486-2-5p	The whole gestation	PE (n = 15) and control (n = 32)	NGS	↑	–	Salomon et al., 2017

(Continued)

TABLE 1 | Continued

Exosomal miRNAs	Gestational weeks	Sample size	Method	Changes in PE plasma	Diagnostic capability	References
	–	PE (n = 20) and control (n = 10)	qRT-PCR	↑	–	Wang Y. et al., 2020
miR-125a-5p	After the diagnosis of PE	PE (n = 18) and control (n = 20)	qRT-PCR	↑	–	Xueya et al., 2020
miR-423-5p	–	PE (n = 20) and control (n = 10)	qRT-PCR	↑	–	Wang Y. et al., 2020
miR-451a	–	PE (n = 20) and control (n = 10)	qRT-PCR	↑	–	Wang Y. et al., 2020
miR-15a-5p	–	PE (n = 20) and control (n = 10)	qRT-PCR	↑	–	Wang Y. et al., 2020
miR-92a-1-3p	–	PE (n = 20) and control (n = 10)	qRT-PCR	↑	–	Wang Y. et al., 2020
miR-92a-2-3p	–	PE (n = 20) and control (n = 10)	qRT-PCR	↑	–	Wang Y. et al., 2020
miR-103a-1-3p	–	PE (n = 20) and control (n = 10)	qRT-PCR	↑	–	Wang Y. et al., 2020
miR-103a-2-3p	–	PE (n = 20) and control (n = 10)	qRT-PCR	↑	–	Wang Y. et al., 2020
miR-126-3p	–	PE (n = 20) and control (n = 10)	qRT-PCR	↑	–	Wang Y. et al., 2020
miR-520a-5p	10–13 weeks	PE (n = 43) and control (n = 50)	qRT-PCR	↓	AUC = 0.63, Sen = 60.47%, Spe = 70.00%	Hromadnikova et al., 2019
miR-517-5p	10–13 weeks	PE (n = 43) and control (n = 50)	qRT-PCR	↓	AUC = 0.699, Sen = 60.47%, Spe = 84.00%	Hromadnikova et al., 2019
miR-525-5p	10–13 weeks	PE (n = 43) and control (n = 50)	qRT-PCR	↓	AUC = 0.698, Sen = 51.16%, Spe = 84.00%	Hromadnikova et al., 2019
miR-210	PE (24–39 weeks) and control (30–39 weeks)	PE (n = 19) and control (n = 34)	qRT-PCR	↑	–	Biro et al., 2017
	PE (31.00 ± 5.07 weeks) and control (36.13 ± 3.00 weeks)	PE (n = 8) and control (n = 8)	qRT-PCR	No significant change	–	Biro et al., 2019

PE, preelampsia; NGS, next generation sequencing; qRT-PCR, reverse transcription-real-time quantitative polymerase chain reaction; Taqman-qPCR, Taqman quantitative polymerase chain reaction; AUC, area under curve; Sen, sensitivity; and Spe, specificity.

Bian et al., 2020). This may reflect the fine-tune features of miRNAs to maintain cellular homeostasis, and also indicate the complicated compensatory routes of various placental miRNAs as well.

Circulating miRNAs Are Promising Biomarkers for the Prediction of PE

Circulating miRNAs can be encapsulated into extracellular vesicles including exosomes or bound to stabilizing proteins (mainly Ago proteins; Arroyo et al., 2011). Plasma miRNAs (including the vesicular form and the non-vesicular form) are relatively stable, being not affected by experimental conditions such as incubation temperature, pH or even RNase A treatment (Chen et al., 2008; Mitchell et al., 2008; Arroyo et al., 2011). The vesicle-packaged miRNAs are more resistant to degradation. Although the exosomal miRNAs constitute only a fraction of the whole plasma miRNA population, they exhibit unique changing pattern PE patients (Biro et al., 2019; Li et al., 2020). Since exosomal miR-885-5p is suggested as the potential predictive marker for PE (Sandrim et al., 2016), increasing attention has been put into this emerging field. The unique characteristics of exosomal miRNAs make them rather promising as non-invasive biomarkers for diagnosing or monitoring the development of PE. We summarize the relevant progress in **Table 1**. Notably, studies from Motawi et al. (2018) indicate significant increase in miR-136, miR-494 and miR-495 in circulating exosomes from PE patients before the 20th week of gestation, and receiver operating characteristic curve analysis reveals promisingly high sensitivity and specificity of these miRNAs to predict PE before the onset of clinical manifestations.

It has to be noticed that the results from various studies may show different changing patterns of the exosomal miRNAs in PE patients (Biro et al., 2017, 2019). The variations may attribute to the differences in sample size, the gestational week at sampling, or the statistical method. Importantly,

the studies using large-scale plasma samples in detailed time points during gestation with normalized statistical methods are needed to achieve reproducible results and confirm the clinical sensitivity and specificity of exosomal miRNAs as the promising biomarkers for PE.

Exosomal miRNAs Are Potentially Useful Tools for the RNA-Based Therapies for PE

In recent years, RNA-based medicine is receiving growing attention for its diverse roles and promising therapeutic capacity (Chow et al., 2020). Interestingly, the exosomes can be engineered to load with miRNAs of interest and delivered to the recipient cells and/or organs, reinforcing the possibility to tailor exosomes as gene-delivery vehicles (Thomou et al., 2017). One technology-barrier is difficulties in introducing anti-miR into exosomes and delivering anti-miR to exosome-recipient cells after intravenous administration. Recently, Yamayoshi (2020) have constructed a novel drug delivery system using anti-exosome antibody-oligonucleotide conjugates to functionally inhibit circulating miRNAs, which sheds light on developing strategy for PE treatment.

CONCLUSION AND PERSPECTIVES

The discovery of placenta-derived miRNAs and their multiple roles in maintaining healthy pregnancy undoubtedly represent one of the most exciting progresses in recent years. In addition to the canonical intracellular silencing functions, placenta-derived miRNAs can also be released to the maternal or fetal circulation via encapsulating into the exosomes, and therefore potentially target various recipient cells to provide a non-hormonal means of intercellular communication between the mother and the fetus. Furthermore, unique exosomal miRNA profiling is potential diagnostic or predictive and prognostic tool for pregnant complications such as PE, and provides novel treatment targets for the disease.

There exist several interesting topics that require further investigations. First, studies regarding exosomal miRNA in pregnant women have been predominantly focusing on the total exosomal miRNAs, while seldom identifying their diverse origins. A recent report reveals that the origin of exosomes determines its target cells and the transfer activity (Sancho-Albero et al., 2019), indicating the importance of further clarifying whether the circulating exosomal miRNAs in the pregnant women are derived from the placenta, the fetus or various maternal organs. This may greatly deepen our understanding of the mechanisms underlying the complicated fetal-maternal interactions during gestation. To follow this concern, the precise trafficking routes and the specific targeting cells or organs of the placental exosomal miRNAs are yet to be clarified. Proper *in vivo* and *ex vivo* models should be constructed to address this point, which is indispensable for developing exosomal miRNA-based therapeutic strategies for pregnant complications such as PE. Finally, the convenient and controllable detection of exosomal miRNA remains challenging, because the adequately simple and robust assay platforms are lacking. A recent wok by Xia et al. (2021) has developed a colorimetric strategy to detect exosomal miR-21 by switching the visible-light-induced oxidase mimic activity of acridone derivate. This may provide a feasible tool for the application in exosomal miRNAs-based diagnosis of PE.

AUTHOR CONTRIBUTIONS

PX and YM drafted the manuscript. HW participated in reference mining. Y-LW designed and supervised the study, and revised the manuscript. All authors contributed to the article and approved the submitted version.

FUNDING

This study was supported by grants from the National Key Research and Development Program of China (2016YFC1000401, 2017YFC1001404, and 2018YFC1004100), the National Natural Science Foundation (81730040 and 21806093), and the China Postdoctoral Science Foundation (2017M621482 and 2019T120342).

ACKNOWLEDGMENTS

We thank Dr. Shao Chin Lee at Jiangsu Normal University, for his critical comments to the manuscript.

REFERENCES

Aghdam, A. M., Amiri, A., Salarinia, R., Masoudifar, A., Ghasemi, F., and Mirzaei, H. (2019). MicroRNAs as diagnostic, prognostic, and therapeutic biomarkers in prostate Cancer. *Crit. Rev. Eukaryot. Gene Exp.* 29, 127–139. doi: 10.1615/CritRevEukaryotGeneExpr.2019025273

Akers, J. C., Gonda, D., Kim, R., Carter, B. S., and Chen, C. C. (2013). Biogenesis of extracellular vesicles (EV): exosomes, microvesicles, retrovirus-like vesicles, and apoptotic bodies. *J. Neurooncol.* 113, 1–11. doi: 10.1007/s11060-013-1084-8

Alisch, R. S., Jin, P., Epstein, M., Caspary, T., and Warren, S. T. (2007). Argonaute2 is essential for mammalian gastrulation and proper mesoderm formation. *PLoS Genet.* 3:e227. doi: 10.1371/journal.pgen.0030227

Anin, S. A., Vince, G., and Quenby, S. (2004). Trophoblast invasion. *Hum. Fertil.* 7, 169–174. doi: 10.1080/14647270400006911

Anton, L., Devine, A., Polyak, E., Olarerin-George, A., Brown, A. G., Falk, M. J., et al. (2019). HIF-1alpha stabilization increases miR-210 eliciting first trimester extravillous trophoblast mitochondrial dysfunction. *Front. Physiol.* 10:699. doi: 10.3389/fphys.2019.00699

Anton, L., Olarerin-George, A. O., Schwartz, N., Srinivas, S., Bastek, J., Hogenesch, J. B., et al. (2013). miR-210 inhibits trophoblast invasion and is a serum biomarker for preeclampsia. *Am. J. Pathol.* 183, 1437–1445. doi: 10.1016/j.ajpath.2013.07.021

Arroyo, J. D., Chevillet, J. R., Kroh, E. M., Ruf, I. K., Pritchard, C. C., Gibson, D. F., et al. (2011). Argonaute2 complexes carry a population of circulating microRNAs independent of vesicles in human plasma. *Proc. Natl. Acad. Sci. U.S.A.* 108, 5003–5008. doi: 10.1073/pnas.1019055108

Asgarpour, K., Shojaei, Z., Amiri, F., Ai, J., Mahjoubin-Tehran, M., Ghasemi, F., et al. (2020). Exosomal microRNAs derived from mesenchymal stem cells:

cell-to-cell messages. *Cell Commun. Signal.* 18:149. doi: 10.1186/s12964-020-00650-6

Awamleh, Z., and Han, V. K. M. (2020). Potential pathophysiological role of microRNA 193b-5p in human placentae from pregnancies complicated by preeclampsia and intrauterine growth restriction. *Mol. Biol. Rep.* 47, 6531–6544. doi: 10.1007/s11033-020-05705-y

Baker, A. H., and Delles, C. (2013). Is microRNA-376c a biomarker or mediator of preeclampsia? *Hypertension* 61, 767–769. doi: 10.1161/HYPERTENSIONAHA.111.00087

Bartel, D. P. (2009). MicroRNAs: target recognition and regulatory functions. *Cell* 136, 215–233. doi: 10.1016/j.cell.2009.01.002

Bentwich, I., Avniel, A., Karov, Y., Aharonov, R., Gilad, S., Barad, O., et al. (2005). Identification of hundreds of conserved and nonconserved human microRNAs. *Nat. Genet.* 37, 766–770. doi: 10.1038/ng1590

Bernstein, E., Kim, S. Y., Carmell, M. A., Murchison, E. P., Alcorn, H., Li, M. Z., et al. (2003). Dicer is essential for mouse development. *Nat. Genet.* 35, 215–217. doi: 10.1038/ng1253

Bian, X., Liu, J., Yang, Q., Liu, Y., Jia, W., Zhang, X., et al. (2020). miR-210 regulates placental adaptation to maternal hypoxic stress during pregnancydagger. *Biol. Reprod.* 104, 418–429. doi: 10.1093/biolre/ioaa187

Biro, O., Alasztics, B., Molvarec, A., Joo, J., Nagy, B., and Rigo, J. Jr. (2017). Various levels of circulating exosomal total-miRNA and miR-210 hypoxamiR in different forms of pregnancy hypertension. *Pregnancy Hypertens* 10, 207–212. doi: 10.1016/j.preghy.2017.09.002

Biro, O., Fothi, A., Alasztics, B., Nagy, B., Orban, T. I., and Rigo, J. Jr. (2019). Circulating exosomal and Argonaute-bound microRNAs in preeclampsia. *Gene* 692, 138–144. doi: 10.1016/j.gene.2019.01.012

Bortolin-Cavaille, M. L., Dance, M., Weber, M., and Cavaille, J. (2009). C19MC microRNAs are processed from introns of large Pol-II, non-protein-coding transcripts. *Nucleic Acids Res.* 37, 3464–3473. doi: 10.1093/nar/gkp205

Chang, G., Mouillet, J. F., Mishima, T., Chu, T., Sadovsky, E., Coyne, C. B., et al. (2017). Expression and trafficking of placental microRNAs at the feto-maternal interface. *FASEB J.* 31, 2760–2770. doi: 10.1096/fj.201601146R

Chen, X., Ba, Y., Ma, L., Cai, X., Yin, Y., Wang, K., et al. (2008). Characterization of microRNAs in serum: a novel class of biomarkers for diagnosis of cancer and other diseases. *Cell Res.* 18, 997–1006. doi: 10.1038/cr.2008.282

Chen, X., Liang, H., Zhang, J., Zen, K., and Zhang, C. Y. (2012). Secreted microRNAs: a new form of intercellular communication. *Trends Cell Biol.* 22, 125–132. doi: 10.1016/j.tcb.2011.12.001

Chiarello, D. I., Salsoso, R., Toledo, F., Mate, A., Vazquez, C. M., and Sobrevia, L. (2018). Foetoplacental communication via extracellular vesicles in normal pregnancy and preeclampsia. *Mol. Aspects Med.* 60, 69–80. doi: 10.1016/j.mam.2017.12.002

Chow, M. Y. T., Qiu, Y., and Lam, J. K. W. (2020). Inhaled RNA therapy: from promise to reality. *Trends Pharmacol. Sci.* 41, 715–729. doi: 10.1016/j.tips.2020.08.002

Cross, J. C. (1998). Formation of the placenta and extraembryonic membranes. *Ann. N. Y. Acad. Sci.* 857, 23–32. doi: 10.1111/j.1749-6632.1998.tb10104.x

Czernek, L., and Duchler, M. (2020). Exosomes as messengers between mother and fetus in pregnancy. *Int. J. Mol. Sci.* 21:4264. doi: 10.3390/ijms21124264

Davoodvandi, A., Marzban, H., Goleij, P., Sahebkar, A., Morshedi, K., Rezaei, S., et al. (2021). Effects of therapeutic probiotics on modulation of microRNAs. *Cell Commun. Signal.* 19:4. doi: 10.1186/s12964-020-00668-w

Devor, E., Santillan, D., Scroggins, S., Warrier, A., and Santillan, M. (2020). Trimester-specific plasma exosome microRNA expression profiles in preeclampsia. *J. Matern. Fetal. Neonatal Med.* 33, 3116–3124. doi: 10.1080/14767058.2019.1569614

Dong, D., Khoong, Y., Ko, Y., and Zhang, Y. (2020). microRNA-646 inhibits angiogenesis of endothelial progenitor cells in pre-eclamptic pregnancy by targeting the VEGF-A/HIF-1alpha axis. *Exp. Ther. Med.* 20, 1879–1888. doi: 10.3892/etm.2020.8929

Donker, R. B., Mouillet, J. F., Chu, T., Hubel, C. A., Stolz, D. B., Morelli, A. E., et al. (2012). The expression profile of C19MC microRNAs in primary human trophoblast cells and exosomes. *Mol. Hum. Reprod.* 18, 417–424. doi: 10.1093/molehr/gas013

Donker, R. B., Mouillet, J. F., Nelson, D. M., and Sadovsky, Y. (2007). The expression of Argonaute2 and related microRNA biogenesis proteins in normal and hypoxic trophoblasts. *Mol. Hum. Reprod.* 13, 273–279. doi: 10.1093/molehr/gam006

Doridot, L., Miralles, F., Barbaux, S., and Vaiman, D. (2013). Trophoblasts, invasion, and microRNA. *Front. Genet.* 4:248. doi: 10.3389/fgene.2013.00248

Forbes, K., Farrokhnia, F., Aplin, J. D., and Westwood, M. (2012). Dicer-dependent miRNAs provide an endogenous restraint on cytotrophoblast proliferation. *Placenta* 33, 581–585. doi: 10.1016/j.placenta.2012.03.006

Friedlander, M. R., Lizano, E., Houben, A. J., Bezdan, D., Banez-Coronel, M., Kudla, G., et al. (2014). Evidence for the biogenesis of more than 1,000 novel human microRNAs. *Genome Biol.* 15:R57. doi: 10.1186/gb-2014-15-4-r57

Fu, G., Ye, G., Nadeem, L., Ji, L., Manchanda, T., Wang, Y., et al. (2013). MicroRNA-376c impairs transforming growth factor-beta and nodal signaling to promote trophoblast cell proliferation and invasion. *Hypertension* 61, 864–872. doi: 10.1161/HYPERTENSIONAHA.111.203489

Gao, W. L., Liu, M., Yang, Y., Yang, H., Liao, Q., Bai, Y., et al. (2012). The imprinted H19 gene regulates human placental trophoblast cell proliferation via encoding miR-675 that targets Nodal Modulator 1 (NOMO1). *RNA Biol.* 9, 1002–1010. doi: 10.4161/rna.20807

Ghaemmaghami, A. B., Mahjoubin-Tehran, M., Movahedpour, A., Morshedi, K., Sheida, A., Taghavi, S. P., et al. (2020). Role of exosomes in malignant glioma: microRNAs and proteins in pathogenesis and diagnosis. *Cell Commun. Signal.* 18:120. doi: 10.1186/s12964-020-00623-9

Groot, M., and Lee, H. (2020). Sorting mechanisms for MicroRNAs into extracellular vesicles and their associated diseases. *Cells* 9:1044. doi: 10.3390/cells9041044

Gunel, T., Zeybek, Y. G., Akcakaya, P., Kalelioglu, I., Benian, A., Ermis, H., et al. (2011). Serum microRNA expression in pregnancies with preeclampsia. *Genet. Mol. Res.* 10, 4034–4040. doi: 10.4238/2011.November.8.5

Hashemian, S. M., Pourhanifeh, M. H., Fadaei, S., Velayati, A. A., Mirzaei, H., and Hamblin, M. R. (2020). Non-coding RNAs and exosomes: their role in the pathogenesis of sepsis. *Mol. Ther. Nucleic Acids* 21, 51–74. doi: 10.1016/j.omtn.2020.05.012

Hromadnikova, I., Dvorakova, L., Kotlabova, K., and Krofta, L. (2019). The prediction of gestational hypertension, preeclampsia and fetal growth restriction via the first trimester screening of plasma exosomal C19MC microRNAs. *Int. J. Mol. Sci.* 20:2972. doi: 10.3390/ijms20122972

Ishibashi, O., Ohkuchi, A., Ali, M. M., Kurashina, R., Luo, S. S., Ishikawa, T., et al. (2012). Hydroxysteroid (17-beta) dehydrogenase 1 is dysregulated by miR-210 and miR-518c that are aberrantly expressed in preeclamptic placentas: a novel marker for predicting preeclampsia. *Hypertension* 59, 265–273. doi: 10.1161/HYPERTENSIONAHA.111.180232

Jeppesen, D. K., Fenix, A. M., Franklin, J. L., Higginbotham, J. N., Zhang, Q., Zimmerman, L. J., et al. (2019). Reassessment of exosome composition. *Cell* 177, 428.e18–445.e18. doi: 10.1016/j.cell.2019.02.029

Ji, L., Brkic, J., Liu, M., Fu, G., Peng, C., and Wang, Y. L. (2013). Placental trophoblast cell differentiation: physiological regulation and pathological relevance to preeclampsia. *Mol. Aspects Med.* 34, 981–1023. doi: 10.1016/j.mam.2012.12.008

Jia, L., Zhou, X., Huang, X., Xu, X., Jia, Y., Wu, Y., et al. (2018). Maternal and umbilical cord serum-derived exosomes enhance endothelial cell proliferation and migration. *FASEB J.* 32, 4534–4543. doi: 10.1096/fj.201701337RR

Jin, J., and Menon, R. (2018). Placental exosomes: a proxy to understand pregnancy complications. *Am. J. Reprod. Immunol.* 79:e12788. doi: 10.1111/aji.12788

Kambe, S., Yoshitake, H., Yuge, K., Ishida, Y., Ali, M. M., Takizawa, T., et al. (2014). Human exosomal placenta-associated miR-517a-3p modulates the expression of PRKG1 mRNA in Jurkat cells. *Biol. Reprod.* 91:129. doi: 10.1095/biolreprod.114.121616

Knofler, M., Haider, S., Saleh, L., Pollheimer, J., Gamage, T., and James, J. (2019). Human placenta and trophoblast development: key molecular mechanisms and model systems. *Cell Mol. Life Sci.* 76, 3479–3496. doi: 10.1007/s00018-019-03104-6

Krawczynski, K., Mishima, T., Huang, X., and Sadovsky, Y. (2016). Intact feto-placental growth in microRNA-210 deficient mice. *Placenta* 47, 113–115. doi: 10.1016/j.placenta.2016.09.007

Li, H., Ouyang, Y., Sadovsky, E., Parks, W. T., Chu, T., and Sadovsky, Y. (2020). Unique microRNA signals in plasma exosomes from pregnancies complicated by preeclampsia. *Hypertension* 75, 762–771. doi: 10.1161/HYPERTENSIONAHA.119.14081

Li, P., Guo, W., Du, L., Zhao, J., Wang, Y., Liu, L., et al. (2013). microRNA-29b contributes to pre-eclampsia through its effects on apoptosis, invasion and angiogenesis of trophoblast cells. *Clin. Sci.* 124, 27–40. doi: 10.1042/CS20120121

Liu, M., Wang, Y., Lu, H., Wang, H., Shi, X., Shao, X., et al. (2018). miR-518b enhances human trophoblast cell proliferation through targeting Rap1b and activating Ras-MAPK signal. *Front. Endocrinol.* 9:100. doi: 10.3389/fendo.2018.00100

Liu, R. F., Xu, X., Huang, J., Fei, Q. L., Chen, F., Li, Y. D., et al. (2013). Down-regulation of miR-517a and miR-517c promotes proliferation of hepatocellular carcinoma cells via targeting Pyk2. *Cancer Lett.* 329, 164–173. doi: 10.1016/j.canlet.2012.10.027

Luo, J., Fan, Y., Shen, L., Niu, L., Zhao, Y., Jiang, D., et al. (2018). The pro-angiogenesis of exosomes derived from umbilical cord blood of intrauterine growth restriction pigs was repressed associated with MiRNAs. *Int. J. Biol. Sci.* 14, 1426–1436. doi: 10.7150/ijbs.27029

Luo, R., Shao, X., Xu, P., Liu, Y., Wang, Y., Zhao, Y., et al. (2014). MicroRNA-210 contributes to preeclampsia by downregulating potassium channel modulatory factor 1. *Hypertension* 64, 839–845. doi: 10.1161/HYPERTENSIONAHA.114.03530

Luo, S. S., Ishibashi, O., Ishikawa, G., Ishikawa, T., Katayama, A., Mishima, T., et al. (2009). Human villous trophoblasts express and secrete placenta-specific microRNAs into maternal circulation via exosomes. *Biol. Reprod.* 81, 717–729. doi: 10.1095/biolreprod.108.075481

Ma, H. Y., Cu, W., Sun, Y. H., and Chen, X. (2020). MiRNA-203a-3p inhibits inflammatory response in preeclampsia through regulating IL24. *Eur. Rev. Med. Pharmacol. Sci.* 24, 5223–5230. doi: 10.26355/eurrev_202005_21304

Marasa, B. S., Srikantan, S., Martindale, J. L., Kim, M. M., Lee, E. K., Gorospe, M., et al. (2010). MicroRNA profiling in human diploid fibroblasts uncovers miR-519 role in replicative senescence. *Aging* 2, 333–343. doi: 10.18632/aging.100159

Mirzaei, H., and Hamblin, M. R. (2020). Regulation of glycolysis by non-coding RNAs in cancer: switching on the warburg effect. *Mol. Ther. Oncolytics* 19, 218–239. doi: 10.1016/j.omto.2020.10.003

Mitchell, M. D., Peiris, H. N., Kobayashi, M., Koh, Y. Q., Duncombe, G., Illanes, S. E., et al. (2015). Placental exosomes in normal and complicated pregnancy. *Am. J. Obstet Gynecol.* 213, S173–S181. doi: 10.1016/j.ajog.2015.07.001

Mitchell, P. S., Parkin, R. K., Kroh, E. M., Fritz, B. R., Wyman, S. K., Pogosova-Agadjanyan, E. L., et al. (2008). Circulating microRNAs as stable blood-based markers for cancer detection. *Proc. Natl. Acad. Sci. U.S.A.* 105, 10513–10518. doi: 10.1073/pnas.0804549105

Motawi, T. M. K., Sabry, D., Maurice, N. W., and Rizk, S. M. (2018). Role of mesenchymal stem cells exosomes derived microRNAs; miR-136, miR-494 and miR-495 in pre-eclampsia diagnosis and evaluation. *Arch. Biochem. Biophys.* 659, 13–21. doi: 10.1016/j.abb.2018.09.023

Mouillet, J. F., Goff, J., Sadovsky, E., Sun, H., Parks, T., Chu, T., et al. (2020). Transgenic expression of human C19MC miRNAs impacts placental morphogenesis. *Placenta* 101, 208–214. doi: 10.1016/j.placenta.2020.09.069

Mouillet, J. F., Ouyang, Y., Coyne, C. B., and Sadovsky, Y. (2015). MicroRNAs in placental health and disease. *Am. J. Obstet Gynecol.* 213, S163–S172. doi: 10.1016/j.ajog.2015.05.057

Nahand, J. S., Vandchali, N. R., Darabi, H., Doroudian, M., Banafshe, H. R., Moghoofei, M., et al. (2020). Exosomal microRNAs: novel players in cervical cancer. *Epigenomics* 12, 1651–1660. doi: 10.2217/epi-2020-0026

Ouyang, Y., Mouillet, J. F., Coyne, C. B., and Sadovsky, Y. (2014). Review: placenta-specific microRNAs in exosomes - good things come in nano-packages. *Placenta* 35(Suppl.), S69–S73. doi: 10.1016/j.placenta.2013.11.002

Pang, R. T., Leung, C. O., Ye, T. M., Liu, W., Chiu, P. C., Lam, K. K., et al. (2010). MicroRNA-34a suppresses invasion through downregulation of Notch1 and Jagged1 in cervical carcinoma and choriocarcinoma cells. *Carcinogenesis* 31, 1037–1044. doi: 10.1093/carcin/bgq066

Pineles, B. L., Romero, R., Montenegro, D., Tarca, A. L., Han, Y. M., Kim, Y. M., et al. (2007). Distinct subsets of microRNAs are expressed differentially in the human placentas of patients with preeclampsia. *Am. J. Obstet Gynecol.* 196, e261–e266. doi: 10.1016/j.ajog.2007.01.008

Razavi, Z. S., Tajiknia, V., Majidi, S., Ghandali, M., Mirzaei, H. R., Rahimian, N., et al. (2021). Gynecologic cancers and non-coding RNAs: epigenetic regulators with emerging roles. *Crit. Rev. Oncol. Hematol.* 157:103192. doi: 10.1016/j.critrevonc.2020.103192

Regnault, T. R., Galan, H. L., Parker, T. A., and Anthony, R. V. (2002). Placental development in normal and compromised pregnancies– a review. *Placenta* 23(Suppl. A), S119–S129. doi: 10.1053/plac.2002.0792

Sabapatha, A., Gercel-Taylor, C., and Taylor, D. D. (2006). Specific isolation of placenta-derived exosomes from the circulation of pregnant women and their immunoregulatory consequences. *Am. J. Reprod. Immunol.* 56, 345–355. doi: 10.1111/j.1600-0897.2006.00435.x

Sadri Nahand, J., Moghoofei, M., Salmaninejad, A., Bahmanpour, Z., Karimzadeh, M., Nasiri, M., et al. (2020). Pathogenic role of exosomes and microRNAs in HPV-mediated inflammation and cervical cancer: a review. *Int. J. Cancer* 146, 305–320. doi: 10.1002/ijc.32688

Salomon, C., Guanzon, D., Scholz-Romero, K., Longo, S., Correa, P., Illanes, S. E., et al. (2017). Placental exosomes as early biomarker of preeclampsia: potential role of exosomal micrornas across gestation. *J. Clin. Endocrinol. Metab.* 102, 3182–3194. doi: 10.1210/jc.2017-00672

Salomon, C., Torres, M. J., Kobayashi, M., Scholz-Romero, K., Sobrevia, L., Dobierzewska, A., et al. (2014). A gestational profile of placental exosomes in maternal plasma and their effects on endothelial cell migration. *PLoS One* 9:e98667. doi: 10.1371/journal.pone.0098667

Sancho-Albero, M., Navascues, N., Mendoza, G., Sebastian, V., Arruebo, M., Martin-Duque, P., et al. (2019). Exosome origin determines cell targeting and the transfer of therapeutic nanoparticles towards target cells. *J. Nanobiotechnol.* 17:16. doi: 10.1186/s12951-018-0437-z

Sandrim, V. C., Luizon, M. R., Palei, A. C., Tanus-Santos, J. E., and Cavalli, R. C. (2016). Circulating microRNA expression profiles in pre-eclampsia: evidence of increased miR-885-5p levels. *BJOG* 123, 2120–2128. doi: 10.1111/1471-0528.13903

Sarker, S., Scholz-Romero, K., Perez, A., Illanes, S. E., Mitchell, M. D., Rice, G. E., et al. (2014). Placenta-derived exosomes continuously increase in maternal circulation over the first trimester of pregnancy. *J. Transl. Med.* 12:204. doi: 10.1186/1479-5876-12-204

Setty, B. A., Jinesh, G. G., Arnold, M., Pettersson, F., Cheng, C. H., Cen, L., et al. (2020). The genomic landscape of undifferentiated embryonal sarcoma of the liver is typified by C19MC structural rearrangement and overexpression combined with TP53 mutation or loss. *PLoS Genet.* 16:e1008642. doi: 10.1371/journal.pgen.1008642

Shao, X., Liu, Y., Liu, M., Wang, Y., Yan, L., Wang, H., et al. (2017). Testosterone represses estrogen signaling by upregulating miR-22: a mechanism for imbalanced steroid hormone production in preeclampsia. *Hypertension* 69, 721–730. doi: 10.1161/HYPERTENSIONAHA.116.08468

Shen, L., Li, Y. J., Li, R. T., Diao, Z. Y., Yany, M. Y., Wu, M. F., et al. (2018). Placenta-associated serum exosomal miR-155 derived from patients with preeclampsia inhibits eNOS expression in human umbilical vein endothelial cells. *Int. J. Mol. Med.* 41, 1731–1739.

Sibai, B. M. (2003). Diagnosis and management of gestational hypertension and preeclampsia. *Obstet Gynecol.* 102, 181–192. doi: 10.1016/s0029-7844(03)00475-7

Stadler, B., Ivanovska, I., Mehta, K., Song, S., Nelson, A., Tan, Y., et al. (2010). Characterization of microRNAs involved in embryonic stem cell states. *Stem Cells Dev.* 19, 935–950. doi: 10.1089/scd.2009.0426

Staff, A. C. (2019). The two-stage placental model of preeclampsia: an update. *J. Reprod. Immunol.* 13, 1–10. doi: 10.1016/j.jri.2019.07.004

Suh, N., Baehner, L., Moltzahn, F., Melton, C., Shenoy, A., Chen, J., et al. (2010). MicroRNA function is globally suppressed in mouse oocytes and early embryos. *Curr. Biol.* 20, 271–277. doi: 10.1016/j.cub.2009.12.044

Takahashi, H., Ohkuchi, A., Kuwata, T., Usui, R., Baba, Y., Suzuki, H., et al. (2017). Endogenous and exogenous miR-520c-3p modulates CD44-mediated extravillous trophoblast invasion. *Placenta* 50, 25–31. doi: 10.1016/j.placenta.2016.12.016

Thomou, T., Mori, M. A., Dreyfuss, J. M., Konishi, M., Sakaguchi, M., Wolfrum, C., et al. (2017). Adipose-derived circulating miRNAs regulate gene expression in other tissues. *Nature* 542, 450–455. doi: 10.1038/nature21365

Ura, B., Feriotto, G., Monasta, L., Bilel, S., Zweyer, M., and Celeghini, C. (2014). Potential role of circulating microRNAs as early markers of preeclampsia. *Taiwan J. Obstet Gynecol.* 53, 232–234. doi: 10.1016/j.tjog.2014.03.001

Valadi, H., Ekstrom, K., Bossios, A., Sjostrand, M., Lee, J. J., and Lotvall, J. O. (2007). Exosome-mediated transfer of mRNAs and microRNAs is a novel mechanism of genetic exchange between cells. *Nat. Cell Biol.* 9, 654–659. doi: 10.1038/ncb1596

van der Pol, E., Boing, A. N., Gool, E. L., and Nieuwland, R. (2016). Recent developments in the nomenclature, presence, isolation, detection and clinical impact of extracellular vesicles. *J. Thromb. Haemost.* 14, 48–56. doi: 10.1111/jth.13190

Wang, D., Na, Q., Song, G. Y., and Wang, L. (2020). Human umbilical cord mesenchymal stem cell-derived exosome-mediated transfer of microRNA-133b boosts trophoblast cell proliferation, migration and invasion in preeclampsia by restricting SGK1. *Cell Cycle* 19, 1869–1883. doi: 10.1080/15384101.2020.1769394

Wang, H., Zhao, Y., Luo, R., Bian, X., Wang, Y., Shao, X., et al. (2020). A positive feedback self-regulatory loop between miR-210 and HIF-1alpha mediated by CPEB2 is involved in trophoblast syncytialization: implication of trophoblast malfunction in preeclampsiadagger. *Biol. Reprod.* 102, 560–570. doi: 10.1093/biolre/ioz196

Wang, Y., Du, X., and Wang, J. (2020). Transfer of miR-15a-5p by placental exosomes promotes pre-eclampsia progression by regulating PI3K/AKT signaling pathway via CDK1. *Mol. Immunol.* 128, 277–286. doi: 10.1016/j.molimm.2020.10.019

Wang, H., Zhang, L., Guo, X., Bai, Y., Li, Y. X., Sha, J., et al. (2018). MiR-195 modulates oxidative stress-induced apoptosis and mitochondrial energy production in human trophoblasts via flavin adenine dinucleotide-dependent oxidoreductase domain-containing protein 1 and pyruvate dehydrogenase phosphatase regulatory subunit. *J. Hypertens.* 36, 306–318. doi: 10.1097/HJH.0000000000001529

Wu, H., Wang, H., Liu, M., Bai, Y., Li, Y. X., Ji, L., et al. (2016). MiR-195 participates in the placental disorder of preeclampsia via targeting activin receptor type-2B in trophoblastic cells. *J. Hypertens.* 34, 1371–1379. doi: 10.1097/HJH.0000000000000948

Xia, Y., Chen, T., Zhang, L., Zhang, X., Shi, W., Chen, G., et al. (2021). Colorimetric detection of exosomal microRNA through switching the visible-light-induced oxidase mimic activity of acridone derivate. *Biosens. Bioelectron.* 173:112834. doi: 10.1016/j.bios.2020.112834

Xu, P., Li, Z., Wang, Y., Yu, X., Shao, X., Li, Y. X., et al. (2020). miR-18a contributes to preeclampsia by downregulating Smad2 (Full Length) and reducing TGF-beta signaling. *Mol. Ther. Nucleic Acids* 22, 542–556. doi: 10.1016/j.omtn.2020.09.019

Xu, P., Zhao, Y., Liu, M., Wang, Y., Wang, H., Li, Y. X., et al. (2014). Variations of microRNAs in human placentas and plasma from preeclamptic pregnancy. *Hypertension* 63, 1276–1284. doi: 10.1161/HYPERTENSIONAHA.113.02647

Xueya, Z., Yamei, L., Sha, C., Dan, C., Hong, S., Xingyu, Y., et al. (2020). Exosomal encapsulation of miR-125a-5p inhibited trophoblast cell migration and proliferation by regulating the expression of VEGFA in preeclampsia. *Biochem. Biophys. Res. Commun.* 525, 646–653. doi: 10.1016/j.bbrc.2020.02.137

Yadava, S. M., Feng, A., Parobchak, N., Wang, B., and Rosen, T. (2020). miR-15b-5p promotes expression of proinflammatory cytokines in human placenta by inhibiting Apelin signaling pathway. *Placenta* 104, 8–15. doi: 10.1016/j.placenta.2020.11.002

Yamayoshi, A. (2020). [Development of novel drug delivery system targeting exosomal microRNA]. *Yakugaku Zasshi* 140, 625–631. doi: 10.1248/yakushi.19-00218-3

Yang, C., Lim, W., Park, J., Park, S., You, S., and Song, G. (2019). Anti-inflammatory effects of mesenchymal stem cell-derived exosomal microRNA-146a-5p and microRNA-548e-5p on human trophoblast cells. *Mol. Hum. Reprod.* 25, 755–771. doi: 10.1093/molehr/gaz054

Yang, H., Ma, Q., Wang, Y., and Tang, Z. (2020). Clinical application of exosomes and circulating microRNAs in the diagnosis of pregnancy complications and foetal abnormalities. *J. Transl. Med.* 18:32. doi: 10.1186/s12967-020-02227-w

Zhang, R., Wang, Y. Q., and Su, B. (2008). Molecular evolution of a primate-specific microRNA family. *Mol. Biol. Evol.* 25, 1493–1502. doi: 10.1093/molbev/msn094

Zhao, G., Yang, C., Yang, J., Liu, P., Jiang, K., Shaukat, A., et al. (2018). Placental exosome-mediated Bta-miR-499-Lin28B/let-7 axis regulates inflammatory bias during early pregnancy. *Cell Death Dis.* 9:704. doi: 10.1038/s41419-018-0713-8

Conflict of Interest: The authors declare that the research was conducted in the absence of any commercial or financial relationships that could be construed as a potential conflict of interest.

frontiers in Cell and Developmental Biology

ORIGINAL RESEARCH
published: 12 April 2021
doi: 10.3389/fcell.2021.640402

Novel circGFRα1 Promotes Self-Renewal of Female Germline Stem Cells Mediated by m^{6}A Writer METTL14

Xiaoyong Li[1], *Geng Tian*[1] *and Ji Wu*[1,2]*

[1] *Key Laboratory for the Genetics of Developmental and Neuropsychiatric Disorders (Ministry of Education), Renji Hospital, School of Medicine, Bio-X Institutes, Shanghai Jiao Tong University, Shanghai, China,* [2] *Key Laboratory of Fertility Preservation and Maintenance of Ministry of Education, Ningxia Medical University, Yinchuan, China*

Circular RNAs (circRNAs) play important roles in the self-renewal of stem cells. However, their significance and regulatory mechanisms in female germline stem cells (FGSCs) are largely unknown. Here, we identified an *N*^{6}-methyladenosine (m^{6}A)-modified circRNA, circGFRα1, which is highly abundant in mouse ovary and stage-specifically expressed in mouse FGSC development. Knockdown of circGFRα1 in FGSCs significantly reduced their self-renewal. In contrast, overexpression of circGFRα1 enhanced FGSC self-renewal. Mechanistically, circGFRα1 promotes FGSC self-renewal by acting as a competing endogenous RNA (ceRNA) that sponges miR-449, leading to enhanced GFRα1 expression and activation of the glial cell derived neurotrophic factor (GDNF) signaling pathway. Furthermore, circGFRα1 acts as a ceRNA based on METTL14-mediated cytoplasmic export through the GGACU motif. Our study should help to understand the mechanisms regulating germ cell development, add new evidence on the mechanism of action of circRNA, and deepen our understanding of the development of FGSCs.

Keywords: circGFRα1, METTL14, ceRNA, female germline stem cells, self-renewal

OPEN ACCESS

Edited by:
Li Meng,
The Chinese University of Hong Kong, China

Reviewed by:
Hao Chen,
School of Medicine, Nantong University, China
Rongjia Zhou,
Wuhan University, China

***Correspondence:**
Ji Wu
jiwu@sjtu.edu.cn

Specialty section:
This article was submitted to Cell Growth and Division, a section of the journal Frontiers in Cell and Developmental Biology

Received: *11 December 2020*
Accepted: *22 March 2021*
Published: *12 April 2021*

Citation:
Li X, Tian G and Wu J (2021) Novel circGFRα1 Promotes Self-Renewal of Female Germline Stem Cells Mediated by m^{6}A Writer METTL14. Front. Cell Dev. Biol. 9:640402. doi: 10.3389/fcell.2021.640402

INTRODUCTION

The infertility rate globally has increased year by year, with an average incidence of 12.5%. Infertility has become the third most common disease threatening human health, after cardiovascular disease and cancer. A shortage and poor quality of oocytes are key factors leading to female infertility. There is thus an urgent need to understand the mechanisms of female reproduction in order to improve the quantity and quality of oocytes. As germline stem cells, female germline stem cells (FGSCs) can increase oocyte number and improve ovarian function, which is of great significance in mammals to improve the quality of oocytes and the pregnancy rate (Zou et al., 2009). These cells are thus becoming a focus of medical care.

With the deepening of the research, great progress has been made in the self-renewal of FGSCs. For example, a series of genes and signal pathways affecting FGSC self-renewal have been identified, such as STPBC, AKT1, AKT3, glial cell derived neurotrophic factor (GDNF) signaling pathway, phosphoinositide-3 kinase–AKT (PI3K–Akt) signaling pathway,

Hippo signaling pathway, and Notch signaling pathway (Xie et al., 2014; Li et al., 2015, 2017a, 2019; Pan et al., 2015; Zhang et al., 2016, 2018; Liu et al., 2017; Ma et al., 2018; Zhu et al., 2018; Wu et al., 2019). GDNF signaling acts by modifying the activity of PI3K–AKT mitogen-activated protein kinase/ERK kinase, and the Src family of downstream substrates, ultimately affecting the expression of genes such as Bcl6b, Lhx1, Etv5, and Egr3.

The main characteristics of circular RNAs (circRNAs) are as follows. Most of circRNAs exist in the cytoplasm, but a small part of circRNAs formed by intron cyclization exist in the nucleus; circRNAs widely exist in human cells, sometimes more common than linear RNA; circRNAs are closed loop structure, not easy to be degraded by RNaseR; circRNAs are highly conservative; most of circRNAs are formed by exon cyclization, and a small part are formed by intron cyclization; Some of circRNAs play the role of miRNA sponge in cells, and a few of them can be translated into proteins (Burd et al., 2010; Memczak et al., 2013; Sun et al., 2013; Zhang et al., 2013). Compared with the miRNA regulatory network, the competing endogenous RNAs (ceRNAs) regulatory network is more sophisticated and complex, involving more RNA molecules, including mRNA, pseudogenes encoding genes, circRNA, lncRNA, and microRNA (Hansen et al., 2013; Zhang et al., 2013; Guo et al., 2014; Ahmed et al., 2016). However, to date, no circRNAs critical in the development of FGSCs, or their functions and/or underlying mechanisms, have been discovered.

N^6-methyladenosine (m^6A) is the most important modification in mRNA epigenetics. Similarly, in the circRNA epigenetic transcriptome, m^6A is also a highly abundant, widely distributed, and functionally important post-transcriptional modification (Shafik et al., 2016; Jacob et al., 2017). Yang et al. (2017) showed that some circRNAs could also recruit translation initiation complexes to start translating proteins by binding with the YTHDF3 recognition protein. In addition, Wu et al. (2019) found that circ_KIAA1429 accelerates the progression of hepatocellular carcinoma through m6A-YTHDF3-Zeb1.

In this study, on the basis of genome-wide circRNA analysis (Li et al., 2019), we identified a novel circRNA, circGFRα1, the biological function in FGSC development of which has not yet been clarified. We found that circGFRα1 was highly abundant in mouse ovary and stage-specifically expressed in mouse FGSC development. Importantly, circGFRα1 promoted the self-renewal of FGSCs. Mechanistically, we found that METTL14-mediated m^6A modification altered circGFRα1 export to the cytoplasm, while circGFRα1 acted as a ceRNA to regulate GFRα1 expression by sponging miR-449 to play regulatory roles in FGSC development. Our findings reveal a novel mechanism regulating FGSC self-renewal and provide a theoretical basis for the study of germ cell development and human reproduction.

MATERIALS AND METHODS

Culture of Female Germline Stem Cells

FGSCs were cultured according to the previously method (Zou et al., 2009; Zhang et al., 2016; Li et al., 2017b). FGSCs passages were performed at a ratio of 1:4 and intervals of 4–7 days.

Plasmid DNA

We used pLCDH-ciR to construct the circGFRα1 overexpression vector to perform transcript circularization. An *Eco*RI restriction enzyme site was discovered within an endogenous flanking sequence located in the front circular frame. On the other hand, a *Bam*HI site was detected within a partially inverted upstream sequence located in the back circular frame. We cloned the fragment amplified into the vector between the front and the back circular frames. We also constructed a control vector that contained only a non-sense insert between the front and back circular frames in the absence of circGFRα1-encoding cDNA. Lentiviral vectors (pGMLV-SC5) loaded with anti-circGFRα1 shRNA and the negative control shRNA (nc-shRNA) with EGFP were provided by Shanghai Genomeditech Company Ltd. In the meantime, we used an irrelevant, scrambled shRNA that was not matched with the mouse genome sequence as the control.

For constructing the METTL14-knockdown lentiviral vectors, we applied molecular biological approaches to insert an interfering fragment in the U6 promoter downstream into the lentiviral vector (pLKD-CMV-G and PR-U6-shRNA). We selected four or more independent siRNAs to examine the target knockdown efficiency. Finally, we selected the optimal siRNA target (targetSeq: GCTAAAGGATGAGTTAAT). To construct METTL14 overexpression vectors, we inserted the candidate gene cDNAs into the *Bam*HI and *Eco*RI restriction sites in an overexpression plasmid (pHBLV-CMVIE-ZsGreen-T2A-puro).

Viral Preparation and Transduction

We used 293T cells to prepare lentiviruses according to a method described previously (Shi et al., 2004). For lentivirus infection, the FGSCs were incubated with 1:1 mixture of culture medium and lentivirus (titer: 2.5×10^8). After 12–16 h of infection, the culture medium containing lentivirus particles was sucked out, and the culture medium was added to the culture plate for further culture. Subsequently, the FGSCs were screened by 100 ng/ml puromycin.

RNA Fluorescence *in situ* Hybridization Assay

The RNA-FISH procedure for circGFRα1 was performed with the RNA-FISH kit of GenePharma Inc. (Shanghai, China), according to the manufacturer's instructions. Briefly, FGSCs were cultured in 48-wells overnight at 37°C and 5% CO2. Next day, cells were rinsed in chilled phosphate-buffered saline (PBS) two times. Cells were fixed with 4% paraformaldehyde in the room temperature for 30 min. Then 0.1% buffer A was added and incubated in the room temperature for 30 min. After that, the cells were washed twice with PBS for 5 min. The RNA-FISH probes targeting circGFRα1 were synthesized by GenePharma Inc. (Shanghai, China). Those probes were mixed well with buffer E to a final concentration 2 μM, then to hybridize with cell's genes and incubate overnight at 37°C. The cells were washed twice with buffer C for 5 min. This was followed by rinsing and staining with DAPI (1:1,000 dilution; Sigma)-containing PBS at room temperature for 5 min. The images were acquired with a fluorescence microscope (Leica, United States).

CCK8 Assay

We cultured FGSCs in each well (containing 200 μL culture medium) of 96-well plates at a density of 5,000 cells/well. At a confluence of 70%–80%, we added 20 μL of the CCK8 reagent into each well of the plate and incubated it for another 2 h at 37°C and 5% CO_2. Then, we used a microplate reader to measure the absorbance (OD) value at 450 nm.

EdU Assay

We cultured FGSCs to 80% confluence and added 50 μM of the EdU reagent into each well, after which the plate was incubated for another 2 h. Thereafter, cells were fixed with 4% PFA for 30 min under ambient temperature and neutralized for 5 min by using 2 mg/mL glycine. Then, the cells were punched with 0.5% Triton X-100, stained with the 1 × Apollo staining solution, incubated for 30 min, and finally washed thrice by using PBS supplemented with 0.5% Triton X-100. Finally, cell nuclei were dyed using 1 × Hoechst 33342. A Leica fluorescence microscope was used to capture images.

m^{6}A Dot Blot

Trizol reagent was used to extract total RNA from FGSCs. After denaturing at 95°C, the RNAs were immediately chilled on ice. Then, they were dropped onto a Hybond-N + membrane. The membrane was cross-linked with a UV cross-linker, followed blocking with 5% skim milk, and overnight incubation with the m6A-specific antibody (1: 1,000) at 4°C. Thereafter, the membrane was rinsed by TBST for 10 min, followed by another 1 h of incubation with a secondary antibody at an ambient temperature. Finally, Tanon 4600SF was used to scan the dots.

qRT-PCR

Trizol reagent was used to extract total cellular RNA from FGSCs that was quantified using Nanodrop Lite. cDNA was prepared by reverse transcribing the RNA (1,000 ng) by using a reverse transcription kit in the 20-μL system. In this qRT-PCR assay, Taq DNA polymerase was used with SYBR Premix Ex Taq in the Applied Biosystems® 7500 Real-Time PCR system. The $2^{-\Delta\Delta Ct}$ approach was used for data analysis.

MeRIP-qPCR

Total RNA was extracted from FGSCs by using the Trizol reagent and quantified using Nanodrop Lite. We bound 1.25 μg of the anti-m6A antibody onto protein A/G magnetic beads dissolved in the IP buffer (consisting of 140 mM NaCl, 20 mM Tris pH 7.5, 2 mM EDTA, and 1% NP-40) 1 h in advance. Thereafter, we incubated the resultant antibody-bound protein A/G beads with the RNA sample at 4°C for 2 h. Then, the obtained samples were rinsed twice by using low-salt wash buffer (composed of 5 mM EDTA and 10 mM Tris; pH 7.5), followed by washing with a high-salt wash buffer (composed of 1 M NaCl, 20 mM Tris pH 7.5, 0.5% sodium deoxycholate, 1% NP-40, 1 mM EDTA and 0.1% SDS) twice and then with the RIPA buffer (150 mM NaCl, 20 mM Tris pH 7.5, 0.5% sodium deoxycholate, 1% NP-40, 1 mM EDTA, and 0.1% SDS) twice. For all the samples, their wash solutions were harvested and considered the EDTA, an fraction. In addition, the beads were incubated with 50 μL N^6-methyladenosine 5-monophosphate sodium salt (20 mM) at 4°C for 1 h to elute the RNA. After precipitation with ethanol, cDNA was prepared by reverse transcribing the RNA in the input, unbound and m6A-bound fractions by using Superscript III random hexamers. Subsequently, qRT-PCR was performed to determine the m6A-containing transcript levels compared with the Rplp0 level. For Rplp0, the primer sequences were GATGGGCAACTGTACCTGACTG and CTGGGCTCCTCTTGGAATG.

Dual-Luciferase Reporter Assay

We inserted the mutant (circGFRα1-MUT) and wild-type (circGFRα1-WT) circGFRα1 miRNA-binding site sequences into *Sac*I and *Kpn*I sites in the pGL3 promoter vector. Thereafter, we cultured the cells in 24-well plates and used Lipofectamine 3000 to transfect 5 ng of the pRL-SV40 *Renilla* luciferase vector and 80 ng plasmid, together with 50 nM of the negative control or miR-449 mimics into the cells. After 48 h, we harvested and examined the cells by performing the dual-luciferase assay according to specific protocols. Each independent experiment was performed thrice.

Statistical Analysis

The significance of difference in graphs was assessed using Student's *t*-test unless specified otherwise. The normally distributed two-sample equal variance was used in this study. Our researchers were aware of sample grouping in each experiment. *P* value of <0.05 indicated statistical significance. Graphs as well as error bars are represented as means ± SEM unless specified otherwise. The R statistical environment and GraphPad Prism 4.0 were used for performing statistical analysis.

RESULTS

Identification and Characterization of circGFRα1

To identify circRNAs involved in FGSC formation, we reanalyzed our previous circRNA expression data (Li et al., 2019) and found that circRNA_12447 (chr19: 58263912–58270163) is upregulated in FGSCs that possibly leads to FGSC differentiation and self-renewal. As discovered using the mouse reference genome (mm10), circRNA_12447 originated from exons 6–8 at the locus of GDNF family receptor alpha 1 (GFRα1) (**Figure 1A**) and was thus referred to as circGFRα1. For investigating the expression profile of circGFRα1 and verifying its circular shape, RT-PCR was performed using divergent primers, through which the expression of circGFRα1 in FGSCs was detected (**Figure 1B**). To confirm the circular shape of circGFRα1, RNase R, a 3′–5′ exoribonuclease with high process ability and no effect on circRNAs, was used. circGFRα1 developed resistance to RNase R exposure compared with the control linear gene GFRα1 (**Figure 1C**). In addition, RT-PCR products obtained after amplification with divergent primers were subjected to Sanger sequencing, which confirmed that circGFRα1 contains

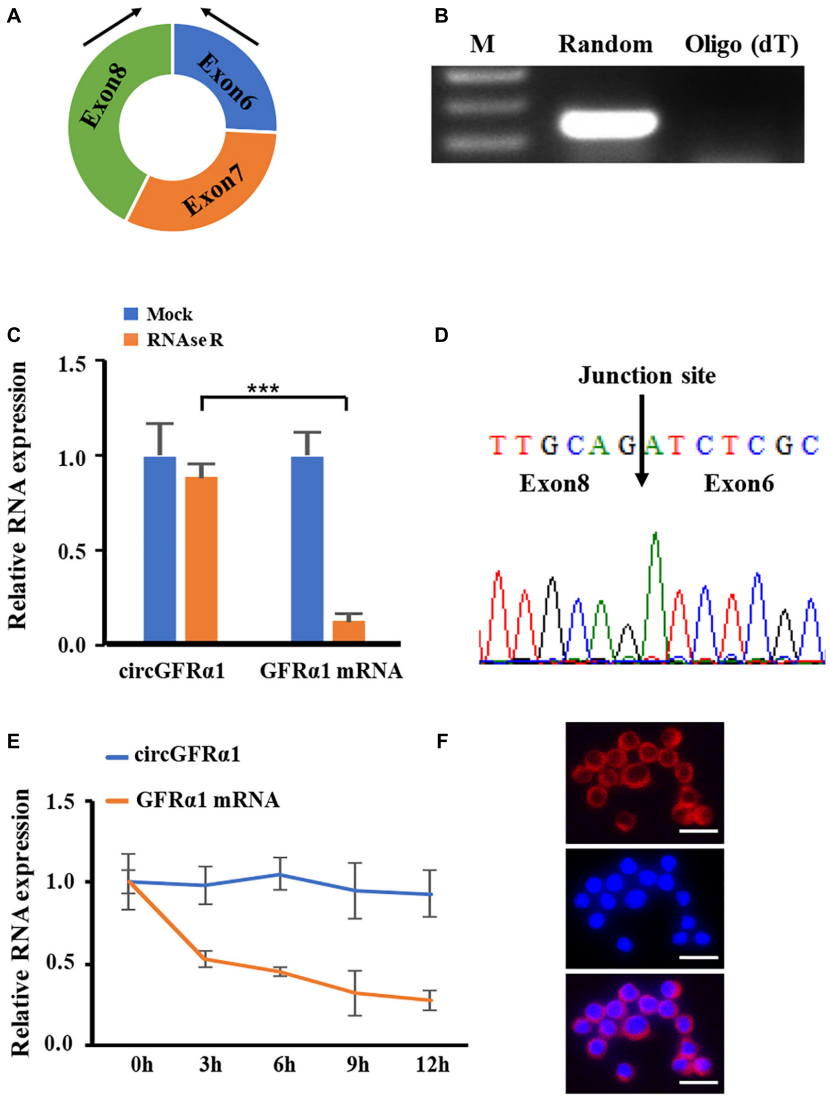

FIGURE 1 | Characterization of circGFRα1 in FGSCs. **(A)** The genomic locus of circGFRα1. **(B)** RT-PCR products showing circularization of circGFRα1 with divergent primers. **(C)** After RNase R treatment in FGSCs, qRT–PCR showing the expression of circGFRα1 and GFRα1 mRNA. **(D)** Sanger sequencing of circGFRα1 demonstrating the head-to-tail splicing. **(E)** After Actinomycin D treatment, qRT–PCR showing the expression of circGFRα1 and GFRα1 mRNAs at the indicated time points. **(F)** RNA FISH for circGFRα1. Scale bars, 20 μm. ***$P < 0.001$.

the back-spliced junction (**Figure 1D**). After exposure of circGFRα1 and the control linear gene to actinomycin D, a transcription inhibitor, our qRT-PCR results revealed that half-life of circGFRα1 is over 12 h, whereas that of the related linear transcript was only 3 h (**Figure 1E**), indicating higher stability of circGFRα1 in FGSCs. Furthermore, we performed fluorescence *in situ* hybridization assays that revealed that circGFRα1 is mostly located in the cytoplasm (**Figure 1F**). Taken together, the findings indicate the stable and rich expression of circGFRα1 in FGSCs.

CircGFRα1 Affects Self-Renewal and Survival of Female Germline Stem Cells

Tissue-specific expression results revealed that circGFRα1 is highly expressed in the mouse ovary (**Supplementary Figure 1A**). Moreover, the circGFRα1 level was found to be stage-specific during the development of mouse FGSCs; a high level of transcript was present in FGSCs, whereas significantly lower levels were detected in germinal vesicle (GV)-stage oocytes ($P < 0.05$) and metaphase II (MII)-stage oocytes (**Supplementary Figure 1B**, $P < 0.001$). To examine the effect of circGFRα1 on FGSC development, we regulated its expression through RNA interference or overexpression by inducing lentivirus infection (**Figure 2A**). As expected, circGFRα1 overexpression was found to significantly upregulate its level (**Figure 2B**, $P < 0.001$). However, relative to negative controls, its expression level was significantly decreased in shRNA-loaded lentivirus-infected FGSCs, which specifically bind to the circGFRα1 junction site (**Figure 2C**, $P < 0.001$).

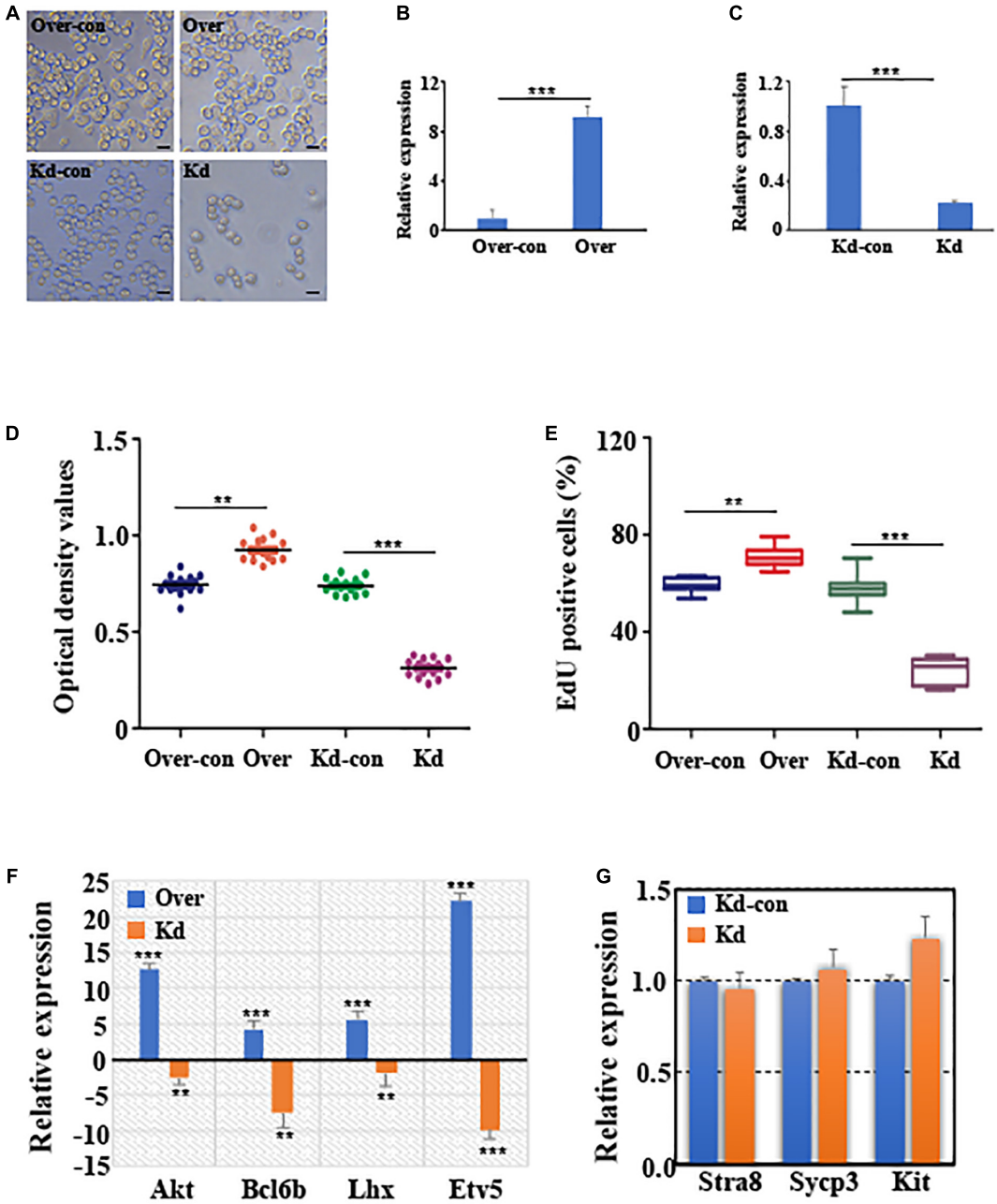

FIGURE 2 | CircGFRα1 affects self-renewal and survival of FGSCs. **(A)** Selected images for FGSCs infected with lentivirus. **(B)** qRT-PCR analyses detected the RNA level of circGFRα1 in cells infected with the circGFRα1 overexpression lentivirus control (over-con), circGFRα1 overexpression lentivirus (over). **(C)** qRT-PCR analyses detected the RNA level of circGFRα1 in cells infected with the circGFRα1 knockdown lentivirus control (kd-con), circGFRα1 knockdown lentivirus (kd). **(D)** CCK-8 assays were conducted using FGSCs infected with the circGFRα1 overexpression lentivirus control (over-con), circGFRα1 overexpression lentivirus (over), circGFRα1 knockdown lentivirus control (kd-con), circGFRα1 knockdown lentivirus (kd). **(E)** EDU assays were conducted using FGSCs infected with the circGFRα1 overexpression lentivirus control (over-con), circGFRα1 overexpression lentivirus (over), circGFRα1 knockdown lentivirus control (kd-con), circGFRα1 knockdown lentivirus (kd). **(F)** Relative expression of Akt, Bcl6b, Lhx, and Etv5 in FGSCs after circGFRα1 overexpression (over) and knockdown (kd). Overexpression control and knockdown control as blank control groups respectively. When calculating the relative expression, the expression of control group was set as 1. A positive value indicates up regulation, and a negative value indicates down regulation. **(G)** Relative expression of Stra8, Sycp3, and Kit, FGSCs infected with the circGFRα1 knockdown lentivirus control (kd-con), circGFRα1 knockdown lentivirus (kd). $^{**}P < 0.01$ and $^{***}P < 0.001$.

Then, we examined the effects of circGFRα1 overexpression and knockdown on FGSC proliferation through CCK-8 and EdU incorporation assays, respectively. According to CCK8 assay results, the OD values of FGSCs with circGFRα1 overexpression markedly increased relative to controls, whereas those of circGFRα1-knockdown FGSCs evidently decreased compared

with those of controls (**Figure 2D**, $P < 0.001$). Moreover, the EdU assay results indicated that EdU-positive FGSCs with circGFRα1 overexpression that were transfected with lentivirus were markedly more in number than controls (**Figure 2E**, $P < 0.001$). However, transfection with circGFRα1-knockdown lentivirus markedly decreased the number of EdU-positive FGSCs compared with that of controls (**Figure 2E**, $P < 0.001$). Thus, we found that genes, including Akt, Bcl6b, Lhx, and Etv5, associated with self-renewal with the highest responsiveness to GDNF signaling within FGSCs are significantly upregulated (**Figure 2F**). Meanwhile, we found that the expression levels of genes associated with FGSC self-renewal were significantly downregulated (**Figure 2F**), whereas the expression levels of genes associated with differentiation, such as Stra8, Sypc3, and Kit, were extremely low and not affected by circGFRα1 knockdown (**Figure 2G**, $P > 0.05$). In summary, these findings suggest that the overexpression of circGFRα1 promoted the self-renewal and maintenance of FGSCs, while its knockdown impaired these characteristics.

CircGFRα1 Serves as a Sponge for miR-449

To explore the potential of circGFRA1 as a miRNA sponge, we performed the RNA hybrid analysis[1]. From our results, we predicted that certain miRNA-binding sites are present in circGFRα1. Of the estimated miRNAs, miR-449, which was also predicted to target the GFRα1 gene based on TargetScan and miRanda, was identified. **Figure 3A** shows the miR-449 seed region nucleotides (denoted in red). Later, CCK-8 and EdU assays were performed for examining the biological effects of miR-449 on FGSCs. We found that FGSCs transfected with miR-449 inhibitors have enhanced proliferation capacity, whereas those transfected with miR-449 mimics have markedly reduced proliferation capacity (**Figures 3B,C**). These findings indicate the role of miR-449 in the regulation of FGSC proliferation.

To verify whether the circGFRα1 transcript interacts with miR-449, the luciferase reported gene assay was performed using the circGFRα1-fused reporter gene (pGL3-circ GFRα1). In addition, a construct containing a non-specific circGFRα1 sequence (pGL3-circEGFR-MUT) and a wild-type construct (pGL3-circGFRα1-WT) were developed (**Figure 3D**). Then, miR-449 mimic and pGL3-circGFRα1-WT were co-transfected into the cells, which markedly reduced the luciferase activity in these cells compared with that in cells co-transfected with control miRNA and pGL3-circGFRα1-WT or co-transfected with mimic and pGL3-circGFRα1-MUT (**Figure 3E**). These findings indicated that miR-449 directly binds to circGFRα1 and adversely targets the latter. Furthermore, to verify whether circGFRα1 directly binds to miR-449, RIP assays were performed using control IgG or anti-AGO2 antibodies. The qRT-PCR assay was used to analyze miR-449 and circGFRα1. We found that anti-AGO2 antibodies markedly downregulate miR-449 and circGFRα1 compared with control IgG (**Figure 3F**), which suggests that miR-449 directly binds to circGFRα1 in the presence of AGO2.

[1]https://bibiserv.cebitec.uni-bielefeld.de/rnahybrid/

CircGFRα1 Acts as a Decoy of miR-449 to Upregulate Their Common Target, GFRα1

To explore the potential of circGFRα1 as a ceRNA for sequestering miR-449 and upregulating GFRα1 expression and activation of the GDNF signaling pathway. We firstly showed that the circGFRα1 expression is comparable to the GDNF signal after removal and replenishment of GDNF; its expression decreased 18 h after GDNF removal but increased after GDNF replenishment (**Figure 4A**). Moreover, TargetScan was used to identify the miR-449 putative target genes, which predicted GFRα1 (**Figure 4B**). To confirm this prediction, luciferase assays were performed using a GFRα1-fused reporter gene. Co-transfection of miR-449 mimic with the GFRα1 UTR significantly reduced the luciferase activity compared with that in control miRNA co-transfected with the GFRα1 UTR or in mimic co-transfected with the GFRα1 UTR (**Figure 4C**). These findings revealed that miR-449 directly binds to the GFRα1 UTR and adversely targets the latter. To verify whether the GFRα1 UTR directly binds to miR-449, RIP assays were performed using control IgG and anti-AGO2 antibodies; miR-449 and the GFRα1 UTR were analyzed through qRT-PCR. We found that anti-AGO2 antibodies markedly downregulate the expression of miR-449 and the GFRα1 UTR compared with control IgG (**Figure 4D**), indicating that the GFRα1 UTR directly binds to circGFRα1 depending on the presence of AGO2. To examine whether circGFRα1 regulates the GFRα1 level by interacting with miR-449, we detected GFRα1 expression in circGFRα1-deleted or circGFRα1-overexpressed FGSCs. As shown in **Figures 4E,F**, circGFRα1 overexpression increased the GFRα1 mRNA and protein expression, whereas circGFRα1 silencing reduced the GFRα1 mRNA and protein expression. Furthermore, the miR-449 inhibitor was co-transfected with si-circGFRα1 in FGSCs, which reversed the repression (**Figure 4G**). Taken together, the findings support the assumption that circGFRα1 modulates the GFRα1 level by directly interacting with miR-449.

METTL14 Promotes Cytoplasmic Export of m^{6}A-Modified circGFRα1 Through the GGACU Motif

As circGFRα1 functioned as a ceRNA, it might be exported to the cytoplasm in an m^{6}A-dependent manner. To study whether m^{6}A modification occurs in circGFRα1, we first predicted the m^{6}A sites using an online bioinformatic tool, m6Avar[2], and found three RRACU m^{6}A sequence motifs located in circGFRα1. Next, we performed methylated RNA immunoprecipitation (Me-RIP)–qPCR assays and found that the m^{6}A level of circGFRα1 in FGSCs was very high (**Figure 5A**). We then performed shRNA-mediated silencing of METTL14, a core component of the m^{6}A methylase complex, and found that downregulation of METTL14 resulted in decreases in the m^{6}A levels of both total RNA and circGFRα1 (**Figures 5B,C**). The results of METTL14 knockdown were confirmed by western blotting (**Supplementary Figure 2A**). We then investigated whether m^{6}A modification

[2]http://m6avar.renlab.org/

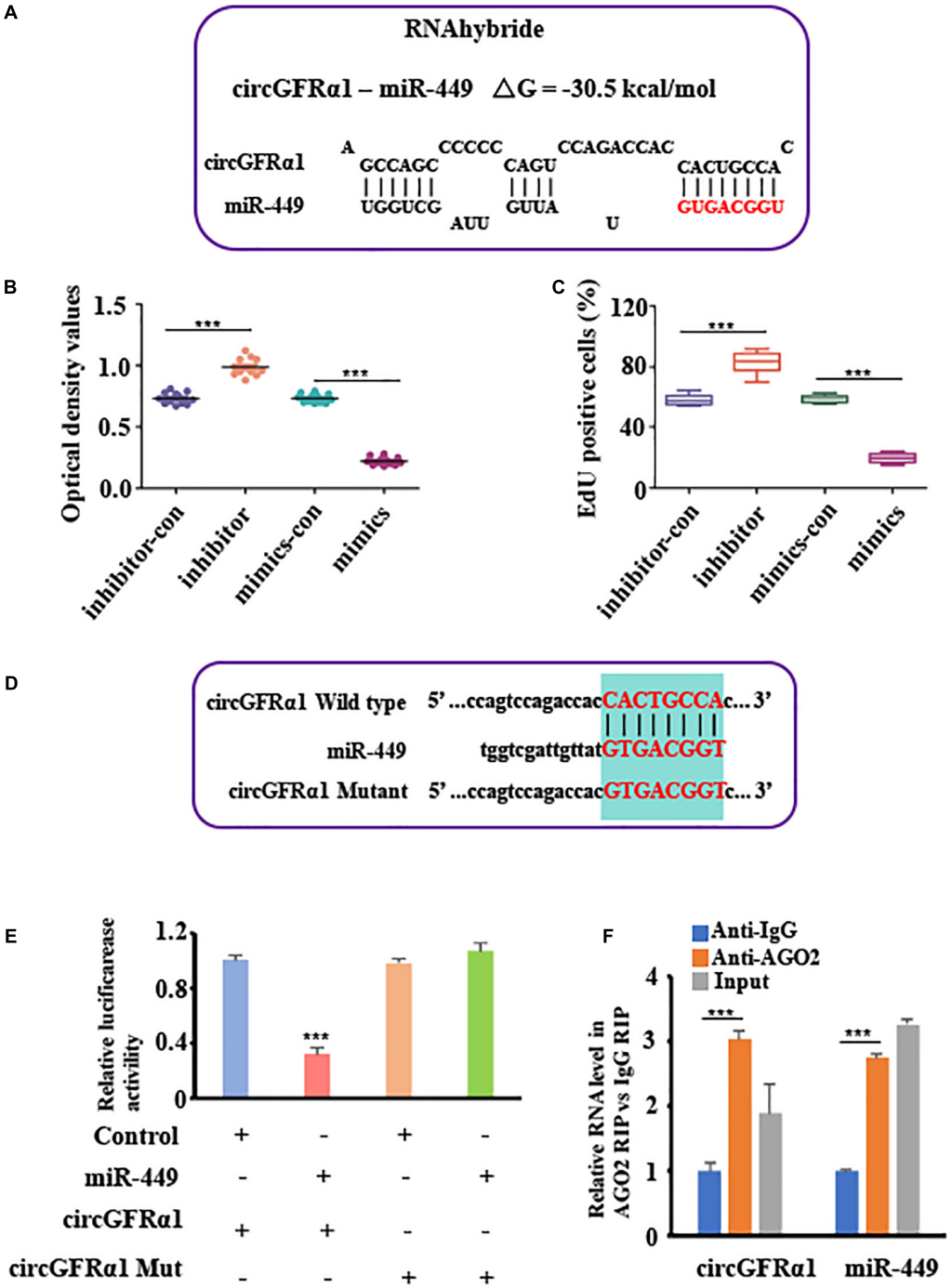

FIGURE 3 | CircGFRα1 serves as a sponge for miR-449. **(A)** RNA hybrid analyses showed putative miR-449 binding sites in CircGFRα1. **(B)** CCK-8 assays were conducted using FGSCs infected with the miR-449 mimics control (mimics-con), miR-449 mimics (over), miR-449 inhibitor control (inhibitor-con), and miR-449 inhibitor (inhibitor). **(C)** EdU assays were conducted using FGSCs infected with the miR-449 mimics control (mimics-con), miR-449 mimics (over), miR-449 inhibitor control (inhibitor-con), and miR-449 inhibitor (inhibitor). **(D)** Target region of the CircGFRα1 for miR-449 and the mutant type of circGFRα1. **(E)** Effects of miR-449 on the activity of firefly luciferase reporters containing either circGFRα1 or mutant type circGFRα1 were assessed by luciferase reporter gene assays. **(F)** RIP assays were performed to detect miR-449 and circGFRα1. ***$P < 0.001$.

could affect the RNA metabolism of circGFRα1. Knockdown of METTL14 did not lead to a change in the expression of circGFRα1 (**Supplementary Figure 2B**).

In addition, we performed FISH and cytoplasmic and nuclear mRNA fractionation experiments, and found that silencing of METTL14 significantly increased the nuclear circGFRα1 content

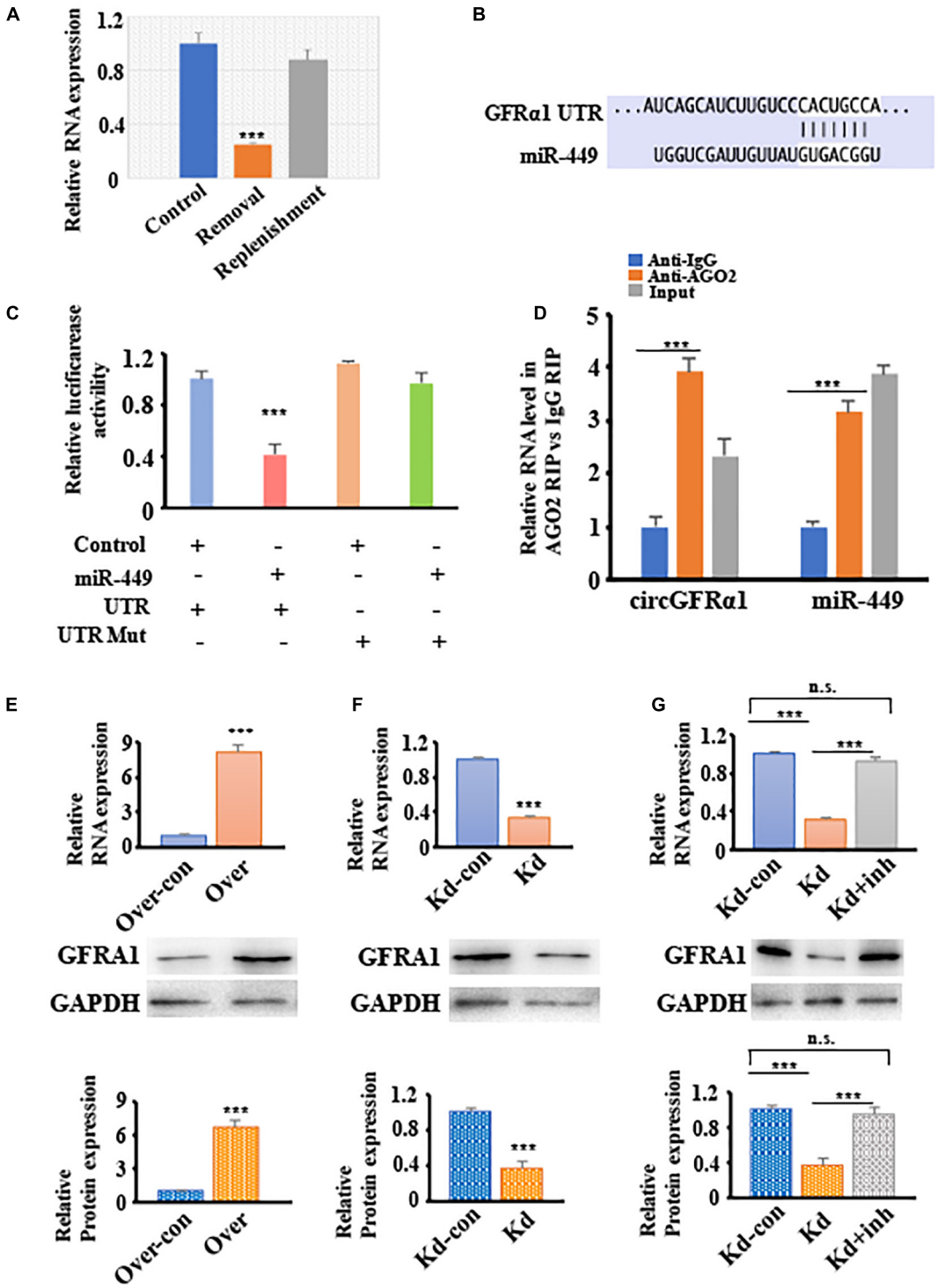

FIGURE 4 | CircGFRα1 functions as a ceRNA to sequester miR-449 and upregulate the expression of GFRα1. **(A)** qRT–PCR analysis for the expression of circGFRα1 after GDNF removal and replenishment. **(B)** Target region of the 3′-UTR GFRα1 for miR-449. **(C)** Effects of miR-449 on the activity of firefly luciferase reporters containing either 3′-UTR GFRα1 or mutant type 3′-UTR GFRα1 were assessed by luciferase reporter gene assays. **(D)** RIP assays were performed to detect miR-449 and 3′-UTR GFRα1. **(E)** qRT–PCR and western blotting analysis for the expression of GFRα1 in FGSCs infected with the circGFRα1 overexpression lentivirus control (over-con), circGFRα1 overexpression lentivirus (over). **(F)** qRT–PCR and western blotting analysis for the expression of GFRα1 in FGSCs infected with the circGFRα1 knockdown lentivirus control (kd-con), circGFRα1 knockdown lentivirus (kd). **(G)** qRT–PCR and western blotting analysis for the expression of GFRα1 in FGSCs infected with the circGFRα1 knockdown lentivirus control (kd-con), circGFRα1 knockdown lentivirus (kd), and co-transfected miR-449 inhibitor and circGFRα1 knockdown lentivirus (kd + inhibitor). ***$P < 0.001$. n.s., no significant.

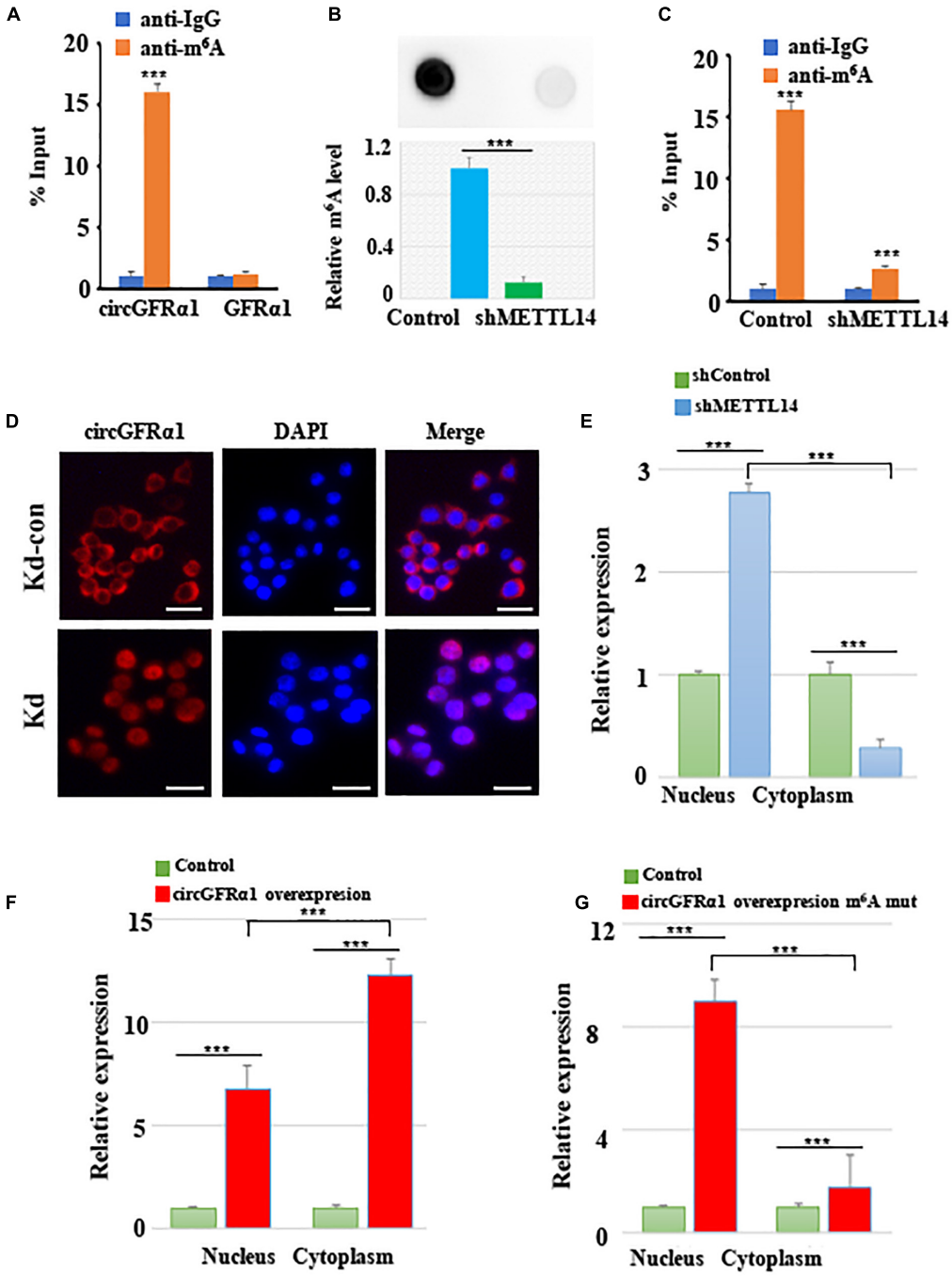

FIGURE 5 | METTL14 promotes cytoplasmic export of m^{6}A methylated circGFRα1. **(A)** MeRIP assay showing that m^{6}A was highly enriched in circGFRα1 **(B)** Relative m^{6}A level of FGSCs after METTL14 knockdown (kd). **(C)** MeRIP assay showing that down- regulation of METTL14 resulted in the decreased m^{6}A level of circGFRα1. **(D)** RNA-FISH showing that the increased nuclear staining of circGFRα1 caused by METTL14 knockdown. **(E)** Cytoplasmic and Nuclear RNA Fractionation assay showing that knockdown of METTL14 increased the nuclear circGFRα1 content. **(F,G)** Cytoplasmic and Nuclear RNA Fractionation assay showing that the nuclear and cytoplasmic circGFRα1 contents were both increased, and mainly in nuclear fraction when mutated the GGACU m^{6}A motif in circGFRα1 overexpressing construct. Scale bars, 20 μm. ***$P < 0.001$.

(**Figures 5D,E**, $p < 0.001$). We also found that, when circGFRα1 was overexpressed, both nuclear and cytoplasmic circGFRα1 levels were increased, particularly in the cytoplasmic fraction (**Figure 5F**, $p < 0.001$). By browsing the junction sequence in circGFRα1, we identified that the GGACU motif was a putative m^{6}A motif. Once we mutated the GGACU m^{6}A motif in a circGFRα1-overexpressing construct, although both nuclear and cytoplasmic circGFRα1 levels were increased, the main

increase occurred in the nuclear fraction (**Figure 5G**, $p < 0.001$). These findings indicated that m^{6}A modification of circGFRα1 facilitated circGFRα1 export from the nucleus to the cytoplasm in an m^{6}A-dependent manner and that m^{6}A modification of circGFRα1 are important for FGSC development.

DISCUSSION

On the basis of the above findings, we propose a model (**Figure 6**) in which METTL14 alters the m^{6}A modification of circGFRα1 and increases its export to the cytoplasm, while circGFRα1 promotes FGSC self-renewal by acting as a ceRNA that sponges miR-449, leading to enhanced GFRα1 expression and activation of the GDNF signaling pathway, finally affecting the development of FGSCs.

Recently, the role of circRNAs has become evident in determining the fate of FGSCs (Li et al., 2017a, 2019). CircRNAs, a newly discovered class of non-coding RNAs, have a covalent bond that links the 3′- and 5′-ends produced through back-splicing (Memczak et al., 2013). The expression of circRNAs is tissue- and stage-specific, and a small portion of circRNAs is highly conserved among different species (Salzman et al., 2013). Functional research on circRNAs has been focused mostly on nuclear transcriptional regulators, miRNA sponges, and RNA-binding proteins (Hansen et al., 2013). In this study, we discovered that miR-449 binds to GFRα1 and circGFRα1, indicating that circGFRα1 possibly plays the role of an miR-449 sponge in regulating the GFRα1 level through the ceRNA mechanism. Therefore, we suggest that circGFRα1 plays the role of a ceRNA for GFRα1 in FGSCs and serves as a miR-449 sponge. First, our bioinformatics analysis results demonstrated the presence of miR-449-binding sites in the 3′-UTR of both circGFRA1 and GFRA1. Second, these results were further validated through luciferase reporter assays. Third, circGFRα1 deletion downregulated the GFRα1 level. Finally, the inhibition of miR-449 reversed the above expression trend.

Increasing evidence has shown that m^{6}A modification plays an important role in mammalian biology. For example, it is involved in upregulation of RNA stability (Wang et al., 2014), localization (Fustin et al., 2013), transport, cleavage (Molinie et al., 2016), and translation (Meyer et al., 2015) at the post-transcriptional level. Alarcon et al. (2015) found that Mettl3-dependent pri-miRNA methylation can promote DGCR recognition and processing, thus promoting microRNA maturation. In addition, HNRNPA2B1, an m^{6}A recognition protein, promotes the processing of pri-miRNA into pre-miRNA (Alarcon et al., 2015). Moreover, the modification of circRNA can promote its translation (Yang et al., 2017). Yang et al. (2018) found that m^{6}A-modified lincRNA 1,281 mediates the regulatory mechanism of ceRNA. Here, we found that m^{6}A is enriched on circGFRα1 in FGSCs. Modification of m^{6}A in circGFRα1 leads to the improvement of its RNA stability, which may partially account for the upregulation of circGFRα1 in FGSCs. In addition to m^{6}A modification, other mechanisms might also be involved in the elevation of circGFRα1, such as DNA methylation, histone modification, and miRNA dysregulation, which warrant further exploration.

GDNF signal regulates the protein phosphorylation of downstream substrates by affecting the activity of protein kinases (PI3K–Akt, mitogen/ERK kinase, and Src family kinases, etc.), ultimately affecting the level of protein expression, which is the most important mechanism regulating SSC self-renewal and differentiation (Brinster and Avarbock, 1994; Oatley et al., 2007; He et al., 2008). GFRα1 is the receptor of GDNF, and GDNF can

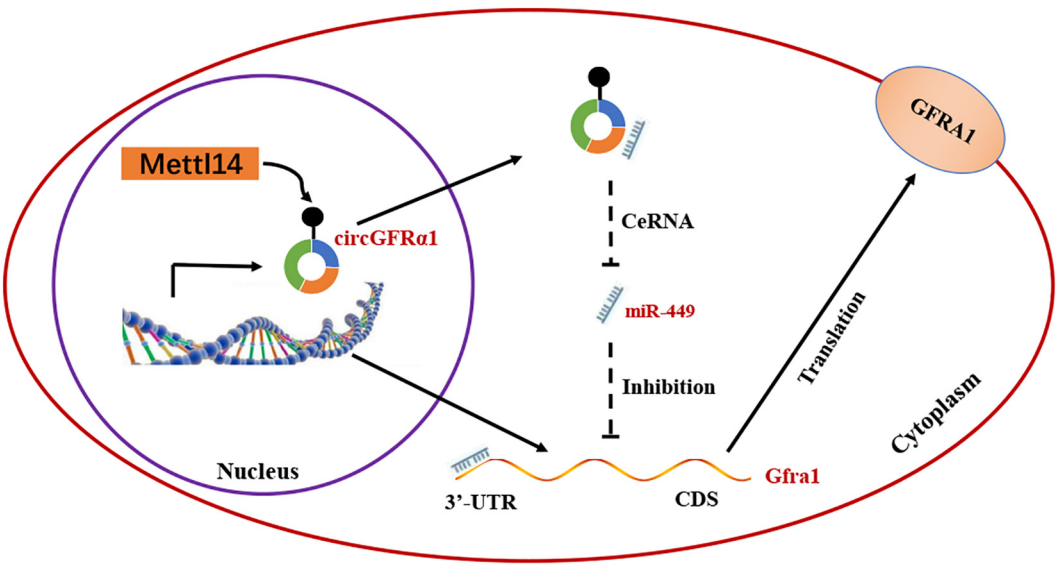

FIGURE 6 | Proposed model of novel circGFRα1 exports to the cytoplasm mediated by METTL14, and promotes self-renewal of FGSCs. METTL14 alters the m^{6}A modification of circGFRα1 and increases its export to the cytoplasm, while circGFRα1 promotes FGSC self-renewal by acting as a ceRNA that sponges miR-449, leading to enhanced GFRα1 expression and activation of the GDNF signaling pathway, and finally affecting self-renewal of FGSCs.

regulate the fate of stem cells only by binding with this receptor. Our previous study showed that GFRα1 was expressed on the surface of FGSCs, and that FGSCs had a mechanism of self-renewal involving GDNF similar to that of SSCs (Li et al., 2019). In this study, we found that circGFRα1 acts as a decoy of miR-449 to upregulate their common target, GFRα1.

Taking our findings together, we found that circGFRα1 promotes FGSC self-renewal by acting as a ceRNA that sponges miR-449, leading to enhanced GFRα1 expression and activation of the GDNF signaling pathway. Furthermore, circGFRα1 acts as a ceRNA based on the METTL14-mediated cytoplasmic export through the GGACU motif. Our study should help to understand the mechanisms regulating germ cell development, add new evidence on the mechanisms of action of circRNA, and clarify female reproductive mechanisms to improve the quantity and quality of oocytes.

DATA AVAILABILITY STATEMENT

The original contributions presented in the study are included in the article/**Supplementary Material**, further inquiries can be directed to the corresponding author/s.

AUTHOR CONTRIBUTIONS

XL conducted all the major experiments, data analysis, and wrote the manuscript. GT performed analysis with RNA Hybrid. JW initiated and supervised the entire project, analyzed data, and wrote the manuscript. All authors reviewed the manuscript and contributed in their areas of expertise.

FUNDING

This work was supported by National Nature Science Foundation of China (32000806 and 81720108017), the National Basic Research Program of China (2017YFA0504201 and 2018YFC1003501), and the China Postdoctoral Science Foundation (2017M621453).

SUPPLEMENTARY MATERIAL

The Supplementary Material for this article can be found online at: https://www.frontiersin.org/articles/10.3389/fcell.2021.640402/full#supplementary-material

REFERENCES

Ahmed, I., Karedath, T., Andrews, S. S., Al-Azwani, I. K., Mohamoud, Y. A., Querleu, D., et al. (2016). Altered expression pattern of circular RNAs in primary and metastatic sites of epithelial ovarian carcinoma. *Oncotarget* 7, 36366–36381. doi: 10.18632/oncotarget.8917

Alarcon, C. R., Lee, H., Goodarzi, H., Halberg, N., and Tavazoie, S. F. (2015). N6-methyladenosine marks primary microRNAs for processing. *Nature* 519, 482–485. doi: 10.1038/nature14281

Brinster, R. L., and Avarbock, M. R. (1994). Germline transmission of donor haplotype following spermatogonial transplantation. *Proc. Natl. Acad. Sci. U.S.A.* 91, 11303–11307. doi: 10.1073/pnas.91.24.11303

Burd, C. E., Jeck, W. R., Liu, Y., Sanoff, H. K., Wang, Z., and Sharpless, N. E. (2010). Expression of linear and novel circular forms of an INK4/ARF-associated non-coding RNA correlates with atherosclerosis risk. *PLoS Genet.* 6:e1001233. doi: 10.1371/journal.pgen.1001233

Fustin, J. M., Doi, M., Yamaguchi, Y., Hida, H., Nishimura, S., Yoshida, M., et al. (2013). RNA-methylation-dependent RNA processing controls the speed of the circadian clock. *Cell* 155, 793–806. doi: 10.1016/j.cell.2013.10.026

Guo, J. U., Agarwal, V., Guo, H., and Bartel, D. P. (2014). Expanded identification and characterization of mammalian circular RNAs. *Genome Biol.* 15:409.

Hansen, T. B., Jensen, T. I., Clausen, B. H., Bramsen, J. B., Finsen, B., Damgaard, C. K., et al. (2013). Natural RNA circles function as efficient microRNA sponges. *Nature* 495, 384–388. doi: 10.1038/nature11993

He, Z., Jiang, J., Kokkinaki, M., Golestaneh, N., Hofmann, M. C., and Dym, M. (2008). Gdnf upregulates c-Fos transcription via the Ras/Erk1/2 pathway to promote mouse spermatogonial stem cell proliferation. *Stem Cells* 26, 266–278. doi: 10.1634/stemcells.2007-0436

Jacob, R., Zander, S., and Gutschner, T. (2017). The dark side of the epitranscriptome: chemical modifications in long non-coding RNAs. *Int. J. Mol. Sci.* 18:2387. doi: 10.3390/ijms18112387

Li, J., Zhou, F., Zheng, T., Pan, Z., Liang, X., Huang, J., et al. (2015). Ovarian germline stem cells (OGSCs) and the hippo signaling pathway association with physiological and pathological ovarian aging in mice. *Cell. Physiol. Biochem.* 36, 1712–1724. doi: 10.1159/000430144

Li, X., Ao, J., and Wu, J. (2017a). Systematic identification and comparison of expressed profiles of lncRNAs and circRNAs with associated co-expression and ceRNA networks in mouse germline stem cells. *Oncotarget* 8, 26573–26590. doi: 10.18632/oncotarget.15719

Li, X., Hu, Z., Yu, X., Zhang, C., Ma, B., He, L., et al. (2017b). Dosage compensation in the process of inactivation/reactivation during both germ cell development and early embryogenesis in mouse. *Sci. Rep.* 7:3729.

Li, X., Tian, G. G., Zhao, Y., and Wu, J. (2019). Genome-wide identification and characterization of long noncoding and circular RNAs in germline stem cells. *Sci. Data* 6:8.

Liu, J., Shang, D., Xiao, Y., Zhong, P., Cheng, H., and Zhou, R. (2017). Isolation and characterization of string-forming female germline stem cells from ovaries of neonatal mice. *J. Biol. Chem.* 292, 16003–16013. doi: 10.1074/jbc.m117.799403

Ma, B., Lee, T. L., Hu, B., Li, J., Li, X., Zhao, X., et al. (2018). Molecular characteristics of early-stage female germ cells revealed by RNA sequencing of low-input cells and analysis of genome-wide DNA methylation. *DNA Res.* 26, 105–117. doi: 10.1093/dnares/dsy042

Memczak, S., Jens, M., Elefsinioti, A., Torti, F., Krueger, J., Rybak, A., et al. (2013). Circular RNAs are a large class of animal RNAs with regulatory potency. *Nature* 495, 333–338. doi: 10.1038/nature11928

Meyer, K. D., Patil, D. P., Zhou, J., Zinoviev, A., Skabkin, M. A., Elemento, O., et al. (2015). 5′ UTR m(6)A promotes cap-independent translation. *Cell* 163, 999–1010. doi: 10.1016/j.cell.2015.10.012

Molinie, B., Wang, J., Lim, K. S., Hillebrand, R., Lu, Z. X., Van Wittenberghe, N., et al. (2016). m(6)A-LAIC-seq reveals the census and complexity of the m(6)A epitranscriptome. *Nat. Methods* 13, 692–698. doi: 10.1038/nmeth.3898

Oatley, J. M., Avarbock, M. R., and Brinster, R. L. (2007). Glial cell line-derived neurotrophic factor regulation of genes essential for self-renewal of mouse spermatogonial stem cells is dependent on Src family kinase signaling. *J. Biol. Chem.* 282, 25842–25851. doi: 10.1074/jbc.m703474200

Pan, Z., Sun, M., Li, J., Zhou, F., Liang, X., Huang, J., et al. (2015). The expression of markers related to ovarian germline stem cells in the mouse ovarian surface epithelium and the correlation with notch signaling pathway. *Cell. Physiol. Biochem.* 37, 2311–2322. doi: 10.1159/000438586

Salzman, J., Chen, R. E., Olsen, M. N., Wang, P. L., and Brown, P. O. (2013). Cell-type specific features of circular RNA expression. *PLoS Genet.* 9:e1003777. doi: 10.1371/journal.pgen.1003777

Shafik, A., Schumann, U., Evers, M., Sibbritt, T., and Preiss, T. (2016). The emerging epitranscriptomics of long noncoding RNAs. *Biochim. Biophys. Acta* 1859, 59–70.

Shi, Y., Chichung Lie, D., Taupin, P., Nakashima, K., Ray, J., Yu, R. T., et al. (2004). Expression and function of orphan nuclear receptor TLX in adult neural stem cells. *Nature* 427, 78–83. doi: 10.1038/nature02211

Sun, J., Lin, Y., and Wu, J. (2013). Long non-coding RNA expression profiling of mouse testis during postnatal development. *PLoS One* 8:e75750. doi: 10.1371/journal.pone.0075750

Wang, X., Lu, Z., Gomez, A., Hon, G. C., Yue, Y., Han, D., et al. (2014). N6-methyladenosine-dependent regulation of messenger RNA stability. *Nature* 505, 117–120. doi: 10.1038/nature12730

Wu, M., Ma, L., Xue, L., Ye, W., Lu, Z., Li, X., et al. (2019). Resveratrol alleviates chemotherapy-induced oogonial stem cell apoptosis and ovarian aging in mice. *Aging (Albany NY)* 11, 1030–1044. doi: 10.18632/aging.101808

Xie, W., Wang, H., and Wu, J. (2014). Similar morphological and molecular signatures shared by female and male germline stem cells. *Sci. Rep.* 4:5580.

Yang, D., Qiao, J., Wang, G., Lan, Y., Li, G., Guo, X., et al. (2018). N6-methyladenosine modification of lincRNA 1281 is critically required for mESC differentiation potential. *Nucleic Acids Res.* 46, 3906–3920. doi: 10.1093/nar/gky130

Yang, Y., Fan, X., Mao, M., Song, X., Wu, P., Zhang, Y., et al. (2017). Extensive translation of circular RNAs driven by N(6)-methyladenosine. *Cell Res.* 27, 626–641. doi: 10.1038/cr.2017.31

Zhang, X., Yang, Y., Xia, Q., Song, H., Wei, R., Wang, J., et al. (2018). Cadherin 22 participates in the self-renewal of mouse female germ line stem cells via interaction with JAK2 and beta-catenin. *Cell. Mol. Life Sci.* 75, 1241–1253. doi: 10.1007/s00018-017-2689-4

Zhang, X. L., Wu, J., Wang, J., Shen, T., Li, H., Lu, J., et al. (2016). Integrative epigenomic analysis reveals unique epigenetic signatures involved in unipotency of mouse female germline stem cells. *Genome Biol.* 17:162.

Zhang, Y., Zhang, X. O., Chen, T., Xiang, J. F., Yin, Q. F., Xing, Y. H., et al. (2013). Circular intronic long noncoding RNAs. *Mol. Cell* 51, 792–806. doi: 10.1016/j.molcel.2013.08.017

Zhu, X., Tian, G. G., Yu, B., Yang, Y., and Wu, J. (2018). Effects of bisphenol A on ovarian follicular development and female germline stem cells. *Arch. Toxicol.* 92, 1581–1591. doi: 10.1007/s00204-018-2167-2

Zou, K., Yuan, Z., Yang, Z., Luo, H., Sun, K., Zhou, L., et al. (2009). Production of offspring from a germline stem cell line derived from neonatal ovaries. *Nat. Cell Biol.* 11, 631–636. doi: 10.1038/ncb1869

Conflict of Interest: The authors declare that the research was conducted in the absence of any commercial or financial relationships that could be construed as a potential conflict of interest.

frontiers in Cell and Developmental Biology

MINI REVIEW
published: 29 April 2021
doi: 10.3389/fcell.2021.641963

Mechanisms of Apoptosis-Related Long Non-coding RNAs in Ovarian Cancer

*Toshihiko Takeiwa[1], Kazuhiro Ikeda[1], Kuniko Horie-Inoue[1] and Satoshi Inoue[1,2]**

[1] Division of Systems Medicine & Gene Therapy, Saitama Medical University, Saitama, Japan, [2] Department of Systems Aging Science and Medicine, Tokyo Metropolitan Institute of Gerontology, Tokyo, Japan

Ovarian cancer is a health-threatening malignancy of ovary in female reproductive systems and one of the most common gynecological malignancies worldwide. Due to rare early symptoms, ovarian cancers are often diagnosed at advanced stages and exhibit poor prognosis. Thus, efforts have been paid to develop alternative diagnostic and therapeutic strategies for the disease. Recent studies have presented that some long non-coding RNAs (lncRNAs) play roles in apoptosis of ovarian cancer cells through various mechanisms involved in the regulation of transcription factors, histone modification complexes, miRNAs, and protein stability. Because evasion of apoptosis in cancer cells facilitates to promote tumor progression and therapy resistance, apoptosis regulatory mechanisms of lncRNAs may be promising new targets in ovarian cancer. In this review, we introduce the recent findings in regard to the molecular mechanisms of apoptosis-related lncRNAs in ovarian cancer cells.

Keywords: ovarian cancer, ovary, apoptosis, long non-coding RNA, transcriptional regulation, histone modification complex, competing endogenous RNA

OPEN ACCESS

Edited by:
Tang Zhonglin,
Agricultural Genomics Institute at Shenzhen, Chinese Academy of Agricultural Sciences, China

Reviewed by:
Andrew Craig,
Queen's University, Canada
Zhigang Tu,
Jiangsu University, China

***Correspondence:**
Satoshi Inoue
sinoue@tmig.or.jp

Specialty section:
This article was submitted to Cell Growth and Division, a section of the journal Frontiers in Cell and Developmental Biology

Received: *15 December 2020*
Accepted: *06 April 2021*
Published: *29 April 2021*

Citation:
Takeiwa T, Ikeda K, Horie-Inoue K and Inoue S (2021) Mechanisms of Apoptosis-Related Long Non-coding RNAs in Ovarian Cancer. Front. Cell Dev. Biol. 9:641963. doi: 10.3389/fcell.2021.641963

OVARY AND OVARIAN CANCER

The ovary is a female reproductive organ where oocyte development occurs (Motta et al., 1997; Virant-Klun, 2015; Yadav et al., 2018) and functions as an endocrine organ involved in the synthesis of the female sex steroid hormones and the regulation of reproduction such as the menstrual cycle, pregnancy, and lactation (Hiller-Sturmhöfel and Bartke, 1998). Thus, the health of ovaries is essential for reproduction and women's lives, rendering finding cures to ovarian diseases crucial. Ovarian cancer is one of the most common gynecological cancers (Momenimovahed et al., 2019). The GLOBOCAN 2018 data estimates ∼300,000 new cases of ovarian cancer and over 180,000 ovarian cancer–related deaths per year worldwide (Bray et al., 2018). Ovarian cancer is a heterogeneous disease and classified by type of originated cell. Epithelial ovarian cancer (EOC) is the most common ovarian cancer (∼90%) (Rojas et al., 2016; Momenimovahed et al., 2019). The disease is often advanced at diagnosis due to lack of early symptoms and the 5-year cause-specific survival rate is <50% (Siegel et al., 2018; Torre et al., 2018; Trinidad et al., 2020). Based on the current limitations, alternative diagnostic and therapeutic approaches for ovarian cancer remain to be explored.

APOPTOSIS IN OVARY AND OVARIAN CANCER

Apoptosis is a process of programmed cell death triggered by intrinsic or extrinsic signals (Wong, 2011). Intrinsic signals are initiated by cellular stresses. These signals increase the mitochondrial permeability and release of the pro-apoptotic factors such as cytochrome-c, resulting in activation of cysteine-aspartic acid proteases (caspases), which are essential enzymes for apoptosis execution. Meanwhile, extrinsic signals are mediated by death receptor signaling pathways. Death receptors, their ligands, and adaptor proteins form the death-inducing signaling complex (DISC), which triggers caspase activation (Wong, 2011).

Apoptosis plays physiological roles in normal ovary functions such as follicular atresia and corpus luteum regression (Vaskivuo and Tapanainen, 2003; Yadav et al., 2018). In malignant tumors, evasion of apoptosis facilitates cancer cell survival and tumor progression (Wong, 2011; Binju et al., 2019), thus efforts have been paid for cancer strategies to discover the molecules to exert apoptosis in cancer cells whereas not in normal cells. For ovarian cancer treatment, small chemicals that modulate apoptosis-related proteins such as inhibitors of apoptotic proteins (IAPs) have entered clinical trials (Binju et al., 2019).

In terms of apoptosis pathways in cancers, several mechanisms of apoptosis-related genes have been well characterized. Transcription factors such as E2F family proteins, nuclear factor kappa B (NF-κB) proteins, and signal transducer and activator of transcription (STAT) family proteins modulate apoptosis via regulating transcription of apoptosis-related genes (Bours et al., 2000; Crosby and Almasan, 2004; Karin, 2006; Kim and Lee, 2007; Kent and Leone, 2019; Verhoeven et al., 2020). Histone modification complexes such as polycomb repressive complex 1/2 (PRC1/2) affect transcription of apoptosis-related genes through histone methylation (Cao et al., 2011; Wang W. et al., 2015; Christofides et al., 2016). Apoptosis-related genes are also modulated by post-transcriptional gene regulation mechanism, such as through miRNAs that regulate apoptosis-related gene mRNAs (Di Leva et al., 2014; Pistritto et al., 2016; Si et al., 2019). Ubiquitin-mediated protein degradation systems are also involved in apoptosis (Zhang et al., 2004; Hoeller and Dikic, 2009; Yang et al., 2009), as some E3 ubiquitin ligases are involved in ubiquitination of apoptosis-related proteins (Hoeller and Dikic, 2009; Yang et al., 2009, 2018; Woo and Kwon, 2019).

Considering the importance of apoptosis in cancer pathophysiology, strategies targeting these apoptosis regulatory mechanisms may contribute to the development of novel ovarian cancer therapies.

LONG NON-CODING RNA (lncRNA)

Long non-coding RNAs (lncRNAs) are defined as >200-nt transcripts that do not encode proteins and tens of thousands of lncRNA transcripts are identified throughout the human genome, the majority with unknown function. However, functional studies of some lncRNAs have revealed that they have a wide range of functions. For example, lncRNAs regulate transcription and chromatin remodeling by modulating the recruitment of transcription factors and PRC to specific genomic loci. Furthermore, lncRNAs are involved in gene regulation at post-transcriptional levels through interacting with mRNAs, miRNAs, and proteins (Marchese et al., 2017). Intriguingly, lncRNAs play important roles in pathophysiology of various cancers (Takayama and Inoue, 2016; Misawa et al., 2017; Arun et al., 2018; Mitobe et al., 2018; Kamada et al., 2020; Takeiwa et al., 2020). Particularly, several lncRNAs have been suggested to regulate the apoptosis of ovarian cancer cells (**Figure 1** and **Table 1**). In the following sections, we will describe some apoptosis-related lncRNAs in ovarian cancer cells according to their mechanisms.

Apoptosis-Related LncRNAs Regulating Transcription Factors

In this section, we will introduce an apoptosis-promotive lncRNA *growth arrest-specific 5 (GAS5)* and apoptosis-suppressive lncRNAs *non-coding RNA in the aldehyde dehydrogenase 1A pathway (NRAD1)/long intergenic non-coding RNA 00284 (LINC00284)* and a non-coding variant of *ceruloplasmin (CP) (lncRNA ceruloplasmin; NRCP)*.

GAS5

Growth arrest-specific 5 is downregulated in ovarian cancer, with this low expression associated with shorter disease-free period and lower overall survival rate of ovarian cancer patients (Gao et al., 2015; Li et al., 2016; Zhao et al., 2018; Long et al., 2019). *GAS5* overexpression promotes apoptosis of ovarian cancer cells such as A2780, HEY, OVCAR3, and SKOV3, and increases the sensitivity of HEY and SKOV3 cells to the anticancer agent cisplatin (Gao et al., 2015; Li et al., 2016; Zhao et al., 2018; Long et al., 2019). A functional study has shown that *GAS5* recruits the E2F4 transcription factor to the *poly(ADP-ribose) polymerase 1 (PARP1)* promoter, repressing *PARP1* transcription in HEY and SKOV3 cells (Long et al., 2019; **Figure 1A**). *GAS5*-mediated *PARP1* repression might contribute to apoptosis by downregulating the mitogen-activated protein kinase (MAPK) pathway, but direct evidence will be required in the future study.

NRAD1/LINC00284

Non-coding RNA in the aldehyde dehydrogenase 1A pathway/long intergenic non-coding RNA 00284 is highly expressed in ovarian cancer. *NRAD1* overexpression and knockdown experiments have shown that it suppresses the apoptosis of HO8910 and OVCAR3 cells. Functional analyses using HO8910 cells have suggested that *NRAD1* binds to NF-κB subunit 1 (NF-κB1) transcription factor and induces NF-κB1–mediated transcriptional repression of *mesoderm specific transcript (MEST)*, contributing to the suppression of apoptosis (Ruan and Zhao, 2019; **Figure 1A**). However, since a previous study has reported that HO8910 is a cross-contaminated cell line, this mechanism is needed to be verified using other ovarian cancer models (Ye et al., 2015).

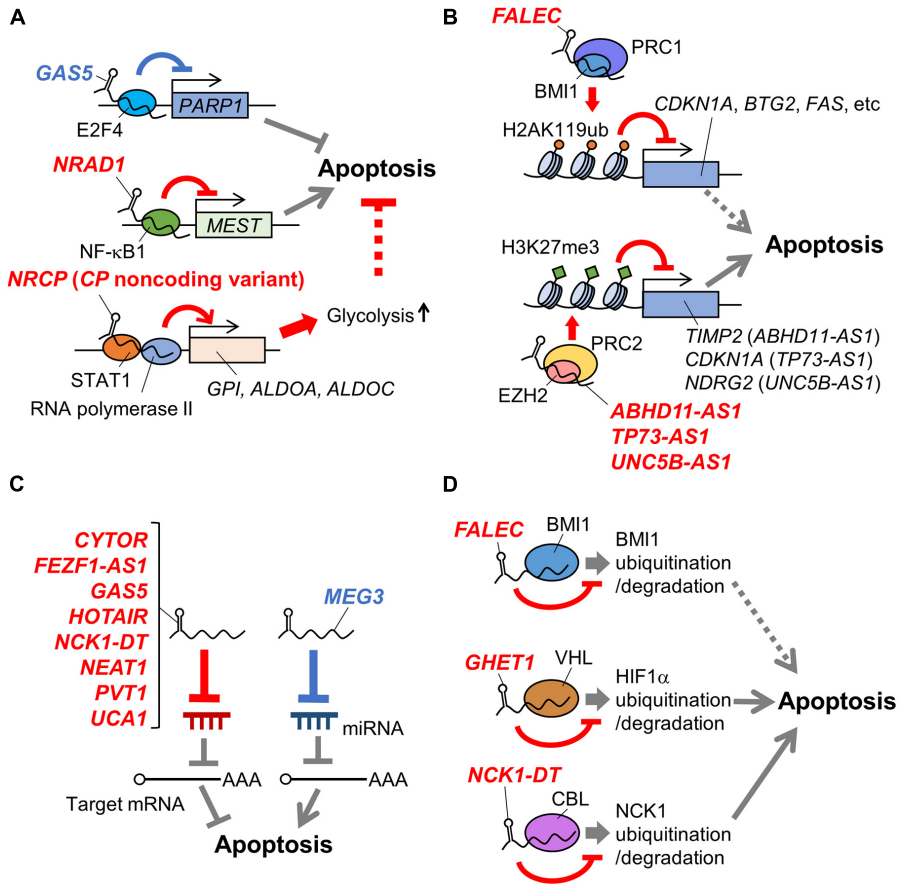

FIGURE 1 | Schematic representation of mechanisms of apoptosis-related lncRNAs in ovarian cancer. LncRNAs involved in apoptosis of ovarian cancer cells via regulating transcription factors **(A)**, histone modification complexes **(B)**, miRNAs **(C)**, and protein stability **(D)** are shown. Names of lncRNAs promoting and suppressing apoptosis are shown in blue and red, respectively. In addition, apoptosis-promotive or suppressive functions of lncRNAs are shown in blue or red lines, respectively. Potential apoptosis-associated biological pathways are shown in dotted lines. *ABHD11-AS1, abhydrolase domain containing 11 antisense RNA 1; ALDOA, aldolase, fructose-bisphosphate A; ALDOC, aldolase, fructose-bisphosphate C*; BMI1, B lymphoma Mo-MLV insertion region 1 homolog; *BTG2, B-cell translocation gene 2*; CBL, casitas B-lineage lymphoma: *CDKN1A, cyclin dependent kinase inhibitor 1A; CP, ceruloplasmin; CYTOR, cytoskeleton regulator RNA*; EZH2, enhancer of zeste homolog 2; *FALEC, focally amplified long non-coding RNA in epithelial cancer; FEZF1-AS1, fasciculation and elongation protein zeta family zinc finger 1 antisense RNA 1; GAS5, growth arrest-specific 5; GHET1, gastric carcinoma high expressed transcript 1; GPI, glucose-6-phosphate isomerase*; H2AK119ub, the ubiquitination at the 119th lysine residue of the histone H2A; H3K27me3, the tri-methylation at the 27th lysine residue of the histone H3; HIF1α, hypoxia-inducible factor 1α; *HOTAIR, HOX transcript antisense RNA; MEG3, maternally expressed gene 3; MEST, mesoderm specific transcript*; NCK1, non-catalytic region of tyrosine kinase adaptor protein 1; *NCK1-DT, NCK1 divergent transcript; NDRG2, n-myc downstream-regulated gene 2; NEAT1, nuclear enriched abundant transcript 1*; NF-κB1, nuclear factor kappa B subunit 1; *NRAD1, non-coding RNA in the aldehyde dehydrogenase 1A pathway; NRCP, lncRNA ceruloplasmin; PARP1, poly(ADP-ribose) polymerase 1; PVT1, plasmacytoma variant translocation 1*; STAT1, signal transducer and activator of transcription 1; *TIMP2, tissue inhibitor of metalloproteinase 2; TP73-AS1, tumor protein p73 antisense RNA 1; UCA1, urothelial carcinoma associated 1; UNC5B-AS1, uncoordinated 5 netrin receptor B antisense RNA 1*.

CP Non-coding Variant (NRCP)

NRCP is a non-coding splice variant of the ceruloplasmin-coding gene that is upregulated in ovarian cancer (Rupaimoole et al., 2015). High *NRCP* expression levels correlate with shorter overall survival in patients with ovarian cancer, while *NRCP* knockdown induces apoptosis in A2780 and SKOV3 cells (Rupaimoole et al., 2015). *NRCP* binds to RNA polymerase II and STAT1 transcription factor, and promotes glycolysis in A2780 and SKOV3 cells by upregulating glycolysis pathway genes such as *glucose-6-phosphate isomerase (GPI), aldolase, fructose-bisphosphate A (ALDOA)*, and *aldolase, fructose-bisphosphate C (ALDOC)* via STAT1 (Rupaimoole et al., 2015; **Figure 1A**). These results suggest a possibility that *NRCP* may modulate apoptosis by regulating cancer metabolism. *NRCP* is not annotated in National Center for Biotechnology Information (NCBI) Reference Sequence (RefSeq) database (on Feb 3rd, 2021) and requires further characterization of sequences and expression profiles.

Apoptosis-Related LncRNAs Regulating Histone Modification Complexes

In this section, we will describe the following apoptosis-suppressive lncRNAs: *abhydrolase domain containing 11*

TABLE 1 | Mechanisms of apoptosis-related lncRNAs in ovarian cancer cells.

lncRNA	Chr. location	Roles in ovarian cancer cells/xenograft tumors	Clinical relevance in ovarian cancer tissues/patients	Effects on apoptosis
GAS5	1q25	↓ in A2780/HEY/HO8910 [a]/OVCAR3/SKOV3 cells Binds to E2F4 and represses *PARP1* in HEY/SKOV3 cells Sponges *miR-196a-5p* to upregulate *HOXA5* in primary tumor cells from HGSOV tissues and A2780/OVCAR3 cells Represses PARP1, growth and cisplatin resistance in SKOV3 tumors	↓ in tumor tissues ↓ is correlated with shorter DFS/OS	+
NRAD1/LINC00284	13q14	↑ in A2780/CAOV3/HO8910/OVCAR3/SKOV3 cells Binds to NF-κB1 and represses *MEST* in HO8910 cells Promotes growth of HO8910 tumors	↑ in ovarian cancer tissues	–
CP non-coding variant *(NRCP)*	3q24-25	↑ in A2780/IGROV1/OVCAR3/SFMAR/SFWAS/SKOV3 cells Binds to RNA Pol II and STAT1, upregulates *GPI, ALDOA*, and *ALDOC* Promotes growth and metastasis of A2780/SKOV3 tumors	↑ in tumor tissues ↑ is correlated with shorter OS	–
ABHD11-AS1	7q11	↑ in HO8910/OVCA429 cells Upregulates RhoC in A2780/OVCAR3 cells Binds to EZH2 and represses *TIMP2* in HO8910/OVCA429 cells Promotes growth and metastasis of A2780 tumors	↑ in tumor tissues	–
FALEC/FAL1	1q21	Promotes PRC1-mediated repression of *CDKN1A, BTG2*, and *FAS* in A2780 cells Binds to and stabilizes BMI1 in A2780 cells Promotes A2780 tumor growth	↑ and copy number gain correlated with shorter OS	–
TP73-AS1	1p36	↑ in CAOV3/HO8910/OV420/SKOV3 cells Binds to EZH2 and represses *CDKN1A* in SKOV3 cells Promotes SKOV3 tumor growth	↑ in tumor tissues ↑ is correlated with poor prognosis	–
UNC5B-AS1	10q22	↑ in A2780/ES2/SKOV3 cells Binds to EZH2 and promotes *NDRG2* in ES2/SKOV3 cells	↑ in tumor tissues	–
FEZF1-AS1	7q31	↑ in A2780/COC1/PEO1/SKOV3 cells Sponges *miR-130a-5p*, upregulates *SOX4* in COC1/SKOV3 cells	↑ in tumors and serum ↑ is correlated with shorter OS	–
HOTAIR	12q13	↑ in cisplatin-resistant A2780/SKOV3 cells Sponges *miR-138-5p*, upregulates *EZH2* and *SIRT1* in A2780/SKOV3 cells Promotes A2780 tumor growth	↑ in tumor tissues ↑ is correlated with shorter OS in HGSOV patients	–
CYTOR/LINC00152	2p11	↑ in A2780/HO8910/SKOV3 cells Sponges *miR-125b* to upregulate *MCL1* in A2780/SKOV3 cells Increases MCL1 level and SKOV3 tumor growth	↑ in tumor tissues ↑ is correlated with shorter OS	–
MEG3	14q32	↓ in OVCAR3/OVCAR5/OVCAR8/SKOV3 cells Sponges *miR-205-5p* in OVCAR8/SKOV3 cells	↓ in tumor tissues	+
NCK1-DT/NCK1-AS1	3q22	↑ in CAOV3/OVCAR3/SKOV3/SNU119/SUN8 cells Sponges *miR-137* to upregulate *NCK1* in CAOV3/SKOV3 cells Prevents CBL-mediated NCK1 degradation in CAOV3/SKOV3 cells	↑ in tumor tissues	–
NEAT1	11q13	↑ in A2780/CAOV3/ES2/HO8910/OV90/OVCAR3/SKOV3 cells ↑ in paclitaxel-resistant HeyA8/SKOV3 cells versus parental cells ↑ in cisplatin-resistant A2780/SKOV3 cells versus parental cells Sponges *miR-34a-5p*, upregulates *BCL2* in OVCAR3/SKOV3 cells Sponges *miR-4500*, upregulates *BZW1* in CAOV3/ES2 cells Sponges *miR-194*, upregulates *ZEB1* in HeyA8/SKOV3 cells Sponges *miR-770-5p*, upregulates *PARP1* in A2780/SKOV3 cells Promotes growth of SKOV3/A2780 tumors and paclitaxel resistance	↑ in tumor tissues ↑ in cisplatin and paclitaxel-resistant cancer tissues ↑ is correlated with shorter OS	–
PVT1	8q24	↑ in A2780/OVCAR3/TOV112D cells Sponges *miR-543*, upregulates *SERPINI1* in OVCAR3/TOV112D cells	↑ in tumor tissues ↑ is correlated with shorter OS	–
UCA1	19p13	↑ in A2780/HeyA8/OAW42/OVCAR4/SKOV3 cells ↑ in paclitaxel-resistant HeyA8/SKOV3 cells ↑ in cisplatin-resistant A2780/SKOV3 cells Sponges *miR-129*, upregulates *ABCB1* in HeyA8/SKOV3 cells Sponges *miR-654-5p*, upregulates *SIK2* in HeyA8/SKOV3 cells Sponges *miR-143*, upregulates *FOSL2* in A2780/SKOV3 cells	↑ in tumor tissues ↑ in tumors and serum exosomes of patients with cisplatin-resistant cancers	–

(Continued)

TABLE 1 | Continued

lncRNA	Chr. location	Roles in ovarian cancer cells/xenograft tumors	Clinical relevance in ovarian cancer tissues/patients	Effects on apoptosis
GHET1	7q36	↑ in 3AO/A2780/OVCAR3/SKOV3 cells Prevents VHL-mediated HIF1α degradation in A2780/SKOV3 cells	↑ in tumor tissues ↑ is correlated with increased tumor size and distant metastasis	–

[a]*Although HO8910 cell line was used as an ovarian cancer cell model in these studies, a previous study has reported that it is a cross-contaminated cell line.*
ABCB1, ATP binding cassette subfamily B member 1; ABHD11-AS1, abhydrolase domain containing 11 antisense RNA 1; ALDOA, aldolase, fructose-bisphosphate A; ALDOC, aldolase, fructose-bisphosphate C; BCL2, B-cell lymphoma 2; BMI1, B lymphoma Mo-MLV insertion region 1 homolog; BTG2, B-cell translocation gene 2; BZW1, basic leucine zipper and W2 domain-containing protein 1; CBL, casitas B-lineage lymphoma; CDKN1A, cyclin dependent kinase inhibitor 1A; CP, ceruloplasmin; CYTOR, cytoskeleton regulator RNA; DFS, disease-free survival; EZH2, enhancer of zeste homolog 2; FAL1, focally amplified lncRNA on chromosome 1; FALEC, focally amplified long non-coding RNA in epithelial cancer; FEZF1-AS1, fasciculation and elongation protein zeta family zinc finger 1 antisense RNA 1; FOSL2, Fos-related antigen 2; GAS5, growth arrest-specific 5; GHET1, gastric carcinoma high expressed transcript 1; GPI, glucose-6-phosphate isomerase; HGSOV, high-grade serous ovarian cancer; HIF1α, hypoxia-inducible factor 1α; HOTAIR, HOX transcript antisense RNA; HOXA5, homeobox A5; LINC00152, long intergenic non-coding RNA 00152; LINC00284, long intergenic non-coding RNA 00284; MCL1, myeloid cell leukemia 1; MEG3, maternally expressed gene 3; MEST, mesoderm specific transcript; NCK1, non-catalytic region of tyrosine kinase adaptor protein 1; NCK1-AS1, NCK1 antisense RNA 1; NCK1-DT, NCK1 divergent transcript; NDRG2, n-myc downstream-regulated gene 2; NEAT1, nuclear enriched abundant transcript 1; NRAD1, non-coding RNA in the aldehyde dehydrogenase 1A pathway; NRCP, lncRNA ceruloplasmin; OS, overall survival; PARP1, poly(ADP-ribose) polymerase 1; PTX, paclitaxel; PVT1, plasmacytoma variant translocation 1; RhoC, ras homolog family member C; SERPINI1, serpin family I member 1; SIK2, salt inducible kinase 2; SIRT1, sirtuin 1; SOX4, sex-determining region Y (SRY)-box transcription factor 4; TIMP2, tissue inhibitor of metalloproteinase 2; TP73-AS1, tumor protein p73 antisense RNA 1; UCA1, urothelial carcinoma associated 1; UNC5B-AS1, uncoordinated 5 netrin receptor B antisense RNA 1; VHL, von Hippel–Lindau tumor suppressor; ZEB1, zinc finger E-box binding homeobox 1.

antisense RNA 1 (ABHD11-AS1), focally amplified long non-coding RNA in epithelial cancer (FALEC)/focally amplified lncRNA on chromosome 1 (FAL1), tumor protein p73 antisense RNA 1 (TP73-AS1), and *uncoordinated 5 netrin receptor B antisense RNA 1 (UNC5B-AS1)*.

ABHD11-AS1

Abhydrolase domain containing 11 antisense RNA 1 is upregulated in ovarian cancer (Wu et al., 2017; Zeng et al., 2019). A functional study has shown that *ABHD11-AS1* modulates the expression of ras homolog family member C (RhoC) by an unknown mechanism, suppressing apoptosis in A2780 and OVCAR3 cells (Wu et al., 2017). Another functional study has shown that *ABHD11-AS1* binds to enhancer of zeste homolog 2 (EZH2), a component of PRC2. *ABHD11-AS1* facilitates tri-methylation at the 27th lysine residue of the histone H3 protein (H3K27me3) on the *tissue inhibitor of metalloproteinase 2 (TIMP2)* promoter, as mediated by PRC2, and likewise suppresses *TIMP2* expression in HO8910 cells and OVCA429 ovarian cancer cells (**Figure 1B**). *TIMP2* suppression mediated by *ABHD11-AS1* promotes the proliferation of OVCA429 cells, suggesting that *ABHD11-AS1* may also modulate apoptosis by this mechanism (Zeng et al., 2019).

FALEC/FAL1

Focally amplified lncRNA in epithelial cancer/focally amplified lncRNA on chromosome 1 was initially identified as an lncRNA whose gene copy number increased in multiple types of cancers, including ovarian cancer (Hu et al., 2014). Its high expression level and gain in genomic copy number correlate with a shorter overall survival rate of late-stage ovarian cancer patients (Hu et al., 2014). A functional study using A2780 cells has suggested that *FALEC* binds to a component of PRC1, B lymphoma Mo-MLV insertion region 1 homolog (BMI1) protein, and recruits PRC1 to the promoters of genes such as *cyclin dependent kinase inhibitor 1A (CDKN1A), B-cell translocation gene 2 (BTG2)*, and *FAS*. Subsequently, PRC1 mediates the ubiquitination at the 119th lysine residue of the histone H2A (H2AK119ub) on these promoter regions and the suppression of these genes (**Figure 1B**). The *FALEC*/PRC1 complex target genes such as *CDKN1A, BTG2*, and *FAS* are suggested to be involved in apoptosis regulation (El-Deiry, 2001; Mao et al., 2015). Thus, *FALEC* can be a regulator of ovarian cancer apoptosis.

TP73-AS1

Tumor protein p73 antisense RNA 1 is upregulated in EOC and associated with poor prognosis in EOC patients (Li Y. et al., 2019). A recent study has shown that *TP73-AS1* knockdown induces apoptosis of SKOV3 cells, suppressing the proliferation in *in vitro* culture and the xenograft tumor formation in athymic mice. In contrast, *TP73-AS1* overexpression suppresses apoptosis in CAOV3 ovarian cancer cells. Functional analyses have suggested that *TP73-AS1* epigenetically suppresses *CDKN1A* expression by recruiting PRC2 to its promoter (**Figure 1B**) and modulates apoptosis of SKOV3 cells through this mechanism (Li Y. et al., 2019).

UNC5B-AS1

Uncoordinated 5 netrin receptor B antisense RNA 1 is highly expressed in ovarian cancer, and a recent study has shown that its knockdown activates caspase 3 in ES2 and SKOV3 cells, suggesting the apoptosis-suppressive role of *UNC5B-AS1* (Wang et al., 2020). Moreover, the same study has suggested that *UNC5B-AS1* promotes PRC2 to repress the *n-myc downstream-regulated gene 2 (NDRG2)* expression epigenetically (**Figure 1B**), which may suppress ovarian cancer cell apoptosis (Wang et al., 2020). This study is limited in the elucidation of the mechanism by which *UNC5B-AS1* regulates PRC2 and its *in vivo* function, and further functional analyses are required.

Apoptosis-Related LncRNAs Regulating miRNAs

In the section, we will introduce an apoptosis-promotive lncRNA GAS5 and the following apoptosis-suppressive lncRNAs: *fasciculation and elongation protein zeta family zinc finger 1 antisense RNA 1 (FEZF1-AS1), HOX transcript antisense RNA (HOTAIR), non-catalytic region of tyrosine kinase adaptor protein 1 (NCK1) divergent transcript (NCK1-DT)/NCK1 antisense RNA 1 (NCK1-AS1), nuclear enriched abundant transcript 1 (NEAT1)*, and *urothelial carcinoma associated 1 (UCA1)*.

FEZF1-AS1

High levels of *FEZF1-AS1* are detected in tumor tissues and the serum of EOC patients, with its high expression associated with shorter overall survival of EOC patients (Sun et al., 2020). Moreover, its knockdown promotes apoptosis in COC1 and SKOV3 ovarian cancer cells, suggesting the apoptosis-suppressive role of *FEZF1-AS1*. *In vitro* analyses of *FEZF1-AS1* have shown that it functions as a competing endogenous RNA (ceRNA) for *miR-130a-5p*, or sponges *miR-130a-5p* (**Figure 1C**). Consequently, *FEZF1-AS1* upregulates the expression of a *miR-130a-5p* target gene, *sex-determining region Y (SRY)-box transcription factor 4 (SOX4)*, that promotes proliferation of COC1 and SKOV3 cells and may contribute to apoptosis suppression (Sun et al., 2020). Further analysis of *FEZF1-AS1* function, especially *in vivo*, will clarify its role and significance in apoptosis of ovarian cancer cells.

GAS5

A recent functional study has suggested that *GAS5* functions as a ceRNA for *miR-196a-5p* to upregulate *homeobox A5 (HOXA5)*, promoting apoptosis of primary tumor cells from high-grade serous ovarian cancer tissues as well as A2780 and OVCAR3 cells (Zhao et al., 2018; **Figure 1C**).

HOTAIR

HOX transcript antisense RNA is upregulated in ovarian cancer, and the elevated expression level correlates with the shorter overall survival of ovarian cancer patients (Qiu et al., 2015; Wang Y. et al., 2015; Zhang et al., 2016; Luo et al., 2017; Yu et al., 2018). *HOTAIR* knockdown induces apoptosis in ovarian cancer cells such as A2780, HeyC2, and OVCA429, and decreases the cisplatin sensitivity of A2780 and SKOV3 cells (Qiu et al., 2015; Wang Y. et al., 2015; Zhang et al., 2016, 2020; Yu et al., 2018). A recent functional study using A2780 and SKOV3 cells has suggested that *HOTAIR* acts as a ceRNA for *miR-138-5p*, leading to cisplatin resistance of these cells (Zhang et al., 2020; **Figure 1C**). This study has shown that *HOTAIR/miR-138-5p* axis modulates *EZH2* and *sirtuin 1 (SIRT1)* expression, but its biological significance has not been elucidated.

NCK1-DT/NCK1-AS1

Non-catalytic region of tyrosine kinase adaptor protein 1 divergent transcript is highly expressed in ovarian cancer. Mechanistically, it acts as a ceRNA for *miR-137* to upregulate *NCK1*, which suppresses apoptosis of CAOV3 and SKOV3 cells and enhances their cisplatin resistance (Chang et al., 2020; **Figure 1C**).

NEAT1

Nuclear enriched abundant transcript 1 is upregulated in ovarian cancer and is associated with shorter overall survival of ovarian cancer patients (Chen et al., 2016). *NEAT1* acts as a ceRNA for *miR-34a-5p* to upregulate BCL2 and suppresses apoptosis of OVCAR3 and SKOV3 cells (Ding et al., 2017). In addition, NEAT1 acts as a ceRNA for *miR-4500*, to upregulate *basic leucine zipper and W2 domain-containing protein 1 (BZW1)* that suppresses apoptosis of CAOV3 and ES2 cells (Xu et al., 2020), and *miR-194* to upregulate the transcription factor zinc finger E-box binding homeobox 1 (ZEB1), promoting resistance to the anticancer agent paclitaxel (PTX) in HeyA8 and SKOV3 cells (An et al., 2017). Furthermore, *NEAT1* sponges *miR-770-5p*, to upregulate *PARP1* and increase cisplatin resistance in A2780 cells *in vivo* (Zhu et al., 2020; **Figure 1C**).

UCA1

The lncRNA *UCA1* is upregulated in ovarian cancer and is detected in exosomes derived from the serum of ovarian cancer patients (Li Z. et al., 2019; Li et al., 2020). Functional studies have shown that UCA1 acts as a ceRNA for *miR-129* and *miR-654-5p* to upregulate *ATP binding cassette subfamily B member 1 (ABCB1)* and *SALT INDUCIBLE KINASE 2 (SIK2)*, respectively, which contribute to the suppression of apoptosis and the enhancement of PTX resistance in HeyA8 and SKOV3 cells (Wang et al., 2018; Li et al., 2020). In addition, *UCA1* functions as a ceRNA for *miR-143* to increase *Fos-related antigen 2 (FOSL2)*, and enhances cisplatin resistance in A2780 and SKOV3 cells (Li Z. et al., 2019; **Figure 1C**). However, the importance of the function of *UCA1* as a ceRNA *in vivo* has not been fully analyzed.

Recent studies have found that many other lncRNAs modulate ovarian cancer apoptosis through regulating miRNAs. For example, *CYTOR/LINC00152* acts as a ceRNA of *miR-125b* to upregulate an antiapoptotic protein MCL1 in A2780 and SKOV3 cells (Chen et al., 2018). *PVT1* suppresses apoptosis in OVACAR3 and TOV112D cells by inhibiting *miR-543* and increasing a *miR-543* target *SERPIN1* (Qu et al., 2020). In contrast, *MEG3* promotes apoptosis in OVCAR8 and SKOV3 cells by sponging *miR-205-5p* (Tao et al., 2020). The detail of lncRNAs regulating miRNAs is also reviewed in other articles (Braga et al., 2020; Salamini-Montemurri et al., 2020).

Apoptosis-Related LncRNAs Regulating Protein Stability

In the section, we will introduce the following apoptosis-suppressive lncRNAs: *FALEC/FAL1*, *gastric carcinoma high expressed transcript 1 (GHET1)*, and *NCK1-DT/NCK1-AS1*.

FALEC/FAL1

As described above, *FALEC* binds to BMI1 and modulates PRC1 function in A2780 cells. In addition, *FALEC* stabilizes BMI1 by suppressing ubiquitin-mediated BMI1 protein degradation (Hu et al., 2014; **Figure 1D**).

GHET1

The lncRNA *GHET1* is upregulated in ovarian cancer and higher expression correlates with increased tumor size and distant metastasis (Liu and Li, 2019). Conversely, its knockdown induces apoptosis and downregulates glycolysis in A2780 and SKOV3 cells, where *GHET1* binds to an E3 ubiquitin ligase, von Hippel–Lindau tumor suppressor (VHL), and prevents VHL-mediated degradation of hypoxia-inducible factor 1α (HIF1α) (**Figure 1D**). Since the *GHET1* function in ovarian cancer cells has been only examined by *in vitro* assays, *in vivo* analyses of *GHET1* are needed. Although the role of the *GHET1*/VHL/HIF1α axis in apoptosis has not yet been elucidated, HIF1α and cancer metabolism have been shown to play important roles in apoptosis regulation, suggesting the possibility that this axis may also be involved in the phenomenon (Zhou et al., 2006; Matsuura et al., 2016).

NCK1-DT/NCK1-AS1

In addition to the function as a ceRNA, *NCK1-AS1* increases the stability of NCK1: *NCK1-AS1* binds to an E3 ubiquitin ligase, casitas B-lineage lymphoma (CBL), and prevents CBL-mediated degradation of NCK1 (Chang et al., 2020; **Figure 1D**). The functions of *NCK-AS1* in ovarian cancer have been suggested based on *in vitro* experiments, and thus needs to be evaluated using ovarian tumor specimens or *in vivo* ovarian cancer models.

CONCLUSION

In this review, we introduced the mechanisms of apoptosis-related lncRNAs in ovarian cancer cells. Considering that dysregulation of apoptosis is involved in the resistance to ovarian cancer therapies, small molecule inhibitors/siRNAs targeting apoptosis-suppressing lncRNAs, or apoptosis-promoting lncRNAs themselves may be applicable to ovarian cancer therapies. For nucleic acid-based therapeutics, it is important to develop the drug delivery systems (DDSs) with high target specificity and less non-specific toxicity *in vivo*. Particularly, for ovarian cancer, DDSs will be useful to treat metastatic cancer cells in peritoneal cavity (Amreddy et al., 2018; van den Brand et al., 2018). Moreover, apoptosis-related lncRNAs may be potential diagnostic and prognostic biomarkers. Especially, *FEZF1-AS1* and *UCA1* are detected in serum and exosomes recovered from serum of ovarian cancer patients, respectively, which suggested their potential as liquid biopsy markers for ovarian cancer.

Apoptosis-related lncRNAs have basically been studied using conventional ovarian cancer cell lines, and the functions of some lncRNAs have been examined by *in vitro* assays alone. For clinical application, it is required to elucidate the lncRNA functions *in vivo*. Moreover, previous studies have indicated some discrepancies between ovarian cancer cell lines and the original tumor clinical tissues in terms of genomic and histological features and gene expression profiles (Domcke et al., 2013; Beaufort et al., 2014). Thus, lncRNA studies using ovarian tumor specimens or other ovarian cancer models are strongly demanded. Three-dimensional cultures of patient-derived cancer cells (PDCs) and cancer models established by transplanting tumor specimens into host mice (patient-derived xenograft [PDX] models) retain the properties of original tumors and have attracted attention as promising models for cancer research and drug screening (Ishiguro et al., 2016; Maru and Hippo, 2019; Namekawa et al., 2019; Shiba et al., 2019). Further studies using PDC and PDX models would advance the application of apoptosis-related lncRNAs to ovarian cancer diagnosis, prognosis, and therapies.

AUTHOR CONTRIBUTIONS

All authors contributed to the conception and provided the data and design. TT contributed to manuscript writing. KI, KH-I, and SI contributed to the conception and final approval of the manuscript.

FUNDING

This work was supported by grants from the Japan Society for the Promotion of Science (20K21667 to SI, 17H04205 and 20H03734 to KH-I, and 20K21636 to KI) and Takeda Science Foundation to SI and KI.

REFERENCES

Amreddy, N., Babu, A., Muralidharan, R., Panneerselvam, J., Srivastava, A., Ahmed, R., et al. (2018). Recent advances in nanoparticle-based cancer drug and gene delivery. *Adv. Cancer Res.* 137, 115–170. doi: 10.1016/bs.acr.2017.11.003

An, J., Lv, W., and Zhang, Y. (2017). LncRNA NEAT1 contributes to paclitaxel resistance of ovarian cancer cells by regulating ZEB1 expression via miR-194. *Onco Targets Ther.* 10, 5377–5390. doi: 10.2147/OTT.S147586

Arun, G., Diermeier, S. D., and Spector, D. L. (2018). Therapeutic targeting of long non-coding RNAs in cancer. *Trends Mol. Med.* 24, 257–277. doi: 10.1016/j.molmed.2018.01.001

Beaufort, C. M., Helmijr, J. C., Piskorz, A. M., Hoogstraat, M., Ruigrok-Ritstier, K., Besselink, N., et al. (2014). Ovarian cancer cell line panel (OCCP): clinical importance of in vitro morphological subtypes. *PLoS One* 9:e103988. doi: 10.1371/journal.pone.0103988

Binju, M., Amaya-Padilla, M. A., Wan, G., Gunosewoyo, H., Suryo Rahmanto, Y., and Yu, Y. (2019). Therapeutic inducers of apoptosis in ovarian cancer. *Cancers (Basel)* 11:1786. doi: 10.3390/cancers11111786

Bours, V., Bentires-Alj, M., Hellin, A. C., Viatour, P., Robe, P., Delhalle, S., et al. (2000). Nuclear factor-kappa B, cancer, and apoptosis. *Biochem. Pharmacol.* 60, 1085–1089. doi: 10.1016/s0006-2952(00)00391-9

Braga, E. A., Fridman, M. V., Moscovtsev, A. A., Filippova, E. A., Dmitriev, A. A., and Kushlinskii, N. E. (2020). LncRNAs in ovarian cancer progression, metastasis, and main pathways: ceRNA and alternative mechanisms. *Int. J. Mol. Sci.* 21:8855. doi: 10.3390/ijms21228855

Bray, F., Ferlay, J., Soerjomataram, I., Siegel, R. L., Torre, L. A., and Jemal, A. (2018). Global cancer statistics 2018: GLOBOCAN estimates of incidence and mortality worldwide for 36 cancers in 185 countries. *CA Cancer J. Clin.* 68, 394–424. doi: 10.3322/caac.21492

Cao, L., Bombard, J., Cintron, K., Sheedy, J., Weetall, M. L., and Davis, T. W. (2011). BMI1 as a novel target for drug discovery in cancer. *J. Cell. Biochem.* 112, 2729–2741. doi: 10.1002/jcb.23234

Chang, H., Li, B., Zhang, X., and Meng, X. (2020). NCK1-AS1 promotes NCK1 expression to facilitate tumorigenesis and chemo-resistance in ovarian cancer. *Biochem. Biophys. Res. Commun.* 522, 292–299. doi: 10.1016/j.bbrc.2019.11.014

Chen, P., Fang, X., Xia, B., Zhao, Y., Li, Q., and Wu, X. (2018). Long noncoding RNA LINC00152 promotes cell proliferation through competitively binding endogenous miR-125b with MCL-1 by regulating mitochondrial apoptosis pathways in ovarian cancer. *Cancer Med.* 7, 4530–4541. doi: 10.1002/cam4.1547

Chen, Z. J., Zhang, Z., Xie, B. B., and Zhang, H. Y. (2016). Clinical significance of up-regulated lncRNA NEAT1 in prognosis of ovarian cancer. *Eur. Rev. Med. Pharmacol. Sci.* 20, 3373–3377.

Christofides, A., Karantanos, T., Bardhan, K., and Boussiotis, V. A. (2016). Epigenetic regulation of cancer biology and anti-tumor immunity by EZH2. *Oncotarget* 7, 85624–85640. doi: 10.18632/oncotarget.12928

Crosby, M. E., and Almasan, A. (2004). Opposing roles of E2Fs in cell proliferation and death. *Cancer Biol. Ther.* 3, 1208–1211. doi: 10.4161/cbt.3.12.1494

Di Leva, G., Garofalo, M., and Croce, C. M. (2014). MicroRNAs in cancer. *Annu. Rev. Pathol.* 9, 287–314. doi: 10.1146/annurev-pathol-012513-104715

Ding, N., Wu, H., Tao, T., and Peng, E. (2017). NEAT1 regulates cell proliferation and apoptosis of ovarian cancer by miR-34a-5p/BCL2. *Onco Targets Ther.* 10, 4905–4915. doi: 10.2147/OTT.S142446

Domcke, S., Sinha, R., Levine, D. A., Sander, C., and Schultz, N. (2013). Evaluating cell lines as tumour models by comparison of genomic profiles. *Nat. Commun.* 4:2126. doi: 10.1038/ncomms3126

El-Deiry, W. S. (2001). Insights into cancer therapeutic design based on p53 and TRAIL receptor signaling. *Cell Death Differ.* 8, 1066–1075. doi: 10.1038/sj.cdd.4400943

Gao, J., Liu, M., Zou, Y., Mao, M., Shen, T., Zhang, C., et al. (2015). Long non-coding RNA growth arrest-specific transcript 5 is involved in ovarian cancer cell apoptosis through the mitochondria-mediated apoptosis pathway. *Oncol. Rep.* 34, 3212–3221. doi: 10.3892/or.2015.4318

Hiller-Sturmhöfel, S., and Bartke, A. (1998). The endocrine system: an overview. *Alcohol Health Res. World* 22, 153–164.

Hoeller, D., and Dikic, I. (2009). Targeting the ubiquitin system in cancer therapy. *Nature* 458, 438–444. doi: 10.1038/nature07960

Hu, X., Feng, Y., Zhang, D., Zhao, S. D., Hu, Z., Greshock, J., et al. (2014). A functional genomic approach identifies FAL1 as an oncogenic long noncoding RNA that associates with BMI1 and represses p21 expression in cancer. *Cancer Cell* 26, 344–357. doi: 10.1016/j.ccr.2014.07.009

Ishiguro, T., Sato, A., Ohata, H., Ikarashi, Y., Takahashi, R. U., Ochiya, T., et al. (2016). Establishment and characterization of an in vitro model of ovarian cancer stem-like cells with an enhanced proliferative capacity. *Cancer Res.* 76, 150–160. doi: 10.1158/0008-5472.CAN-15-0361

Kamada, S., Takeiwa, T., Ikeda, K., Horie-Inoue, K., and Inoue, S. (2020). Long non-coding RNAs involved in metabolic alterations in breast and prostate cancers. *Front. Oncol.* 10:593200. doi: 10.3389/fonc.2020.593200

Karin, M. (2006). Nuclear factor-κB in cancer development and progression. *Nature* 441, 431–436. doi: 10.1038/nature04870

Kent, L. N., and Leone, G. (2019). The broken cycle: E2F dysfunction in cancer. *Nat. Rev. Cancer* 19, 326–338. doi: 10.1038/s41568-019-0143-7

Kim, H. S., and Lee, M. S. (2007). STAT1 as a key modulator of cell death. *Cell. Signal.* 19, 454–465. doi: 10.1016/j.cellsig.2006.09.003

Li, J., Huang, H., Li, Y., Li, L., Hou, W., and You, Z. (2016). Decreased expression of long non-coding RNA GAS5 promotes cell proliferation, migration and invasion, and indicates a poor prognosis in ovarian cancer. *Oncol. Rep.* 36, 3241–3250. doi: 10.3892/or.2016.5200

Li, Y., Jiao, Y., Hao, J., Xing, H., and Li, C. (2019). Long noncoding RNA TP73-AS1 accelerates the epithelial ovarian cancer via epigenetically repressing p21. *Am. J. Transl. Res.* 11, 2447–2454.

Li, Z., Niu, H., Qin, Q., Yang, S., Wang, Q., Yu, C., et al. (2019). lncRNA UCA1 mediates resistance to cisplatin by regulating the mir-143/FOSL2-signaling pathway in ovarian cancer. *Mol. Ther. Nucleic Acids* 17, 92–101. doi: 10.1016/j.omtn.2019.05.007

Li, Z. Y., Wang, X. L., Dang, Y., Zhu, X. Z., Zhang, Y. H., Cai, B. X., et al. (2020). Long non-coding RNA UCA1 promotes the progression of paclitaxel resistance in ovarian cancer by regulating the miR-654-5p/SIK2 axis. *Eur. Rev. Med. Pharmacol. Sci.* 24, 591–603. doi: 10.26355/eurrev_202001_20035

Liu, D., and Li, H. (2019). Long non-coding RNA GEHT1 promoted the proliferation of ovarian cancer cells via modulating the protein stability of HIF1α. *Biosci. Rep.* 39:BSR20181650. doi: 10.1042/BSR20181650

Long, X., Song, K., Hu, H., Tian, Q., Wang, W., Dong, Q., et al. (2019). Long non-coding RNA GAS5 inhibits DDP-resistance and tumor progression of epithelial ovarian cancer via GAS5-E2F4-PARP1-MAPK axis. *J. Exp. Clin. Cancer Res.* 38:345. doi: 10.1186/s13046-019-1329-2

Luo, P., Liu, X. F., Wang, Y. C., Li, N. D., Liao, S. J., Yu, M. X., et al. (2017). Prognostic value of abnormally expressed lncRNAs in ovarian carcinoma: a systematic review and meta-analysis. *Oncotarget* 8, 23927–23936. doi: 10.18632/oncotarget.14760

Mao, B., Zhang, Z., and Wang, G. (2015). BTG2: a rising star of tumor suppressors (review). *Int. J. Oncol.* 46, 459–464. doi: 10.3892/ijo.2014.2765

Marchese, F. P., Raimondi, I., and Huarte, M. (2017). The multidimensional mechanisms of long noncoding RNA function. *Genome Biol.* 18:206. doi: 10.1186/s13059-017-1348-2

Maru, Y., and Hippo, Y. (2019). Current status of patient-derived ovarian cancer models. *Cells* 8:505. doi: 10.3390/cells8050505

Matsuura, K., Canfield, K., Feng, W., and Kurokawa, M. (2016). Metabolic regulation of apoptosis in cancer. *Int. Rev. Cell Mol. Biol.* 327, 43–87. doi: 10.1016/bs.ircmb.2016.06.006

Misawa, A., Takayama, K. I., and Inoue, S. (2017). Long non-coding RNAs and prostate cancer. *Cancer Sci.* 108, 2107–2114. doi: 10.1111/cas.13352

Mitobe, Y., Takayama, K. I., Horie-Inoue, K., and Inoue, S. (2018). Prostate cancer-associated lncRNAs. *Cancer Lett.* 418, 159–166. doi: 10.1016/j.canlet.2018.01.012

Momenimovahed, Z., Tiznobaik, A., Taheri, S., and Salehiniya, H. (2019). Ovarian cancer in the world: epidemiology and risk factors. *Int. J. Womens Health* 11, 287–299. doi: 10.2147/IJWH.S197604

Motta, P. M., Makabe, S., and Nottola, S. A. (1997). The ultrastructure of human reproduction. I. The natural history of the female germ cell: origin, migration and differentiation inside the developing ovary. *Hum. Reprod. Update* 3, 281–295. doi: 10.1093/humupd/3.3.281

Namekawa, T., Ikeda, K., Horie-Inoue, K., and Inoue, S. (2019). Application of prostate cancer models for preclinical study: advantages and limitations of cell lines, patient-derived xenografts, and three-dimensional culture of patient-derived cells. *Cells* 8:74. doi: 10.3390/cells8010074

Pistritto, G., Trisciuoglio, D., Ceci, C., Garufi, A., and D'Orazi, G. (2016). Apoptosis as anticancer mechanism: function and dysfunction of its modulators and targeted therapeutic strategies. *Aging (Albany NY)* 8, 603–619. doi: 10.18632/aging.100934

Qiu, J. J., Wang, Y., Ding, J. X., Jin, H. Y., Yang, G., and Hua, K. Q. (2015). The long non-coding RNA HOTAIR promotes the proliferation of serous ovarian cancer cells through the regulation of cell cycle arrest and apoptosis. *Exp. Cell Res.* 333, 238–248. doi: 10.1016/j.yexcr.2015.03.005

Qu, C., Dai, C., Guo, Y., Qin, R., and Liu, J. (2020). Long non-coding RNA PVT1-mediated miR-543/SERPINI1 axis plays a key role in the regulatory mechanism of ovarian cancer. *Biosci. Rep.* 40:BSR20200800. doi: 10.1042/BSR20200800

Rojas, V., Hirshfield, K. M., Ganesan, S., and Rodriguez-Rodriguez, L. (2016). Molecular characterization of epithelial ovarian cancer: implications for diagnosis and treatment. *Int. J. Mol. Sci.* 17:2113. doi: 10.3390/ijms17122113

Ruan, Z., and Zhao, D. (2019). Long intergenic noncoding RNA LINC00284 knockdown reduces angiogenesis in ovarian cancer cells. *FASEB J.* 33, 12047–12059. doi: 10.1096/fj.201900101RR

Rupaimoole, R., Lee, J., Haemmerle, M., Ling, H., Previs, R. A., Pradeep, S., et al. (2015). Long noncoding RNA ceruloplasmin promotes cancer growth by altering glycolysis. *Cell Rep.* 13, 2395–2402. doi: 10.1016/j.celrep.2015.11.047

Salamini-Montemurri, M., Lamas-Maceiras, M., Barreiro-Alonso, A., Vizoso-Vázquez, Á, Rodríguez-Belmonte, E., Quindós-Varela, M., et al. (2020). The challenges and opportunities of lncRNAs in ovarian cancer research and clinical use. *Cancers (Basel)* 12:1020. doi: 10.3390/cancers12041020

Shiba, S., Ikeda, K., Suzuki, T., Shintani, D., Okamoto, K., Horie-Inoue, K., et al. (2019). Hormonal regulation of patient-derived endometrial cancer stem-like

cells generated by three-dimensional culture. *Endocrinology* 160, 1895–1906. doi: 10.1210/en.2019-00362

Si, W., Shen, J., Zheng, H., and Fan, W. (2019). The role and mechanisms of action of microRNAs in cancer drug resistance. *Clin. Epigenetics* 11:25. doi: 10.1186/s13148-018-0587-8

Siegel, R. L., Miller, K. D., and Jemal, A. (2018). Cancer statistics, 2018. *CA Cancer J. Clin.* 68, 7–30. doi: 10.3322/caac.21442

Sun, Z., Gao, S., Xuan, L., and Liu, X. (2020). Long non-coding RNA FEZF1-AS1 induced progression of ovarian cancer via regulating miR-130a-5p/SOX4 axis. *J. Cell. Mol. Med.* 24, 4275–4285. doi: 10.1111/jcmm.15088

Takayama, K., and Inoue, S. (2016). The emerging role of noncoding RNA in prostate cancer progression and its implication on diagnosis and treatment. *Brief. Funct. Genomics* 15, 257–265. doi: 10.1093/bfgp/elv057

Takeiwa, T., Ikeda, K., Mitobe, Y., Horie-Inoue, K., and Inoue, S. (2020). Long noncoding rnas involved in the endocrine therapy resistance of breast cancer. *Cancers (Basel)* 12:1424. doi: 10.3390/cancers12061424

Tao, P., Yang, B., Zhang, H., Sun, L., Wang, Y., and Zheng, W. (2020). The overexpression of lncRNA MEG3 inhibits cell viability and invasion and promotes apoptosis in ovarian cancer by sponging miR-205-5p. *Int. J. Clin. Exp. Pathol.* 13, 869–879.

Torre, L. A., Trabert, B., DeSantis, C. E., Miller, K. D., Samimi, G., Runowicz, C. D., et al. (2018). Ovarian cancer statistics, 2018. *CA Cancer J. Clin.* 68, 284–296. doi: 10.3322/caac.21456

Trinidad, C. V., Tetlow, A. L., Bantis, L. E., and Godwin, A. K. (2020). Reducing ovarian cancer mortality through early detection: approaches using circulating biomarkers. *Cancer Prev. Res. (Phila.)* 13, 241–252. doi: 10.1158/1940-6207.CAPR-19-0184

van den Brand, D., Mertens, V., Massuger, L. F. A. G., and Brock, R. (2018). siRNA in ovarian cancer – delivery strategies and targets for therapy. *J. Control. Release* 283, 45–58. doi: 10.1016/j.jconrel.2018.05.012

Vaskivuo, T. E., and Tapanainen, J. S. (2003). Apoptosis in the human ovary. *Reprod. Biomed. Online* 6, 24–35. doi: 10.1016/s1472-6483(10)62052-4

Verhoeven, Y., Tilborghs, S., Jacobs, J., De Waele, J., Quatannens, D., Deben, C., et al. (2020). The potential and controversy of targeting STAT family members in cancer. *Semin. Cancer Biol.* 60, 41–56. doi: 10.1016/j.semcancer.2019.10.002

Virant-Klun, I. (2015). Postnatal oogenesis in humans: a review of recent findings. *Stem Cells Cloning* 8, 49–60. doi: 10.2147/SCCAA.S32650

Wang, H., Su, H., and Tan, Y. (2020). UNC5B-AS1 promoted ovarian cancer progression by regulating the H3K27me on NDRG2 via EZH2. *Cell Biol. Int.* 44, 1028–1036. doi: 10.1002/cbin.11300

Wang, J., Ye, C., Liu, J., and Hu, Y. (2018). UCA1 confers paclitaxel resistance to ovarian cancer through miR-129/ABCB1 axis. *Biochem. Biophys. Res. Commun.* 501, 1034–1040. doi: 10.1016/j.bbrc.2018.05.104

Wang, W., Qin, J. J., Voruganti, S., Nag, S., Zhou, J., and Zhang, R. (2015). Polycomb group (PcG) proteins and human cancers: multifaceted functions and therapeutic implications. *Med. Res. Rev.* 35, 1220–1267. doi: 10.1002/med.21358

Wang, Y., Wang, H., Song, T., Zou, Y., Jiang, J., Fang, L., et al. (2015). HOTAIR is a potential target for the treatment of cisplatin-resistant ovarian cancer. *Mol. Med. Rep.* 12, 2211–2216. doi: 10.3892/mmr.2015.3562

Wong, R. S. (2011). Apoptosis in cancer: from pathogenesis to treatment. *J. Exp. Clin. Cancer Res.* 30:87. doi: 10.1186/1756-9966-30-87

Woo, S. M., and Kwon, T. K. (2019). E3 ubiquitin ligases and deubiquitinases as modulators of TRAIL-mediated extrinsic apoptotic signaling pathway. *BMB Rep.* 52, 119–126. doi: 10.5483/BMBRep.2019.52.2.011

Wu, D. D., Chen, X., Sun, K. X., Wang, L. L., Chen, S., and Zhao, Y. (2017). Role of the lncRNA ABHD11-AS1 in the tumorigenesis and progression of epithelial ovarian cancer through targeted regulation of RhoC. *Mol. Cancer* 16:138. doi: 10.1186/s12943-017-0709-5

Xu, H., Sun, X., Huang, Y., Si, Q., and Li, M. (2020). Long non-coding RNA NEAT1 modifies cell proliferation, colony formation, apoptosis, migration and invasion via the miR-4500/BZW1 axis in ovarian cancer. *Mol. Med. Rep.* 22, 3347–3357. doi: 10.3892/mmr.2020.11408

Yadav, P. K., Tiwari, M., Gupta, A., Sharma, A., Prasad, S., Pandey, A. N., et al. (2018). Germ cell depletion from mammalian ovary: possible involvement of apoptosis and autophagy. *J. Biomed. Sci.* 25:36. doi: 10.1186/s12929-018-0438-0

Yang, L., Chen, J., Huang, X., Zhang, E., He, J., and Cai, Z. (2018). Novel insights into E3 ubiquitin ligase in cancer chemoresistance. *Am. J. Med. Sci.* 355, 368–376. doi: 10.1016/j.amjms.2017.12.012

Yang, Y., Kitagaki, J., Wang, H., Hou, D. X., and Perantoni, A. O. (2009). Targeting the ubiquitin-proteasome system for cancer therapy. *Cancer Sci.* 100, 24–28. doi: 10.1111/j.1349-7006.2008.01013.x

Ye, F., Chen, C., Qin, J., Liu, J., and Zheng, C. (2015). Genetic profiling reveals an alarming rate of cross-contamination among human cell lines used in China. *FASEB J.* 29, 4268–4272. doi: 10.1096/fj.14-266718

Yu, Y., Zhang, X., Tian, H., Zhang, Z., and Tian, Y. (2018). Knockdown of long non-coding RNA HOTAIR increases cisplatin sensitivity in ovarian cancer by inhibiting cisplatin-induced autophagy. *J. BUON* 23, 1396–1401.

Zeng, X. Y., Jiang, X. Y., Yong, J. H., Xie, H., Yuan, J., Zeng, D., et al. (2019). lncRNA ABHD11-AS1, regulated by the EGFR pathway, contributes to the ovarian cancer tumorigenesis by epigenetically suppressing TIMP2. *Cancer Med.* 8, 7074–7085. doi: 10.1002/cam4.2586

Zhang, H. G., Wang, J., Yang, X., Hsu, H. C., and Mountz, J. D. (2004). Regulation of apoptosis proteins in cancer cells by ubiquitin. *Oncogene* 23, 2009–2015. doi: 10.1038/sj.onc.1207373

Zhang, Y., Ai, H., Fan, X., Chen, S., Wang, Y., and Liu, L. (2020). Knockdown of long non-coding RNA HOTAIR reverses cisplatin resistance of ovarian cancer cells through inhibiting miR-138-5p-regulated EZH2 and SIRT1. *Biol. Res.* 53:18. doi: 10.1186/s40659-020-00286-3

Zhang, Z., Cheng, J., Wu, Y., Qiu, J., Sun, Y., and Tong, X. (2016). LncRNA HOTAIR controls the expression of Rab22a by sponging miR-373 in ovarian cancer. *Mol. Med. Rep.* 14, 2465–2472. doi: 10.3892/mmr.2016.5572

Zhao, H., Yu, H., Zheng, J., Ning, N., Tang, F., Yang, Y., et al. (2018). Lowly-expressed lncRNA GAS5 facilitates progression of ovarian cancer through targeting miR-196-5p and thereby regulating HOXA5. *Gynecol. Oncol.* 151, 345–355. doi: 10.1016/j.ygyno.2018.08.032

Zhou, J., Schmid, T., Schnitzer, S., and Brüne, B. (2006). Tumor hypoxia and cancer progression. *Cancer Lett.* 237, 10–21. doi: 10.1016/j.canlet.2005.05.028

Zhu, M., Yang, L., and Wang, X. (2020). NEAT1 knockdown suppresses the cisplatin resistance in ovarian cancer by regulating miR-770-5p/PARP1 axis. *Cancer Manag. Res.* 12, 7277–7289. doi: 10.2147/CMAR.S257311

Conflict of Interest: The authors declare that the research was conducted in the absence of any commercial or financial relationships that could be construed as a potential conflict of interest.

frontiers in Cell and Developmental Biology

ORIGINAL RESEARCH
published: 11 May 2021
doi: 10.3389/fcell.2021.642916

Hsa-miR-100-3p Controls the Proliferation, DNA Synthesis, and Apoptosis of Human Sertoli Cells by Binding to SGK3

*Bang Liu, Yinghong Cui, Wei Chen, Li Du, Chunyun Li, Cailin Wan and Zuping He**

The Key Laboratory of Model Animals and Stem Cell Biology in Hunan Province, School of Medicine, Hunan Normal University, Changsha, China

Human Sertoli cell is required for completing normal spermatogenesis, and significantly, it has important applications in reproduction and regenerative medicine because of its great plasticity. Nevertheless, the molecular mechanisms underlying the fate decisions of human Sertoli cells remain to be clarified. Here, we have demonstrated the expression, function, and mechanism of Homo sapiens-microRNA (hsa-miR)-100-3p in human Sertoli cells. We revealed that miR-100-3p was expressed at a higher level in human Sertoli cells by 10% fetal bovine serum (FBS) than 0.5% FBS. MiR-100-3p mimics enhanced the DNA synthesis and the proliferation of human Sertoli cells, as indicated by 5-ethynyl-2′-deoxyuridine (EdU) and Cell Counting Kit-8 (CCK-8) assays. Flow cytometry showed that miR-100-3p mimics reduced the apoptosis of human Sertoli cells, and notably, we predicted and further identified serum/glucocorticoid regulated kinase family member 3 (SGK3) as a direct target of MiR-100-3p. SGK3 silencing increased the proliferation and decreased the apoptosis of human Sertoli cells, while SGK3 siRNA 3 assumed a similar role to miR-100-3p mimics in human Sertoli cells. Collectively, our study indicates that miR-100-3p regulates the fate decisions of human Sertoli cells by binding to SGK3. This study is of great significance, since it provides the novel epigenetic regulator for the proliferation and apoptosis of human Sertoli cells and it may offer a new clue for gene therapy of male infertility.

Keywords: human Sertoli cells, hsa-miR-100-3p, proliferation, apoptosis, SGK3

OPEN ACCESS

Edited by:
Tang Zhonglin, Agricultural Genomics Institute at Shenzhen, Chinese Academy of Agricultural Sciences, China

Reviewed by:
Elena Goncharova, University of California, Davis, United States
Gang Zhang, Qingdao University, China

***Correspondence:**
Zuping He
zupinghe@hunnu.edu.cn

Specialty section:
This article was submitted to Cell Growth and Division, a section of the journal Frontiers in Cell and Developmental Biology

Received: *17 December 2020*
Accepted: *31 March 2021*
Published: *11 May 2021*

Citation:
Liu B, Cui Y, Chen W, Du L, Li C, Wan C and He Z (2021) Hsa-miR-100-3p Controls the Proliferation, DNA Synthesis, and Apoptosis of Human Sertoli Cells by Binding to SGK3. Front. Cell Dev. Biol. 9:642916. doi: 10.3389/fcell.2021.642916

INTRODUCTION

Abnormal spermatogenesis causes male infertility. Sertoli cell is one of the most important somatic cells within the testis because it is essential for regulating normal spermatogenesis and male germ cell development. In anatomical structure, the Sertoli cell is surrounded by male germ cells in the seminiferous tubules, and it directly contacts with male germ cells of different stages. Sertoli cell is tightly linked by multiprotein complexes that constitute the blood–testis barrier (BTB), which protects male germ cells from immunological rejection (Shi et al., 2018). Besides, Sertoli cell can provide a number of growth factors for the signaling transduction of male germ cells (Hofmann, 2008), e.g., bone morphogenetic protein 4 (BMP4), stem cell factor (SCF), glial cell-derived neurotrophic factor (GDNF), and fibroblast growth factor 2 (FGF2). Androgen receptor (AR)

is specifically expressed in Sertoli cell, and its functional failure leads to immature Sertoli cells and spermatogenesis arrest (Singh et al., 1995; Meachem et al., 1997; Meroni et al., 2019). Finally, Sertoli cells can remove apoptotic germ cells with an aim to retain the homeostasis of the testis (Gong et al., 2018). Significantly, recent studies demonstrate that Sertoli cells have the potential to become the cells of other lineages, including the induced pluripotent stem (iPS) cells, neural stem cells (Alamoudi et al., 2018), and Leydig cells (Fu et al., 2019), reflecting that Sertoli cells might have significant applications in cell transplantation and tissue engineering for human diseases.

MicroRNA (known as the miRNA) has been demonstrated to play essential roles in mediating cellular proliferation, differentiation, transdifferentiation, and apoptosis. We have recently demonstrated that a number of miRNAs regulate the fate decisions of human spermatogonial stem cell (SSC). For example, miR-1908-3p controls human SSC renewal and apoptosis by binding to Kruppel-like factor 2 (KLF2) (Chen et al., 2020), while miR-122-5p regulates human SSC fate decisions *via* targeting casitas B-lineage lymphoma (CBL) (Zhou et al., 2020). Moreover, we have revealed that P21-activated kinase 1 (PAK1)/miR-31-5p controls human SSC proliferation and the apoptosis *via* targeting juxtaposed with another zinc finger protein 1 (JAZF1) (Fu et al., 2019), and miR-663a mediates human SSC proliferation and apoptosis by targeting transcription factor nuclear factor I X-type (NFIX) (Zhou et al., 2018). We have also compared the global miRNA profiles in human spermatogonia, pachytene spermatocytes, and spermatids between normal men and non-obstructive azoospermia patients (Yao et al., 2017). Nevertheless, the roles and molecular mechanisms of miRNAs in mediating human Sertoli cell remain elusive. It has been reported that miR-638 suppresses the growth of immature Sertoli cells by regulating sperm-associated antigen 1 (SPAG1) (Hu et al., 2017). MiR-130a has been shown to stimulate the proliferation of the immature porcine Sertoli cells *via* the activation of SMAD5 (Luo et al., 2020), while miR-320-3p is specifically expressed in mouse Sertoli cells and it reduces the lactate production of Sertoli cells through suppressing the level of glucose transporter 3 (Zhang et al., 2018). Recently, we have revealed the expression and the effect of miR-202-3p on regulating human Sertoli cells (Yang et al., 2019). These studies indicate that miRNA may be involved in controlling the fate determinations of Sertoli cells. It is well known that 10% fetal bovine serum (FBS) can significantly promote the proliferation of human Sertoli cells. Therefore, we compared the miRNA expression profiles in human Sertoli cells between 10% FBS and 0.5% FBS with an aim to identify novel miRNAs that could promote the proliferation of human Sertoli cells, and we revealed that miR-100-3p was expressed at a higher level in human Sertoli cells by 10% FBS than 0.5% FBS. In this study, we have uncovered that has-miR-100-3p promotes the proliferation and DNA synthesis and that it inhibits the apoptosis of human Sertoli cells by binding to serum/glucocorticoid regulated kinase family member 3 (SGK3). Thus, this study offers new epigenetic mechanisms controlling human Sertoli cell fate decisions, and importantly, it might provide new biomarkers for the treatment of male infertility.

MATERIALS AND METHODS

Culture of Human Sertoli Cells

We isolated human Sertoli cells from six obstructive azoospermia (OA) patient testicular tissues by the two steps enzymatic digestion followed by differential plating (Yang et al., 2019). Human Sertoli cells were seeded onto the culture dish, and they were cultured with Dulbecco's modified Eagle's medium (DMEM)/F12 (Gibco, United States) by the addition of 10% FBS (Gibco, United States) and 1% penicillin and streptomycin (Gibco, United States) at 34°C in 5% CO_2 incubator. This study was approved by the Institutional Ethical Review Committee of Hunan Normal University, and an informed consent of testis tissues for research only was obtained from each OA patient.

RNA Extraction and RT-PCR

We extracted total RNA from human Sertoli cells when they were cultured with 10% or 0.5% FBS for 3 h, respectively, by the RNAiso Plus reagent (Takara, Japan). NanoDrop (Thermo Fisher Scientific, United States) was utilized to determine the concentrations of total RNA, and RNA with good quality was employed for RT-PCR. We performed RT of RNA to obtain the cDNA by the First Strand cDNA Synthesis Kit (Thermo Fisher Scientific, United States) and PCR reaction of the cDNA in terms of the protocol (Yang et al., 2014). We chose the following gene primers, including Wilms' tumor gene 1 (WT1), GATA binding protein 4 (GATA4), GDNF, SCF, follicle-stimulating hormone receptor (FSHR), SRY-related high-mobility group-box gene 9 (SOX9), AR, and FGF2, and the sequences of those genes were shown in **Supplementary Table 1**.

The PCR reactions of cDNA were completed for 35 cycles pursuant to the conditions we previously described (Yang et al., 2014). The PCR products were separated by electrophoresis with 2% agarose gels stained with Safer ethidium bromide Alternatives-GelGreen (Biotium, United States). Images were exposed to the Gel Documentation and Image Analysis System ChampGel 5000 (SageCreation, China). No cDNA but with PCR of glyceraldehyde 3-phosphate dehydrogenase (*GAPDH*) primers was used as a negative control.

Real-Time qPCR

The RNAiso Plus reagent (Takara, Japan) was employed to isolate total RNA from human Sertoli cells and these cells without or with the treatment of miR-100-3p mimics, miR-100-3p inhibitor, miRNA mimics control, miRNA inhibitor control, SGK3 siRNAs, or siRNA control. RT reactions were performed for 60 min at 37°C using the mixture consisting of 100 ng RNA, 10 μl 2× TS miRNA Reaction Mix, 1 μl miRNA RT Enzyme Mix, and RNase-free water in a total volume of 20 μl, and heat inactivation of RT was done for 5 s at 85°C in a Veriti 96-Well Thermal Cycler (Bio-Rad, United States). Nuclease-free water was employed to dilute the RT reaction mixture by five times. The miRNA primer sequences for real-time qPCR were shown in **Supplementary Table 1**. Real-time qPCR was performed three times utilizing Power SYBR Green PCR Master Mix (Biosystems, United Kingdom) and a CFX

Connect Real-Time System (Bio-Rad, United States), pursuant to the protocol described previously (Wang et al., 2017). The levels of miRNAs were normalized to U6, and their relative expression was calculated using the $2^{-\Delta\Delta Ct}$ method (Wang et al., 2017).

The levels of *SGK3* gene were measured by real-time qPCR in human Sertoli cells with treatment of miR-100-3p mimics, miRNA mimics control, miR-100-3p inhibitors, miRNA inhibitor control, SGK3-siRNAs, or siRNA control, pursuant to the protocol described previously (Wang et al., 2017). *SGK3* primers were designed and shown in **Supplementary Table 1**, and the relative levels of *SGK3* gene were calculated by the $2^{-\Delta\Delta Ct}$ method after normalization to housekeeping gene *GAPDH* (Wang et al., 2017).

Immunocytochemistry

For the immunocytochemical staining, 4% paraformaldehyde (PFA; Beyotime, China) was used for fixation of human Sertoli cells for 20 min, and 0.5% Triton X-100 (Sigma, United States) was employed to permeabilize these cells for 15 min. These cells were blocked with 5% bovine serum albumin (BSA) for 90 min, and they were incubated with primary antibodies as shown in **Supplementary Table 2** overnight at 4°C. Primary antibodies were replaced with isotype IgGs to serve as negative controls. The secondary antibody IgG (Sigma, United States) with 1:2,000 dilution was used to recognize the primary antibodies. Cell nuclei were labeled by 4′,6-diamidino-2-phenylindole (DAPI), while the images were screened by a fluorescence microscope (Leica, Germany).

Transfection of MiR-100-3p Mimics, MiR-100-3p Inhibitors, or SGK3 siRNAs to Human Sertoli Cells

The mimics, inhibitors, and the controls for miR-100-3p were bought from GenePharma (Shanghai, China). The oligonucleotide sequences for miR-100-3p mimics and inhibitors were shown in **Supplementary Table 3**. Human Sertoli cells were planted to the culture dish at 1×10^5 Sertoli cells/cm^2 density, and they were cultured with DMEM/F12 containing the 10% FBS overnight. Human Sertoli cells were classified into four groups, namely, miR-100-3p mimics, miRNA mimics control, miR-100-3p inhibitor, and miRNA inhibitor control. Similarly, human Sertoli cells were categorized into four groups, including SGK3 siRNA 1, SGK3 siRNA 2, SGK3 siRNA 3, and the control siRNA. Transfection of miR-100-3p mimics, inhibitor, or SGK3 siRNA1-3 was completed, respectively, utilizing Lipofectamine 3000 transfection agent (Life Technologies, Carlsbad, CA, United States). Forty-eight or seventy-two hours after transfection, the cells were used for determining the mRNA or protein levels.

Cell Counting Kit-8 Assay

For the proliferation assay, human Sertoli cells were plated onto 96-well microtiter plates (Corning, United States) at a density of 2,000 Sertoli cells/well, and they were transfected with miR-100-3p mimics, miRNA mimics control, miR-100-3p inhibitor, miRNA inhibitor control, SGK3 siRNA 3, or the control siRNA. After 5 days of culture, Cell Counting Kit-8 (CCK-8) assay (Dojin Laboratories, Japan) was performed to measure human Sertoli cell proliferation pursuant to the manufacturer's direction. The culture medium was changed with 10% CCK-8 solution (Dojin Laboratories, Kumamoto, Japan), and the cells were incubated with it for 3 h. The absorbance was determined at 450 nm by a microplate reader.

Western Blots

Human Sertoli cells were transfected with miR-100-3p mimics, miRNA mimics control, miR-100-3p inhibitor, miRNA inhibitor control, SGK3 siRNAs, or the control siRNA, and the RIPA buffer (Beyotime Biotechnology, China) was used for protein extraction from these cells. Centrifugation of cell lysates was performed at 12,000 × g for 20 min, while the protein concentrations were determined by bicinchoninic acid (BCA) kit (Dingguo, China). Thirty micrograms of cell lysate were employed for Western blots using the antibodies (**Supplementary Table 2**) in terms of the method (He et al., 2007), while the blots were detected with chemiluminescence (SageCreation, China).

5-Ethynyl-20-Deoxyuridine (EdU) Incorporation Assay

In total, 3,000 human Sertoli cells/well were plated onto 96-well plates (Corning, United States) in DMEM/F12 with the addition of 50 mM 5-ethynyl-2′-deoxyuridine (EdU; RiboBio, China). These cells were treated with miRNA mimics control, miR-100-3p mimics, miRNA inhibitor control, miR-100-3p inhibitor, SGK3 siRNA 3, or the control siRNA. We fixed the cells after 12 h of culture with 4% PFA, and they were neutralized by 1.8 mg/ml glycine and permeabilized with 0.5% Triton X-100 for 15 min. Apollo staining reaction buffer was utilized for EdU immunostaining, while Hoechst 33342 was employed for labeling cell nuclei. The EdU-positive cells were calculated from at least 500 cells by fluorescence microscopy (Leica, Germany).

Annexin V and Propidium Iodide Staining and Flow Cytometry

The apoptosis of human Sertoli cells was examined by the allophycocyanin (APC) Annexin V and propidium iodide (PI) apoptosis detection kit (BioLegend, London, United Kingdom) and flow cytometry (BD, United States) after transfecting without or with the treatment of miR-100-3p mimics, miR-100-3p inhibitors, miRNA mimics control, miRNA inhibitor control, SGK3 siRNAs, or the control siRNA. Human Sertoli cells were seeded onto six-well plates (Corning, United States) at a density of 5×10^4 cells/well, and they were collected by centrifuging at 1,000 rpm for 5 min. Meanwhile, the cells were labeled by the non-vital dye PI and Annexin V-fluorescein isothiocyanate (FITC), which was employed to detect different cell populations, including the intact cells (i.e., $FITC^-PI^-$ cells), the early apoptotic cells (i.e., $FITC^+PI^-$ cells), and the late apoptotic cells (i.e., $FITC^+PI^+$ cells).

Terminal Deoxynucleotidyl Transferase dUTP Nick End Labeling Assay

The terminal deoxynucleotidyl transferase dUTP nick end labeling (TUNEL) Apoptosis Detection Kit (Yeasen, China) was utilized to further examine the apoptotic cells. In total, 5×10^4 human Sertoli cells/well were treated with miRNA mimics control, miR-100-3p mimics, miRNA inhibitor control, miR-100-3p inhibitor, SGK3 siRNA 3, or the control siRNA, and 4% PFA was used for fixing these cells for 30 min at 4°C. After extensive washes by phosphate buffered saline (PBS), the cells were treated with 20 mg/ml Proteinase K, 1× DNaseI Buffer for 6 min and 10 U/ml DNaseI for 10 min, and they were washed with deionized water and incubated with 1× Equilibration Buffer for 30 min. These cells were stained with Alexa Fluor 647 in buffer mixed with TdT Enzyme for 70 min at 37°C. After extensive washes by PBS, DAPI was used for labeling the cell nuclei, and the TUNEL-positive cells were counted by the fluorescence microscope (Leica, Germany).

Dual Luciferase Assay

A total of 3,000 human Sertoli cells were seeded onto 96-well plates (Corning, United States). After 24 h of culture, Lipofectamine 3000 transfection agent (Sigma, United States) was employed to transfect miR-100-3p mimics or the mimics control to these cells. Forty-eight hours later, human Sertoli cells were transfected with 500 ng plasmids containing the binding sequence in 3′ untranslated regions (UTRs) of SGK3, firefly luciferase (reporter), or the renilla luciferase (internal control) (Genecreate, China) using the Lipofectamine 3000 reagent (Sigma, United States). Forty-eight hours after transfection, human Sertoli cells were lysed, and luciferase activity was determined using the 96-well plate luminometer (Corning, United States). The results were normalized to cells transfected with miRNA mimics control.

Statistical Analysis

All results were shown as the mean ± SEM. Comparisons between two groups were performed using the unpaired *t*-test, and *P*-value < 0.05 was regarded as statistically significant. Each experiment was conducted at least three times independently.

RESULTS

Biochemical Phenotype of Primary Human Sertoli Cells

We first verified the identity of the cells used in this study using numerous markers for human primary Sertoli cell. The transcripts of *GDNF*, *GATA4*, *WT1*, *SCF*, *FSHR*, *SOX9*, *AR*, and *FGF2* were detected in the isolated human cells (**Figure 1A**) as shown by RT-PCR. No PCR product was detected in the no cDNA samples but with PCR by the primers of *GAPDH*. Furthermore, immunocytochemistry showed that the cells were positively stained for WT1 (**Figure 1B**), GDNF (**Figure 1C**), GATA4 (**Figure 1D**), SCF (**Figure 1E**), and SOX9 (**Figure 1F**). No immunostaining was seen in the cells when the isotype IgGs were used for the replacement of primary antibodies (**Figure 1G**),

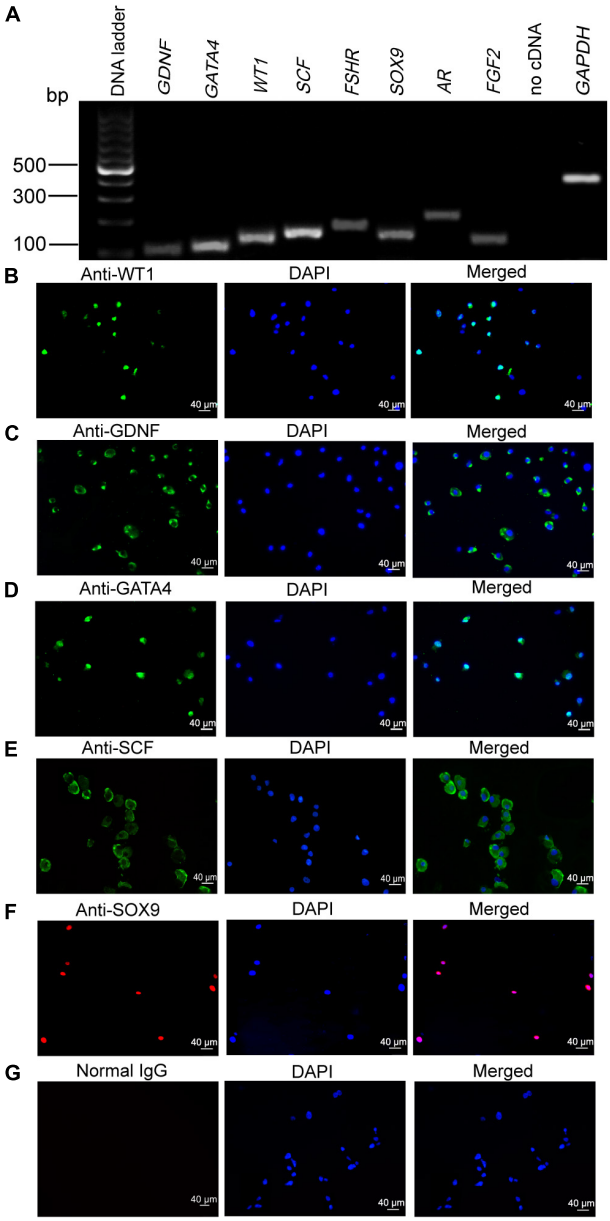

FIGURE 1 | Phenotype of human Sertoli cells. **(A)** The transcripts of glial cell-derived neurotrophic factor (*GDNF*), GATA binding protein 4 (*GATA4*), Wilms' tumor gene 1 (*WT1*), stem cell factor (*SCF*), follicle-stimulating hormone receptor (*FSHR*), SRY-related high-mobility group-box gene 9 (*SOX9*), androgen receptor (*AR*), and fibroblast growth factor 2 (*FGF2*) were detected by RT-PCR in human Sertoli cells. Housekeeping gene glyceraldehyde 3-phosphate dehydrogenase (*GAPDH*) was used to be the RNA loading control. **(B–G)** Immunocytochemistry revealed the positive cells of WT1 **(B)**, GDNF **(C)**, GATA4 **(D)**, SCF **(E)**, SOX9 **(F)**, and isotype IgGs **(G)** in human Sertoli cells. Scale bar in panels **(B–G)** = 40 μm.

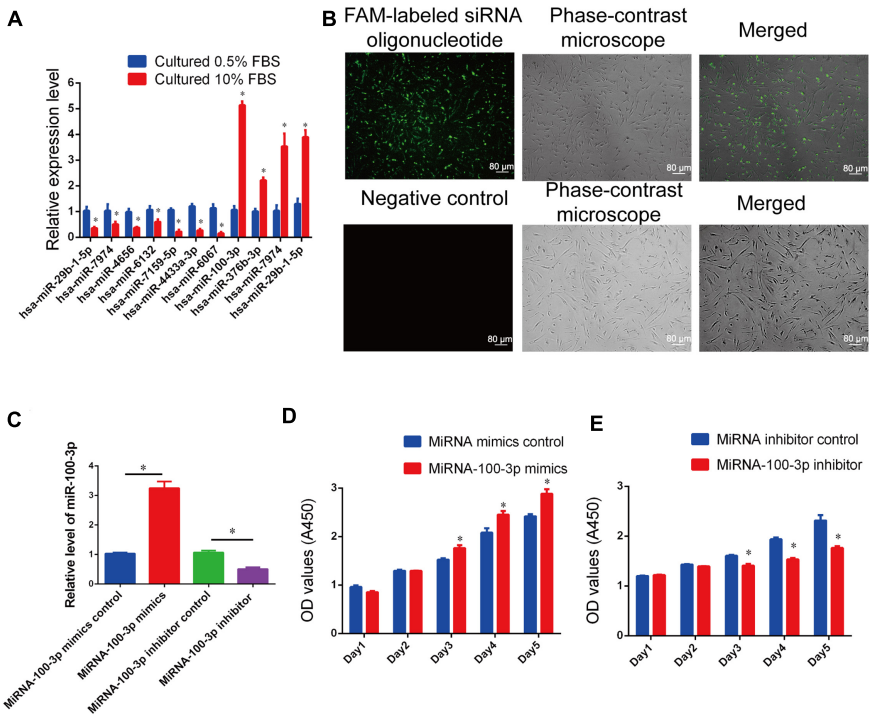

FIGURE 2 | MiR-100-3p controls human Sertoli cell proliferation. **(A)** Real-time qPCR showed the relative expression levels of Homo sapiens-microRNA (hsa-miR)-29b-1-5p, hsa-miR-7974, hsa-miR-4656, hsa-miR-6132, hsa-miR-7159-5p, hsa-miR-4433a-3p, hsa-miR-6067, hsa-miR-100-3p, hsa-miR-376b-3p, hsa-miR-7974, and hsa-miR-29b-1-5p in human Sertoli cells by 10% fetal bovine serum (FBS) compared with 0.5% FBS. **(B)** The transfection efficiency of miR-100-3p mimics and inhibitor was evaluated by fluorescence microscope and phase-contrast microscope. Scale bar = 80 μm. **(C)** The relative expression levels of miR-100-3p in human Sertoli cells treated with miR-100-3p mimics or inhibitor. **(D,E)** The cell growth of human Sertoli cells treated with miR-100-3p mimics **(D)** and miR-100-3p inhibitor **(E)** for 5 days. * denoted the statistical difference between miR-100-3p mimics and miRNA mimics control or miR-100-3p inhibitor and miRNA inhibitor control.

which verified the specific expression of these proteins mentioned above.

Differential Expression of MiR-100-3p in Human Sertoli Cells Between 10% and 0.5% Fetal Bovine Serum

We have found that FBS promotes human Sertoli cell proliferation. To seek novel miRNAs that are involved in the DNA synthesis and proliferation of human Sertoli cells, we compared the differences in the global miRNA profiles of human Sertoli cells cultured in different serum concentrations (10% vs. 0.5% FBS) using miRNA microarrays. The representative miRNAs that were upregulated and downregulated in human Sertoli cells cultured with 10% FBS compared to 0.5% FBS were identified and listed in **Supplementary Table 4**. Among the miRNAs with differential expression (fold changes $\geq$ 1.5 and $p < 0.05$), miR-100-3p was expressed at a higher level in human Sertoli cells by 10% FBS than 0.5% FBS. Real-time qPCR reflected the highest level of miR-100-3p in human Sertoli cells by 10% FBS compared with 0.5% FBS (**Figure 2A**), which was consistent with miR-10-3p expression in human Sertoli cells affected by 10% FBS and 0.5% FBS, as detected by miRNA microarrays. These data suggest that miR-100-3p is involved in regulating the proliferation of human Sertoli cells.

MiR-100-3p Stimulates Human Sertoli Cell Growth and DNA Synthesis

We examined the role of miR-100-3p in regulating human Sertoli cells using miR-100-3p mimics and inhibitors. As shown in **Figure 2B**, the transfection efficiency of miR-100-3p mimics or inhibitors was more than 80% in human Sertoli cells. MiRNA mimics control, miR-100-3p mimics, miRNA inhibitor control, or miR-100-3p inhibitor was transfected to human Sertoli cells by Lipofectamine 3000. Twenty-four hours after transfection, real-time qPCR demonstrated that the level of miR-100-3p was upregulated by miR-100-3p mimics in human Sertoli cells when compared to miRNA mimics control (**Figure 2C**). In contrast, miR-100-3p inhibitor reduced miR-100-3p expression in human Sertoli cells compared to miRNA inhibitor control (**Figure 2C**).

The influence of miR-100-3p on human Sertoli cell proliferation was measured by various kinds of methods. Cell proliferation assays were performed from 1 day to 5 days after transfection of miR-100-3p mimics and miR-100-3p inhibitors, and miR-100-3p mimics increased the numbers of human Sertoli cells compared to miRNA mimics control (**Figure 2D**), whereas miR-100-3p inhibitor reduced the growth of human Sertoli cells when compared with miRNA inhibitor control (**Figure 2E**). The levels of proliferating cell nuclear antigen (PCNA) protein were increased by miR-100-3p mimics

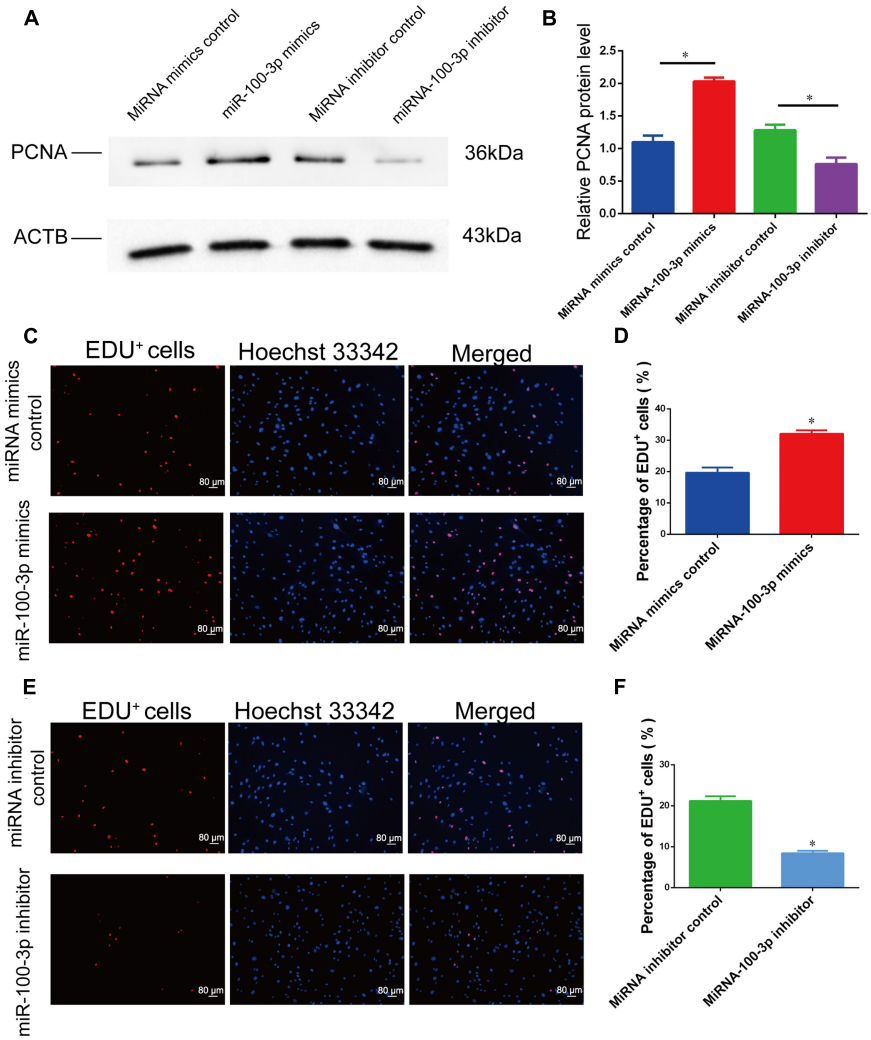

FIGURE 3 | MiR-100-3p affects human Sertoli cell DNA synthesis. **(A)** Proliferating cell nuclear antigen (PCNA) expression was shown by Western blots in human Sertoli cells at 72 h after miR-100-3p mimics or inhibitor transfection. **(B)** The relative expression of PCNA in human Sertoli cells at 72 h after miR-100-3p mimics and inhibitor transfection. **(C–F)** The ratios of 5-ethynyl-2′-deoxyuridine (EdU)-positive cells were illustrated by EdU incorporation assays in human Sertoli cell treatment with miRNA mimics control vs. the miR-100-3p mimics **(C,D)** as well as miR-100-3p inhibitor vs. miRNA inhibitor **(E,F)**. Scale bar in panels **(C,E)** = 80 μm. * indicated the statistical difference between miR-100-3p mimics and miRNA mimics control or miR-100-3p inhibitor and miRNA inhibitor control.

and decreased by miR-100-3p inhibitor, as shown by Western blots (**Figures 3A,B**). The percentages of EdU-positive cells were enhanced by miR-100-3p mimics (**Figures 3C,D**) and decreased by miR-100-3p inhibitor (**Figures 3E,F**), as indicated by EdU incorporation assay. Collectively, these results implicate that miR-100-3p can stimulate human Sertoli cell growth and DNA synthesis.

MiR-100-3p Inhibits Human Sertoli Cell Apoptosis

We further determined the influence of miR-100-3p on human Sertoli cell apoptosis. As shown by APC Annexin V and PI staining and analyzed by flow cytometry, miR-100-3p mimics decreased human Sertoli cell apoptosis vs. miRNA mimics control (**Figures 4A,B**). By contrast, the percentage of human Sertoli cell apoptosis was enhanced by the miR-100-3p inhibitor compared to miRNA inhibitor control (**Figures 4C,D**). The percentages of TUNEL-positive cells were decreased by miR-100-3p mimics and enhanced by miR-100-3p inhibitor, as shown by TUNEL assay (**Figures 4E,F,G,H**). Therefore, our results indicate that miR-100-3p inhibits human Sertoli cell apoptosis.

SGK3 Is a Direct Target of MiR-100-3p in Human Sertoli Cells

We next sought to find miR-100-3p targets in controlling human Sertoli cells. Because miRNAs act *via* their seed sequence through the base-pair binding to the 3′ UTR of mRNAs. We used various kinds of miRNA prediction software (TargetScan, miRwalk, and miRDB) and predicted that SGK3, EBF1, and PSD3 were the potential targets for miR-100-3p (**Figure 5A**).

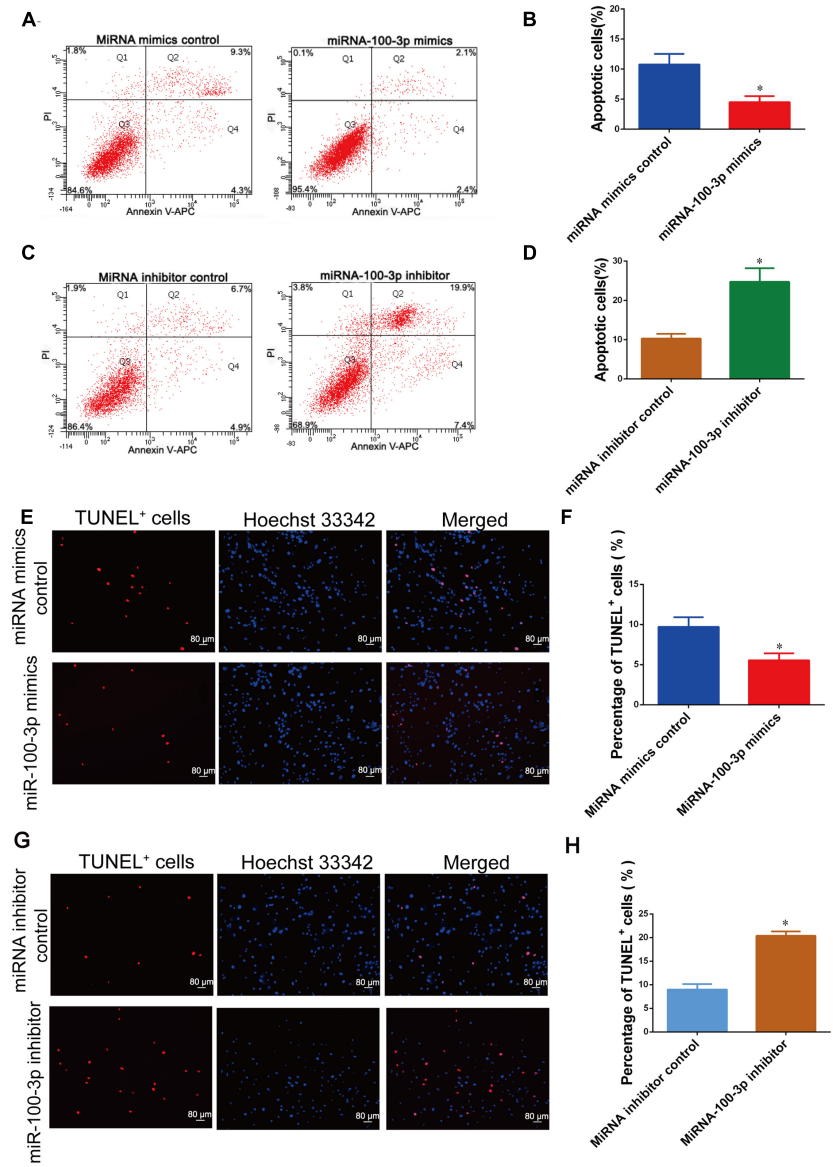

FIGURE 4 | MiR-100-3p inhibits human Sertoli cell apoptosis. **(A–D)** The percentages of human Sertoli cell early and late apoptosis affected by miR-100-3p mimics **(A,B)** and miR-100-3p inhibitor **(C,D)** by comparison to the respective control. **(E–H)** The ratios of terminal deoxynucleotidyl transferase dUTP nick end labeling (TUNEL)-positive cells in human Sertoli cells treated with miR-100-3p mimics and miR-100-3p inhibitor by comparison to the respective control. Scale bar in panels **(E,G)** = 80 μm. * denoted the statistical difference between miR-100-3p mimics and miRNA mimics control or miR-100-3p inhibitor and miRNA inhibitor control.

To determine whether SGK3 is a binding target for miR-100-3p in human Sertoli cells, we performed real-time qPCR and Western blots showing that *SGK3* transcripts were reduced by miR-100-3p mimics but increased by miR-100-3p inhibitors (**Figure 5B**), while SGK3 protein was diminished by miR-100-3p mimics but enhanced by miR-100-3p inhibitor (**Figures 5C,D**). The second to eighth nucleotides (known as the seed region) of miR-100-3p were able to bind to the 3′ UTR sequence of *SGK3* mRNA (**Figure 5E**), and the binding site of *SGK3* mRNA was further illustrated by the dual luciferase assay. The luciferase activity of the fusion genes was reduced by the sequence in 3′ UTR of *SGK3* mRNA in human Sertoli cells by miR-100-3p mimics (**Figure 5F**, left panel), whereas the mutated target sequences had no effect on the luciferase activity (**Figure 5F**, right panel). Considered together, these data indicate that SGK3 may be a direct target for miR-100-3p in human Sertoli cells.

The Effect of Serum/Glucocorticoid Regulated Kinase Family Member 3 Knockdown on the Proliferation and Apoptosis of Human Sertoli Cells

We asked the impact of SGK3 on human Sertoli cell proliferation and apoptosis. We used SGK3 small interfering RNAs (siRNAs),

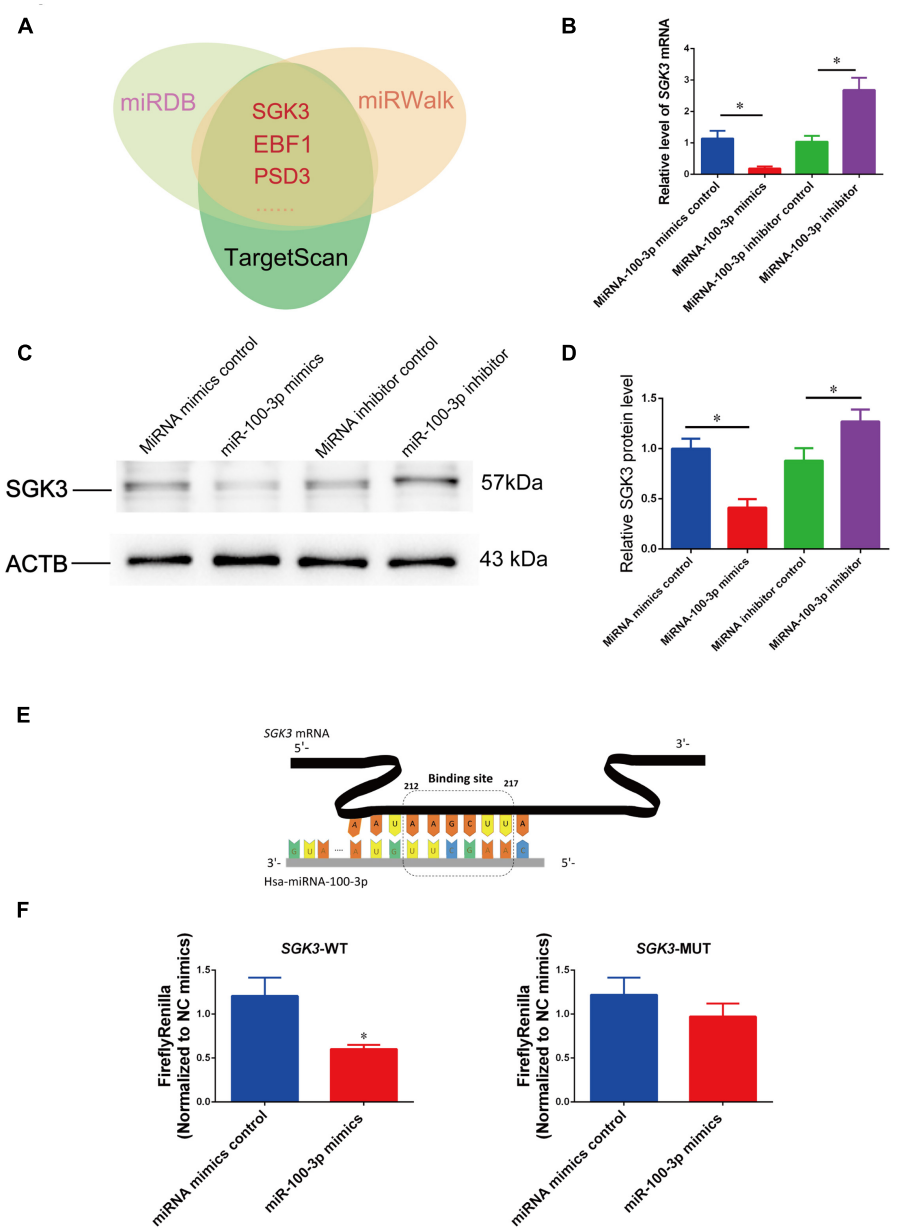

FIGURE 5 | MiR-100-3p binds to serum/glucocorticoid regulated kinase family member 3 (SGK3) in human Sertoli cells. **(A)** MiR-100-3p targets were predicted by three bioinformatics tools. **(B)** The relative levels of *SGK3* mRNA in human Sertoli cells affected by miR-100-3p mimics or miR-100-3p inhibitor by comparison to the respective control. **(C,D)** The relative level of SGK3 in human Sertoli cells at day 3 after transfection of miR-100-3p mimics or miR-100-3p inhibitor after normalization to ACTB (beta-actin). **(E)** Schematic diagram illustrated the binding site of miR-100-3p to *SGK3* mRNA. **(F)** The binding of miR-100-3p to wild-type SGK3 by dual luciferase assays in human Sertoli cells after transfection of miR-100-3p mimics or the miRNA mimics control. * indicated the statistical difference between miR-100-3p mimics and miRNA mimics control or miR-100-3p inhibitor and miRNA inhibitor control.

including SGK3 siRNA 1–3, with different base-pair binding sites, to knock down the SGK3 level of human Sertoli cells. The transfection efficiency of SGK3 siRNAs in human Sertoli cells was more than 80%, as indicated by the transfection of FAM-labeled fluorescent oligo (**Figure 2A**). SGK3 siRNAs could knock down the levels of *SGK3* transcripts and proteins, while SGK3 siRNA 3 had the highest effectiveness for SGK3 silencing (**Figures 6A,B**).

SGK3 siRNA 3 caused the enhancement of human Sertoli cell number from 24 to 120 h of culture (**Figure 6C**). The PCNA protein level (**Figure 6D**) and the ratio of EdU-positive cells (**Figure 6E**) of human Sertoli cells were increased by SGK3 siRNAs, especially by SGK3 siRNA 3. By contrast, SGK3 knockdown reduced the apoptosis of the human Sertoli cells (**Figures 6F,G**). Together, these results reflect that SGK3 silencing stimulates the

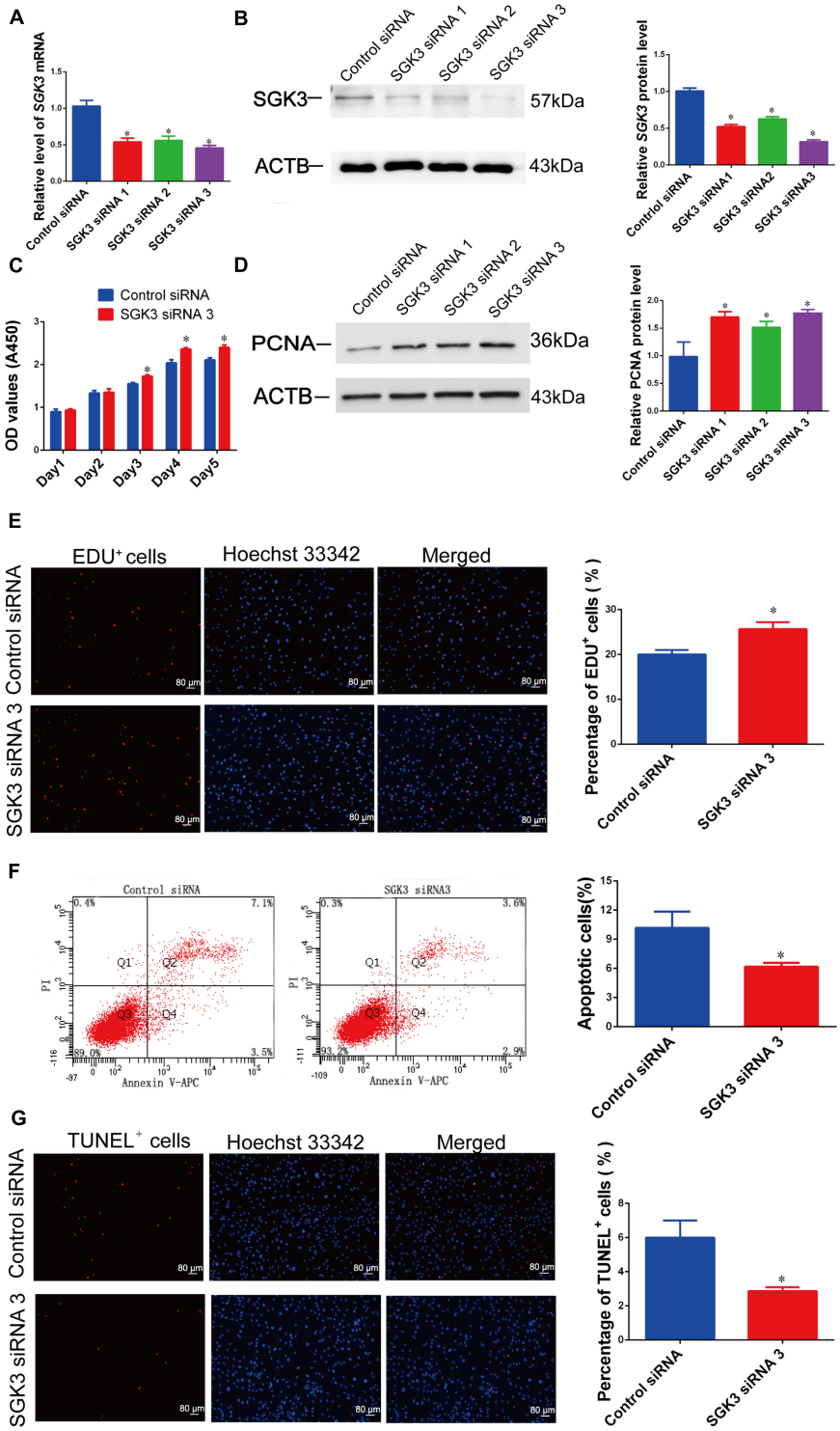

FIGURE 6 | Serum/glucocorticoid regulated kinase family member 3 (SGK3) knockdown regulates human Sertoli cell proliferation, DNA synthesis, and apoptosis. **(A)** The relative levels of *SGK3* mRNA in human Sertoli cells after transfection of SGK3 siRNA 1–3 or the control siRNA. **(B)** The relative level of SGK3 protein in human Sertoli cells after transfection of SGK3 siRNA 1-3 or the control siRNA. **(C)** The cell growth of human Sertoli cells treated with SGK3 siRNA 3 and the control siRNA for 5 days. **(D)** The relative level of proliferating cell nuclear antigen (PCNA) protein in human Sertoli cells at day 3 transfected by SGK3 siRNA 1-3 or the control siRNA. **(E)** The 5-ethynyl-2′-deoxyuridine (EdU)-positive cells of human Sertoli cells treated with SGK3 siRNA 3 or the control siRNA. Scale bar in panel **(E)** = 80 μm. **(F)** The percentages of apoptosis in human Sertoli cells transfected with control siRNA or SGK3 siRNA 3. **(G)** The percentages of terminal deoxynucleotidyl transferase dUTP nick end labeling (TUNEL)-positive cells in human Sertoli cells transfected with control siRNA or SGK3 siRNA 3. Scale bar in panels **(E,G)** = 80 μm. * indicated the statistical difference between SGK3 siRNAs and the control siRNA.

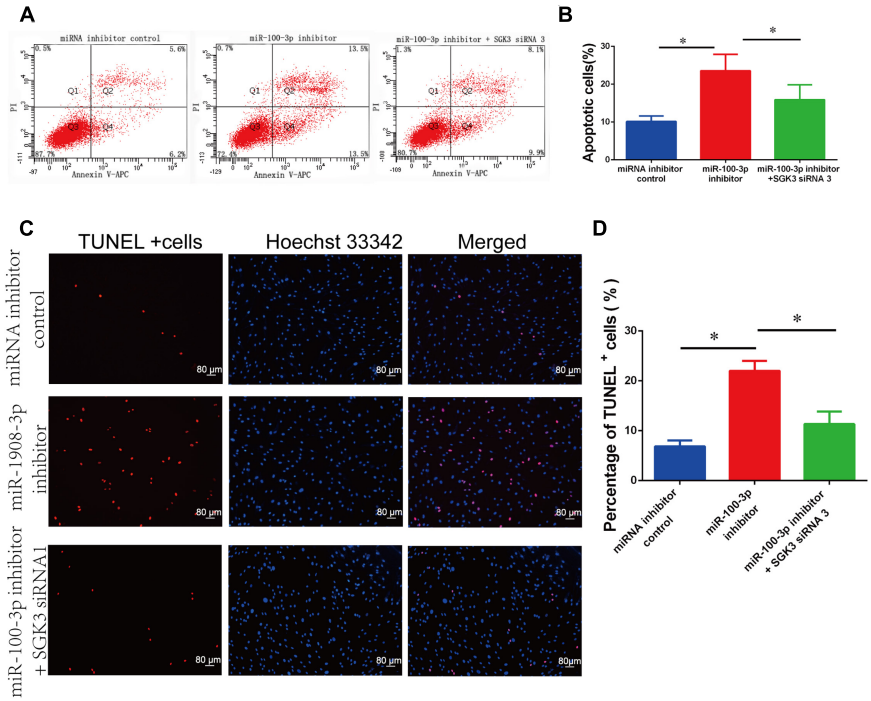

FIGURE 7 | The impact of miR-100-3p and serum/glucocorticoid regulated kinase family member 3 (SGK3) siRNA 3 on the apoptosis of human Sertoli cells. **(A,B)** Allophycocyanin (APC) Annexin V/propidium iodide (PI) staining and flow cytometry showed the apoptotic percentages of human Sertoli cells affected by miRNA inhibitor control, miR-100-3p inhibitor, as well as miR-100-3p inhibitor and SGK3 siRNA 3. **(C,D)** Terminal deoxynucleotidyl transferase dUTP nick end labeling (TUNEL) assay revealed the percentages of TUNEL-positive cells in human Sertoli cells affected by miRNA inhibitor control, miR-100-3p inhibitor, as well as miR-100-3p inhibitor and SGK3 siRNA 3. Scale bar in panel **(C)** = 80 μm. * indicates the statistical differences between miR-100-3p inhibitor and SGK3 siRNA 3 and miR-100-3p inhibitor or between miR-100-3p inhibitor and miRNA inhibitor control.

proliferation and suppresses the apoptosis of human Sertoli cells, which was in accordance with the influence of miR-100-3p mimics.

The Synergetic Effect of MiR-100-3p and Serum/Glucocorticoid Regulated Kinase Family Member 3 SiRNA 3 on the Apoptosis of Human Sertoli Cells

We further inquired whether there was the synergetic effect of miR-100-3p inhibitor and SGK3 siRNA 3 on the apoptosis of human Sertoli cells. MiR-100-3p inhibitor and SGK3 siRNA 3 were co-transfected to these cells with Lipofectamine 3000 reagent. After 48 h of transfection, the number of early and late apoptosis was decreased in human Sertoli cells with the co-transfection of miR-100-3p inhibitor and SGK3 siRNA 3 compared with the cells transfected with miR-100-3p inhibitor (**Figures 7A,B**). TUNEL assay showed that the percentages of TUNEL-positive cells were decreased in human Sertoli cells co-transfected with miR-100-3p inhibitor and SGK3 siRNA 3 when compared to those cells transfected with miR-100-3p inhibitor (**Figures 7C,D**). These data implicate that there is a synergetic effect of miR-100-3p inhibitor and SGK3 siRNA 3 on the apoptosis of human Sertoli cells.

The Synergetic Effect of MiR-100-3p and Serum/Glucocorticoid Regulated Kinase Family Member 3 SiRNA 3 on DNA Synthesis and Proliferation of Human Sertoli Cells

We finally explored the influence of miR-100-3p inhibitor and SGK3 siRNA 3 on the DNA synthesis and proliferation of human Sertoli cells. Western blots showed that the expression levels of SGK3 (**Figures 8A,B**) and PCNA (**Figures 8E,F**) proteins were enhanced in human Sertoli cells with the co-transfection of miR-100-3p inhibitor and SGK3 siRNA 3 compared with the cells transfected with miR-100-3p inhibitor. Similarly, the EdU incorporation assay displayed that the percentages of EdU-positive cells were increased in human Sertoli cells co-transfected with miR-100-3p inhibitor and SGK3 siRNA 3 in comparison to these cells transfected with miR-100-3p inhibitor (**Figures 8C,D**). Together, these results indicate that there is the synergetic influence of miR-100-3p inhibitor and SGK3 siRNA 3 on the DNA synthesis and proliferation of human Sertoli cells.

DISCUSSION

Sertoli cell is required for regulating spermatogenesis because it provides the niche and the nutrition for the proliferation and

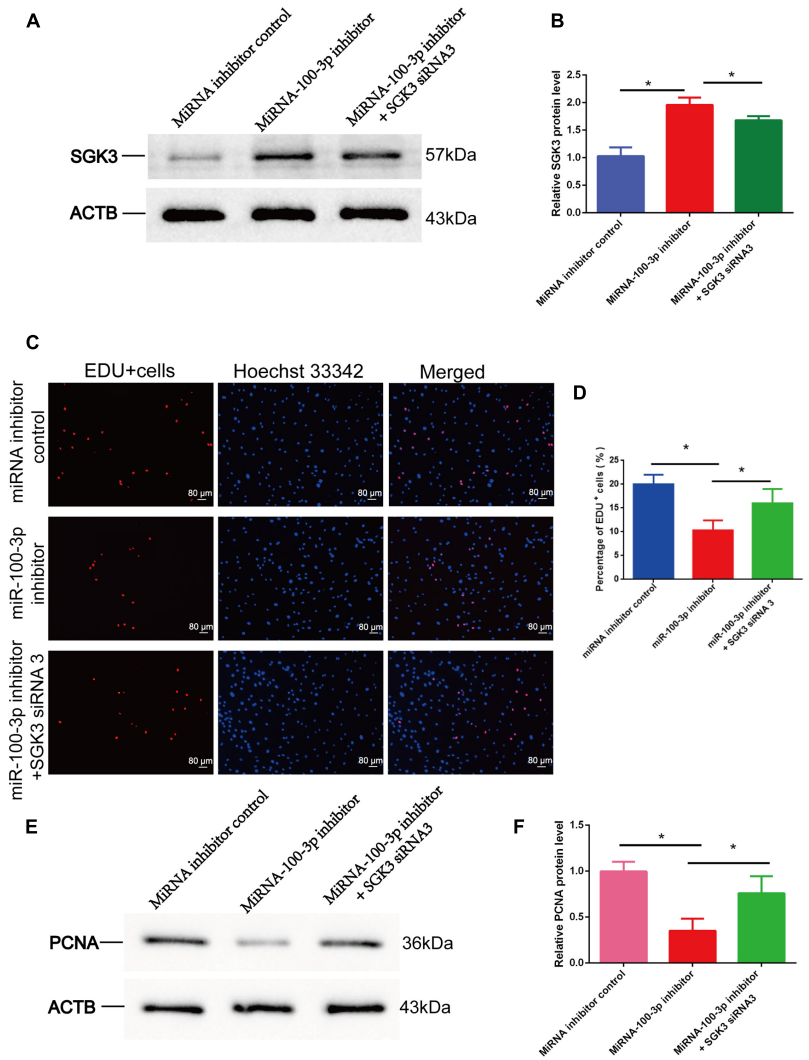

FIGURE 8 | The effect of miR-100-3p and serum/glucocorticoid regulated kinase family member 3 (SGK3) siRNA 3 on the DNA synthesis and proliferation of human Sertoli cells. **(A,B,E,F)** Western blots displayed the expression levels of SGK3 **(A,B)** and proliferating cell nuclear antigen (PCNA) **(E,F)** proteins in human Sertoli cells affected by miRNA inhibitor control, miR-100-3p inhibitor, as well as miR-100-3p inhibitor and SGK3 siRNA 3. **(C,D)** The 5-ethynyl-2′-deoxyuridine (EdU) incorporation assay revealed the percentages of EdU-positive cells in human Sertoli cells affected by miRNA inhibitor control, miR-100-3p inhibitor, as well as miR-100-3p inhibitor and SGK3 siRNA 3. Scale bar in panel **(C)** = 80 μm. * denoted the statistical differences between miR-100-3p inhibitor and SGK3 siRNA 3 and miR-100-3p inhibitor or between miR-100-3p inhibitor and miRNA inhibitor control.

differentiation of male germ cells (Franca et al., 2016). It has been shown that the amount of male germ cells is positively correlated with the number of Sertoli cells (Rebourcet et al., 2017). In addition, Sertoli cell can be reprogrammed to become Leydig cell by Wt1 ablation (Zhang et al., 2015) and neural stem cells (Alamoudi et al., 2018), highlighting that Sertoli cell has significant applications in male reproduction and cell therapy of various diseases. Although great progress has been made in understanding the biology of rodent Sertoli cells, the molecular mechanisms for human Sertoli cell fate decisions, especially epigenetic regulators, are still unknown.

By comparing the expression levels of miRNAs between 0.5% FBS and 10% FBS in human Sertoli cells, we revealed that miR-100-3p was enhanced by 10% FBS, as demonstrated by miRNA microarray and verified by real-time qPCR. MiR-100-3p has been shown to control the proliferation and the apoptosis of human gastric cancer cells *via* binding to bone morphogenic protein type 2 receptor (BMPR2) (Peng et al., 2019), and it may be involved in producing interleukin (IL)-8 and IL-1β in mesangial cells (Liang et al., 2016). In this study, we have shown that miR-100-3p stimulates human Sertoli cell proliferation and DNA synthesis, as determined by CCK-8 assay, PCNA expression, and EdU incorporation assay. We have uncovered that miR-100-3p suppresses human Sertoli cell apoptosis, as indicated by Annexin V and PI staining and flow cytometry as well as TUNEL assay.

Predicted by miRWalk and miRDB software, we assumed that SGK3 is a potential target. Furthermore, we uncovered that the level of SGK3 was reduced by miR-100-3p mimics and increased by miR-100-3p inhibitor, reflecting that SGK3 is the binding target for miR-100-3p in human Sertoli cells. Dual luciferase reporter assays further demonstrated that miR-100-3p is able to bind to SGK3 in human Sertoli cells. SGK3 knockdown led to changes in human Sertoli cell proliferation and apoptosis, which was consistent with the influence of the miR-100-3p mimics. SGK3, belonging to the SGK family of acylglycerol kinase (AGK) kinases, is expressed in many kinds of cells, especially in testis and pancreas, and it exerts broad functions (Lang et al., 2006). It has been shown that SGK3 plays a role as a carcinogen in breast cancer, ovarian cancer, and hepatocellular carcinoma, and it participates in controlling cell survival, differentiation, and material transport (Lang et al., 2006; Wang et al., 2019). SGK3 is composed of a 3′ UTR that is the target seed region of numerous miRNAs. The transcription and location of SGK3 are affected by many factors, e.g., miRNA-335-5p (Yao et al., 2018), and it is involved in many intracellular signaling transduction pathways, including phosphoinositide 3-kinase (PI3K)/AKT pathway (Basnet et al., 2018). In the current study, we identified SGK3 as a direct and binding target of miR-100-3p in human Sertoli cell fate decisions.

In conclusion, we have reported for the first time that miR-100-3p promotes DNA synthesis and proliferation and suppresses the apoptosis of human Sertoli cells. We have also identified that miR-100-3p binds to SGK3 in human Sertoli cells. Therefore, miR-100-3p controls human Sertoli cell proliferation and apoptosis by targeting SGK3. As such, this study offers new mechanisms by uncovering epigenetic regulators for determining the fate determinations of human Sertoli cells. Given the functional importance of miRNAs in mediating human reproduction, our study could provide novel targets for gene therapy of male infertility.

DATA AVAILABILITY STATEMENT

The original contributions presented in the study are included in the article/**Supplementary Material**, and further inquiries can be directed to the corresponding author/s.

AUTHOR CONTRIBUTIONS

BL performed the experiments, analyzed the data, and wrote the manuscript. YC, WC, LD, CL, and CW performed the experiments. ZH designed the study, analyzed the data, and wrote the manuscript. All authors contributed to the article and approved the submitted version.

FUNDING

This work was supported by grants from the National Key R&D Project (2016YFC1000606), National Natural Science Foundation of China (31671550 and 31872845), High Level Talent Gathering Project in Hunan Province (2018RS3066), Major Scientific and Technological Projects for Collaborative Prevention and Control of Birth Defect in Hunan Province (2019SK1012), Key Grant of Research and Development in Hunan Province (2020DK2002), and The Open Fund of the NHC Key Laboratory of Male Reproduction and Genetics (KF201802).

SUPPLEMENTARY MATERIAL

The Supplementary Material for this article can be found online at: https://www.frontiersin.org/articles/10.3389/fcell.2021.642916/full#supplementary-material

REFERENCES

Alamoudi, A. A., Alnoury, A., and Gad, H. (2018). miRNA in tumour metabolism and why could it be the preferred pathway for energy reprograming. *Brief. Funct. Genomics* 17, 157–169. doi: 10.1093/bfgp/elx023

Basnet, R., Gong, G. Q., Li, C., and Wang, M. W. (2018). Serum and glucocorticoid inducible protein kinases (SGKs): a potential target for cancer intervention. *Acta Pharm. Sin. B* 8, 767–771. doi: 10.1016/j.apsb.2018.07.001

Chen, W., Cui, Y., Liu, B., Li, C., Du, L., Tang, R., et al. (2020). Hsa-miR-1908-3p mediates the self-renewal and apoptosis of human spermatogonial stem cells via targeting KLF2. *Mol. Ther. Nucleic Acids* 20, 788–800. doi: 10.1016/j.omtn.2020.04.016

Franca, L. R., Hess, R. A., Dufour, J. M., Hofmann, M. C., and Griswold, M. D. (2016). The Sertoli cell: one hundred fifty years of beauty and plasticity. *Andrology* 4, 189–212. doi: 10.1111/andr.12165

Fu, H., Zhou, F., Yuan, Q., Zhang, W., Qiu, Q., Yu, X., et al. (2019). miRNA-31-5p mediates the proliferation and apoptosis of human spermatogonial stem cells via targeting JAZF1 and cyclin A2. *Mol. Ther. Nucleic Acids* 14, 90–100. doi: 10.1016/j.omtn.2018.11.004

Gong, Y., Zhang, Z., Chang, Z., Zhou, H., Zhao, R., and He, B. (2018). Inactivation of glycogen synthase kinase-3alpha is required for mitochondria-mediated apoptotic germ cell phagocytosis in Sertoli cells. *Aging (Albany NY)* 10, 3104–3116. doi: 10.18632/aging.101614

He, Z., Jiang, J., Hofmann, M. C., and Dym, M. (2007). Gfra1 silencing in mouse spermatogonial stem cells results in their differentiation via the inactivation of RET tyrosine kinase. *Biol. Reprod.* 77, 723–733. doi: 10.1095/biolreprod.107.062513

Hofmann, M. C. (2008). Gdnf signaling pathways within the mammalian spermatogonial stem cell niche. *Mol. Cell. Endocrinol.* 288, 95–103. doi: 10.1016/j.mce.2008.04.012

Hu, P., Guan, K., Feng, Y., Ma, C., Song, H., Li, Y., et al. (2017). miR-638 Inhibits immature Sertoli cell growth by indirectly inactivating PI3K/AKT pathway via SPAG1 gene. *Cell Cycle* 16, 2290–2300. doi: 10.1080/15384101.2017.1380130

Lang, F., Bohmer, C., Palmada, M., Seebohm, G., Strutz-Seebohm, N., and Vallon, V. (2006). (Patho)physiological significance of the serum- and glucocorticoid-inducible kinase isoforms. *Physiol. Rev.* 86, 1151–1178. doi: 10.1152/physrev.00050.2005

Liang, Y., Zhao, G., Tang, L., Zhang, J., Li, T., and Liu, Z. (2016). MiR-100-3p and miR-877-3p regulate overproduction of IL-8 and IL-1beta in mesangial cells activated by secretory IgA from IgA nephropathy patients. *Exp. Cell Res.* 347, 312–321. doi: 10.1016/j.yexcr.2016.08.011

Luo, H., Chen, B., Weng, B., Tang, X., Chen, Y., Yang, A., et al. (2020). miR-130a promotes immature porcine Sertoli cell growth by activating SMAD5 through the TGF-β-PI3K/AKT signaling pathway. *FASEB J.* 34, 15164–15179. doi: 10.1096/fj.202001384R

Meachem, S. J., Wreford, N. G., Robertson, D. M., and Mclachlan, R. I. (1997). Androgen action on the restoration of spermatogenesis in adult rats: effects of

human chorionic gonadotrophin, testosterone and flutamide administration on germ cell number. *Int. J. Androl.* 20, 70–79. doi: 10.1046/j.1365-2605.1997.d01-121.x

Meroni, S. B., Galardo, M. N., Rindone, G., Gorga, A., Riera, M. F., and Cigorraga, S. B. (2019). Molecular mechanisms and signaling pathways involved in Sertoli cell proliferation. *Front. Endocrinol. (Lausanne)* 10:224. doi: 10.3389/fendo.2019.00224

Peng, C. W., Yue, L. X., Zhou, Y. Q., Tang, S., Kan, C., Xia, L. M., et al. (2019). miR-100-3p inhibits cell proliferation and induces apoptosis in human gastric cancer through targeting to BMPR2. *Cancer Cell Int.* 19:354. doi: 10.1186/s12935-019-1060-2

Rebourcet, D., Darbey, A., Monteiro, A., Soffientini, U., Tsai, Y. T., Handel, I., et al. (2017). Sertoli cell number defines and predicts germ and leydig cell population sizes in the adult mouse testis. *Endocrinology* 158, 2955–2969. doi: 10.1210/en.2017-00196

Shi, J. F., Li, Y. K., Ren, K., Xie, Y. J., Yin, W. D., and Mo, Z. C. (2018). Characterization of cholesterol metabolism in Sertoli cells and spermatogenesis (Review). *Mol. Med. Rep.* 17, 705–713. doi: 10.3892/mmr.2017.8000

Singh, J., O'neill, C., and Handelsman, D. J. (1995). Induction of spermatogenesis by androgens in gonadotropin-deficient (hpg) mice. *Endocrinology* 136, 5311–5321. doi: 10.1210/endo.136.12.7588276

Wang, H., Huang, F., Zhang, Z., Wang, P., Luo, Y., Li, H., et al. (2019). Feedback activation of SGK3 and AKT contributes to rapamycin resistance by reactivating mTORC1/4EBP1 Axis via TSC2 in breast cancer. *Int. J. Biol. Sci.* 15, 929–941. doi: 10.7150/ijbs.32489

Wang, H., Yuan, Q., Sun, M., Niu, M., Wen, L., Fu, H., et al. (2017). BMP6 regulates proliferation and apoptosis of human Sertoli cells Via Smad2/3 and Cyclin D1 pathway and DACH1 and TFAP2A activation. *Sci. Rep.* 7:45298. doi: 10.1038/srep45298

Yang, C., Yao, C., Tian, R., Zhu, Z., Zhao, L., Li, P., et al. (2019). miR-202-3p regulates Sertoli cell proliferation, synthesis function, and apoptosis by targeting LRP6 and Cyclin D1 of Wnt/beta-Catenin signaling. *Mol. Ther. Nucleic Acids* 14, 1–19. doi: 10.1016/j.omtn.2018.10.012

Yang, S., Ping, P., Ma, M., Li, P., Tian, R., Yang, H., et al. (2014). Generation of haploid spermatids with fertilization and development capacity from human spermatogonial stem cells of cryptorchid patients. *Stem Cell Rep.* 3, 663–675. doi: 10.1016/j.stemcr.2014.08.004

Yao, C., Yuan, Q., Niu, M., Fu, H., Zhou, F., Zhang, W., et al. (2017). Distinct expression profiles and novel targets of microRNAs in Human spermatogonia, pachytene spermatocytes, and round spermatids between OA patients and NOA patients. *Mol. Ther. Nucleic Acids* 9, 182–194. doi: 10.1016/j.omtn.2017.09.007

Yao, L., Li, M., Hu, J., Wang, W., and Gao, M. (2018). MiRNA-335-5p negatively regulates granulosa cell proliferation via SGK3 in PCOS. *Reproduction* 156, 439–449. doi: 10.1530/REP-18-0229

Zhang, L., Chen, M., Wen, Q., Li, Y., Wang, Y., Wang, Y., et al. (2015). Reprogramming of Sertoli cells to fetal-like Leydig cells by Wt1 ablation. *Proc Natl Acad Sci U.S.A.* 112, 4003–4008. doi: 10.1073/pnas.1422371112

Zhang, L. L., Ma, J., Yang, B., Zhao, J., Yan, B. Y., et al. (2018). Interference with lactate metabolism by mmu-miR-320-3p via negatively regulating GLUT3 signaling in mouse Sertoli cells. *Cell Death Dis.* 9:964. doi: 10.1038/s41419-018-0958-2

Zhou, F., Chen, W., Cui, Y., Liu, B., Yuan, Q., Li, Z., et al. (2020). MiRNA-122-5p stimulates the proliferation and DNA synthesis and inhibits the early apoptosis of human spermatogonial stem cells by targeting CBL and competing with LncRNA CASC7. *Aging (Albany NY)* 12, 25528–25546. doi: 10.18632/aging.104158

Zhou, F., Yuan, Q., Zhang, W., Niu, M., Fu, H., Qiu, Q., et al. (2018). MiR-663a stimulates proliferation and suppresses early apoptosis of human spermatogonial stem cells by targeting NFIX and regulating cell cycle. *Mol. Ther. Nucleic Acids* 12, 319–336. doi: 10.1016/j.omtn.2018.05.015

Conflict of Interest: The authors declare that the research was conducted in the absence of any commercial or financial relationships that could be construed as a potential conflict of interest.

frontiers in Cell and Developmental Biology

ORIGINAL RESEARCH
published: 13 May 2021
doi: 10.3389/fcell.2021.633937

Urothelial Cancer Associated 1 (UCA1) and miR-193 Are Two Non-coding RNAs Involved in Trophoblast Fusion and Placental Diseases

Clara Apicella[1†], Camino S. M. Ruano[1†], Sébastien Jacques[1], Géraldine Gascoin[2,3], Céline Méhats[1], Daniel Vaiman[1†] and Francisco Miralles[1†]*

[1] Institut Cochin, Université de Paris, U1016 INSERM, UMR 8104, CNRS, Paris, France, [2] Unité Mixte de Recherche MITOVASC, Équipe Mitolab, CNRS 6015, INSERM U1083, Université d'Angers, Angers, France, [3] Réanimation et Médecine Néonatales, Centre Hospitalier Universitaire, Angers, France

OPEN ACCESS

Edited by:
Tang Zhonglin, Agricultural Genomics Institute at Shenzhen, Chinese Academy of Agricultural Sciences, China

Reviewed by:
Marie Van Dijk, Amsterdam University Medical Centers, Netherlands
Stephen Lye, Lunenfeld-Tanenbaum Research Institute, Canada

***Correspondence:**
Daniel Vaiman
daniel.vaiman@inserm.fr

[†] These authors have contributed equally to this work

Specialty section:
This article was submitted to Cell Growth and Division, a section of the journal Frontiers in Cell and Developmental Biology

Received: *26 November 2020*
Accepted: *19 April 2021*
Published: *13 May 2021*

Citation:
Apicella C, Ruano CSM, Jacques S, Gascoin G, Méhats C, Vaiman D and Miralles F (2021) Urothelial Cancer Associated 1 (UCA1) and miR-193 Are Two Non-coding RNAs Involved in Trophoblast Fusion and Placental Diseases. Front. Cell Dev. Biol. 9:633937. doi: 10.3389/fcell.2021.633937

A bioinformatics screen for non-coding genes was performed from microarrays analyzing on the one hand trophoblast fusion in the BeWo cell model, and on the other hand, placental diseases (preeclampsia and Intra-Uterine Growth Restriction). Intersecting the deregulated genes allowed to identify two miRNA (mir193b and miR365a) and one long non-coding RNA (UCA1) that are pivotal for trophoblast fusion, and deregulated in placental diseases. We show that miR-193b is a hub for the down-regulation of 135 cell targets mainly involved in cell cycle progression and energy usage/nutrient transport. UCA1 was explored by siRNA knock-down in the BeWo cell model. We show that its down-regulation is associated with the deregulation of important trophoblast physiology genes, involved in differentiation, proliferation, oxidative stress, vacuolization, membrane repair and endocrine production. Overall, UCA1 knockdown leads to an incomplete gene expression profile modification of trophoblast cells when they are induced to fuse into syncytiotrophoblast. Then we performed the same type of analysis in cells overexpressing one of the two major isoforms of the STOX1 transcription factor, STOX1A and STOX1B (associated previously to impaired trophoblast fusion). We could show that when STOX1B is abundant, the effects of UCA1 down-regulation on forskolin response are alleviated.

Keywords: trophoblast, placenta, preeclampsia, intra uterine growth restriction, syncytialisation, non-coding RNAs

INTRODUCTION

In humans, abnormal placental development is associated with two major pregnancy diseases: preeclampsia (PE) and intrauterine growth restriction (IUGR).

PE occurs in a range of 2–5% pregnancies, and it is characterized by hypertension and proteinuria, surging from the mid-gestation at the earliest (Steegers et al., 2010). Despite a certain degree of heterogeneity in its pathogenesis, a consensus exists that abnormal placentation or placenta development could be at the origin of the disease. Notably, placental ischemia would

cause intermittent hypoxia, oxidative stress, cell death, and the release to the maternal circulation of anti-angiogenic factors and debris that promote inflammation and a systemic endothelial dysfunction (Rana et al., 2019). In some cases, the disease poses a real threat to the survival of the mother requiring the delivery of the feto-placental unit. Thus, PE is one of the major causes of premature births (before 37 completed weeks of pregnancy), with their cortege of neonate complications (Goldenberg et al., 2008). The symptoms of the disease disappear after delivery. However, epidemiological studies have shown that the women who have suffered a preeclamptic pregnancy have an increased risk of developing a cardiovascular disease (CVD) later in life (Newstead et al., 2007; Brouwers et al., 2018), as well as other diseases affecting strongly vascularized tissues, such as the brain (Basit et al., 2018).

IUGR refers to a somehow loosely defined condition in which the unborn baby is smaller than expected for his or her gestational age (Nardozza et al., 2017). IUGR babies typically have an estimated weight that falls below that of 90% of unborn babies of the same gestational age. In addition, IUGR babies are sometimes born prematurely. Babies with IUGR are at increased risk of health problems before, and after birth. These problems include low oxygen levels while in the womb and high levels of distress during labor and delivery. In the long term, IUGR increases the risk of developing a metabolic disease such as type 2 diabetes and CVD (Darendeliler, 2019).

In about one third of the cases, PE is complicated with IUGR, suggesting that there could be an overlap in the etiology of both diseases. The considerable similarity in histopathology and gene expression in the placentas has been recently reported between both diseases (Awamleh et al., 2019; Gibbs et al., 2019; Medina-Bastidas et al., 2020).

In the human placenta, the maternal blood is in direct contact with a continuous multinucleated layer, the syncytiotrophoblast (STB). This polarized interface releases hormones and mediates the exchange of nutrients, gases and waste between mother and the developing fetus (Turco and Moffett, 2019). The STB is mitotically inactive, formation and constant renewal of the syncytium depends on the underlying mononuclear cytotrophoblasts (CTB). Throughout gestation, CTBs proliferate, differentiate and eventually fuse with the STB via cell-syncytial fusion. This process is balanced by a concomitant release of apoptotic material as syncytial knots from the STB to the maternal circulation. Hence, the process of syncytialization is critical to the integrity of the STB and in maintaining the essential functions of the placenta. Several *in vitro* and *in vivo* studies have demonstrated a close, if not a causal, relationship between structural/functional deficiency of the syncytium and the development of PE and IUGR (Guller et al., 2008; Roland et al., 2016; Costa, 2016).

Genome-wide transcriptomic and epigenomic studies have greatly contributed to the understanding of the molecular mechanisms involved in either normal or pathological placenta development. Thus, numerous studies have revealed altered placental expression of various genes in PE and IUGR (Cox et al., 2015; Deyssenroth et al., 2017; Chabrun et al., 2019; Majewska et al., 2019; Benny et al., 2020). A particular category concerns those genes encoding for non-protein coding RNAs (ncRNAs). Classes of ncRNAs include transfer RNAs (tRNAs), ribosomal RNAs (rRNAs), small RNAs, such as microRNAs (miRNAs), siRNAs, piRNAs, snoRNAs, snRNAs, exRNAs, scaRNAs and the long ncRNAs (Hombach and Kretz, 2016). The ncRNAs display a great variety of mechanisms of action including: post-transcriptional gene regulation through controlling processes like protein synthesis, RNA maturation, transport and decay, but also, transcriptional gene regulation through the modification of chromatin structure (Fernandes et al., 2019). They are an important basis of epigenetic regulation in the human placenta, in normal and pathological situations (Hayder et al., 2018; Apicella et al., 2019). Structurally different ncRNAs engage diverse mechanisms that lead to different regulatory outcomes. The discovery of the diversity of functions played by the ncRNAs in the cell physiology has boosted the exploration of their role in placental development, physiology and pathology.

The central role of the STB in the physiology of the placenta, suggests that deregulation of ncRNAs specifically required for its formation and/or maintenance could be potentially involved in placental diseases. Here we combined two microarray analyses, one carried out on the classical fusogenic trophoblast model BeWo (under the accession number GSE148088) (Kudo et al., 2004; Ramos et al., 2008; Orendi et al., 2010; Shankar et al., 2015; Zheng et al., 2016), and one carried out on total human placentas with normal controls, PE and IUGR placentas (under the accession number E-MTAB-9416). A cross-analysis was carried out with a drastic filtering in order to identify ncRNA that are associated to disease (in the placentas) and to fusion (induced by forskolin treatment in the BeWo cells), in parallel.

This cross-analysis allowed the identification of a small subset of ncRNAs which are consistently modified both during fusion of trophoblast cells, and in the pathological placentas. We then carried on our analysis focusing upon the miRNA miR-193b (by a bioinformatic approach) and the lncRNA UCA1 (through knock-down (KD) experiments). In addition, we analyzed the effects of this KD in BeWo cells, overexpressing specifically one of the two major isoforms of the STOX1 transcription factor (STOX1A and STOX1B), previously identified as a key player in preeclampsia (George and Bidwell, 2013), and recently shown to modulate fusion through a specific equilibrium between its two isoforms (Vaiman and Miralles, 2016; Ducat et al., 2020). The chart of the present study is shown as **Figure 1**.

RESULTS

Transcriptional Modifications in BeWo Cells Following Forskolin Treatment

BeWo cells were cultured in the presence of 20 μM forskolin to induce cell fusion (BeWo-FSK). Control cells were grown with the vehicle, DMSO (BeWo-CO). After 72 h, the total RNA was extracted, and global gene-expression profiles were analyzed with microarrays. Comparison of BeWo-FSK relative to BeWo-CO detected 2109 genes differentially expressed (DEGs) with a fold change (FC) either $\leq$-2 or $\geq$2, and

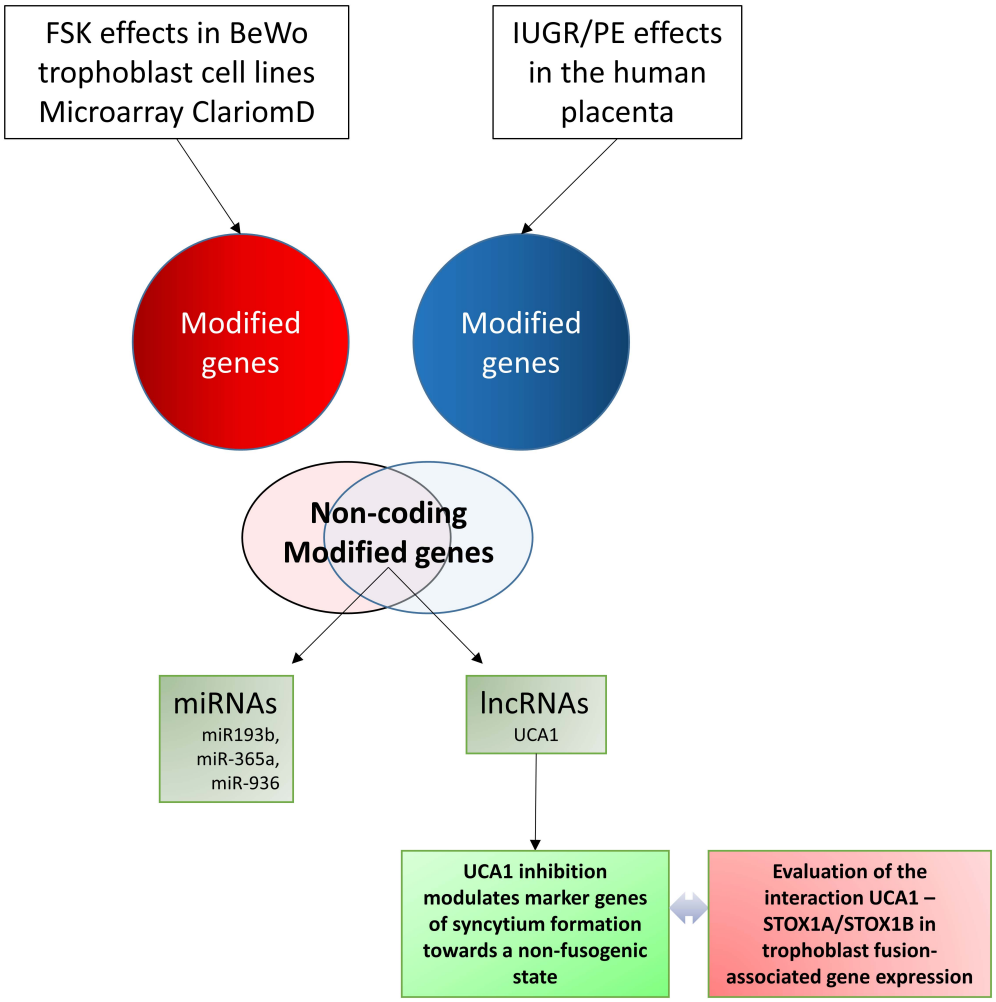

FIGURE 1 | Chart of the study, explaining the pivotal aim: connecting non-protein coding genes involved in trophoblast fusion with placental genes altered in human placental pathologies (Preeclampsia and Intra-Uterine Growth Restriction).

P-value $\leq$ 0.05 (**Figure 2A** and **Supplementary Table 1**). Of these, 828 genes were up-regulated and 1,281 down-regulated (**Supplementary Table 1**). Gene set enrichment analysis (GSEA), and over representation analysis (ORA) confirmed that our results were accurately consistent with previous reports having analyzed transcriptomic changes in BeWo cells after forskolin treatment (**Supplementary Figure 1**). In the BeWo-FSK we detected substantially increased expression of key markers of syncytialization such as CGA (*FC* = 10.1; $P = 2.1 \times 10^{-11}$), CGB1 (*FC* = 20.5; $P = 2.81 \times 10^{-12}$) or ERVFRD-1 (aka Syncytin2, *FC* = 10.6; $P = 6.23 \times 10^{-12}$). Up-regulated DEGs were associated with biological processes such as cell migration, vascular development, response to TGF-Beta and response to hypoxia. Down-regulated DEGs are mainly involved in cell cycle progression, amino-acid metabolism, and mitochondrial gene expression (**Figure 2B**). In terms of hallmarks present in the GSEA Broad database, inflammation and hypoxia pathways were particularly enriched in up-regulated genes, while cell cycle, nutrient sensing via mTORC1 pathway, were strongly enriched in down-regulated genes, suggesting a whole silencing of basic pathways of cell physiology and energy expenditure slow down, accompanying the differentiation of the trophoblast cells into a syncytial structure.

Differentially Expressed Non-coding RNAs in Forskolin-Treated BeWo Cells

Three hundred and seven (307) of the DEGs detected in the BeWo-FSK relative to BeWo-CO, encode annotated ncRNAs. They belong to different categories including: sense-intronic RNA, antisense RNA, long non-coding RNA (lncRNA), circular (circRNA), microRNA (miRNA) and housekeeping ncRNAs (Y-RNAs, ribosomal RNAs, Small nucleolar RNAs and transfer RNAs) (**Figure 3**). The category of housekeeping ncRNAs was the most represented (111 genes). Nonetheless, we focused our study on the categories corresponding to regulatory ncRNAs. A selection of the most significantly modified regulatory ncRNAs detected

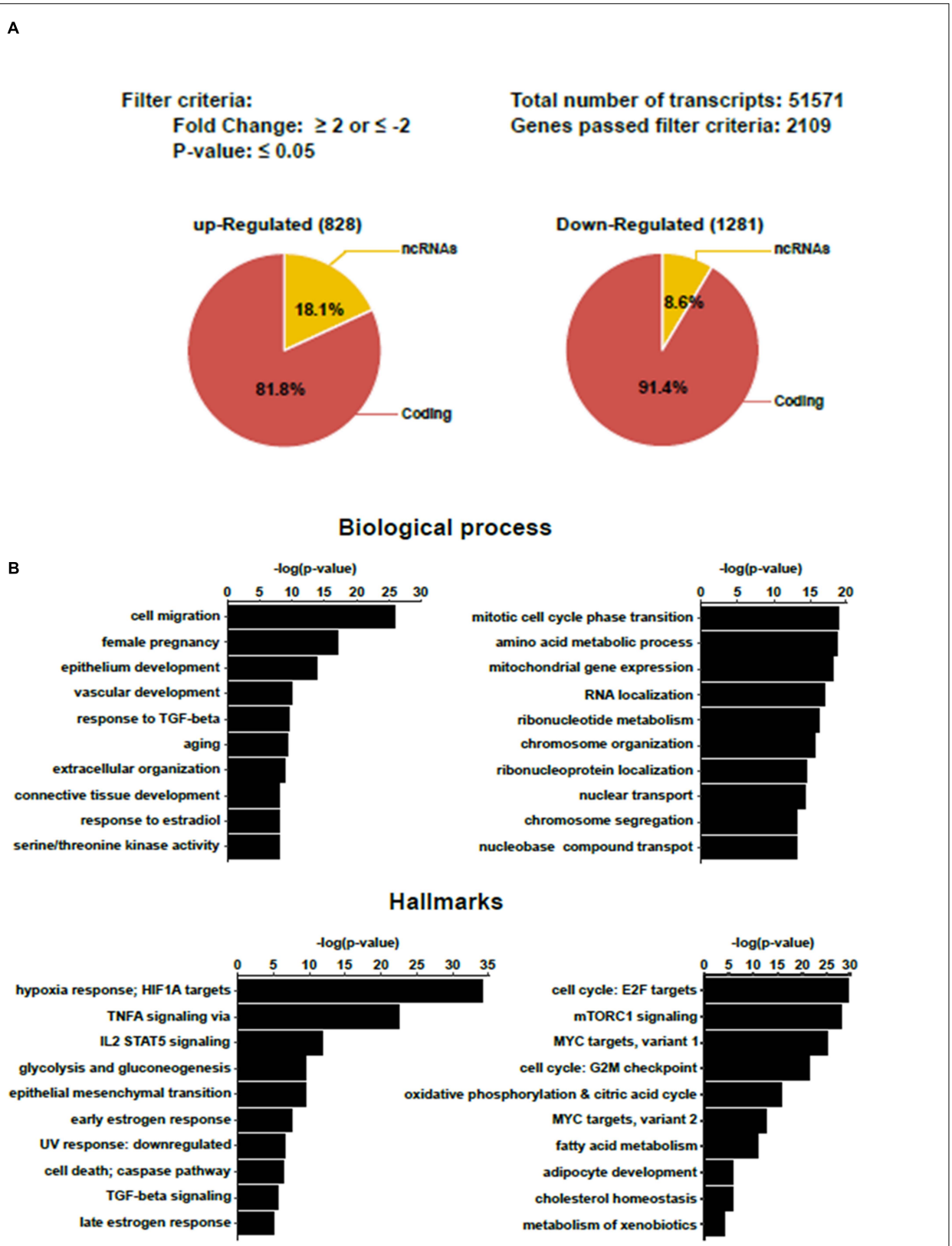

FIGURE 2 | Transcriptomic analysis of BeWo cells after 72 h treatment with forskolin. **(A)** Summary of transcriptomic analysis. Genes with a fold change (FC) either $\leq$-2 or $\geq$2, and $P \leq 0.05$ were considered differentially expressed in the BeWo cells treated with forskolin (BeWo-FSK) relative to the untreated cells (BeWo-CO). **(B)** Over Representation Analysis (ORA) showing principal Biological processes and Hallmarks enriched by the up-regulated (left) and down-regulated (right) DEGs in the BeWo-FSK compared to the BeWo-CO.

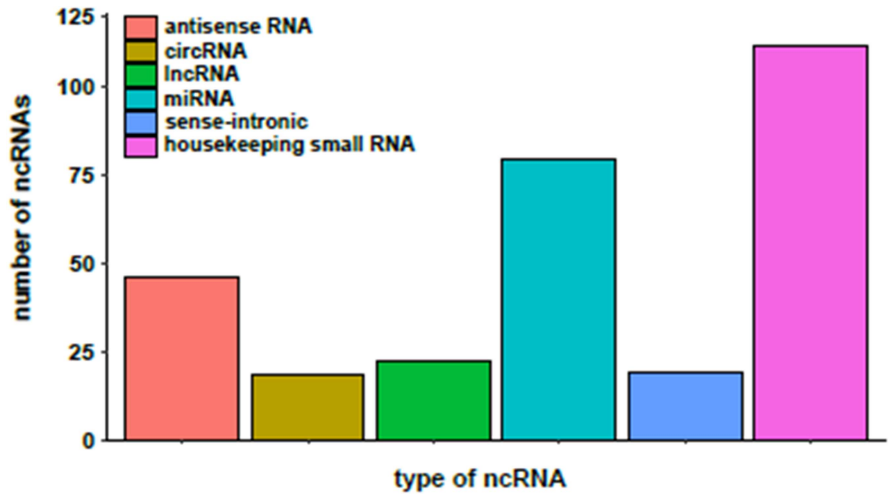

FIGURE 3 | Distribution of the different categories of non-coding RNAs (ncRNAs) differentially expressed in the BeWo-FSK.

TABLE 1 | Top 25 differentially expressed regulatory ncRNAs in the BeWo cells after 72 h of forskolin treatment.

Gene symbol	ncRNA class	Fold change	*P*-value	FDR *P*-value
hsa-miR-147b	miRNA	28.94	8.33E-11	3.53E-07
LINC01511	lncRNA	14.88	8.43E-13	1.63E-08
hsa-miR-4632	miRNA	8.93	6.38E-09	7.80E-06
RP11-420L9.5	antisenseRNA	7.6	1.61E-08	1.48E-05
LINC01237	lncRNA	4.45	2.70E-07	1.00E-04
MYCNUT	lncRNA	4.31	3.72E-09	5.15E-06
LINC01164	lncRNA	3.98	1.37E-07	8.14E-05
UCA1	lncRNA	3.76	2.19E-06	7.00E-04
CTB-60B18.12	antisenseRNA	3.46	2.06E-06	7.00E-04
hsa-miR-6810	miRNA	3.36	3.13E-06	9.00E-04
hsa-miR-936	miRNA	3.35	5.99E-06	1.50E-03
SLC2A1-AS1	antisenseRNA	3.23	6.17E-06	1.50E-03
IL10RB-AS1	antisenseRNA	3.14	5.32E-06	1.30E-03
hsa-miR-193b	miRNA	2.91	8.00E-04	4.54E-02
hsa-miR-365a	miRNA	2.73	3.90E-06	1.10E-03
hsa-miR-6888	miRNA	2.54	8.24E-05	9.80E-03
hsa-miR-3941	miRNA	2.16	3.18E-05	5.10E-03
Hsa-miR-636	miRNA	−2.16	4.69E-05	6.70E-03
hsa-miR-301a	miRNA	−2.27	2.92E-05	4.90E-03
RP11-884K10.7	antisenseRNA	−2.84	4.00E-04	2.68E-02
COX10-AS1	antisenseRNA	−3.12	5.63E-05	7.60E-03
OLMALINC	lncRNA	−3.33	9.98E-05	1.12E-02
hsa-miR-1908	miRNA	−3.45	6.12E-07	3.00E-04
DLEU2	lncRNA	−3.75	8.74E-05	1.03E-02
hsa-miR-6758	miRNA	−4.31	8.16E-07	3.00E-04

following forskolin treatment in the BeWo cells is shown in **Table 1**. These include the lncRNAs, antisenseRNAs and miRNAs. The list of the totality of ncRNAs (classified by category) detected as differentially expressed is provided as **Supplementary Table 2**.

Identification of Regulatory ncRNAs Targets Reveals Their Potential Roles in Syncytialization

To investigate the role of these ncRNAs in the process of BeWo fusion we identified their putative targets (when known) using appropriate databases (miRBase, starBase v2.0. and DianaTools LncBase v.2). Since miRbase tends to provide a more limited list of putative target genes (∼10% of the others) for a given miRNA, and since these were generally largely covered in the other databases, this constituted the major basis for the establishment of our lists of targets. Next, we selected among these targets those which are indeed detected as DEGs in the BeWo-FSK relative to the BeWo-CO cells. These resulted in a list of 278 up-regulated and 572 down-regulated DEGs. Out of the deregulated DEG list (**Supplementary Table 1**), this represents 33.6% for the up-regulated and 44.6% for the down-regulated DEGs. Assuming a total of 50,000 genes including the non-protein coding ones, the expected proportions are 1.6 and 1.1%, respectively, thus we observed a significant enrichment of putative targets in both cases (χ^2 contingency test, $p < 10^{-20}$).

Hallmark enrichment analysis using the ncRNAs targeted-DEGs revealed that the most significantly impacted functions are related to the cell cycle progression for the down-regulated DEGs, while TNF-signaling and hypoxia response are the most enriched processes for the up-regulated DEGs. Strikingly, these enriched pathways are quite similar to those obtained with the total DEG gene set, suggesting that many DEGs contributing to the definition of the hallmarks are targeted by the ncRNAs.

Network Analysis of ncRNAs and Their Targets Identifies miR-193b as a Hub

To further analyze the role of the differentially expressed ncRNAs in the process of BeWo fusion we used the Cytoscape tool to construct a regulatory network integrating these ncRNAs and their targets. This resulted in a network composed of

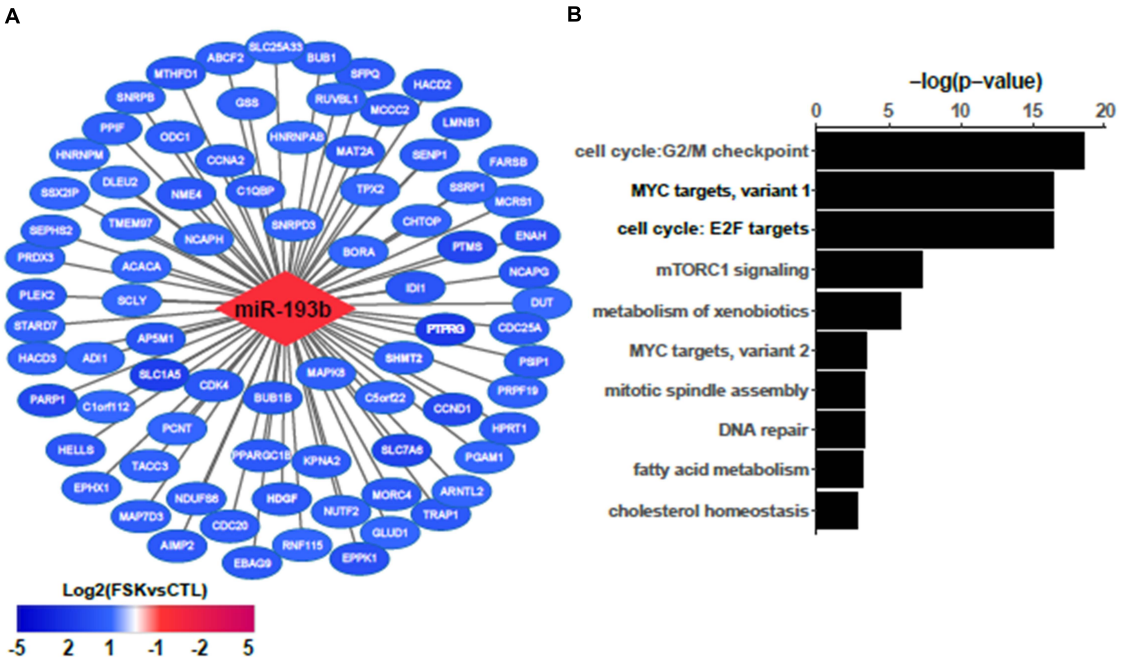

FIGURE 4 | Network analysis identifies miR193b as a hub regulator **(A)** Most significantly down-regulated genes in BeWo-FSK targeted by miR193b. **(B)** Hallmarks enrichment analysis of the targets of miR193b deregulated in the BeWo-FSK relative to the BeWo-CO.

985 nodes (representing ncRNAs and targets) and 1,775 edges (representing interactions). Next, we submitted our network to topological analysis. MiR-193b was identified as the principal hub of our network, with 135 predicted targets (**Figure 4A**). Other lesser hubs corresponding to miR-16, miR-455, and miR-365 are presented as **Supplementary Figure 2**. Most of the targets of miR-193b were down-regulated (108 out of 135) in the BeWo-FSK relative to BeWo-CO, while miR-193b was significantly up-regulated (FC = 2.91; P = 0.0008). Hallmarks enrichment analysis shows that the down-regulated genes targeted by mir-193b are mainly involved in the control of cell cycle progression and energy usage/nutrient metabolism (**Figure 4B**).

A Small Subset of ncRNAs Involved in Syncytialization Is Also Associated With Preeclampsia and Intrauterine Growth Restriction

To identify ncRNAs associated with syncytialization in BeWo which could be also involved in PE and/or IUGR we compared the list of ncRNAs identified in BeWo with those identified in a list from our study on total human placentas with normal controls, PE and IUGR placentas (E-MTAB-9416) and other published datasets (GSE114349, GSE114691, GSE75010, GSE93839, and GSE66273). Comparison of all differentially expressed ncRNAs, revealed that two miRNAs (miR-193b and miR-365a) and one lncRNA (UCA1) were found most consistently up-regulated in both PE and IUGR. Therefore, miR-193b is associated to trophoblast fusion, together with pathological placentation, suggesting its overall implication in normal placental function. A few additional miRNAs where also found simultaneously differentially expressed in preeclamptic placentas and in the BeWo-FSK (miR-936; miR-6886; miR-7110; miR-518A1; miR-4454, and miR-1283-2), but those were not studied further in the present paper.

We next focused our attention on the lncRNA UCA1. This was justified by the following: (i) UCA1 is up-regulated in PE and IUGR but also in primary cultures of human syncytiotrophoblasts exposed for 24 h to 1% oxygen as compared to the same cells exposed to 20% oxygen (**Table 2**), (ii) also, a study coupling laser microdissection to isolate specific trophoblast subpopulations and microarray analysis, identified UCA1 as the most differentially expressed ncRNA in STBs isolated from the placentas of pregnancies with severe PE relative to controls (Gormley et al., 2017), (iii) *in situ* hybridization confirmed up-regulation of UCA1 in the STBs compartment of the placenta. Alternative splicing isoforms have been described for UCA1 (Xue et al., 2016). We found that UCA1 was increased

TABLE 2 | Genome-wide transcriptomic studies showing up-regulation of UCA1 either in preeclampsia or intrauterine growth retardation.

Data set	Study	Fold change	*P*-value
E-MTAB-9416	IUGR vs. CO	8.91	3.20×10^{-03}
GSE75010	PE vs. CO	2.04	2.81×10^{-10}
GSE93839	PE STB vs. CO STB	5.93	1.55×10^{-03}
GSE66273	PE vs. CO	6.19	3.33×10^{-04}
GSE147776	IUGR vs. CO	2.01	3.58×10^{-02}
GSE41331	CTB 1%O2 vs. 20%O2	1.86	1.61×10^{-02}

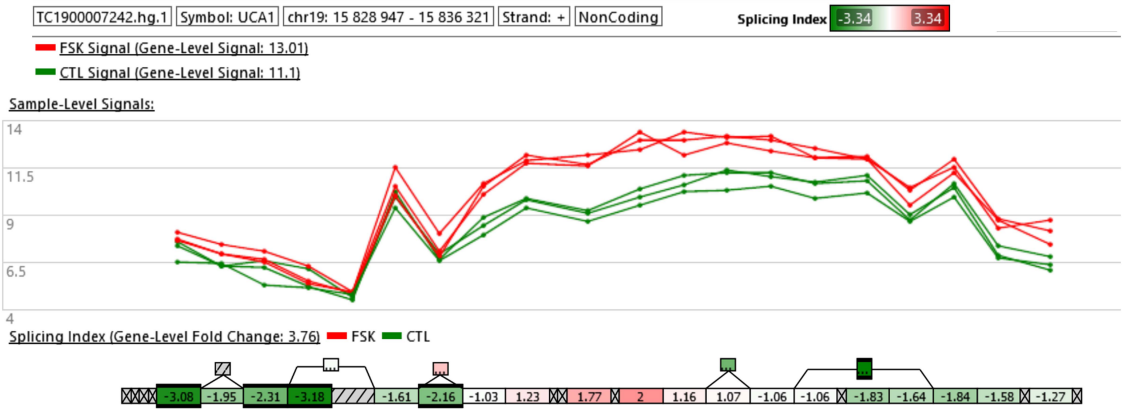

FIGURE 5 | Exon level analysis of UCA1. The microarray ClariomD provides information on the local fluorescence level of a series of probe and allows to calculate a local splicing index, comparing BeWo cells treated with FSK vs. BeWo cells treated by the DMSO as a vehicle. Isoforms lacking the first portion of the full transcript are more strongly expressed in the BeWo-FSK comparatively to the BeWo-CO.

in expression by 3.76-fold following FSK treatment. Exon level analysis of UCA1 (accessible through the ClariomD array used in this study) shows that probes located in the terminal part of the gene have a higher level of fluorescence in the forskolin-treated compared to the control cells (**Figure 5**). Thus, it shows that in the BeWo-FSK there is a specific increase in the production of the shorter isoforms (ENST00000600160.2, ENST00000589333.2) of UCA1, while the level of expression of the most complete isoform (ENST00000397381.4) is apparently unaffected.

UCA1 siRNA Knockdown Lead to Altered Regulation of Genes Involved in Fusion Mechanisms in BeWo Cells

The effect of the si-RNAs was evaluated by qRT-PCR. UCA1 levels were drastically affected (reduction ranging from 90 to 98% compared to the si-SCR, according to the experiment, **Figure 6A**). In a first characterization, we analyzed in BeWoC cells the expression of genes involved in cell proliferation (*ki67*, *ITIH5*), oxidative stress (*NOS3*, *GCLM* and *CAV1*-also involved in exosome physiology), membrane repair *(ANXA1, ANXA2*, *CAV1*), trophoblast fusion (*Syncytin1*, *Syncytin2*), endocrine differentiation of trophoblast (*CGA*/*CGB*), syncytiotrophoblast stabilization (*TGM2*) cell migration (*MMP9*), oxygen sensing (*INHA*), and apoptosis (*BAX*, *BCL2*, *DAPK1* and *BAD*). The KD of UCA1 led to significant alterations of almost all the genes involved in these pathways (**Figure 6**). A principal component analysis was carried out on the qPCR data and showed a clear separation of the cell replicates (**Figure 7**). The first axis (79% of the variation) is driven by the FSK treatment, while the second axis (10%) contrasts markers of differentiation vs. markers of proliferation. The analysis reveals that in terms of gene expression, the KD of UCA1 reduced the differences between FSK treated cells and control group in the center of the graph. This means that when levels of UCA1 are strongly reduced, the expression profile remains closer to that of untreated control cells. These observations suggest that UCA1 is important for a successful syncytialisation process.

A statistical test by two-ways ANOVA revealed significant modifications for most genes except GCLM and DAPK1 (**Table 3** and **Figure 6**). The knockdown of UCA1 by itself affected all the genes, but MMP9. The FSK effect was significant in all the genes except UCA1, CGB, KI67 (in addition to GCLM and DAPK1). Finally, there was a significant interaction effect between the FSK treatment and the UCA1 KD in the case of UCA1, CGB, SYNCYTIN2, TGM2, ANXA2, ITIH5, and BAD. These interaction effects indicate a differential effect of the UCA1 KD according to the FSK treatment leading to cell fusion.

Interference Between UCA1 and the Trophoblast Differentiation Factor STOX1 in BeWo Cells

Previously, we have identified STOX1 as a major actor of the syncytialisation process in BeWo cells. More specifically, we showed that the short isoform of STOX1, STOX1B, antagonizes cell fusion when overexpressed and that disturbing the STOX1A/B balance mimics specific gene perturbations seen in PE CTBs in three well-characterized cell lines BeWoA, BeWoB and BeWoC, the first two overexpressing STOX1A and STOX1B, 20–30- and 6-fold, respectively (Ducat et al., 2020). In the present paper, analyzing exon-level microarrays, we show now for the first time that STOX1 isoforms are differentially spliced when the BeWo cells fuse under forskolin (**Supplementary Figure 3**), strengthening the idea that the two isoforms are associated with different pivotal stages of trophoblast differentiation.

To explore the putative role of UCA1 in the syncytialization in normal and pathological conditions, we silenced this lncRNA using a specific small interfering RNA (si-RNA) in BeWo cells lines permanently transfected either with an empty plasmid (encoding G418 resistance), or with the same plasmid encoding for the expression of either STOX1A or STOX1B (These cells are

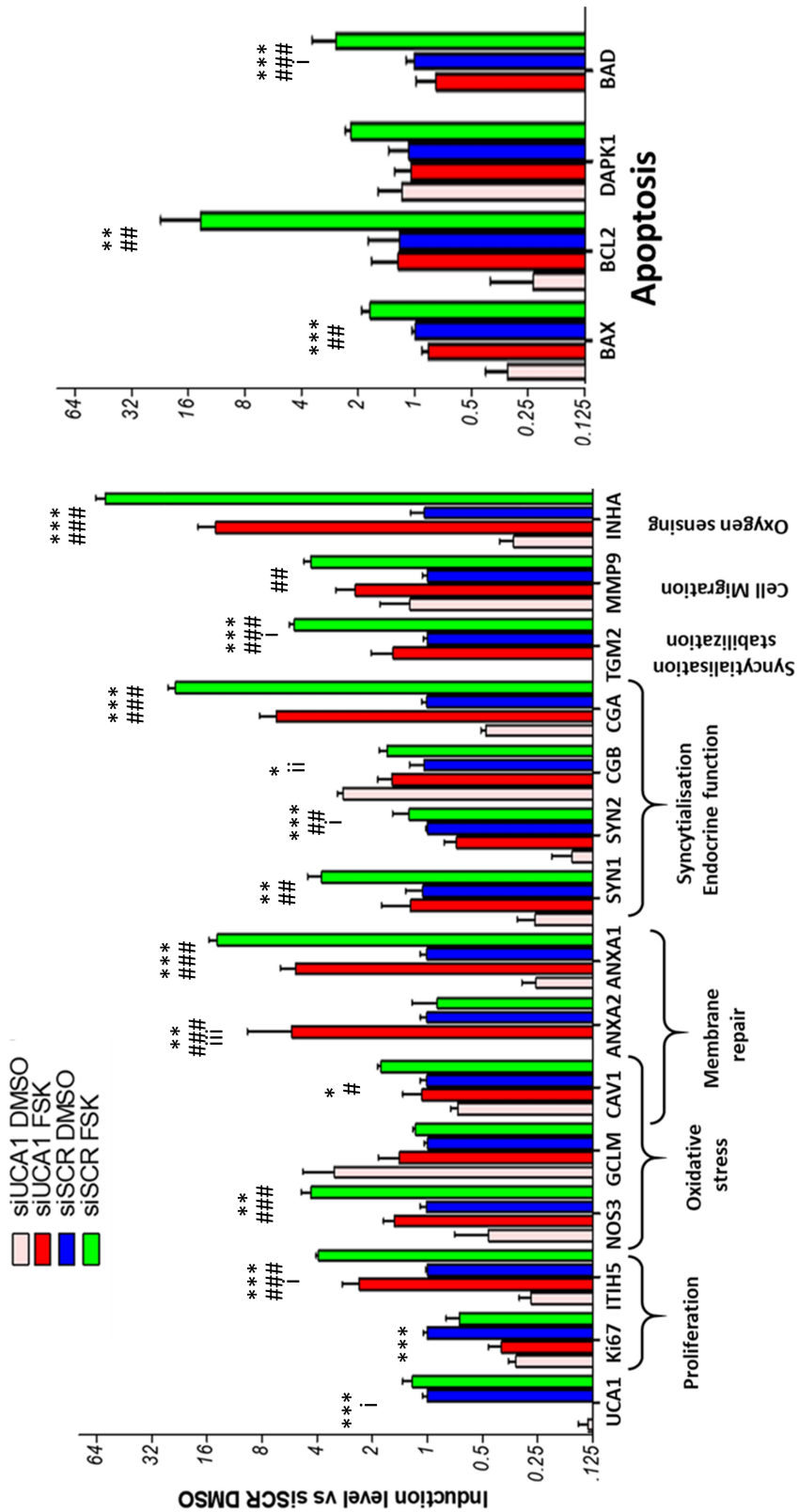

FIGURE 6 | qRT-PCR analysis of the efficiency of UCA1 silencing in BeWo cells with or without forskolin treatment, and its effects on several markers of syncytialization. Genes involved in apoptosis are on the right panel. Stars (*) are marks of a significant effect of the siRNA against UCA1, hashes (#) are marks of significant effects of the forskolin-induced fusion, and (i) are marks of interaction effects (*, #, i represent p-values below 0.05; **, ##, ii $p < 0.01$; ***, ###, iii$p < 0.001$).

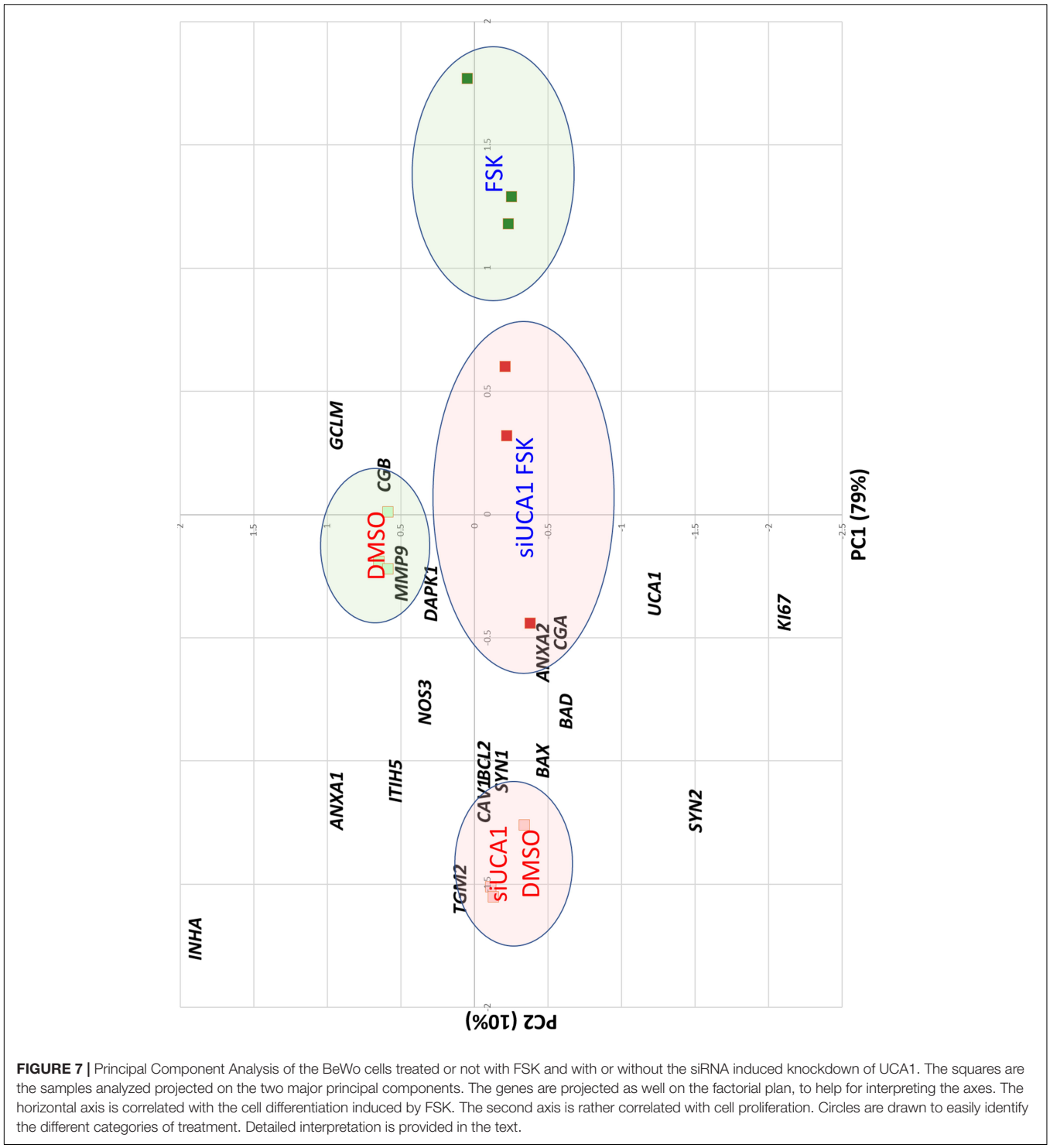

FIGURE 7 | Principal Component Analysis of the BeWo cells treated or not with FSK and with or without the siRNA induced knockdown of UCA1. The squares are the samples analyzed projected on the two major principal components. The genes are projected as well on the factorial plan, to help for interpreting the axes. The horizontal axis is correlated with the cell differentiation induced by FSK. The second axis is rather correlated with cell proliferation. Circles are drawn to easily identify the different categories of treatment. Detailed interpretation is provided in the text.

called BeWoC, BeWoA or BeWoB, respectively). The cells were transfected with the si-UCA1 or a scrambled siRNA, si-SCR, used as control. We analyzed by qPCR a panel of 8 genes (including UCA1), The choice of these 8 genes was motivated by the fact that strong correlations exist between the 19 genes analyzed in the first experiment. The chosen genes are representative of the different pathways analyzed (proliferation-KI67, oxidative stress-INHA, trophoblast differentiation-SYN1, apoptosis-BCL2, BAX, invasion-MMP9, endocrine differentiation-CGA). The results are presented as a histogram (**Figure 8A**), with statistical values presented in **Supplementary Table 3** (ANOVA), and as a PCA analysis, where the two first axes account for 40 and 19.5% of the variance (**Figure 8B**). BeWoC cells (represented by squares) harbor the same profile with the 8 genes from the

TABLE 3 | Statistical analyses of individual gene effects following UCA1 knock-down ± FSK treatment (significant values are in red fonts).

Overall tests of univariate models			Tests of univariate effects		
Y variable	**F**	**Prob.**	**Source**	**F**	**Prob.**
UCA1	22.504	0.00029659	Si treatment	56.948	6.6307×10^{-05}
			Fusion	4.288	0.07213567
			Si treatment*Fusion	6.275	0.03665572
CGB	8.208	0.00797657	Si treatment	10.373	0.01222583
			Fusion	0.283	0.60936093
			Si treatment*Fusion	13.967	0.00572781
CGA	127.930	4.243×10^{-07}	Si treatment	43.849	0.00016558
			Fusion	336.346	8.0411×10^{-08}
			Si treatment*Fusion	3.596	0.09452054
GCLM	2.521	0.13152052	Si treatment	4.143	0.07620217
			Fusion	0.975	0.3524659
			Si treatment*Fusion	2.445	0.15650114
NOS3	14.589	0.00131394	Si treatment	15.149	0.0045949
			Fusion	28.613	0.0006866
			Si treatment*Fusion	0.004	0.95003544
CAV1	5.155	0.02833346	Si treatment	7.939	0.02257829
			Fusion	7.147	0.02821257
			Si treatment*Fusion	0.379	0.55505375
KI67	13.163	0.00184323	Si treatment	34.327	0.00037894
			Fusion	0.891	0.37283458
			Si treatment*Fusion	4.272	0.07257943
SYN2	23.107	0.00027009	Si treatment	39.848	0.00022968
			Fusion	18.244	0.00271954
			Si treatment*Fusion	11.229	0.01006638
TGM2	51.718	1.3944×10^{-05}	Si treatment	63.473	4.4987×10^{-05}
			Fusion	84.869	1.5606×10^{-05}
			Si treatment*Fusion	6.811	0.0311362
ANXA2	39.218	3.939×10^{-05}	Si treatment	23.397	0.00129298
			Fusion	43.573	0.00016922
			Si treatment*Fusion	50.685	0.00010006
ITIH5	56.208	1.0168×10^{-05}	Si treatment	37.157	0.00029085
			Fusion	125.667	3.5958×10^{-06}
			Si treatment*Fusion	5.801	0.04260521
SYN1	10.209	0.00413556	Si treatment	15.939	0.00399228
			Fusion	14.682	0.00500579
			Si treatment*Fusion	0.005	0.94569912
ANXA1	96.898	1.2527×10^{-06}	Si treatment	45.870	0.00014171
			Fusion	243.711	2.8262×10^{-07}
			Si treatment*Fusion	1.114	0.32213654
MMP9	5.171	0.02810927	Si treatment	1.134	0.31791426
			Fusion	13.560	0.00619729
			Si treatment*Fusion	0.819	0.39182403
INHA	137.727	3.1788×10^{-07}	Si treatment	40.502	0.00021729
			Fusion	372.037	5.4151×10^{-08}
			Si treatment*Fusion	0.641	0.44650823
BAX	21.540	0.00034606	Si treatment	36.796	0.00030055
			Fusion	25.245	0.00102124
			Si treatment*Fusion	2.580	0.14686479
BCL2	8.774	0.00654947	Si treatment	13.427	0.00636233
			Fusion	12.786	0.00723255
			Si treatment*Fusion	0.110	0.74867557

(Continued)

TABLE 3 | Continued

Overall tests of univariate models			Tests of univariate effects		
Y variable	**F**	**Prob.**	**Source**	**F**	**Prob.**
DAPK1	2.339	0.14975061	Si treatment	2.106	0.18480454
			Fusion	2.027	0.1923598
			Si treatment*Fusion	2.884	0.12788132
BAD	32.681	7.7268×10^{-05}	Si treatment	55.723	7.1629×10^{-05}
			Fusion	36.270	0.0003154
			Si treatment*Fusion	6.050	0.03934242

previous analysis: in the condition where the KD of UCA1 is combined with FSK treatment, the expression profile is close to the one of BeWoC cells without FSK and not treated with the siUCA1. Overall, the FSK effects were all oriented in the same direction of the first axis (clear to dark colors), which can thus be interpreted as a mark of FSK-induced trophoblast differentiation. A strong difference Between BeWoA, BeWoB and the control BeWoC comes from the variation along the second axis, showing that in this case, STOX1-overexpressing cells in the presence of forskolin are positioned with increasing abcissae, suggesting that this axis correlate with STOX1-driven differentiation in the presence of forskolin. When UCA1 is KD, the effect of STOX1 are less pronounced on the second axis (red squares, lozenges-BeWoA and circles-BeWoB). In the absence of FSK the STOX effects are less obvious and the dots are all in the middle of the graph.

Interestingly, the gene expression profiles are very peculiar in BeWoB cells under FSK treatment when analyzing UCA1 effects. On the first axis, UCA1 KD is not able to modify strongly the x-axis in these cells (from ∼2.3 to 1.5, $\Delta = 0.8$), while in control BeWoC, the modification on the x-axis ranges from ∼1.9 to −0.5, $\Delta = 2.4$, and in BeWoA from ∼2.2 to 0.5, $\Delta = 1.7$. The effect on gene differentiation was thus less reduced in BeWoB cells, comforting the idea that BeWoB overexpression and UCA1 KD act similarly but not synergistically against trophoblast fusion. This may be associated to the fact that STOX1B overexpression is associated with deficits of syncytialization (Ducat et al., 2020).

DISCUSSION

In the placenta, the STB acts as a barrier between the mother and fetus, and functions in gas exchange, nutrient, waste transport and hormone production. The STB is mitotically inactive and is formed by the constant cell-cell fusion of the underlying mononuclear CTBs. STB fragments are continuously shed into the maternal circulation. Thus, maintenance of the STB requires a finely regulated turnover. Excessive or restricted CTB-STB fusion may lead to PE, IUGR, and implantation failure (Gauster et al., 2009).

Although derived from human choriocarcinoma, the BeWo cells, display structural and physiological features of human primary trophoblast (Burres and Cass, 1986; Ramos et al., 2008; Orendi et al., 2010) and have been largely used as a model to study the process of trophoblasts fusion induced by forskolin treatment (Chen et al., 2008; Zhou et al., 2013; Wang et al., 2014). Several transcriptomic studies have helped to identify important genes involved in trophoblast fusion (Kudo et al., 2004; Depoix et al., 2011; Shankar et al., 2015; Zheng et al., 2016). However, the majority of these studies have focused on the role of protein-coding genes. The role that ncRNAs could have in the trophoblast fusion remains to be explored.

Here, we have conducted a microarray transcriptomic analysis of BeWo cells under forskolin treatment (BeWo-FSK) and focused our analysis on the differentially expressed ncRNAs relative to controls (BeWo-CO). We identified a number of ncRNAs (antisense-RNAs, lncRNAs, miRNAs) which might be involved in the process of syncytialization *in vivo*. We have generated a network displaying the putative regulatory interactions among the differentially expressed ncRNAs and differentially expressed genes (DEGs) in the BeWo-FSK relative to the BeWo-CO. The analysis of this network shows that the majority of ncRNAs targets are involved in cell proliferation and metabolism. Topological analysis of the network identified miR193b as a principal hub of the network. Hallmarks enrichment analysis shows that most targets of miR193b are down-regulated genes involved in cell cycle progression such as CCND1, CCNA2, or BUB1B. Previous studies have shown that miR193b acts as tumor suppressor by repressing cell proliferation (Mazzu et al., 2017; Zhang et al., 2017; Bhayadia et al., 2018). In the context of placental development, it has been reported that mir193b-3p overexpression significantly decreases the migration and invasion of the trophoblast cells (HTR-8/SVneo) by targeting the 3′UTR of TGF-beta2 (Zhou et al., 2016). The miR193b has been found consistently up-regulated in PE and IUGR placentas in our study and others (Ishibashi et al., 2012; Xu et al., 2014; Zhou et al., 2016; Awamleh et al., 2019). This miRNA is thought to contribute to these pathologies because of its inhibitory effect on the migration and invasion of trophoblasts. Here we show that miR193b is also involved in the process of syncytialization. A prior, and key step in syncytialisation, is the acquisition of fusion competence, which requires the CTB to exit the cell cycle (Lu et al., 2017). Therefore, by targeting genes involved in the control of cell cycle progression, miR193b could play a pivotal role in this crucial step of the process of syncytialisation. Overexpression of miR193b in PE could negatively impact placental development by accelerating CTB-STB fusion, thus leading to a premature depletion of the pool of CTBs necessary to ensure the constant renewal of the STB. Alternatively, increased miR193b expression in PE could reflect a mechanism seeking to

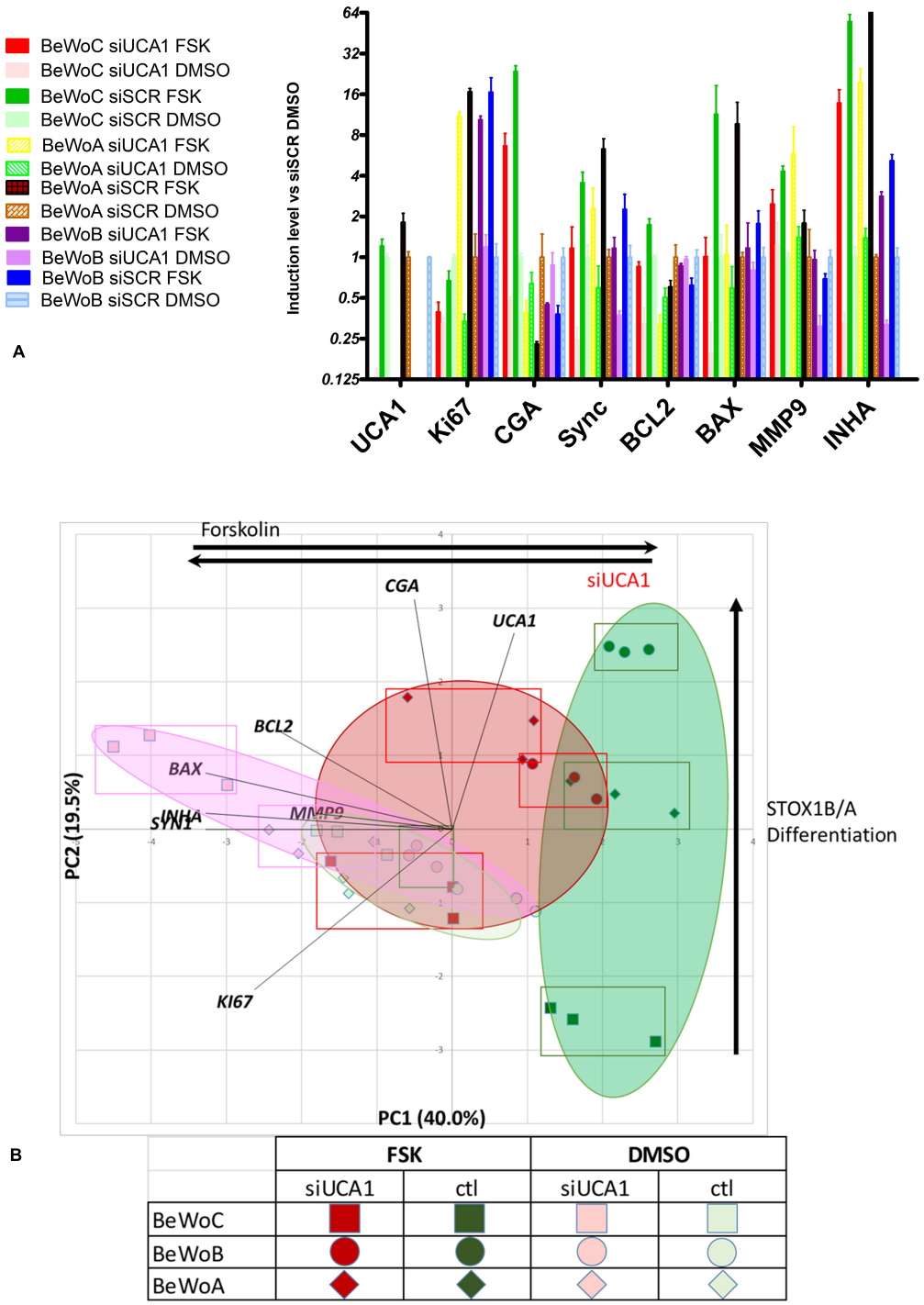

FIGURE 8 | (A) qRT-PCR analysis of the efficiency of UCA1 silencing in controls BeWoC and BeWo overexpressing either STOX1A or STOX1B, with or without forskolin treatment, and its effects on several markers of syncytialization. **(B)** Principal Component Analysis of the BeWo cells [controls BeWoC (circles) and overexpressing either STOX1A (lozenges) or STOX1B (circles)]. The genes are represented in black bold characters. The rectangles show the position of the different replicates. Red color marks UCA1 KD, while green are control cases. Dark colors mark FSK treatment. The interpretation of the axes is marked by black arrows.

compensate an excessive apoptotic shedding of the syncytium by facilitating the entering of CTB into the fusion process.

Since a dysfunctional syncytium could be at the origin of placental diseases, we systematically searched for lncRNAs involved in the CTBs fusion that were deregulated in placentas from PE or IUGR. An exhaustive literature search, as well and the reanalysis of datasets available in the GEO Database resulted in the identification of three lncRNAs consistently up-regulated

in PE and IUGR and involved in syncytialization: miR193b, miR365a and UCA1.

UCA1 (Urothelial Cancer Associated 1), is a lncRNA initially identified in a bladder cancer cell line (Wang et al., 2006). The involvement of lncRNAs in placental diseases has been previously described for the HELLP syndrome, a serious complication of preeclampsia (van Dijk et al., 2012). In the case of UCA1 high expression has previously been reported in different types of cancer. UCA1 promotes cell proliferation, tumor progression, migration and drug resistance. UCA1 mediates the transcriptional regulation at an epigenetic level by interaction with chromatin modifiers (EZH2, CTCF, YAP,. . .), by direct regulation via chromatin looping and/or by sponging miRNAs (Neve et al., 2018). The oncogenic functions of UCA1 have been extensively studied, but its role in development and differentiation remains unknown. A recent study, using the HTR-8/SVneo and JAR trophoblast cells suggests that UCA1 could inhibit trophoblast cell invasion and proliferation by down-regulating JAK2 (Liu et al., 2020). Knockdown of UCA1 in these cells suppressed the apoptotic rate and accelerated cell proliferation. Increased expression of UCA1 in PE had been reported previously and confirmed by our study (Liu et al., 2020). In addition, increased expression of UCA1, specifically in the STB of preeclamptic placentas, has been reported (Gormley et al., 2017). Thus, these data suggest that similar to miR193b, UCA1 might contribute in driving CTBs toward syncytialisation by inhibiting the genes involved in cell proliferation. The increased expression of UCA1 in the preeclamptic syncytium could reflect an increase in the turnover of the syncytium, to compensate for an increased apoptotic rate (Sharp et al., 2010; Fogarty et al., 2013). However, suppression of UCA1 in the HTR-8/SVneo and JAR cells decreased their apoptotic rates, indicating that UCA1 could also be involved in the induction of apoptosis (Liu et al., 2020). To explore more deeply the role that UCA1 might play in the process of syncytialization, we silenced its expression in the BeWo cells (BeWo-CO and BeWo-FSK) using a specific small interfering RNA (siRNA). Our results show that silencing UCA1 results in the downregulation of proliferation, attenuation of the expression of several markers of syncytialization, and most significantly downregulation of the expression of the antiapoptotic marker BCL2. As mentioned above in the HTR-8/SVneo and JAR cells, the Knockdown of UCA1, suppressed the apoptotic rate and accelerated cell proliferation (Liu et al., 2020). Thus, suppression of UCA1 in BeWo cells seems to have a different impact concerning the proliferation and apoptosis rates. These differences could be attributed to the fact that these cell lines are akin to different types of CTBs or either to particularities linked to the tumoral transformation process undergone by these cells. Nevertheless, our results on the BeWo cells are consistent with other studies indicating that in many cell types, UCA1 stimulates proliferation and inhibits apoptosis (Jun et al., 2018; Liu et al., 2018; Chen et al., 2019; Li et al., 2019; Wang et al., 2019). One limit of our study is that we did not carry out cell visualization experiments of the fusion; we can nevertheless assume that the alterations of syncytialisation marks that we observe here will likely be associated to phenotypic effects, that will have to be further assessed in future works.

Having in hand a model of altered fusion by STOX1A (BeWoA) or STOX1B (BeWoB) overexpression we attempted to evaluate the effect of UCA1 KD in these specific models. The overexpression of STOX1B (inhibiting fusion) led to more limited gene alterations than the other cells when forskolin was added in the Knock down of UCA1, suggesting that the alterations of gene expression induced by STOX1B overexpression render the UCA1 down-regulation alterations less visible.

Interestingly, hypoxia which plays a central role in the development of PE is known to induce UCA1 expression through HIF1A in both cancer cell lines and primary cultures of STB (Yuen et al., 2013; Xue et al., 2014; Zhu et al., 2019; Wang et al., 2020). In addition, it has been shown that UCA1 inhibits ischemia/reperfusion-induced apoptosis in cardiomyocytes (Chen et al., 2019; Wang et al., 2020). Given that ischemia/reperfusion is a known hallmark of severe PE and knowing that UCA1 has been detected as overexpressed specifically in the STB of severe preeclamptic patients (Gormley et al., 2017), it is tempting to speculate that UCA1 overexpression could reflect a protective mechanism aimed to attenuate apoptosis. However, in other cell types UCA1 has proved to exert pleiotropic effects, thus it might be involved in many other aspects of the trophoblast physiology. Although the BeWo cells are a good model to study the cell fusion process they are transformed carcinoma-like cells missing many trophoblast functions. Therefore, a more in-depth analysis of the functions of UCA1 in the placenta requires more physiological models such as primary trophoblast cultures, or placental organocultures. Another direction for future work is the assessment of the specific effects of the short isoforms of UCA1 that appear to be specifically modified when fusion occur. To note, we have recently demonstrated that alternative splicing is a general feature of placental disease, affecting hundreds of genes (Ruano et al., 2021). This could be achieved by lentiviral transformation of the cell lines, or even primary cultures with this short isoform. Finally, to understand better how UCA1 is actually functioning is an interesting challenge for further studies.

METHODS

Cell Culture

BeWo cell lines were cultivated in F12 medium (Life Technologies) supplemented with 10% fetal bovine serum (FBS) and 1% penicillin/streptomycin in 6-cm diameter plates, up to 60% confluence and with 50 μg/ml of geneticin G-418. The generation of the BeWoA (overexpressing constitutively STOX1A), BeWoB (overexpressing constitutively STOX1B) and BeWoC cell lines is described in detail in Ducat et al. (2020). The concentration of forskolin chosen for this study was based on preliminary studies (Ducat et al., 2020). At the end of the treatment, total RNA was extracted as previously described (Ducat et al., 2016). The siRNA against UCA1 was Ambion silencer select provided by ThermoFisher scientific. After plating in 12-well plates (1 ml) at 70% confluency, the cells were transfected the nest morning using RNAiMAx transfection

reagent (Invitrogen). Each well was transfected with 200 μl of Optimem™ with 1 μl of RNAiMax and 0.5 μl of siRNA or si scrambled at 5 pmol/μl, following the manufacturer's protocol. To induce syncytialization the cells were treated 1 day later with 20 μM forskolin or vehicle (DMSO) for 72 h.

Microarray Assay

One hundred ng of RNA per sample were analyzed using the ClariomD (Affymetrix) microarray assay. Library preparation, hybridization and data acquisition were performed by GENOM'IC platform according to manufacturer's instructions. Gene and exon level expressions were processed and extracted from the ClariomD microarray using the Transcriptomic Analysis Console (TAC) provided by Affymetrix.

Quantitative Reverse Transcribed-PCR

Five hundred nanograms of total RNA were reverse transcribed with MMLV using the Invitrogen kit and random primers. qPCR was carried out under standard conditions in a LightCycler480 (Roche) in 96 well plates as previously described (Ducat et al., 2020), with a Sybrgreen kit from BioLine (Meridian Bioscience). In the case of UCA1, the analysis was carried out using a TaqMan probe and the Roche LightCycler® TaqMan® Master. The PPIA gene (cyclophilin) was used as reporter in all experiment, since we have shown previously an excellent stability of this gene in trophoblast cells. All the cell qPCR experiments were carried out three to four independent times, and every time in triplicates. Primers for the different genes are listed as **Supplementary Table 4**.

Functional Annotation of the Differentially Expressed Genes (DEGs)

For the functional annotation of the DEGs we performed Over-representation analysis (ORA) using the WebGestalt[1] bioinformatics resource (Liao et al., 2019). Databases interrogated include: Gene Ontology (GO), Kyoto Encyclopedia of Genes and Genomes (KEGG), and Hallmarks. The significance of the detected enrichments was calculated using the Benjamini and Hochberg multiple test adjustment.

Gene Set Enrichment Analysis (GSEA)

GSEA was conducted using GSEA software from the Broad Institute[2]. The BeWo fusion gene set was generated using the top up-regulated and down-regulated genes after 72 h forskolin treatment reported by Shankar et al. (2015). We used as input the gene expression matrix generated by the Transcriptomic Analysis Console (Affymetrix) including all samples and replicates. The permutation value was set as 1,000. *P*-values were corrected for multiple testing and the cutoff for significant enrichment corresponds to an FDR < 0.25.

Prediction of ncRNAs Targets

To identify targets for the differentially expressed ncRNAs in the BeWo-FSK relative to BeWo-Co cells we used *ad hoc* databases. These include miRBase[3], starBase v2.0.[4] and the DianaTools LncBase v.2[5].

ncRNAs Regulatory Network

The ncRNAs and corresponding differentially expressed targets were used to generate a regulatory network. The network was constructed, visualized and analyzed using the Cytoscape 3.2.1 software[6] and its complementary applications (Shannon et al., 2003). The centrality parameters of the network were analyzed using the Cytoscape application NetworkAnalyzer (Shannon et al., 2003). Two topological parameters Betweenness Centrality (BC) and node degree were used to identify hub genes. The network is available as a **Supplementary XML File**.

DATA AVAILABILITY STATEMENT

The datasets presented in this study can be found in online repositories. The names of the repository/repositories and accession number(s) can be found below: https://www.ebi.ac.uk/metagenomics/, E-MTAB-9416 and https://www.ncbi.nlm.nih.gov/genbank/, GSE148088.

ETHICS STATEMENT

This study was approved by the Ethics Committee and CCPPRB (Comité Consultatif de Protection des Personnes dans la Recherche Biomédicale) of Paris Cochin. All patients gave their written consent for the use of their placenta and blood samples. For Angers, the collection and use for research purpose (including genetic analyses) of placentas from pregnancies complicated with IUGR or healthy pregnancy have been approved by the Ethics Committee of Angers. The patients/participants provided their written informed consent to participate in this study.

AUTHOR CONTRIBUTIONS

DV, FM, and CM conceived the work and drafted it. DV performed qRT-PCR experiments. SJ performed the microarray work. GG drafted the manuscript and contributed human samples. CR and CA performed RNA and qPCR experiments and drafted the manuscript. All authors contributed to the article and approved the submitted version.

FUNDING

The Ph.D. projects of CR and CA were funded by the European Union's Horizon 2020 Research and Innovation

[1]http://bioinfo.vanderbilt.edu/webgestalt

[2]https://www.gsea-msigdb.org/gsea/index.jsp

[3]http://www.mirbase.org/

[4]http://starbase.sysu.edu.cn

[5]http://diana.imis.athena-innovation.gr/DianaTools/index.php?r=lncBase/index

[6]https://cytoscape.org/

Program under Marie Skłodowska-Curie Actions Innovative Training Network (H2020-MSCA-ITN 2017, Grant No. 765274, acronym iPLACENTA).

SUPPLEMENTARY MATERIAL

The Supplementary Material for this article can be found online at: https://www.frontiersin.org/articles/10.3389/fcell.2021.633937/full#supplementary-material

Supplementary Figure 1 | GSEA analysis of the data from the present paper in comparison with published data, demonstrating an extreme similarity of our data compared to published datasets (Shankar et al., 2015).

Supplementary Figure 2 | Presentation of the network of deregulated genes in the predicted targets of miR-16, miR-455, and miR-365.

Supplementary Figure 3 | STOX1 expression levels at the probe level along the gene. Junction probes analysis revealed that a large part of the 3′ exon is less present in FSK-streated cells. This decrease in a series of probes reveal that STOX1A is twice as abundant as STOX1B when the cells are not fused, while in the context of fusion the ratio STOX1A/STOX1B drastically changes.

REFERENCES

Apicella, C., Ruano, C. S. M., Mehats, C., Miralles, F., and Vaiman, D. (2019). The role of epigenetics in placental development and the etiology of preeclampsia. *Int. J. Mol. Sci.* 20:2837. doi: 10.3390/ijms20112837

Awamleh, Z., Gloor, G. B., and Han, V. K. M. (2019). Placental microRNAs in pregnancies with early onset intrauterine growth restriction and preeclampsia: potential impact on gene expression and pathophysiology. *BMC Med. Genomics* 12:91. doi: 10.1186/s12920-019-0548-x

Basit, S., Wohlfahrt, J., and Boyd, H. A. (2018). Pre-eclampsia and risk of dementia later in life: nationwide cohort study. *BMJ* 363:k4109. doi: 10.1136/bmj.k4109

Benny, P. A., Alakwaa, F. M., Schlueter, R. J., Lassiter, C. B., and Garmire, L. X. (2020). A review of omics approaches to study preeclampsia. *Placenta* 92, 17–27. doi: 10.1016/j.placenta.2020.01.008

Bhayadia, R., Krowiorz, K., Haetscher, N., Jammal, R., Emmrich, S., Obulkasim, A., et al. (2018). Endogenous tumor suppressor microRNA-193b: therapeutic and prognostic value in acute myeloid leukemia. *J. Clin. Oncol.* 36, 1007–1016. doi: 10.1200/JCO.2017.75.2204

Brouwers, L., van der Meiden-van Roest, A. J., Savelkoul, C., Vogelvang, T. E., Lely, A. T., Franx, A., et al. (2018). Recurrence of pre-eclampsia and the risk of future hypertension and cardiovascular disease: a systematic review and meta-analysis. *BJOG* 125, 1642–1654. doi: 10.1111/1471-0528.15394

Burres, N. S., and Cass, C. E. (1986). Density-dependent inhibition of expression of syncytiotrophoblastic markers by cultured human choriocarcinoma (BeWo) cells. *J. Cell. Physiol.* 128, 375–382. doi: 10.1002/jcp.1041280305

Chabrun, F., Huetz, N., Dieu, X., Rousseau, G., Bouzille, G., Chao de la Barca, J. M., et al. (2019). Data-mining approach on transcriptomics and methylomics placental analysis highlights genes in fetal growth restriction. *Front. Genet.* 10:1292. doi: 10.3389/fgene.2019.01292

Chen, J., Hu, Q., Zhang, B. F., Liu, X. P., Yang, S., and Jiang, H. (2019). Long noncoding RNA UCA1 inhibits ischaemia/reperfusion injury induced cardiomyocytes apoptosis via suppression of endoplasmic reticulum stress. *Genes Genomics* 41, 803–810. doi: 10.1007/s13258-019-00806-w

Chen, Y., Qian, H., Zhang, Y., Ma, Y., Lin, C., and Xiang, Y. (2008). Effect of Ad-TIMP3 on biologic behavior of choriocarcinoma cells in vitro. *J. Reprod. Med.* 53, 608–614.

Costa, M. A. (2016). Scrutinising the regulators of syncytialization and their expression in pregnancy-related conditions. *Mol. Cell. Endocrinol.* 420, 180–193. doi: 10.1016/j.mce.2015.11.010

Cox, B., Leavey, K., Nosi, U., Wong, F., and Kingdom, J. (2015). Placental transcriptome in development and pathology: expression, function, and methods of analysis. *Am. J. Obstet. Gynecol.* 213, S138–S151. doi: 10.1016/j.ajog.2015.07.046

Darendeliler, F. (2019). IUGR: genetic influences, metabolic problems, environmental associations/triggers, current and future management. *Best Pract. Res. Clin. Endocrinol. Metab.* 33:101260. doi: 10.1016/j.beem.2019.01.001

Depoix, C., Tee, M. K., and Taylor, R. N. (2011). Molecular regulation of human placental growth factor (PlGF) gene expression in placental villi and trophoblast cells is mediated via the protein kinase a pathway. *Reprod. Sci.* 18, 219–228. doi: 10.1177/1933719110389337

Deyssenroth, M. A., Peng, S., Hao, K., Lambertini, L., Marsit, C. J., and Chen, J. (2017). Whole-transcriptome analysis delineates the human placenta gene network and its associations with fetal growth. *BMC Genomics* 18:520. doi: 10.1186/s12864-017-3878-0

Ducat, A., Couderc, B., Bouter, A., Biquard, L., Aouache, R., Passet, B., et al. (2020). Molecular mechanisms of trophoblast dysfunction mediated by imbalance between STOX1 isoforms. *iScience* 23:101086. doi: 10.1016/j.isci.2020.101086

Ducat, A., Doridot, L., Calicchio, R., Mehats, C., Vilotte, J. L., Castille, J., et al. (2016). Endothelial cell dysfunction and cardiac hypertrophy in the STOX1 model of preeclampsia. *Sci. Rep.* 6:19196. doi: 10.1038/srep19196

Fernandes, J. C. R., Acuna, S. M., Aoki, J. I., Floeter-Winter, L. M., and Muxel, S. M. (2019). Long non-coding RNAs in the regulation of gene expression: physiology and disease. *Noncoding RNA* 5:17. doi: 10.3390/ncrna5010017

Fogarty, N. M., Ferguson-Smith, A. C., and Burton, G. J. (2013). Syncytial knots (Tenney-Parker changes) in the human placenta: evidence of loss of transcriptional activity and oxidative damage. *Am. J. Pathol.* 183, 144–152. doi: 10.1016/j.ajpath.2013.03.016

Gauster, M., Moser, G., Orendi, K., and Huppertz, B. (2009). Factors involved in regulating trophoblast fusion: potential role in the development of preeclampsia. *Placenta* 30 Suppl. A, S49–S54. doi: 10.1016/j.placenta.2008.10.011

George, E. M., and Bidwell, G. L. (2013). STOX1: a new player in preeclampsia? *Hypertension* 61, 561–563. doi: 10.1161/HYPERTENSIONAHA.111.00721

Gibbs, I., Leavey, K., Benton, S. J., Grynspan, D., Bainbridge, S. A., and Cox, B. J. (2019). Placental transcriptional and histologic subtypes of normotensive fetal growth restriction are comparable to preeclampsia. *Am. J. Obstet. Gynecol.* 220, e1–e110. doi: 10.1016/j.ajog.2018.10.003

Goldenberg, R. L., Culhane, J. F., Iams, J. D., and Romero, R. (2008). Epidemiology and causes of preterm birth. *Lancet* 371, 75–84. doi: 10.1016/S0140-6736(08)60074-4

Gormley, M., Ona, K., Kapidzic, M., Garrido-Gomez, T., Zdravkovic, T., and Fisher, S. J. (2017). Preeclampsia: novel insights from global RNA profiling of trophoblast subpopulations. *Am. J. Obstet. Gynecol.* 217, e1–e200. doi: 10.1016/j.ajog.2017.03.017

Guller, S., Ma, Y. Y., Fu, H. H., Krikun, G., Abrahams, V. M., and Mor, G. (2008). The placental syncytium and the pathophysiology of preeclampsia and intrauterine growth restriction: a novel assay to assess syncytial protein expression. *Ann. N. Y. Acad. Sci.* 1127, 129–133. doi: 10.1196/annals.1434.015

Hayder, H., O'Brien, J., Nadeem, U., and Peng, C. (2018). MicroRNAs: crucial regulators of placental development. *Reproduction* 155, R259–R271. doi: 10.1530/REP-17-0603

Hombach, S., and Kretz, M. (2016). Non-coding RNAs: classification, biology and functioning. *Adv. Exp. Med. Biol.* 937, 3–17. doi: 10.1007/978-3-319-42059-2_1

Ishibashi, O., Ohkuchi, A., Ali, M. M., Kurashina, R., Luo, S. S., Ishikawa, T., et al. (2012). Hydroxysteroid (17-beta) dehydrogenase 1 is dysregulated by miR-210 and miR-518c that are aberrantly expressed in preeclamptic placentas: a novel marker for predicting preeclampsia. *Hypertension* 59, 265–273. doi: 10.1161/HYPERTENSIONAHA.111.180232

Jun, T., Zheng, F. S., Ren, K. M., Zhang, H. Y., Zhao, J. G., and Zhao, J. Z. (2018). Suppression of long non-coding RNA UCA1 inhibits proliferation and invasion and induces apoptosis in human lung cancer cells. *Eur. Rev. Med. Pharmacol. Sci.* 22, 7274–7281.

Kudo, Y., Boyd, C. A., Sargent, I. L., Redman, C. W., Lee, J. M., and Freeman, T. C. (2004). An analysis using DNA microarray of the time course of gene expression during syncytialization of a human placental cell line (BeWo). *Placenta* 25, 479–488. doi: 10.1016/j.placenta.2003.12.001

Li, J. L., Liu, X. L., Guo, S. F., Yang, Y., Zhu, Y. L., and Li, J. Z. (2019). Long noncoding RNA UCA1 regulates proliferation and apoptosis in multiple myeloma by targeting miR-331-3p/IL6R axis for the activation of JAK2/STAT3 pathway. *Eur. Rev. Med. Pharmacol. Sci.* 23, 9238–9250.

Liao, Y., Wang, J., Jaehnig, E. J., Shi, Z., and Zhang, B. (2019). WebGestalt 2019: gene set analysis toolkit with revamped UIs and APIs. *Nucleic Acids Res.* 47, W199–W205. doi: 10.1093/nar/gkz401

Liu, J., Luo, C., Zhang, C., Cai, Q., Lin, J., Zhu, T., et al. (2020). Upregulated lncRNA UCA1 inhibits trophoblast cell invasion and proliferation by downregulating JAK2. *J. Cell. Physiol.* 235, 7410–7419. doi: 10.1002/jcp.29643

Liu, Q., Li, Y., Lv, W., Zhang, G., Tian, X., Li, X., et al. (2018). UCA1 promotes cell proliferation and invasion and inhibits apoptosis through regulation of the miR129-SOX4 pathway in renal cell carcinoma. *Onco. Targets Ther.* 11, 2475–2487. doi: 10.2147/OTT.S160192

Lu, X., Wang, R., Zhu, C., Wang, H., Lin, H. Y., Gu, Y., et al. (2017). Fine-tuned and cell-cycle-restricted expression of fusogenic protein Syncytin-2 maintains functional placental syncytia. *Cell Rep.* 21, 1150–1159. doi: 10.1016/j.celrep.2017.10.019

Majewska, M., Lipka, A., Paukszto, L., Jastrzebski, J. P., Szeszko, K., Gowkielewicz, M., et al. (2019). Placenta transcriptome profiling in intrauterine growth restriction (IUGR). *Int. J. Mol. Sci.* 20:1510. doi: 10.3390/ijms20061510

Mazzu, Y. Z., Hu, Y., Soni, R. K., Mojica, K. M., Qin, L. X., Agius, P., et al. (2017). miR-193b-regulated signaling networks serve as tumor suppressors in liposarcoma and promote adipogenesis in adipose-derived stem cells. *Cancer Res.* 77, 5728–5740. doi: 10.1158/0008-5472.CAN-16-2253

Medina-Bastidas, D., Guzman-Huerta, M., Borboa-Olivares, H., Ruiz-Cruz, C., Parra-Hernandez, S., Flores-Pliego, A., et al. (2020). Placental microarray profiling reveals common mRNA and lncRNA expression patterns in preeclampsia and intrauterine growth restriction. *Int. J. Mol. Sci.* 21:3597. doi: 10.3390/ijms21103597

Nardozza, L. M. M., Zamarian, A. C. P., and Araujo Junior, E. (2017). New definition of fetal growth restriction: consensus regarding a major obstetric complication. *Rev. Bras. Ginecol. Obstet.* 39, 315–316. doi: 10.1055/s-0037-1603741

Neve, B., Jonckheere, N., Vincent, A., and Van Seuningen, I. (2018). Epigenetic regulation by lncRNAs: an overview focused on UCA1 in colorectal cancer. *Cancers (Basel)* 10:440. doi: 10.3390/cancers10110440

Newstead, J., von Dadelszen, P., and Magee, L. A. (2007). Preeclampsia and future cardiovascular risk. *Expert Rev. Cardiovasc. Ther.* 5, 283–294. doi: 10.1586/14779072.5.2.283

Orendi, K., Gauster, M., Moser, G., Meiri, H., and Huppertz, B. (2010). The choriocarcinoma cell line BeWo: syncytial fusion and expression of syncytium-specific proteins. *Reproduction* 140, 759–766. doi: 10.1530/REP-10-0221

Ramos, A. J., Cantero, M. R., Zhang, P., Raychowdhury, M. K., Green, A., MacPhee, D., et al. (2008). Morphological and electrical properties of human trophoblast choriocarcinoma. BeWo cells. *Placenta* 29, 492–502. doi: 10.1016/j.placenta.2008.02.013

Rana, S., Lemoine, E., Granger, J. P., and Karumanchi, S. A. (2019). Preeclampsia: pathophysiology, challenges, and perspectives. *Circ. Res.* 124, 1094–1112. doi: 10.1161/CIRCRESAHA.118.313276

Roland, C. S., Hu, J., Ren, C. E., Chen, H., Li, J., Varvoutis, M. S., et al. (2016). Morphological changes of placental syncytium and their implications for the pathogenesis of preeclampsia. *Cell. Mol. Life Sci.* 73, 365–376. doi: 10.1007/s00018-015-2069-x

Ruano, C. S. M., Apicella, C., Jacques, S., Gascoin, G., Gaspar, C., Miralles, F., et al. (2021). Alternative splicing in normal and pathological human placentas is correlated to genetic variants. *Hum. Genet.* 140, 827–848. doi: 10.1007/s00439-020-02248-x

Shankar, K., Kang, P., Zhong, Y., Borengasser, S. J., Wingfield, C., Saben, J., et al. (2015). Transcriptomic and epigenomic landscapes during cell fusion in BeWo trophoblast cells. *Placenta* 36, 1342–1351. doi: 10.1016/j.placenta.2015.10.010

Shannon, P., Markiel, A., Ozier, O., Baliga, N. S., Wang, J. T., Ramage, D., et al. (2003). Cytoscape: a software environment for integrated models of biomolecular interaction networks. *Genome Res.* 13, 2498–2504. doi: 10.1101/gr.1239303

Sharp, A. N., Heazell, A. E., Crocker, I. P., and Mor, G. (2010). Placental apoptosis in health and disease. *Am. J. Reprod. Immunol.* 64, 159–169. doi: 10.1111/j.1600-0897.2010.00837.x

Steegers, E. A., von Dadelszen, P., Duvekot, J. J., and Pijnenborg, R. (2010). Pre-eclampsia. *Lancet* 376, 631–644. doi: 10.1016/S0140-6736(10)60279-6

Turco, M. Y., and Moffett, A. (2019). Development of the human placenta. *Development* 146, doi: 10.1242/dev.163428

Vaiman, D., and Miralles, F. (2016). Targeting STOX1 in the therapy of preeclampsia. *Expert Opin. Ther. Targets* 20, 1433–1443. doi: 10.1080/14728222.2016.1253682

van Dijk, M., Thulluru, H. K., Mulders, J., Michel, O. J., Poutsma, A., Windhorst, S., et al. (2012). HELLP babies link a novel lincRNA to the trophoblast cell cycle. *J. Clin. Invest.* 122, 4003–4011. doi: 10.1172/JCI65171

Wang, C. J., Zhu, C. C., Xu, J., Wang, M., Zhao, W. Y., Liu, Q., et al. (2019). The lncRNA UCA1 promotes proliferation, migration, immune escape and inhibits apoptosis in gastric cancer by sponging anti-tumor miRNAs. *Mol. Cancer* 18:115. doi: 10.1186/s12943-019-1059-2

Wang, Q. S., Zhou, J., and Li, X. (2020). LncRNA UCA1 protects cardiomyocytes against hypoxia/reoxygenation induced apoptosis through inhibiting miR-143/MDM2/p53 axis. *Genomics* 112, 574–580. doi: 10.1016/j.ygeno.2019.04.009

Wang, R., Dang, Y. L., Zheng, R., Li, Y., Li, W., Lu, X., et al. (2014). Live cell imaging of in vitro human trophoblast syncytialization. *Biol. Reprod.* 90:117. doi: 10.1095/biolreprod.113.114892

Wang, X. S., Zhang, Z., Wang, H. C., Cai, J. L., Xu, Q. W., Li, M. Q., et al. (2006). Rapid identification of UCA1 as a very sensitive and specific unique marker for human bladder carcinoma. *Clin. Cancer Res.* 12, 4851–4858. doi: 10.1158/1078-0432.CCR-06-0134

Xu, P., Zhao, Y., Liu, M., Wang, Y., Wang, H., Li, Y. X., et al. (2014). Variations of microRNAs in human placentas and plasma from preeclamptic pregnancy. *Hypertension* 63, 1276–1284. doi: 10.1161/HYPERTENSIONAHA.113.02647

Xue, M., Chen, W., and Li, X. (2016). Urothelial cancer associated 1: a long noncoding RNA with a crucial role in cancer. *J. Cancer Res. Clin. Oncol.* 142, 1407–1419. doi: 10.1007/s00432-015-2042-y

Xue, M., Li, X., Li, Z., and Chen, W. (2014). Urothelial carcinoma associated 1 is a hypoxia-inducible factor-1alpha-targeted long noncoding RNA that enhances hypoxic bladder cancer cell proliferation, migration, and invasion. *Tumour Biol.* 35, 6901–6912. doi: 10.1007/s13277-014-1925-x

Yuen, R. K., Chen, B., Blair, J. D., Robinson, W. P., and Nelson, D. M. (2013). Hypoxia alters the epigenetic profile in cultured human placental trophoblasts. *Epigenetics* 8, 192–202. doi: 10.4161/epi.23400

Zhang, J., Qin, J., and Su, Y. (2017). miR-193b-3p possesses anti-tumor activity in ovarian carcinoma cells by targeting p21-activated kinase 3. *Biomed. Pharmacother.* 96, 1275–1282. doi: 10.1016/j.biopha.2017.11.086

Zheng, R., Li, Y., Sun, H., Lu, X., Sun, B. F., Wang, R., et al. (2016). Deep RNA sequencing analysis of syncytialization-related genes during BeWo cell fusion. *Reproduction* doi: 10.1530/REP-16-0343

Zhou, X., Li, Q., Xu, J., Zhang, X., Zhang, H., Xiang, Y., et al. (2016). The aberrantly expressed miR-193b-3p contributes to preeclampsia through regulating transforming growth factor-beta signaling. *Sci. Rep.* 6:19910. doi: 10.1038/srep19910

Zhou, Z., Zhang, Q., Lu, X., Wang, R., Wang, H., Wang, Y. L., et al. (2013). The proprotein convertase furin is required for trophoblast syncytialization. *Cell Death Dis.* 4:e593. doi: 10.1038/cddis.2013.106

Zhu, T. T., Sun, R. L., Yin, Y. L., Quan, J. P., Song, P., Xu, J., et al. (2019). Long noncoding RNA UCA1 promotes the proliferation of hypoxic human pulmonary artery smooth muscle cells. *Pflugers Arch.* 471, 347–355. doi: 10.1007/s00424-018-2219-8

Conflict of Interest: The authors declare that the research was conducted in the absence of any commercial or financial relationships that could be construed as a potential conflict of interest.

Advantages of publishing in Frontiers

OPEN ACCESS
Articles are free to read for greatest visibility and readership

FAST PUBLICATION
Around 90 days from submission to decision

HIGH QUALITY PEER-REVIEW
Rigorous, collaborative, and constructive peer-review

TRANSPARENT PEER-REVIEW
Editors and reviewers acknowledged by name on published articles

Frontiers
Avenue du Tribunal-Fédéral 34
1005 Lausanne | Switzerland

Visit us: www.frontiersin.org
Contact us: frontiersin.org/about/contact

REPRODUCIBILITY OF RESEARCH
Support open data and methods to enhance research reproducibility

DIGITAL PUBLISHING
Articles designed for optimal readership across devices

FOLLOW US
@frontiersin

IMPACT METRICS
Advanced article metrics track visibility across digital media

EXTENSIVE PROMOTION
Marketing and promotion of impactful research

LOOP RESEARCH NETWORK
Our network increases your article's readership